

Transcriptional regulation of CNS regeneration

Dissertation

zur Erlangung des Grades eines Doktors
der Naturwissenschaften

der Mathematisch-Naturwissenschaftlichen Fakultät
und
der Medizinischen Fakultät
der Eberhard-Karls-Universität Tübingen

vorgelegt
von

Yashashree Shrikant Joshi
Goregaon, India
Mai 2014

Tag der mündlichen Prüfung:

:

:

Tag der mündlichen Prüfung:

Dekan der Math.-Nat. Fakultät:

Prof. Dr. W. Rosenstiel

Dekan der Medizinischen Fakultät

Prof. Dr. I. B. Autenrieth

1. Berichterstatter

Prof. Dr. / PD Dr. Di Giovanni

2. Berichterstatter

Prof. Dr. / PD Dr. Schlosshauer

Prüfungskommission:

Prof. Dr. Di Giovanni

Prof. Dr. Knipper

Prof. Dr. Schlosshauer

PD Dr. Wizenmann

I hereby declare that I have produced the work entitled: "Transcriptional regulation of CNS regeneration",

submitted for the award of a doctorate, on my own (without external help), have used only the sources and aids indicated and have marked passages included from other works, whether verbatim or in content, as such. I swear upon oath that these statements are true and that I have not concealed anything. I am aware that making a false declaration under oath is punishable by a term of imprisonment of up to three years or by a fine.

Tübingen, _____

Date

Signature

Contents

1 Summary.....	7
Zusammenfassung.....	10
1.1 Synopsis.....	13
1.1.1 CNS regeneration-Cellular and molecular mechanisms following injury.....	13
1.1.2 CNS regeneration- Identified molecular mechanisms.....	16
1.1.3 Ubiquitin ligases and p53-related signalling in CNS regeneration.....	21
1.1.4 CNS regeneration and ubiquitin ligases.....	24
1.1.5 Role of histone acetyl transferases p300 and PCAF in CNS regeneration.....	32
1.2 Concluding remarks and outlook.....	39
1.3 Abbreviations.....	40
1.4 Acknowledgement.....	41
1.5 References.....	42
2 Publications.....	48
2.1 Modulation of MDM4-p53-IGF1R axis promotes CNS axonal regeneration and sprouting after CNS injury.....	49
2.2 The histone acetyl transferase p300 promotes intrinsic axonal regeneration.....	89
2.3 PCAF dependent epigenetic changes promote axonal regeneration in the central nervous system.....	109
3 Curriculum Vitae.....	139

1 Summary

It was a long held belief that adult mammalian central nervous is unable to regenerate in any condition and reiterated in Ramon y Cajal's seminal work (Santiago Ramón y Cajal, 1991). This idea was disproved when injured CNS axons were able to regenerate in PNS lesion environment and embryonic grafts shedding light on the reasons contributing to CNS regeneration failure (Richardson *et al.*, 1980, Aguayo *et al.*, 1981). Regeneration in the CNS is inhibited by myelin and astrocyte based inhibitors along with the presence of an inhibitory transcriptional environment, elicited and/or enhanced by the cascades induced by injury (Yiu and He, 2006).

Extensive research has identified transcription factors and proteins which when modulated enhance regeneration of the injured adult CNS axons (Liu *et al.*, 2011). Traditional approaches to promote a permissive molecular environment in neurons have provided crucial leads but not therapeutic options. Hence, novel approaches and targets need to be identified by studying molecules involved in developmental processes like neurogenesis, axon path-finding and neuronal morphogenesis. Ubiquitin ligases and ubiquitin ligase like proteins have been identified to play a role in neuronal morphogenesis, connectivity and degeneration after injury (Yamada *et al.*, 2013). MDM4, a ubiquitin ligase like enzyme, has p53 as its prime substrate and interacts also with molecules like PTEN, Smads, p21, previously implicated in regeneration (Toledo and Wahl, 2006, Eva *et al.*, 2012). MDM4 occludes the transcriptional activation domain of p53 limiting its transactivation while another E3 ubiquitin ligase MDM2 reduces the level and hence the activity of p53 (Marine, 2011, Marine and Jochemsen, 2004).

In this study, we have investigated the effect of modulating novel factors MDM2 and MDM4 on CNS regeneration using optic nerve crush as an injury model. Genetic ablation of MDM4 and pharmacological inhibition of MDM2 in retinal ganglion cells induced regeneration of optic axons, without substantially affecting neuronal survival. Genome wide gene expression analysis from FACS sorted pure RGCs revealed up-regulation of IGF1R gene

and its role was confirmed by its specific pharmacological inhibition. Hence this study represents MDM2-MDM4-p53-IGF1R as a neuronal signaling pathway that might present novel therapeutic targets for neuro-trauma patients.

Along with identifying the role of p53 and its negative regulators MDM2 and MDM4 in regeneration, we also studied the role of histone acetyl transferases P/CAF and p300 which are known to be epigenetic modulators in neurons (as collaboration between colleagues at the same lab). Expression of p300, which acetylates specific lysine residues of p53 and histone H3, was decreases in RGCs upon maturation and hence was a potential valid target. Viral overexpression of p300 in RGCs enhanced regeneration after optic nerve crush coupled with boosting the pre-conditioning effect of lens injury. The pre-conditioning lesion primes the neurons to enter a regenerative state and enables the axons to overcome the inhibitory extrinsic environment. Pre-conditioning lesion effect can be induced in the spinal system (i.e in the dorsal root ganglia) by lesioning the peripheral axons which permits the regeneration of their central branches in the CNS. Regenerative effect of the conditioning lesion is elicited due to the expression of regeneration associated genes (RAGs), but the mechanism controlling their expression remains unknown. Here, we were able to clarify a unique role of p300/ CBP associated Factor (PCAF) following conditioning lesion. PCAF dependent acetylation at histone H3 lysine 9 (H3K9) along with a reduction in methylation of H3K9 (H3K9me₂), was observed at the promoters of RAGs exclusively after PNS axonal injury. PCAF dependent acetylation of these promoters increased RAGs expression, which was mediated by extracellular signal regulated kinase (ERK) axonal retrograde signaling. Hence we have established a unifying role for PCAF as a broad regulator for regeneration, following a conditioning lesion. Viral PCAF overexpression also promoted axonal regeneration after CNS injury in spinal ascending sensory fibers, though such an effect was not observed in the ONC system, owing mainly due lower PCAF expression levels observed.

To conclude, in this study we were able to identify novel ubiquitin ligases, MDM4 and MDM2 which when deleted promote regeneration in the adult CNS. Additionally

overexpression of epigenetic modulators p300 and P/CAF was found to induce regeneration in the CNS. Development and validation of drugs that can specifically modify the activity of these targets can present novel therapeutic options.

Zusammenfassung

Die lang vertretene Überzeugung, dass das adulte Zentralnervensystem nicht in der Lage ist sich zu regenerieren, wurde wiederholt in den bahnbrechenden Arbeiten Ramon y Cajals widerlegt (Santiago Ramón y Cajal, 1991). Es war gezeigt, dass sich verletzte ZNS Axone in PNS Läsionen und embryonalen Transplantaten regenerieren können (Richardson *et al.*, 1980). Die Regeneration im ZNS wird von Myelin- und Astrozyten- Inhibitoren und einer inhibitorischen Transkriptions Umgebung, die durch Verletzungs-Kaskaden induziert und/oder verstärkt wird, gehemmt (Yiu and He, 2006). Umfangreiche Forschungen haben Transkriptionsfaktoren und Proteine identifiziert, die nach Modulation die Regeneration verletzter adulter ZNS Axone verbessern (Liu *et al.*, 2011). Obwohl traditionelle Ansätze, die eine selektive molekulare Umgebung in Neuronen fördern, Wegweisende Ergebnisse geliefert haben, müssen neue Herangehensweisen und Ziele, durch die Erforschung von Molekülen, die in Entwicklungsprozessen wie der Neurogenese, der axonalen Wegfindung und der neuronalen Morphogenese beteiligt sind, identifiziert werden. Es hat sich herausgestellt, dass Ubiquitin-Ligasen und Ubiquitin-Ligase-ähnliche Proteine eine Rolle in der neuronalen Morphogenese, der Konnektivität und der Degeneration nach einer Verletzung spielen (Yamada *et al.*, 2013). MDM4, ein Ubiquitin-Ligase-ähnliches Enzym, dessen primäres Substrat p53 ist und das mit Proteinen wie PTEN, Smads und p21 interagiert, wurde schon zuvor eine regenerative Wirkung beigemessen (Toledo and Wahl, 2006, Eva *et al.*, 2012). MDM4 verschließt die transkriptionelle Aktivierungsdomäne von p53, wodurch die Transkriptionsaktivierung von p53 begrenzt wird, während eine weitere E3-Ubiquitin-Ligase MDM2 die p53 Konzentration und damit die Aktivität von p53 reduziert (Toledo and Wahl, 2006, Eva *et al.*, 2012, Marine, 2011, Marine and Jochemsen, 2004). Für die vorliegende Arbeit haben wir die Wirkung der neuen modulierenden Faktoren MDM2 und MDM4 auf die Regenerationsfähigkeit des ZNS mittels Zerquetschung des Sehnerv als Verletzungs Modell untersucht. Die genetische Ablation von MDM4 und die pharmakologische Inhibition von MDM2 in retinalen Ganglienzellen, induzierte die

Regeneration von Axonen des N. Optikus, ohne das neuronale Überleben wesentlich zu beeinflussen. Genom-weite Genexpressions-Analysen von FACS-sortierten reinen RGCs, offenbarten eine Hochregulation des IGF1R -Gens. Dies wurde zusätzlich durch die spezifische pharmakologische Hemmung des IGF1R-Gens bestätigt. Deshalb stellt diese Studie den neuronalen MDM2 - p53 - MDM4 - IGF1R-Signalweg als neues therapeutisches Ziel für die Behandlung von Neuro-Trauma-Patienten vor. Neben der Identifizierung der Rolle von p53 und seiner negativen Regulatoren MDM2 und MDM4 bei der Regeneration, untersuchten wir auch die Rolle der Histon-Acetyl-Transferasen P/ CAF und p300, die bekanntlich epigenetische Modulatoren in Neuronen (als Zusammenarbeit zwischen Kollegen im gleichen Labor) sind. Die Expression von p300, welches spezifisch Lysin-Reste von p53 und Histon H3 acetyliert, war nach der Reifung der RGCs verringert. Dies machte p300 zu einem sehr vielversprechenden Ziel. Die virale Überexpression von p300 in RGCs, verbesserte die Regeneration nach Zerquetschung des Sehnervs und förderte den präkonditionierenden Linsen-Verletzungs Effekt. Die präkonditionierende Läsion sorgt dafür, dass die Neuronen in einen regenerativen Zustand übergehen und ermöglicht den Axonen die hemmende extrinsische Umgebung zu überwinden. Der präkonditionierende Läsions-Effekt kann im spinalen System (d. h. in den Spinalganglien) durch Läsion der peripheren Axone induziert werden und ermöglicht die Regeneration ihrer zentralen Verzweigungsstellen im ZNS. Die regenerative Wirkung der konditionierenden Läsion wird durch die Expression Regenerations-assoziiierter Gene (RAGs) hervorgerufen. Der Mechanismus der ihre Expression kontrolliert ist allerdings noch unbekannt. In dieser Arbeit gelang es die einzigartige Rolle von p300/ CBP assoziierter Faktor (PCAF) nach einer konditionierenden Läsion zu klären. Die PCAF-abhängige Acetylierung an Histon H3 Lysin 9 (H3K9) und die Verringerung der Methylierung von H3K9 (H3K9me2), wurde bei den Promotoren der RAGs ausschließlich nach einer PNS axonalen Schädigung beobachtet. Es zeigte sich, dass die PCAF-abhängige Acetylierung dieser Promotoren die RAGs Expression, vermittelt durch die Extracellular-signal Regulated Kinase (ERK) und axonal retrograde Signalwege, erhöht wurde. Somit haben wir eine übergreifende Rolle für PCAF

als umfassenden Regulator der Regeneration nach einer konditionierenden Läsion nachgewiesen. Die virale PCAF Überexpression förderte auch die axonale Regeneration nach ZNS-Verletzung der spinalen aufsteigenden sensorischen Fasern, obwohl ein solcher Effekt nicht im ONC -System beobachtet werden konnte. was vor allem auf eine niedrigere PCAF Expression zurückzuführen sein könnte.

Abschließend lässt sich sagen, dass wir in dieser Studie die neuartigen Ubiquitinligasen, MDM4 und MDM2 identifizieren konnten, die wenn sie ausgeschaltet werden die Regeneration im adulten ZNS fördern. Desweiteren zeigte sich, dass die Überexpression der epigenetischen Modulatoren p300 und PCAF die Regeneration im ZNS induziert Die Entwicklung und Validierung von Medikamenten, die gezielt die Aktivität dieser Ziele verändern , könnten neue therapeutische Möglichkeiten eröffnen.

1.1 Synopsis

In this work, I describe the role of transcriptional regulation of CNS regeneration with a focus on ubiquitin ligase MDM2 and ubiquitin ligase like protein MDM4 along with the role of histone acetyl transferases p300 and P/CAF. Key results are followed by the relevant discussion, while the publications from the primary and collaborative works have been attached at the end.

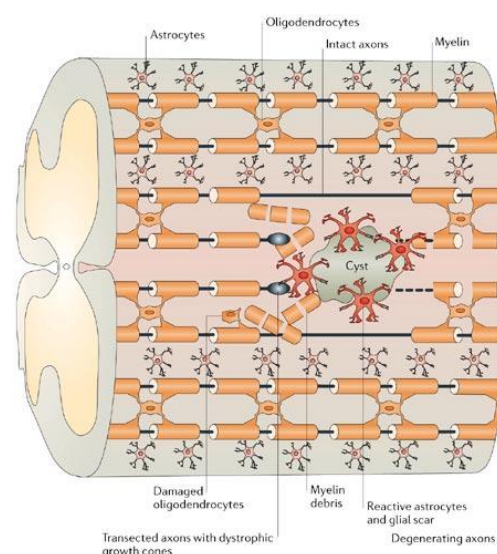
1.1.1 CNS regeneration- Cellular and molecular mechanisms following injury

The central nervous system (CNS) is a remarkable plastic system functional, structural and molecular level and controls complex functions like sensory input, conscious motor, and behavioral output and subconscious autonomic physiological control. The CNS adapts and responds to various cues from physiological stimuli related to learning and memory to pathological insults like traumatic brain/spinal cord injury, stroke or neurodegenerative diseases.

Injury to the adult mammalian CNS leads to severe clinical debility due to failure of damaged axons to instinctively regenerate. This failure can be (Yiu and He, 2006) attributed to inhibitory myelin environment and lack of neuronal intrinsic response. The immediate endogenous reaction to CNS trauma includes structural damage to the axons and/or their cell bodies, triggering a series of events. Injured axons retract from the injury site while a few axons are able sprout for a millimeter or less (Windle, 1980). Mammalian CNS axons lack the capacity to regenerate, but develop dystrophic growth cones or boutons, implicating the failed attempt to regenerate owing to intrinsic properties of the neurons and their interaction with the inhibitory extrinsic properties. Active secondary processes that follow after the primary insult also lead to additional structural and functional loss. SCI primarily leads to the disruption of the axonal tracts leading to paraplegia or quadriplegia, depending upon the site and the extent of the injury (Bradbury and McMahon, 2006).

Extensive research in the past decade has disputed Ramon y Cajal work stated in “Degeneration and Regeneration of the Nervous system” which mentioned “in adult centres, nerve pathways are something that are fixed, ended and immutable. Everything may die, nothing may be regenerated”(Llinas, 2003). Seminal work by Aguayo and colleagues demonstrated that injured CNS axons are able to regrow on transplanted peripheral nervous system grafts, indicating the inhibitory role of CNS myelin (David and Aguayo, 1981, Aguayo *et al.*, 1981, Richardson *et al.*, 1980).

Regeneration failure of adult mammalian CNS is attributed to growth inhibitory extrinsic adult CNS myelin and CSPG associated inhibitors , inadequate growth supporting environment at the lesion site as well as limited intrinsic neuronal growth potential of the adult CNS (Schwab and Thoenen, 1985, David and Aguayo, 1981, Silver and Miller, 2004, Lu and Tuszynski, 2008). Following injury, severed axons are exposed to myelin and oligodendrocyte-associated inhibitors along with CSPGs secreted by reactive astrocytes. Myelin associated inhibitors like Nogo (or Rtn4 ,a member of reticulon membrane-proteins family), myelin associated glycoprotein (MAG) (Mukhopadhyay *et al.*, 1994, McKerracher *et al.*, 1994), oligodendrocyte myelin glycoprotein (OMgp) (Wang *et al.*, 2002), trans-membrane semaphorin 4D (Moreau-Fauvarque *et al.*, 2003), ephrin B3 (Benson *et al.*, 2005) have been



Copyright © 2006 Nature Publishing Group
Nature Reviews | Neuroscience

Figure 1: Extrinsic inhibitors of CNS regeneration Transsection of nerve fibres following an injury exposes the damaged axons to the inhibitory myelin environment. Astrocyte activation leads to the development of the glial scar, which together with myelin associated inhibitor represents an insurmountable barrier for the severed axons(Yiu and He, 2006).

identified by *in vitro* and/or *in vivo* studies. Nogo, MAG and OmGP have been found to bind receptors Nogo-66 receptor (NgR) and PirB as well as co-receptors like p75, TROY and LINGO (Yiu and He, 2006). Binding of these myelin associated inhibitors to their receptors has been shown to induce GTPase RhoA and its effector Rho activated kinase (ROCK)(Schmandke and Strittmatter, 2007). Activation of ROCK induces growth cone collapse and axon guidance repulsion (Hall, 1998). Pharmacological or genetic ablation of these inhibitors have led enhance sprouting following spinal cord injury but to minimal or no regeneration without any functional recovery (Lee *et al.*, 2010, Schmandke and Strittmatter, 2007).

Reactive astrocytes, initiated after the injury, are known secrete various types of CSPGs (aggrecan, brevican, neurocan, phosphacan, versican and NG2) neutralization of which by chondroitinase ABC promoted regeneration of corticospinal axons to enhance regeneration (Morgenstern *et al.*, 2002, Bradbury *et al.*, 2002). Discovery of these extrinsic inhibitors and the possibility of enhancing regeneration following neutralization was a breakthrough in CNS regeneration research, but did not lead to functional recovery. This pointed to the crucial role intrinsic neuronal potential played in inducing regeneration and the focus switched to identifying the important endogenous regulators of neuronal potential.

Though the central hypothesis for limited CNS axonal regeneration has always been the inhibitory extrinsic environment, evidence from the past decade points towards lack of neuronal response after injury. This inability of neurons to excite a response can be attributed to locking the neuro-regeneration potential through maturation as well as the cascades initiated by injury could inhibit the neurons from responding (Liu *et al.*, 2011).

1.1.2 CNS regeneration- Identified Molecular Mechanisms eliciting a response

CNS regeneration potential, along with being dependent on external environment, is also dependent on and synchronized by the elicited neuronal gene expression of the extracellular and cellular signaling proteins, which remodel the cytoskeleton and alter axon growth cone activity and plasticity (Carmichael *et al.*, 2005, Tedeschi, 2011, Liu *et al.*, 2011).

Responses to the injury

Following an injury, the injured end of the axon reseals itself while the distal segment of the axons undergoes Wallerian degeneration (Fishman and Bittner, 2003, Schlaepfer and Bunge, 1973). Injured neurons then form a growth cone like structure or a retraction bulb and either initiate regenerative growth as observed in PNS or lead to dystrophic growth cones as seen in the CNS (Bradke *et al.*, 2012). Local cytoskeletal remodeling at the growth cone allows the axon to sprout or to retract away from the lesion site. Adult mammalian CST axons are known to form retraction bulbs after an axotomy and withdraw themselves away from the lesion site (Bernstein and Stelzner, 1983, Bregman *et al.*, 1989). Retrograde signals from the injury site induce chromatolysis in the cell body, severity of which depends upon the extent and distance of the lesion site from the cell body (Bradke *et al.*, 2012).

Development-dependent decline of axon growth ability

Seminal work by the Aguayo lab showed that embryonic neurons are able to regenerate in the inhibitory CNS environment suggesting that CNS neurons have a reduced capacity for axon growth (Brown *et al.*, 2009, Bernstein and Stelzner, 1983). Molecules like Bcl-2, KLFs and mTOR show a developmental dependent decline in Retinal ganglion cells and cortical spinal neurons (Park *et al.*, 2008, Moore *et al.*, 2009, Cho *et al.*, 2005). Down-regulation of these crucial players has led to the enhanced regeneration in the CNS. These evidences suggest that various pathways and molecules contribute to the development dependent decline of axonal growth ability of CNS neurons (Liu *et al.*, 2011).

Axon regenerative ability regulators in the mammalian CNS

Reactivating trophic responses:

Establishment of a concrete role of neurotrophins in axonal elongation and synaptogenesis during development hinted towards the possible positive role of trophic molecules in enhancing regeneration in the CNS (Reichardt, 2006, Zhou and Snider, 2006, Zweifel *et al.*, 2005). Growth promoting pathways have been re-activated in the injured CNS neurons by exogenous application of trophic molecules or overexpression of downstream signaling molecules (Leaver *et al.*, 2006). In the optic nerve system, CNTF enhanced the regeneration elicited by the RGCs along with increasing the survival while BDNF intra-vitreous application resulted only in higher survival rates (Smith *et al.*, 2009, Leaver *et al.*, 2006, Nakazawa *et al.*, 2002, Pernet and Di Polo, 2006). However, in the CST only NT-3 was able to initiate sprouting rostral to the lesion site but BDNF and NGF did illicit any effect in this system. Ectopic IGF delivery was able to increase the survival rates of CST neurons but did not affect the regeneration ability (Hollis *et al.*, 2009). Activation of the ERK pathways via the lent viral TrkB expression in cortical neurons led to higher sprouting which was shown to be dependent on Shc/FRS-2 activation domain of ERK (Hollis *et al.*, 2009). Overexpression of ERK1/2 promoted neuronal survival but failed to induce neuroregeneration (Pernet *et al.*, 2005).

Conditioning effect of a lesion in sensory neurons:

Conditioning lesion effect, discovered in the primary sensory neurons from the dorsal root ganglia (DRGs), has elucidated transcriptional mechanisms involved in PNS and consequently CNS regeneration. Conditioning lesion effect, prompted by injuring the peripheral branch of the sensory neurons leads to activation of the gene expression program in the neurons, priming them to have a boosted regenerative response in a subsequent PNS or CNS lesion (Oblinger and Lasek, 1984). In the visual system, a conditioning lesion effect is stimulated by lens injury or zymosan injection which leads to macrophage activation

(Fischer *et al.*, 2001, Leon *et al.*, 2000, Yin *et al.*, 2003). Macrophage activation induces the secretion of inflammatory factors with positive effects (eg: BDNF, IL-6, PDGF, GDNF) as well as negative effects (TNF- α and IL-1 β). Also, it leads to clearance of the inhibitory myelin associated debris along with activating the RGCs transcriptional response(Yin *et al.*, 2003). Hence, lens injury in the visual system or lesion to the peripheral branch in DRG system augments a recapitulation of development patterns of growth associated proteins (GAP43, CAP23, Sprrr1A and cytoskeletal associated proteins), up-regulation of transcription factors (ATF3, c-Jun, Sox11, Smad1), transcriptional regulators (p300, Smads, STAT3, SMARCC1, NF- κ B) along with polyamine synthesis enzyme arginase 1. All these genes together have been termed as regeneration associated genes and are elaborated further, along with a few known vital transcriptional pathways.

Transcriptional pathways involved CNS regeneration

Conditioning lesion model has shown numerous transcription factors and activators like C/EBP, CREB, ATF3, c-jun, KLF4 that directly or indirectly regulate axon outgrowth and regeneration(Herdegen *et al.*, 1997, Lane and Bailey, 2005, Makwana and Raivich, 2005, Raivich and Behrens, 2006). On this framework, cytokines ciliary neurotrophic factor (CNTF) and leukemia inhibitory factor (LIF) were investigated and found to be directly involved in eliciting a conditioning lesion response, since CNTF and LIF knockouts were unable to induce conditioning lesion effect after lens injury(Leibinger *et al.*, 2009). Purified exogenous cytokines were hoped to mimic the conditioning lesion effect but presented only a moderate response(Muller *et al.*, 2009, Leaver *et al.*, 2006). This elusive effect was explained by recent work showing suppressor of cytokine signaling (SOCS) proteins to limit the efficacy of cytokines in promoting regeneration. SOCS3 conditional deletion led to a higher regenerative response in RGCs following optic nerve crush(Smith *et al.*, 2009). Concurrent deletion of cytokine receptor gp130 and SOCS3 was found to interrupt this regenerative response explaining involvement of gp130 dependent pathway(Smith *et al.*, 2009). Failed regenerative

response of optic nerve axons in a PNS graft after viral overexpression of SOCS3 in RGCs, confirmed the role of this SOCS3 pathway(Hellstrom *et al.*, 2011).

CREB dependent transcription induced by specific PTMs regulates axon regeneration via Arginase I up regulation and polyamine synthesis, in the PNS as well as the CNS regeneration(Cai *et al.*, 2002, Gao *et al.*, 2004, Spencer and Filbin, 2004). Also, JNK/c-Jun transcriptional pathway might act as a sensor in response to nerve injury and is known to mediate nerve regeneration, though the response elicited in CNS regeneration by activation of JNK pathway was found to be highly context dependent(Raivich *et al.*, 2004, Carulli *et al.*, 2002).

Deletion of Phosphatase and tensin (PTEN) homolog leads to enhanced regeneration in the optic nerve as well as following spinal cord injury(Park *et al.*, 2008, Liu *et al.*, 2010). PTEN deletion accumulates PIP3, leading to activation of phosphatidylinositol dependent kinase, hence activating AKT. AKT activation was found to activate the mTOR pathway inducing the S6 kinase and Elf4 dependent transcription of genes for cell growth, resulting in axonal regeneration after optic nerve injury(Park *et al.*, 2010). But PTEN deletion was also found to activate TSC1, suggesting the role of more than one downstream pathway in enhancing regeneration(Park *et al.*, 2010).

KLF (Krüppel-like factor) mediated transcriptional pathway, already known to control cellular functions like cell cycle, proliferation, and cell death, also was recently found to regulate developmental axonal growth. Klf4, a transcriptional regulator and tumor suppressor, was also found to play a negative role in inhibiting CNS regeneration *in vivo*. Deletion of KLF4 specifically in RGCs using tissue specific conditional knockout system, led to higher regeneration after optic nerve crush injury(Moore *et al.*, 2009). KLF4 is also acts as a direct transcriptional repressor of p53(Rowland *et al.*, 2005).

P53 is ubiquitously expressed in the brain and the spinal cord and controls cell cycle regulation, apoptosis and has been recently identified to regulate neurite and axonal

outgrowth(Di Giovanni and Rathore, 2012). P53 has been lately shown to control axon outgrowth by transcriptional regulation mechanisms rather than spatial response at the growth cones of outgrowing axons(Di Giovanni *et al.*, 2006, Gaub *et al.*, 2010, Qin *et al.*, 2010b, Qin *et al.*, 2010a, Tedeschi *et al.*, 2009a). Analysis in the primary cerebellar and cortical neurons showed p53 to regulate genes associated with outgrowth and cytoskeletal remodeling, namely Coronin1b, Rab13 and GAP43(Di Giovanni *et al.*, 2006, Moore *et al.*, 2009). Additionally p53 was shown to be involved in the facial motor nerve regeneration by occupying GAP43 promoter, further strengthening the role of p53 in axonal regeneration(Fishman and Bittner, 2003). Posttranslational acetylation of p53 lysine residues K 320-372-3-82 by acetyl transferases p300 and P/CAF were credited for neuro regeneration observed post injury, giving an insight into the transcriptional mechanisms post injury in neurons(Moore *et al.*, 2009, Tedeschi and Di Giovanni, 2009)

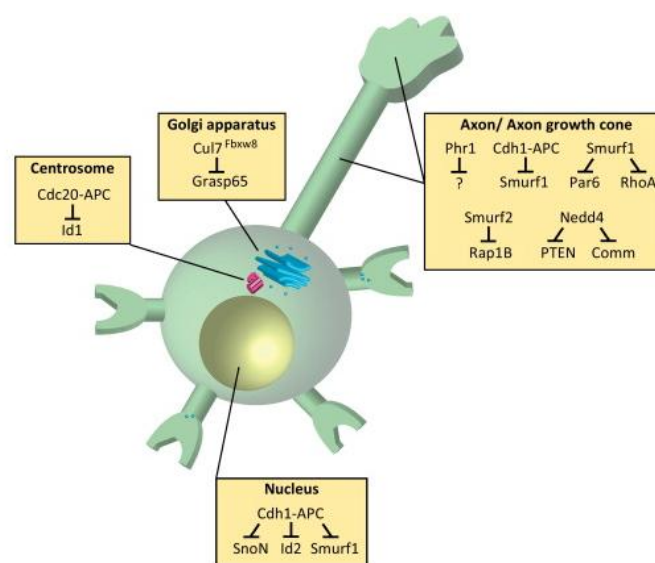
Transcriptional pathways converge upon regeneration associated genes (RAGs) which are involved in axonal outgrowth and path-finding during development, and their up-regulation is known to induce sprouting and axonal regeneration after injury. Proteins coded by RAGs belong to varied functional proteins families like cytoskeletal associated proteins (α -tubulin, MAP1a and MAP2)(Gloster *et al.*, 1994, Knoop and Octave, 1997), cell adhesion molecules (NCAM-L1CAM, TAG1) (Kamiguchi and Lemmon, 2000, Panicker *et al.*, 2003), the synaptic and extracellular matrix components (SNAP-25, cp15/neuritin) (Naeve *et al.*, 1997, Kimura *et al.*, 2003, Di Giovanni *et al.*, 2005) and growth associated proteins (SPRR1a, CAP-23 and GAP-43)(Caroni and Grandes, 1990, Aigner and Caroni, 1993, Aigner and Caroni, 1995).

Successful regeneration is hence a cumulative effect of appropriate transcriptional activation of pro-growth molecules and factors countering the growth cone collapse and repulsive guidance signals (Liu *et al.*, 2008). Understanding and enhancing the neuronal transcriptional response that boosts axonal outgrowth, sprouting and regeneration as well as

inhibit growth cone collapse will allow the de-encryption of the molecular mechanisms of the nervous system.

1.1.3 Ubiquitin Ligases and p53-related signalling in CNS regeneration

Vital cellular functions are dynamically regulated by the post-translational modifications of proteins, including ubiquitination which is mediated by ubiquitin ligases. Ubiquitin-activating enzymes (E1), ubiquitin activating enzyme (E2) and ubiquitin ligases (E3) effect the ATP-dependent covalent linking of 76-amino acid ubiquitin moiety to protein residues. Ubiquitinated proteins are recognized by cellular machineries like endosomal sorting complex, DNA repair complex and ubiquitin proteasome enabling processes such as protein localization and degradation, cell proliferation and differentiation and apoptosis. Different E3 ubiquitin ligases are localized to distinct subcellular compartments in neurons and play critical roles in neuronal morphogenesis and connectivity. The nucleus, centrosome, Golgi apparatus, axon and dendrite cytoskeleton, and synapse are main milieus for E3 ubiquitin ligase function in neurons. APC (E3 RING finger) protein complex activators Cdh1 and Cdc20 are highly expressed in the developing brain, overlapping with the axon and dendrite morphogenesis and synaptogenesis phases (Konishi et al., 2004, Kim et al., 2009).



TRENDS in Neurosciences

Figure 2: E3 ubiquitin ligases localized to distinct subcellular compartments control neuronal morphogenesis. E3 ubiquitin ligases operate in the nucleus, centrosome, Golgi apparatus, and axon and dendrite cytoskeleton in neurons. This figure summarizes the role of various ubiquitin ligases and their spatial control in regulating neuronal functions.

Nuclear E3 ubiquitin ligase complex Cdh1–APC regulates SnoN, Id2 and Smurf thereby controlling axon growth and patterning in cerebellar cortex granule neurons. On the other hand, centrosomal E3 ubiquitin ligase complex, Cdc20–APC, targets Id1 for degradation to induce dendrite growth and arborization of granule neurons in the rat cerebellar cortex. Along with this function, Cdh1–APC may also act in the cytoplasm to regulate Smurf1 levels to inhibit axon growth. Ubiquitin ligase Smurf1 and Smurf2 operate locally at the axon to regulate neuronal polarity by degrading Par6 and RhoA (Cheng et al., 2011, Schwamborn et al., 2007, Wang et al., 2003). Another E3 ubiquitin ligase Nedd4 functions at the axon growth cone to ubiquitinate the proteins PTEN and Comm in the control of axon morphogenesis. It is worth noting that the ubiquitin ligases are negatively regulating target implicated in molecular mechanisms controlling axonal regeneration.

Ubiquitin ligases MDM2 and ubiquitin ligase like protein MDM4 negatively regulate transactivation of p53. Recent work from our laboratory has shown tumour suppressor and transcription factor p53 to be required for neurite outgrowth, axonal sprouting and

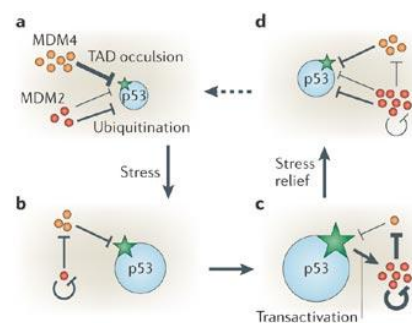


Figure 3: p53 regulation by MDM2 and MDM4 explained in a dynamic model. a. This figure describes the p53 response in an unstressed cell and after stress. MDM2 (orange circle) ubiquitinates p53 (blue circle, star signifies activity and size of circle shows amount of p53) while MDM4 binds to the transcriptional activation domain (TAD) inhibiting transactivation. b. After stress, MDM2 degrades itself and MDM4, leading to the accumulation and activation of p53, mounting a transcriptional response. c p53 transactivation leads to MDM2 expression, the increasingly abundant MDM2 degrades MDM4 more efficiently, enabling full p53 activation. d The accumulated MDM2 preferentially targets p53 again and p53 levels decrease, and as MDM4 levels increase, p53 activity also decreases. The switch that makes MDM2 preferentially target p53 for degradation in unstressed cells (a), then target itself and MDM4 after stress (b and c), and target p53 again after stress relief (d) is not precisely understood. (Toledo and Wahl, 2006)

regeneration both after facial nerve injury and spinal cord injury in mice (Tedeschi *et al.*, 2009a, Floriddia *et al.*, 2012, Tedeschi and Di Giovanni, 2009, Tedeschi *et al.*, 2009b, Di

Giovanni *et al.*, 2006). Transcriptionally active p53 acetylated at K372-3-82 forms a transcriptional complex with acetyl transferases CBP/p300 and P/CAF that occupies promoters of selected RAGs, leading to neurite outgrowth(Tedeschi, 2011, Gaub *et al.*, 2010). Numerous stress signals following axonal injury converge on p53, which is tightly regulated at its protein levels and subcellular localization(Di Giovanni *et al.*, 2005, Di Giovanni, 2009). As already stated, transcriptional activity of p53 is regulated by many factors, including the well-defined negatively regulators MDM2 and MDM4. MDM2, a E3 ubiquitin ligase, targets p53 for degradation via the ubiquitin proteasome pathway and negatively regulates p53 cytoplasmic-nuclear shuttling. MDM4 is structurally similar to MDM2 but is devoid of ubiquitin ligase function but occupies p53 transcriptional activation domain thereby inhibiting its transactivation. MDM4 prevents p53 nuclear translocation in association with MDM2 and competes with the acetyl transferases CBP and p300 for binding to lysines on p53 C-terminus, overall hindering p53 transcriptional activity (Markey, 2011, Toledo and Wahl, 2006, Francoz *et al.*, 2006).

Therefore we investigated whether disruption of MDM4-MDM2-p53 interaction would affect the axonal regeneration. The key results obtained by genetic and pharmacological inhibition of MDM4 or MDM2 specifically in RGCs have been summarized in the next section (Section: 1.1.4).

1.1.4 CNS regeneration and ubiquitin ligases

As described already, lack of neuronal intrinsic regenerative response after CNS axonal injury might be credited to the inhibitory molecular environment, which exists prior to axonal injury or is elicited and/or empowered by the signalling cascades initiated by the injury. Post-translationally modified proteins/transcription factors and enzymes involved in these modifications play an important role in controlling the molecular environment of the neurons, during development and post-maturation. Ubiquitin ligases and ubiquitin ligase like proteins coordinate neuronal morphogenesis and connectivity both during development and after axonal injury. They mediate the turnover, localization and activity of a number of crucial proteins and transcription factors involved in the axonal regeneration program, including PTEN, p300, KLFs, Smads, p21 and p53(Yamada *et al.*, 2013).In fact, a newly identified E3 ubiquitin ligase Pirh2 was found to induce degeneration of distal segment of injured axons, via NMDA2. All this evidence makes strong case for modulation of ubiquitin ligases *in vivo* to investigate their role in controlling the molecular environment following injury. Such proteins in conjunction with their regulators like ubiquitin ligases may represent a signalling hub synchronizing the post-injury regenerative neuronal response. Despite the appreciation of role of these indirect but decisive components in modulating the neuronal morphogenesis, connectivity during development and after injury, their role in regulation regeneration in injured post-mitotic neurons remains unanswered. MDM4, an ubiquitin ligase like enzyme, forms inhibitory protein complexes with at least four key proteins involved in the axonal outgrowth program: Smad1/2, p300, p53 and MDM2 (Markey, 2011, Kadakia *et al.*, 2002). MDM4 expression is regulated during development in the retina and reaches its maximal levels upon maturation in adults, possibly keeping the post-injury RGC growth expression program under control.

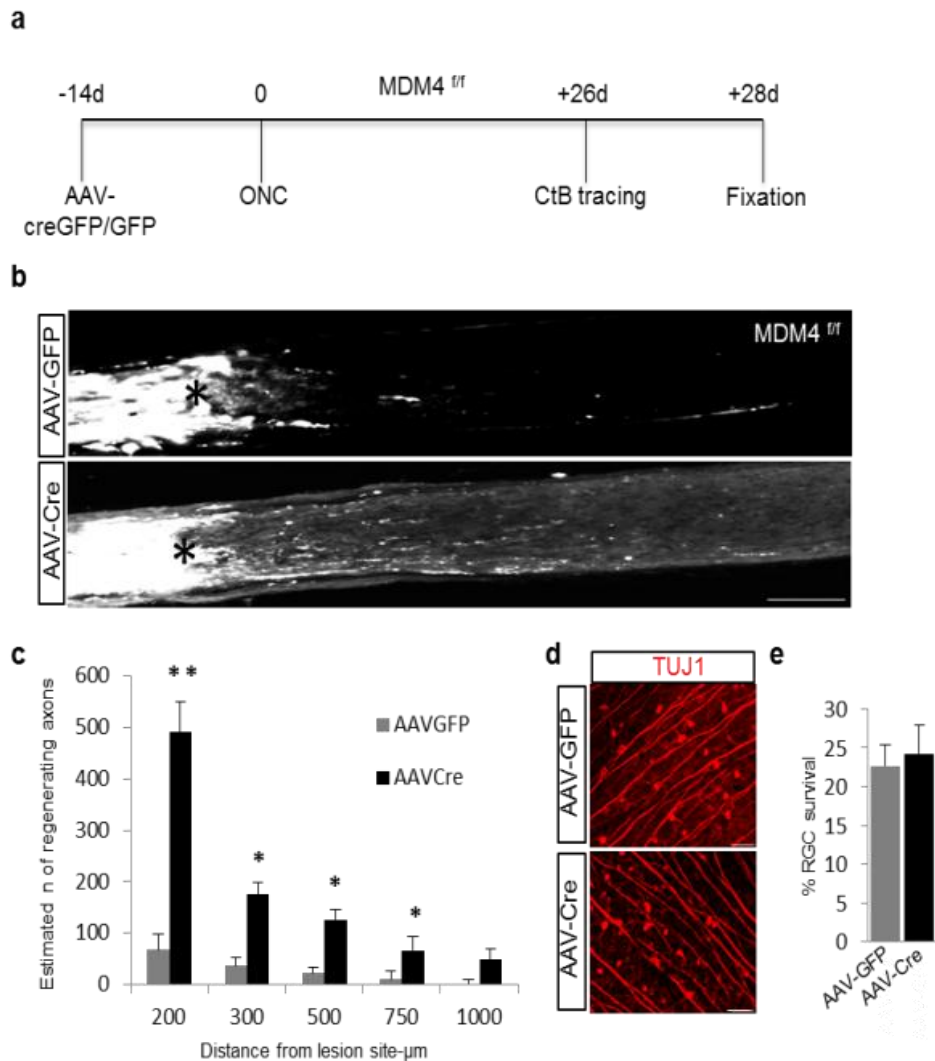


Figure 4. Conditional deletion of MDM4 in retinal ganglion cells enhances axonal regeneration after optic nerve crush. **a.** Schematic of the experimental design showing AAV-Cre or AAV-GFP intra-vitreous infection of RGC in MDM4^{fl/fl} mice 14 days before optic nerve crush. Regenerating axons were traced with Cholera toxin B (CtB). **b.** High magnification images of regenerating CtB labeled optic nerve axons 28d post-crush (asterisk) in MDM4^{fl/fl} mice after infection with AAV-Cre or AAV-GFP. Scale bar 100 μm. **c.** Quantification of regenerating optic nerve axons post-crush (experiment as in b). At least 4 serial sections were analysed from each animal (Student t-test, *p< 0.05 or **p<0.01 n= 7, each group). **d.** Anti-Tuj1 immunofluorescence shows surviving retinal ganglion cells (Tuj1+) 28 days post-optic nerve crush. Scale bar 50 μm. **e.** Quantification of surviving RGC as total percentage of surviving cells as compared to the intact contralateral retina (n=7, AAV-Cre infected animals; n=6, AAV-GFP infected animals).

MDM4 hence is an appealing target to be modulated in the injured CNS. Therefore, we wanted to define the role of MDM4-MDM2/p53 pathway via genetic ablation of MDM4 specifically in RGCs. MDM2 was pharmacologically inhibited by Nutlin-3a, a drug that inhibits

the binding of p53 and MDM2 and stabilises p53. We performed conditional deletion of MDM4 specifically in RGC by intra-vitreous injection of AAV2-CreGFP virus in $MDM4^{fl/fl}$ mice two weeks before ONC, while an AAV2-GFP vector was employed as control (Fig. 4a). AAV2 infects RGCs very efficiently and rather specifically due to physical proximity although about 10% of other neuronal populations can also be infected. Significantly, MDM4 deletion promoted robust axonal regeneration of the optic nerve as measured 28d after ONC (Fig. 4b, c), while it did not affect RGC survival (Fig. 4d, e). Concomitant deletion of p53 and MDM4,

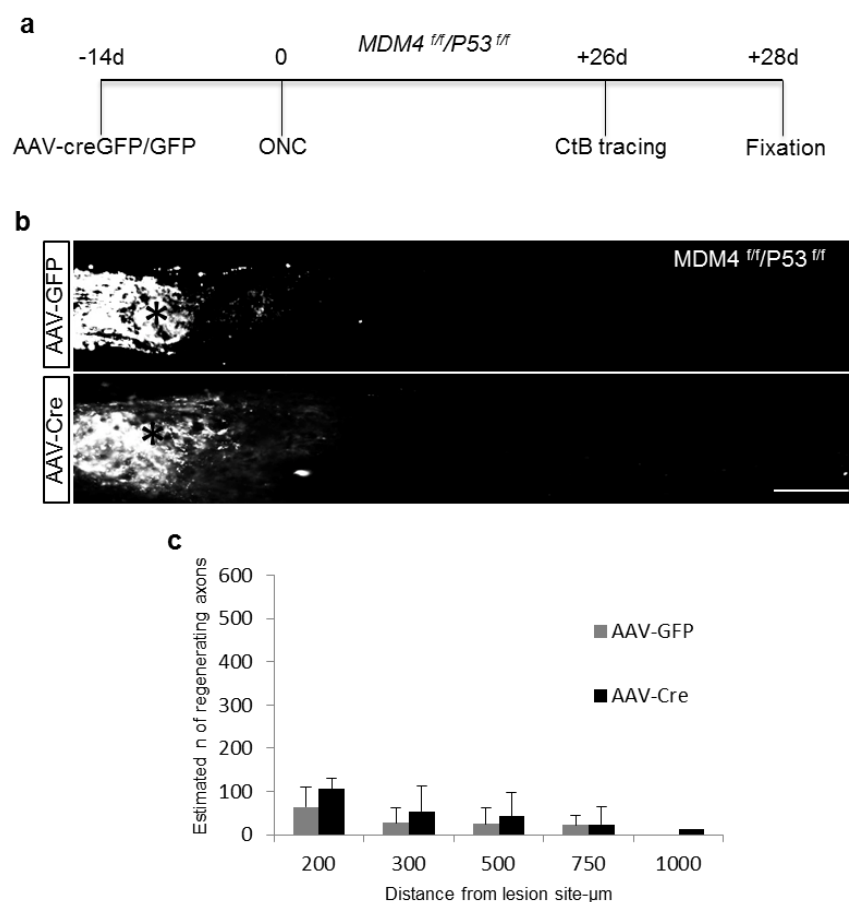


Figure 5: Conditional co-deletion of MDM4 and p53 does not lead to axonal regeneration

a. Schematic of the experimental design showing AAV-Cre or AAV-GFP intra-vitreous infection of RGC in $MDM4^{fl/fl}p53^{fl/fl}$ mice 14 days before optic nerve crush. Regenerating axons were traced with Cholera toxin B (CtB). **b.** Representative images of CtB labelled optic nerve axons from $MDM4^{fl/fl}p53^{fl/fl}$ mice infected with AAV-CreGFP/AAV-GFP. No regenerating axons were observed past the lesion site (asterisk). Scale bar 100 μ m. **c.** Quantification of CtB labelled axons regenerating past the lesion site. At least 4 serial sections were analyzed from each animal (n=5, AAV-CreGFP group, n=4, AAV-GFP).

abrogated the regenerative effect suggesting a role of p53 dependent pathways in enhancing regeneration after MDM4 deletion (Figure 5a,b). MDM4 interacting proteins p300 and Smads have already been described to have a pro-neurite outgrowth and axon regeneration function and hence p300 dependent acetylation of regenerative promoters as well as TGF β -Smad signalling could possibly play a role (Gaub *et al.*, Zou *et al.*, 2009, Parikh *et al.*). This is further supported by the fact that p300 acetylates p53 in RGC after ONC during p300-dependent axonal regeneration, assisting the presence of this signalling network during

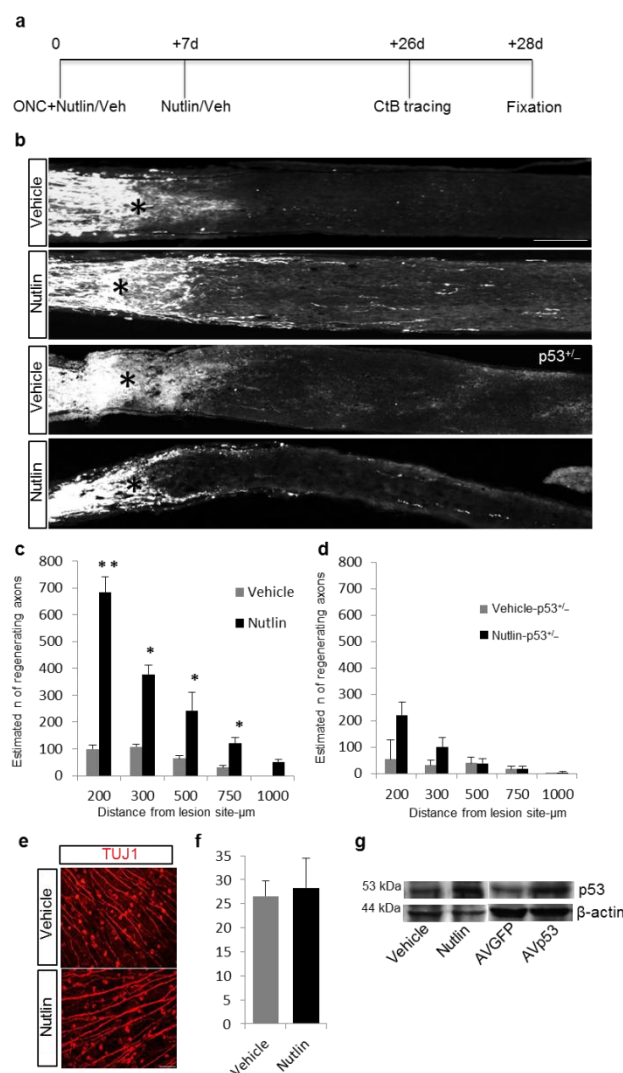


Figure 6: Inhibition of MDM2/p53 interaction enhances axonal regeneration after optic nerve crush. **a.** Schematic of the experimental design showing intra-vitreous injection of Nutlin-3a (100nM). **b.** Regenerating CtB labeled optic nerve axons 28d post-crush (asterisk) in Nutlin treated wildtype mice. Scale bar 100 μ m. **c.& d.** Quantification of regenerating optic nerve axons post-crush (experiment as in b). At least 4 serial sections were analysed from each animal (Student t-test, * $p < 0.05$ or ** $p < 0.01$ for each distance, $n = 7$, each group). **e.** Anti-Tuj1 immunofluorescence shows surviving retinal ganglion cells (Tuj1+) 28 days post-optic nerve crush. Scale bar 50 μ m. **f.** Quantification of surviving RGC as total percentage of surviving cells as compared to the intact contralateral retina ($n = 7$, Nutlin; $n = 6$, vehicle). **g.** Immunoblotting from retinas treated with vehicle or Nutlin (100nM) at the time of ONC, 3 days post-ONC. Nutlin enhances P53 expression.

axonal regeneration(Gaub *et al.*, 2011). MDM4 also forms a complex with p21, whose function in axon regeneration and sprouting has been previously described(Tanaka *et al.*, 2004),(Markey). P21 being a p53 target gene may also play a role in axonal regeneration. P21 and classical regeneration associated genes expression was enhanced after MDM4 deletion in primary neurons, corroborating inhibitory role of MDM4 in limiting the regenerative gene expression program. While MDM4 controls the transcriptional activity of p53, MDM2 controls the stability by ubiquitinating and targeting it for proteasomal degradation(Toledo and Wahl, 2006).

To stabilise p53, we employed a small molecular MDM2 antagonist Nutlin-3a, which competes for the p53 binding site(Vassilev *et al.*, 2004). Intravitreal administration of Nutlin-3a(100nm) on the day of the crush and 7 days later was able to enhance axonal regeneration after optic nerve crush, mounting a response similar to MDM4 deletion (Figure 6a,b,c) cell survival rate did not change (Figure 6c,d). Axonal regeneration of the optic nerve axons after crush was significantly reduced in Nutlin-3a treated p53^{+/-} mice as compared to wildtype (Figure 6b,d). These results further support the overall model where regeneration after deletion of MDM4 and inhibition of MDM2 both depend upon p53 transactivation.

To further dissect in to the molecular pathways that might be modulated after MDM4 deletion specifically in RGCs, we performed a genome wide analysis from FACS sorted pure RGCs, by injecting a fluorescent retrograde tracer in the superior colliculus thus tracing specifically RGCs. This assay revealed that MDM4 conditional deletion was accompanied by the expression of transcripts involved in cytoskeleton remodelling, axonal development and signalling, including genes involved in neuronal maturation (Table 1). This very elegantly suggests that MDM4 deletion modulates developmentally regulated pathways, which may support axonal regrowth. Along with controlling these complex development pathways, MDM4 deletion triggered optic nerve regeneration via IGF1R signalling. IGF1R inhibition using an established antagonist picropodophyllin (1µm) annulled regeneration, observed

after MDM4 deletion, confirming the role of IGF1R signalling (Girnita *et al.*, 2004) (Figure 7b,c).

Table 1: List of selected differentially regulated genes from RGC after ONC in MDM4^{fl/fl} mice- AAV *Cre* vs *GFP*

<i>Functional Class</i>	<i>Fold change (Cre vs GFP)</i>	<i>p value</i>	<i>Function</i>
<u>Axonal signalling</u>			
IGF1R	2,12	0,0122	Intracell signalling
CXCR2	2,18	0,0222	Chemoattraction
Klf11	1,764	0,0391	Axonal transport
Cited4	1,69	0,0324	Transcription co-activ
Spr2b	1,866	0,004	Axon growth
<u>Neuronal morphology and cytoskeleton organization</u>			
DCC	-2,031	0,0476	Axon guidance
GAD1	1,569	0,0365	Glut/GABA metab
Arf1	3,505	0,02	GTP-bind prot
FCER1A	1,71	0,018	IgE rec
NKX2-2	-1,66	0,014	NeuroD1-cofact
Nrg1	-1,84	0,006	Neuronal differ
Rab23	1,516	0,01	GTPase
Rin2	1,797	0,029	GTPase
Mast3	-1,797	0,043	Microtub ass kinase
<u>Neuronal development</u>			
GAD1	1,569	0,0365	Glut/GABA metab
CAMKK2	1,595	0,004	CREB activator
ZIC1	1,632	0,0385	Transc Activ-Neurogenesis
ZNF423	1,762	0,0226	Smad coact-Neurogenesis
LYNX1	2,222	0,0004	Synaptic plasticity
ST8SIA2	1,683	0,02704	NCAM1 binding protein-rec
DCC	-2,031	0,0476	Axon guidance

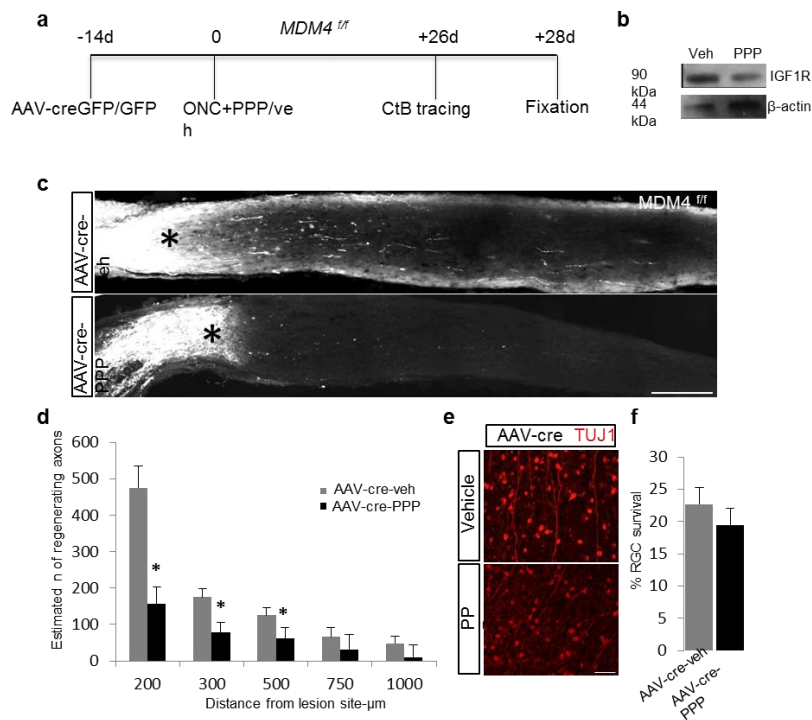


Figure 7 : Regeneration elicited by MDM4 deletion is reduced by inhibition of IGF1R signalling. **a.** Schematic of the experimental design. Conditional MDM4 deletion in MDM4^{fl/fl} mice was followed by ONC and pharmacological inhibition of IGF1R with the antagonist picropodophyllin (PPP). Axonal tracing was performed with CtB. **b.** Immunoblotting from retinæ 3d after ONC and administration of PPP or vehicle. Shown is a strong reduction in the expression of IGF1R. **c.** Representative images of optic nerves showing regenerating CtB labelled axons of MDM4^{fl/fl} animals after MDM4 conditional deletion and vehicle. Not a significant number of regenerating axons were found after PPP administration post-ONC (asterisk). Scale bar 100 μ m. **d.** Quantification of regenerating optic nerve axons post-crush (experiment as in c). At least 4 serial sections were analysed from each animal (Student t-test, $p < 0.05$ for each distance, $n = 6$, each group). The number of regenerating axons was significantly hampered following AAV-cre-PPP treatment versus AAV-cre-veh. **e.** Anti-Tuj1 immunofluorescence shows surviving retinal ganglion cells (Tuj1+) 28 days post-optic nerve crush. Scale bar 50 μ m. **f.** Quantification of surviving RGC as total percentage of surviving cells as compared to the intact contralateral retina ($n = 6$).

The best characterized IGF1R targets include PI3K and JAK/STAT3, which are typically activated by IGF1R (Kim *et al.*, 2012, Subbiah *et al.*, 2011, Staerk *et al.*, 2005, Serra *et al.*, 2007). Both PI3K and JAK/STAT3 activation is dependent upon phosphorylation of specific residues that has been shown to be necessary to promote axonal regeneration following deletion of PTEN or after JAK binding to IL-6 respectively (Park *et al.*, 2008, Cao *et al.*, 2006, Shah *et al.*, 2006, Teng and Tang, 2006, Hakkoum *et al.*, 2007). This points to a likely engagement of MDM4-MDM2/p53-IGF1R signalling and related regenerative pathways, supporting the importance of our novel findings. In this study focussing on the ubiquitin ligase

proteins, we have identified MDM4-MDM2/p53 as a regeneration-repressive protein complex, whose disruption activates the axonal regenerative program via IGF1R signalling. Discovery of MDM4-MDM2/p53-IGF1R signalling pathway helps in de-encrypting the causes for failed regeneration and may provide a target for regenerative therapy, after CNS insult. Genetic ablation of MDM4 or pharmacological inhibition of MDM2-p53 interaction has been conclusively shown to induce tumour suppression and are currently in trials for cancer treatment (Brown *et al.*, 2009). The recent discovery of specific small molecule inhibitors of MDM4 (Vogel *et al.*, 2012, Reed *et al.*, 2010) which are still awaiting confirmation in multiple studies, may also expand our regenerative therapeutic options.

1.1.5 Role of histone acetyl transferases p300 and P/CAF in CNS regeneration

Gene expression is regulated by transcription, tightly controlling the neuronal intrinsic capacity to synthesize new proteins necessary for mounting a pro-axonal regeneration signaling. Indeed, transcriptional regulation controls axonal outgrowth during development as well as axon regrowth after injury in the adult (Butler and Tear, 2007, Goldberg *et al.*, 2002, Raivich *et al.*, 2004, Moore *et al.*, 2009). Post-injury extrinsic signals are assembled to determine the intrinsic response of the cell. Modulation of these signaling pathways is sufficient to promote axonal outgrowth without additional inhibition of the inhibitory environment. In this work, we have attempted to determine if the pro-regenerative transcriptional machinery is repressed in adult CNS neurons post-maturation and injury. Gene expression is determined by the state of chromatin as well as by the occupancy of specific transcriptional complexes near gene promoters. The state of chromatin and the activity of transcription factors contributes to the fine-tuning of gene expression which is regulated by histone acetyl transferases and histone deacetylases. HATs and HDACs regulate and maintain a balance between the level of histone and transcription factor acetylation (Yang and Seto, 2007). Chromatin relaxation and transcription factor activation via histone deacetylases inhibition by trichostatin A enhances neurite outgrowth on permissive and non-permissive substrates. Specifically, this was due to an increased expression of the histone acetyltransferases CBP/p300 and p300/CBP-associated factor (P/CAF) that enhanced acetylation of H3 and p53, which stimulated the expression of several proregenerative genes (Tedeschi and Di Giovanni, 2009, Tedeschi *et al.*, 2009a, Gaub *et al.*, 2010). However, this work described the role of histone acetyltransferases in axonal regeneration *in vitro* and we have here investigated its role *in vivo*.

In the present study, we investigated the regulation and expression of HATs- p300, CBP and P/CAF- and their role in retinal ganglion cell maturation. Indeed, histone acetylation and the expression of CBP and p300 are repressed in mature retinal ganglion cells and after optic nerve crush and hence were potential candidates to test in the ability of retinal ganglion cells to regenerate axons following optic nerve crush (Figure 8).

Overexpression of p300 but not histone deacetylases inhibition, promotes axonal regeneration after optic nerve crush (Figure 9 C, D). P300 leads to hyperacetylation of histone H3 and the transcription factors p53 and C/EBP, as well as increased p300 occupancy and H3 acetylation of selected pro-axonal outgrowth gene promoters.

Furthermore, p300 overexpression along with a conditioning lesion boosted the axonal

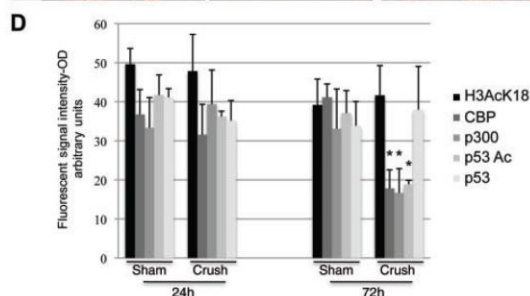
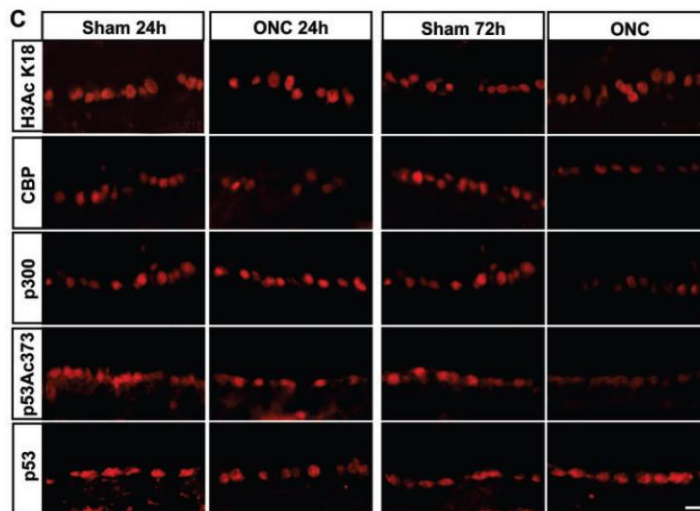
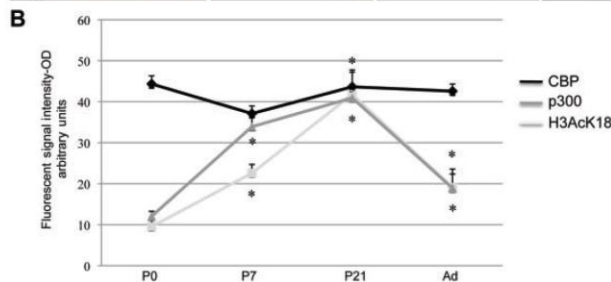
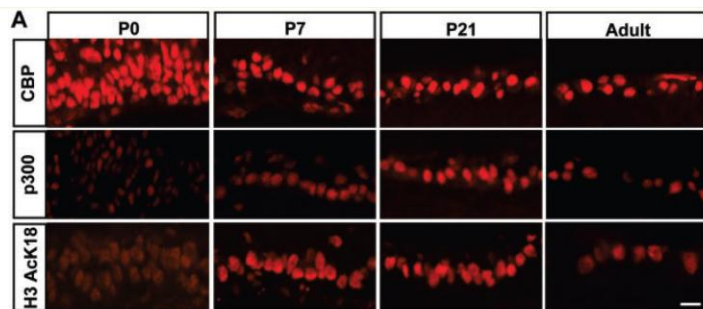


Figure 8: Maturation and optic nerve crush are associated with decrease in expression of histone acetyltransferase p300 in the retinal ganglion cell layer.

A. Representative pictures of RGC layer at different time points during the RGC maturation stained against CBP, p300 and H3K18, Scale bar 20µm. B. The level of protein was analyzed by analysis of fluorescence intensity and represented arbitrary units. and a decrease in adult, whereas CBP expression was not altered. P300 and H3 AcK18 level show a similar expression pattern during RGC maturation (n=3). Asterisks = unpaired two-tailed t-test, *P-value0.01; n=3. Each average value per time point was measured against the average value of all time points together.(C)RGC layer stained against H3 AcK18, CBP, p300, p53 Ac373 and p53, 24 h and 72 h after optic nerve crush compared with sham. No change is observed for H3K18 acetylation at either 24 h or at 72 h after optic nerve crush compared with sham, whereas a decrease of p300 and CBP expression is shown along with a decrease of p53 Ac373, while p53 basal level was stable. Scale bar = 20 um. (D) The graph represents quantification of the protein level obtained by measurement of the fluorescence signal.

Asterisks=unpaired 2-tailed t-test, *P-value0.01; n=3. Error bars represent SD. OD=optical density.

regeneration (Figure 9 C, D). This for the first time shows that specific modification of epigenetic environment can promote axonal regeneration *in vivo*, likely by redirecting the transcriptional program on pro-regeneration promoters.

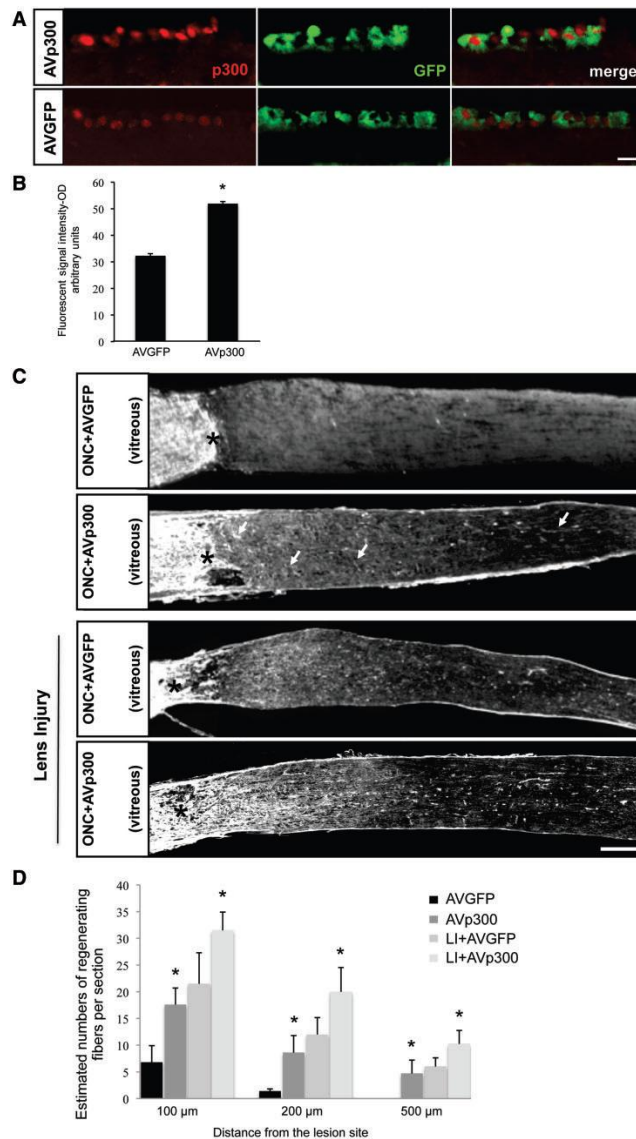


Figure 9. p300 over-expression by adenovirus infection induces axonal regeneration of the optic nerve. (A) Representative pictures of RGC layer after immunostaining in the retina against p300 shows expression of p300 in green fluorescence protein (GFP)-positive cells 24 h after optic nerve crush (ONC) and AVp300 or AVGFP infection. An increase of p300 expression in the retinal ganglion cell layer is shown following AVp300-GFP versus AVGFP infection. Scale bar 20 μm. (B) Bar graph represents quantification of p300 protein levels analyzed by measurement of the fluorescence signal. Asterisks = unpaired two-tailed t-test, *P-value 0.01; n=3. (C) Representative pictures of longitudinal optic nerve sections immunostained against GAP-43 14d after optic nerve crush and infected with AVGFP or AVp300-GFP (alone or in combination with lens injury) show axonal regeneration in AVp300-infected rats, which is enhanced by lens injury. Scale bar = 100 μm. (D) Adenoviral overexpression of p300 alone or in combination with lens injury induces a significant increase in the number of axons past the lesion site compared with AVGFP-infected nerves alone or in combination with lens injury as shown in the bar graph (n = 4 per condition). Asterisks = unpaired two-tailed t-test, *P-value < 0.05. Error bars represent SD.

This study further highlights the need for an intrinsic response to be elicited by neurons after injury. Hyper acetylation of histones results in euchromatin, a higher transcription permissive state of the chromatin (Berger, 2007, Fraser and Bickmore, 2007). Hyperacetylation of histones can be induced by pan-HDAC inhibitors like Trichostatin A, which inhibits the activity of class I and II HDACs (Saha and Pahan, 2005). In our study, treatment of RGCs with TSA increased the survival of RGCs but did not induce regeneration after ONC. Pan-HDAC inhibition leads to an overall hyper-acetylation of histones and hence it is not possible to predict which gene would be induced in response to the treatment (Saha and Pahan, 2006, Dokmanovic *et al.*, 2007). Hence to have a more specific epigenetic modulation, we chose to virally overexpress p300 in RGCs. P300 is a transcriptional coactivator and histone-modifying enzyme, thus contributing to epigenetic changes responsible for enhanced transcriptional activity (Ogryzko *et al.*, 1996). We had also recently reported that overexpression of CBP and p300 was able to promote neurite outgrowth on permissive and inhibitory myelin substrates in primary cerebellar neurons (Gaub *et al.*, 2010). Here, in vivo overexpression of p300 in RGCs led to higher axonal regeneration after optic nerve crush. This could be due to p300-dependent hyper-acetylation of histone H3, and of the promoters of several regeneration-associated genes leading to their expression. p300 overexpression also led to acetylation of p53 and C/EBP, which have been implicated in regeneration. Acetylation of p53 at lysine residue 373 been previously shown to promote neurite outgrowth in primary neurons and to be a hallmark of active p53 that is required for axonal regeneration (Tedeschi *et al.*, 2009; Gaub *et al.*, 2010). Acetylation of C/EBP enhances its transcription potential and has been shown to be induced in retinal ganglion cells after conditional lesion mediated axonal regeneration, and has been shown to be necessary for axonal regeneration in the PNS (Nadeau *et al.*, 2005). All this data points to scenario where in p300 may initiate a silent pro-regenerative gene expression program by driving the expression of several regeneration-associated genes by promoting transcription.

Along with p300, we also studied the role of another histone acetyl transferase in controlling the transcriptional response mounted by dorsal root ganglia after conditioning lesion. Conditioning lesion as already mentioned induces strong transcriptional response in which several modulators have been identified. But, a broader transcriptional regulator was not identified until date. Studying dorsal root ganglia (DRG) after a sciatic nerve axotomy (SNA), showed an increase in P/CAF dependent acetylation of RAG promoters, along with a reduction of H3K9Me2, suggesting a unifying role for P/CAF in enhancing transcription.

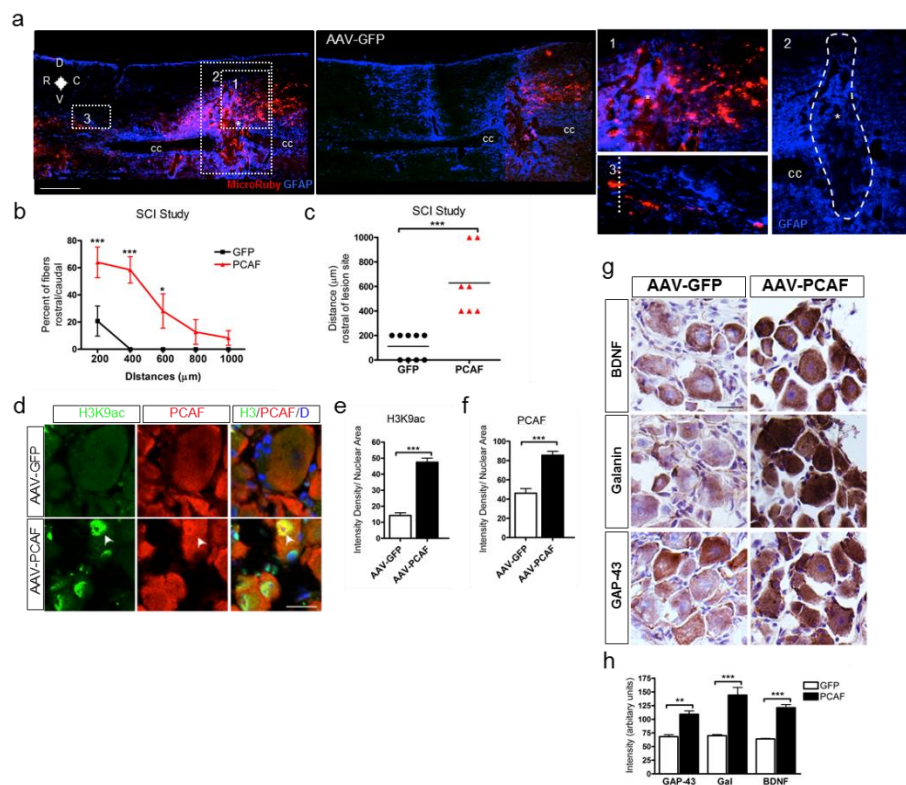


Figure 10: PCAF overexpression induces spinal axonal regeneration and expression of RAGs. **a**, MicroRuby tracing of the dorsal columns shows regenerating fibers invading into and past the lesion site after AAV-PCAF overexpression (upper right) versus a control AAV-GFP virus (upper left). Insets show higher magnification of regenerating axons. D-R-C-V: anatomical coordinates, dorsal-rostral-caudal-ventral. **cc**: central canal. Scale bar, 250μm. **b**, Quantification of regenerating axons, N = 9 (AAV-GFP), N = 7 (AAV-PCAF), **c**, Quantification of longest regenerating axon per animal from PCAF overexpression SCI study and conditioning SCI study with PCAF $-/-$ mice shows PCAF is required for regeneration from a conditioning lesion which can be mimicked by PCAF overexpression. **d-f**, Overexpression of AAV-PCAF in the SCI study promotes H3K9ac (8 weeks post-infection) (arrowheads) as shown by IHC (**d**). Nuclear intensity density analysis of H3K9ac (**e**) and PCAF (**f**) show enhanced PCAF and H3K9ac after PCAF overexpression. **g,h**, IHC RAG analysis of corresponding L4-L6 DRGs from infected AAV-PCAF and AAV-GFP animals show an increase in GAP-43, Galanin and BDNF expression, IHC (**g**) and DAB intensity analysis (**h**). Scale bars, 25μm. Error bars, s.e., (**b**) Welch's t -test, * $P < 0.05$, ** $P < 0.01$ and *** $P < 0.001$. (**c, h**) $P < 0.0001$, ANOVA, Bonferroni post-hoc tests, ** $P < 0.01$ and *** $P < 0.001$, (**e, f**) Student's t -test, *** $P < 0.001$, N = 3, performed in triplicate.

Viral P/CAF overexpression in dorsal root ganglia also showed an increase in fibers across CNS lesion and up to a distance of 1 mm rostral of the lesion site (Figure 10 a-d). To test if P/CAF overexpression is also able to modulate regeneration in another CNS model, optic nerve crush, we delivered P/CAF to RGCs using AAV1 virus followed by optic nerve crush.

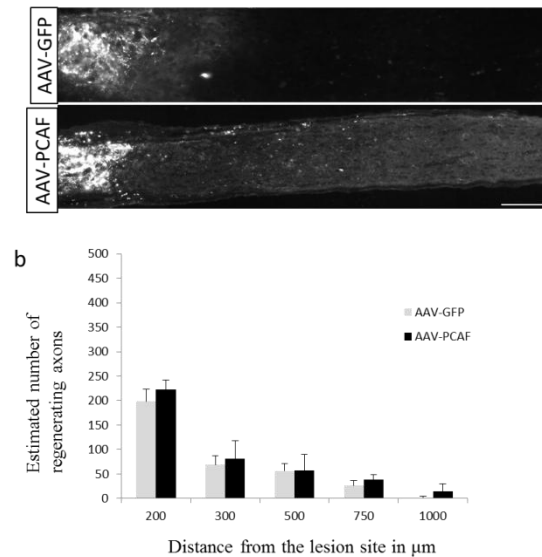


Figure 11: P/CAF overexpression in RGCs using AAV1 does not induce axonal regeneration in optic nerve axons after optic nerve crush. a Representative pictures of longitudinal optic nerve sections traced using fluorescently labeled cholera toxin subunit B (CTB), 28 days after optic nerve crush and infected with AAV1-GFP or AAV1-P/CAF show no axonal regeneration. Scale bar = 100 μm. b. Quantification of regenerating optic nerve axons post-crush. At least 4 serial sections were analysed from each animal (n= 6, each group). The number of regenerating axons after AAV-P/CAF infection did not increase regeneration

But this approach failed to induce any effect even after 28 days in this system, which could be explained due to lesser infection efficiency of AAV1 for RGCs (Figure 11 a, b). Employment of AAV2 to target RGCs might induce a higher expression in RGCs and might induce better regeneration.

Hence, this work shows that P/CAF is required for conditioning-dependent spinal regeneration and the overexpression of P/CAF is also able to promote regeneration of sensory fibers after spinal cord injury. Moreover, P/CAF induced regeneration also led to a significant increase in H3K9 acetylation levels along with expression of GAP-43, Galanin and BDNF in the L4-L6 DRGs. Peripheral axonal injury leads to cascade of events which also

includes a rise in cAMP levels and phosphorylation of multiple players involved transmitting information to the cell body (Bradke *et al.*, 2012, Hanz and Fainzilber, 2006, Rishal *et al.*, 2010). These signals are transmitted to the cell body via retrograde transport machinery (Hanz *et al.*, 2003, Perlson *et al.*, 2005, Yudin *et al.*, 2008, Shin *et al.*, 2012), but the mechanisms translating these signals into gene expression inhibition are unknown. Expression of key axonal regeneration players, such as RAGs, is inhibited after injury but no mechanism has been shown until date that mediates the injury-triggered signals and chromatin remodeling. Here, for the first time we show that after a PNS injury (SNA), PCAF is activated by phosphoERK. This leads to translocation of PCAF to the nucleus and acetylation of H3K9 as well as increased PCAF and H3K9ac at the promoters of GAP-43, Galanin and BDNF. We observed that PCAF epigenetically communicates RAGs and induction of these genes is sufficient to simulate the regeneration response seen after a conditioning lesion. In fact, PCAF overexpression has been shown to induce higher regenerative ability than overexpression of single RAGs or transcription factors (Buffo *et al.*, 1997, Bomze *et al.*, 2001, Gao *et al.*, 2004, Seijffers *et al.*, 2007). Hence here we have attempted to decode the complex epigenetic changes that occur to chromatin surrounding RAGs following a PNS injury. Hence in this study we shed light on the epigenetic scenario existing after neuronal injury and this hints towards the development of epigenetic-related regenerative therapies for SCI patients.

1.2 Concluding remarks and outlook

Extensive research in the last decade has helped in understanding the complex scenario after a CNS injury. In spite of these advances, our knowledge about the cellular and molecular mechanisms controlling neuroregeneration in the adult CNS is still quite limited. Though many pathways have been shown to be involved in neuroregeneration, therapeutic optic targeting druggable pathways are still not known.

This work identifies ubiquitin ligase MDM2 and ubiquitin ligase like protein MDM4 as important regulators of intrinsic neuroregeneration mechanisms. MDM2 and MDM4 are extensively studied targets in for cancer. MDM2 antagonist Nutlin-3a is already being tested in clinical trials for cancer, making it a possible therapeutic option for spinal cord injury (SCI) patients. Development of drugs specific for MDM4 will also widen the options of therapeutic strategies available for spinal cord injury patients.

Along with this, we were also able to identify epigenetic regulators p300 and P/CAF as crucial regulators involved in regeneration. While viral p300 overexpression induces regeneration in the optic nerve, P/CAF was shown to have a unifying role in mounting a transcriptional response following conditioning lesion. Viral P/CAF overexpression also enhanced the outgrowth of the ascending spinal fibers, suggesting a role in CNS regeneration. Role of P/CAF in another clinically relevant injury model awaits investigation. Viral overexpression is an impractical therapeutic approach, but these studies do present multiple pathways that can be targeted. This study we sheds light on the epigenetic scenario existing after neuronal injury and this hints towards the development of epigenetic-related regenerative therapies for SCI patients.

Hence these studies provide an insight into the intrinsic neuronal mechanisms following injury along with a robust base for development of therapeutics targeting the mentioned pathways.

1.3 Abbreviations

AAV	Adeno associated virus	NF-κB	Nuclear factor kappa light chain enhancer of activated B cells
AP	Activator protein	NCAM	Neural cell adhesion molecule
APC	Anaphase promoting complex	NgR	Nogo receptor
ATF	Activating transcription factor	NT	Neurotrophin
Bcl	B-cell leukemia protein	OMgp	Oligodendrocyte myelin glycoprotein
BDNF	Brain derived neurotrophic factor	ONC	Optic nerve crush
BMP	Bone morphogenetic protein	p21Cip1/Waf1	Cyclin dependent kinase interacting protein
cAMP	Cyclic adenosine monophosphate	p300	E1-A binding protein p300
CAP	Cytoskeletal associated protein	PCAF	P300/CBP associated factor
CBP	CREB binding protein	PDGF	Platelet derived growth factor
Cdc	Cell division cycle protein	PKA	Protein kinase A
Cdh	Cadherin	PNS	Peripheral nervous system
cGKI	cGMP dependent protein kinase	PTM	Post-translational modification
CNS	Central nervous system	PTEN	Phosphatase and tensin homolog
CSPG	Chondroitin Sulphate proteo glycan	RAG	Regeneration associated gene
CST	Cortico spinal tract	Rho	Ras homolog gene
CREB	Cyclic AMP response element binding protein	RGC	Retinal ganglion cell
ERK	Extracellular signal-related kinase	ROCK	Rho associated protein kinase
FACS	Fluorescence activated cell sorting	RTN	Reticulon family protein
GAP	Growth associated protein	Smad	mothers against decapentaplegic homolog
GDNF	Glial cell derived neurotrophic factor	SCI	Spinal cord injury
H3	Histone H3	SMARCC	SWI/SNF complex subunit
HAT	Histone acetyl transferase	Smurf	Smad ubiquitination regulatory factor
HDAC	Histone de-acetylase	SNAP	Synaptosomal associated protein
Hsp	Heat shock protein	SnoN	Ski-related novel protein
IGF1R	Insulin related growth factor 1	Sp1	Specificity protein
JAK	Janus Kinase	Sprr1	Small protein rich repeat protein
JNK	Jun N terminal kinase	STAT3	Signal transducer and activator of transcription
KLF	Krüppel like factor	TFs	Transcription factors
L1CAM	L1 cell adhesion molecule	TNF	Tumor necrosis factor
MAG	Myelin associated glycoprotein	TSC1	Tuberous sclerosis
MDM	Murine double minute protein	Trk	Trompomycin receptor kinase B
mTOR	Mammalian target of rapamycin		

1.4 Acknowledgement

Thank you to each and every person who has supported me in innumerable ways during this work.

Firstly, I would like to thank Prof. Dr. Simone Di Giovanni, my thesis advisor, for the opportunity to work in his lab, his support and guidance throughout this period. I would also take the opportunity to thank the DZNE, for giving me a scholarship during this tenure, without which the whole endeavor would have been impossible. A special thanks to all my present and past colleagues for their support, assistance, help, discussions, feedback and encouragement. Also, I would like to thank the members of my advisory committee Prof. Dr. Schlosshauer and PD. Dr. Andrea Wizenmann for all their help, time and constructive criticisms. The excellent support provided by the Prof. Herbert, Dr. Deiss-Thielgtes, Dr. Lampe of Graduate Training Centre in helping and developing all the students, is unparalleled. I would like to thank them for all their help and patience.

A special thanks to all my friends in Tuebingen who constantly supported me in innumerable ways and the encouragement they provided kept me going.

Lastly, the support of my family, especially of Tai and Nikhil, is unfathomable, to whom this thesis is dedicated.

Yashashree Joshi

1.5 References

- Aguayo, A. J., David, S. & Bray, G. M. 1981. Influences of the glial environment on the elongation of axons after injury: transplantation studies in adult rodents. *J Exp Biol*, 95, 231-40.
- Aigner, L. & Caroni, P. 1993. Depletion of 43-kD growth-associated protein in primary sensory neurons leads to diminished formation and spreading of growth cones. *J Cell Biol*, 123, 417-29.
- Aigner, L. & Caroni, P. 1995. Absence of persistent spreading, branching, and adhesion in GAP-43-depleted growth cones. *J Cell Biol*, 128, 647-60.
- Benson, M. D., Romero, M. I., Lush, M. E., Lu, Q. R., Henkemeyer, M. & Parada, L. F. 2005. Ephrin-B3 is a myelin-based inhibitor of neurite outgrowth. *Proc Natl Acad Sci U S A*, 102, 10694-9.
- Bernstein, D. R. & Stelzner, D. J. 1983. Plasticity of the corticospinal tract following midthoracic spinal injury in the postnatal rat. *J Comp Neurol*, 221, 382-400.
- Bradbury, E. J. & McMahon, S. B. 2006. Spinal cord repair strategies: why do they work? *Nat Rev Neurosci*, 7, 644-653.
- Bradbury, E. J., Moon, L. D., Popat, R. J., King, V. R., Bennett, G. S., Patel, P. N., Fawcett, J. W. & McMahon, S. B. 2002. Chondroitinase ABC promotes functional recovery after spinal cord injury. *Nature*, 416, 636-40.
- Bradke, F., Fawcett, J. W. & Spira, M. E. 2012. Assembly of a new growth cone after axotomy: the precursor to axon regeneration. *Nat Rev Neurosci*, 13, 183-93.
- Bregman, B. S., Kunkel-Bagden, E., Mcatee, M. & O'Neill, A. 1989. Extension of the critical period for developmental plasticity of the corticospinal pathway. *J Comp Neurol*, 282, 355-70.
- Brown, C. J., Lain, S., Verma, C. S., Fersht, A. R. & Lane, D. P. 2009. Awakening guardian angels: drugging the p53 pathway. *Nat Rev Cancer*, 9, 862-73.
- Butler, S. J. & Tear, G. 2007. Getting axons onto the right path: the role of transcription factors in axon guidance. *Development*, 134, 439-48.
- Cai, D., Deng, K., Mellado, W., Lee, J., Ratan, R. R. & Filbin, M. T. 2002. Arginase I and polyamines act downstream from cyclic AMP in overcoming inhibition of axonal growth MAG and myelin in vitro. *Neuron*, 35, 711-9.
- Cao, Z., Gao, Y., Bryson, J. B., Hou, J., Chaudhry, N., Siddiq, M., Martinez, J., Spencer, T., Carmel, J., Hart, R. B. & Filbin, M. T. 2006. The cytokine interleukin-6 is sufficient but not necessary to mimic the peripheral conditioning lesion effect on axonal growth. *J Neurosci*, 26, 5565-73.
- Carmichael, S. T., Archibeque, I., Luke, L., Nolan, T., Momiy, J. & Li, S. 2005. Growth-associated gene expression after stroke: evidence for a growth-promoting region in peri-infarct cortex. *Exp Neurol*, 193, 291-311.
- Caroni, P. & Grandes, P. 1990. Nerve sprouting in innervated adult skeletal muscle induced by exposure to elevated levels of insulin-like growth factors. *J Cell Biol*, 110, 1307-17.
- Carulli, D., Buffo, A., Botta, C., Altruda, F. & Strata, P. 2002. Regenerative and survival capabilities of Purkinje cells overexpressing c-Jun. *Eur J Neurosci*, 16, 105-18.
- Cheng, P.-L., Lu, H., Shelly, M., Gao, H. & Poo, M.-M. 2011. Phosphorylation of E3 Ligase Smurf1 Switches Its Substrate Preference in Support of Axon Development. *Neuron*, 69, 231-243.
- Cho, K. S., Yang, L., Lu, B., Feng Ma, H., Huang, X., Pekny, M. & Chen, D. F. 2005. Re-establishing the regenerative potential of central nervous system axons in postnatal mice. *J Cell Sci*, 118, 863-72.
- David, S. & Aguayo, A. J. 1981. Axonal elongation into peripheral nervous system "bridges" after central nervous system injury in adult rats. *Science*, 214, 931-3.
- Di Giovanni, S. 2009. Molecular targets for axon regeneration: focus on the intrinsic pathways. *Expert Opin Ther Targets*, 13, 1387-98.
- Di Giovanni, S., Faden, A. I., Yakovlev, A., Duke-Cohan, J. S., Finn, T., Thouin, M., Knobloch, S., De Biase, A., Bregman, B. S. & Hoffman, E. P. 2005. Neuronal

- plasticity after spinal cord injury: identification of a gene cluster driving neurite outgrowth. *FASEB J*, 19, 153-4.
- Di Giovanni, S., Knights, C. D., Rao, M., Yakovlev, A., Beers, J., Catania, J., Avantaggiati, M. L. & Faden, A. I. 2006. The tumor suppressor protein p53 is required for neurite outgrowth and axon regeneration. *EMBO J*, 25, 4084-96.
- Di Giovanni, S. & Rathore, K. 2012. p53-Dependent pathways in neurite outgrowth and axonal regeneration. *Cell Tissue Res*, 349, 87-95.
- Eva, R., Andrews, M. R., Franssen, E. H. & Fawcett, J. W. 2012. Intrinsic mechanisms regulating axon regeneration: an integrin perspective. *Int Rev Neurobiol*, 106, 75-104.
- Fischer, D., Heiduschka, P. & Thanos, S. 2001. Lens-injury-stimulated axonal regeneration throughout the optic pathway of adult rats. *Exp Neurol*, 172, 257-72.
- Fishman, H. M. & Bittner, G. D. 2003. Vesicle-mediated restoration of a plasmalemmal barrier in severed axons. *News Physiol Sci*, 18, 115-8.
- Floriddia, E. M., Rathore, K. I., Tedeschi, A., Quadrato, G., Wuttke, A., Lueckmann, J. M., Kigerl, K. A., Popovich, P. G. & Di Giovanni, S. 2012. p53 Regulates the Neuronal Intrinsic and Extrinsic Responses Affecting the Recovery of Motor Function following Spinal Cord Injury. *J Neurosci*, 32, 13956-70.
- Francoz, S., Froment, P., Bogaerts, S., De Clercq, S., Maetens, M., Doumont, G., Bellefroid, E. & Marine, J. C. 2006. Mdm4 and Mdm2 cooperate to inhibit p53 activity in proliferating and quiescent cells in vivo. *Proc Natl Acad Sci U S A*, 103, 3232-7.
- Gao, Y., Deng, K., Hou, J., Bryson, J. B., Barco, A., Nikulina, E., Spencer, T., Mellado, W., Kandel, E. R. & Filbin, M. T. 2004. Activated CREB is sufficient to overcome inhibitors in myelin and promote spinal axon regeneration in vivo. *Neuron*, 44, 609-21.
- Gaub, P., Joshi, Y., Wuttke, A., Naumann, U., Schnichels, S., Heiduschka, P. & Di Giovanni, S. The histone acetyltransferase p300 promotes intrinsic axonal regeneration. *Brain*, 134, 2134-48.
- Gaub, P., Joshi, Y., Wuttke, A., Naumann, U., Schnichels, S., Heiduschka, P. & Di Giovanni, S. 2011. The histone acetyltransferase p300 promotes intrinsic axonal regeneration. *Brain*, 134, 2134-48.
- Gaub, P., Tedeschi, A., Puttagunta, R., Nguyen, T., Schmandke, A. & Di Giovanni, S. 2010. HDAC inhibition promotes neuronal outgrowth and counteracts growth cone collapse through CBP/p300 and P/CAF-dependent p53 acetylation. *Cell Death Differ*, 17, 1392-408.
- Girnita, A., Girnita, L., Del Prete, F., Bartolazzi, A., Larsson, O. & Axelson, M. 2004. Cyclolignans as inhibitors of the insulin-like growth factor-1 receptor and malignant cell growth. *Cancer Res*, 64, 236-42.
- Gloster, A., Wu, W., Speelman, A., Weiss, S., Causing, C., Pozniak, C., Reynolds, B., Chang, E., Toma, J. G. & Miller, F. D. 1994. The T alpha 1 alpha-tubulin promoter specifies gene expression as a function of neuronal growth and regeneration in transgenic mice. *J Neurosci*, 14, 7319-30.
- Goldberg, J. L., Klassen, M. P., Hua, Y. & Barres, B. A. 2002. Amacrine-signaled loss of intrinsic axon growth ability by retinal ganglion cells. *Science*, 296, 1860-4.
- Hakkoum, D., Stoppini, L. & Muller, D. 2007. Interleukin-6 promotes sprouting and functional recovery in lesioned organotypic hippocampal slice cultures. *J Neurochem*, 100, 747-57.
- Hall, A. 1998. Rho GTPases and the actin cytoskeleton. *Science*, 279, 509-14.
- Hellstrom, M., Muhling, J., Ehler, E. M., Verhaagen, J., Pollett, M. A., Hu, Y. & Harvey, A. R. 2011. Negative impact of rAAV2 mediated expression of SOCS3 on the regeneration of adult retinal ganglion cell axons. *Mol Cell Neurosci*, 46, 507-15.
- Herdegen, T., Skene, P. & Bahr, M. 1997. The c-Jun transcription factor--bipotential mediator of neuronal death, survival and regeneration. *Trends Neurosci*, 20, 227-31.
- Hollis, E. R., 2nd, Jamshidi, P., Low, K., Blesch, A. & Tuszynski, M. H. 2009. Induction of corticospinal regeneration by lentiviral trkB-induced Erk activation. *Proc Natl Acad Sci U S A*, 106, 7215-20.

- Kadakia, M., Brown, T. L., Mcgorry, M. M. & Berberich, S. J. 2002. MdmX inhibits Smad transactivation. *Oncogene*, 21, 8776-85.
- Kamiguchi, H. & Lemmon, V. 2000. Recycling of the cell adhesion molecule L1 in axonal growth cones. *J Neurosci*, 20, 3676-86.
- Kim, A. H., Puram, S. V., Bilimoria, P. M., Ikeuchi, Y., Keough, S., Wong, M., Rowitch, D. & Bonni, A. 2009. A centrosomal Cdc20-APC pathway controls dendrite morphogenesis in postmitotic neurons. *Cell*, 136, 322-36.
- Kim, J. G., Kang, M. J., Yoon, Y. K., Kim, H. P., Park, J., Song, S. H., Han, S. W., Park, J. W., Kang, G. H., Kang, K. W., Oh Do, Y., Im, S. A., Bang, Y. J., Yi, E. C. & Kim, T. Y. 2012. Heterodimerization of glycosylated insulin-like growth factor-1 receptors and insulin receptors in cancer cells sensitive to anti-IGF1R antibody. *PLoS One*, 7, e33322.
- Kimura, K., Mizoguchi, A. & Ide, C. 2003. Regulation of growth cone extension by SNARE proteins. *J Histochem Cytochem*, 51, 429-33.
- Knoops, B. & Octave, J. N. 1997. Alpha 1-tubulin mRNA level is increased during neurite outgrowth of NG 108-15 cells but not during neurite outgrowth inhibition by CNS myelin. *Neuroreport*, 8, 795-8.
- Konishi, Y., Stegmuller, J., Matsuda, T., Bonni, S. & Bonni, A. 2004. Cdh1-APC controls axonal growth and patterning in the mammalian brain. *Science*, 303, 1026-30.
- Lane, M. A. & Bailey, S. J. 2005. Role of retinoid signalling in the adult brain. *Prog Neurobiol*, 75, 275-93.
- Leaver, S. G., Cui, Q., Plant, G. W., Arulpragasam, A., Hisheh, S., Verhaagen, J. & Harvey, A. R. 2006. AAV-mediated expression of CNTF promotes long-term survival and regeneration of adult rat retinal ganglion cells. *Gene Ther*, 13, 1328-41.
- Lee, J. K., Geoffroy, C. G., Chan, A. F., Tolentino, K. E., Crawford, M. J., Leal, M. A., Kang, B. & Zheng, B. 2010. Assessing spinal axon regeneration and sprouting in Nogo-, MAG-, and OMgp-deficient mice. *Neuron*, 66, 663-70.
- Leibinger, M., Muller, A., Andreadaki, A., Hauk, T. G., Kirsch, M. & Fischer, D. 2009. Neuroprotective and axon growth-promoting effects following inflammatory stimulation on mature retinal ganglion cells in mice depend on ciliary neurotrophic factor and leukemia inhibitory factor. *J Neurosci*, 29, 14334-41.
- Leon, S., Yin, Y., Nguyen, J., Irwin, N. & Benowitz, L. I. 2000. Lens injury stimulates axon regeneration in the mature rat optic nerve. *J Neurosci*, 20, 4615-26.
- Liu, K., Lu, Y., Lee, J. K., Samara, R., Willenberg, R., Sears-Kraxberger, I., Tedeschi, A., Park, K. K., Jin, D., Cai, B., Xu, B., Connolly, L., Steward, O., Zheng, B. & He, Z. 2010. PTEN deletion enhances the regenerative ability of adult corticospinal neurons. *Nat Neurosci*, 13, 1075-81.
- Liu, K., Tedeschi, A., Park, K. K. & He, Z. 2011. Neuronal intrinsic mechanisms of axon regeneration. *Annu Rev Neurosci*, 34, 131-52.
- Liu, R., Chen, X. P. & Tao, L. Y. 2008. Regulation of axonal regeneration following the central nervous system injury in adult mammalian. *Neurosci Bull*, 24, 395-400.
- Llinas, R. R. 2003. The contribution of Santiago Ramon y Cajal to functional neuroscience. *Nat Rev Neurosci*, 4, 77-80.
- Lu, P. & Tuszynski, M. H. 2008. Growth factors and combinatorial therapies for CNS regeneration. *Exp Neurol*, 209, 313-20.
- Makwana, M. & Raivich, G. 2005. Molecular mechanisms in successful peripheral regeneration. *FEBS J*, 272, 2628-38.
- Marine, J. C. 2011. MDM2 and MDMX in cancer and development. *Curr Top Dev Biol*, 94, 45-75.
- Marine, J. C. & Jochemsen, A. G. 2004. Mdmx and Mdm2: brothers in arms? *Cell Cycle*, 3, 900-4.
- Markey, M. P. Regulation of MDM4. *Front Biosci*, 16, 1144-56.
- Markey, M. P. 2011. Regulation of MDM4. *Front Biosci*, 16, 1144-56.

- Mckerracher, L., David, S., Jackson, D. L., Kottis, V., Dunn, R. J. & Braun, P. E. 1994. Identification of myelin-associated glycoprotein as a major myelin-derived inhibitor of neurite growth. *Neuron*, 13, 805-11.
- Moore, D. L., Blackmore, M. G., Hu, Y., Kaestner, K. H., Bixby, J. L., Lemmon, V. P. & Goldberg, J. L. 2009. KLF family members regulate intrinsic axon regeneration ability. *Science*, 326, 298-301.
- Moreau-Fauvarque, C., Kumanogoh, A., Camand, E., Jaillard, C., Barbin, G., Boquet, I., Love, C., Jones, E. Y., Kikutani, H., Lubetzki, C., Dusart, I. & Chedotal, A. 2003. The transmembrane semaphorin Sema4D/CD100, an inhibitor of axonal growth, is expressed on oligodendrocytes and upregulated after CNS lesion. *J Neurosci*, 23, 9229-39.
- Morgenstern, D. A., Asher, R. A. & Fawcett, J. W. 2002. Chondroitin sulphate proteoglycans in the CNS injury response. *Prog Brain Res*, 137, 313-32.
- Mukhopadhyay, G., Doherty, P., Walsh, F. S., Crocker, P. R. & Filbin, M. T. 1994. A novel role for myelin-associated glycoprotein as an inhibitor of axonal regeneration. *Neuron*, 13, 757-67.
- Muller, A., Hauk, T. G., Leibinger, M., Marienfeld, R. & Fischer, D. 2009. Exogenous CNTF stimulates axon regeneration of retinal ganglion cells partially via endogenous CNTF. *Mol Cell Neurosci*, 41, 233-46.
- Naeve, G. S., Ramakrishnan, M., Kramer, R., Hevroni, D., Citri, Y. & Theill, L. E. 1997. Neuritin: a gene induced by neural activity and neurotrophins that promotes neurogenesis. *Proc Natl Acad Sci U S A*, 94, 2648-53.
- Nakazawa, T., Tamai, M. & Mori, N. 2002. Brain-derived neurotrophic factor prevents axotomized retinal ganglion cell death through MAPK and PI3K signaling pathways. *Invest Ophthalmol Vis Sci*, 43, 3319-26.
- Oblinger, M. & Lasek, R. 1984. A conditioning lesion of the peripheral axons of dorsal root ganglion cells accelerates regeneration of only their peripheral axons. *The Journal of Neuroscience*, 4, 1736-1744.
- Panicker, A. K., Buhusi, M., Thelen, K. & Maness, P. F. 2003. Cellular signalling mechanisms of neural cell adhesion molecules. *Front Biosci*, 8, d900-11.
- Parikh, P., Hao, Y., Hosseinkhani, M., Patil, S. B., Huntley, G. W., Tessier-Lavigne, M. & Zou, H. Regeneration of axons in injured spinal cord by activation of bone morphogenetic protein/Smad1 signaling pathway in adult neurons. *Proc Natl Acad Sci U S A*, 108, E99-107.
- Park, K. K., Liu, K., Hu, Y., Kanter, J. L. & He, Z. 2010. PTEN/mTOR and axon regeneration. *Exp Neurol*, 223, 45-50.
- Park, K. K., Liu, K., Hu, Y., Smith, P. D., Wang, C., Cai, B., Xu, B., Connolly, L., Kramvis, I., Sahin, M. & He, Z. 2008. Promoting axon regeneration in the adult CNS by modulation of the PTEN/mTOR pathway. *Science*, 322, 963-6.
- Pernet, V. & Di Polo, A. 2006. Synergistic action of brain-derived neurotrophic factor and lens injury promotes retinal ganglion cell survival, but leads to optic nerve dystrophy in vivo. *Brain*, 129, 1014-26.
- Pernet, V., Hauswirth, W. W. & Di Polo, A. 2005. Extracellular signal-regulated kinase 1/2 mediates survival, but not axon regeneration, of adult injured central nervous system neurons in vivo. *J Neurochem*, 93, 72-83.
- Qin, Q., Liao, G., Baudry, M. & Bi, X. 2010a. Cholesterol Perturbation in Mice Results in p53 Degradation and Axonal Pathology through p38 MAPK and Mdm2 Activation. *PLoS One*, 5, e9999.
- Qin, Q., Liao, G., Baudry, M. & Bi, X. 2010b. Role of calpain-mediated p53 truncation in semaphorin 3A-induced axonal growth regulation. *Proc Natl Acad Sci U S A*, 107, 13883-7.
- Raivich, G. & Behrens, A. 2006. Role of the AP-1 transcription factor c-Jun in developing, adult and injured brain. *Prog Neurobiol*, 78, 347-63.
- Raivich, G., Bohatschek, M., Da Costa, C., Iwata, O., Galiano, M., Hristova, M., Nateri, A. S., Makwana, M., Riera-Sans, L., Wolfer, D. P., Lipp, H. P., Aguzzi, A., Wagner, E. F. &

- Behrens, A. 2004. The AP-1 transcription factor c-Jun is required for efficient axonal regeneration. *Neuron*, 43, 57-67.
- Reed, D., Shen, Y., Shelat, A. A., Arnold, L. A., Ferreira, A. M., Zhu, F., Mills, N., Smithson, D. C., Regni, C. A., Bashford, D., Cicero, S. A., Schulman, B. A., Jochemsen, A. G., Guy, R. K. & Dyer, M. A. 2010. Identification and characterization of the first small molecule inhibitor of MDMX. *J Biol Chem*, 285, 10786-96.
- Reichardt, L. F. 2006. Neurotrophin-regulated signalling pathways. *Philos Trans R Soc Lond B Biol Sci*, 361, 1545-64.
- Richardson, P. M., McGuinness, U. M. & Aguayo, A. J. 1980. Axons from CNS neurons regenerate into PNS grafts. *Nature*, 284, 264-5.
- Rowland, B. D., Bernards, R. & Peeper, D. S. 2005. The KLF4 tumour suppressor is a transcriptional repressor of p53 that acts as a context-dependent oncogene. *Nat Cell Biol*, 7, 1074-1082.
- Schlaepfer, W. W. & Bunge, R. P. 1973. Effects of calcium ion concentration on the degeneration of amputated axons in tissue culture. *J Cell Biol*, 59, 456-70.
- Schmandke, A. & Strittmatter, S. M. 2007. ROCK and Rho: biochemistry and neuronal functions of Rho-associated protein kinases. *Neuroscientist*, 13, 454-69.
- Schwab, M. E. & Thoenen, H. 1985. Dissociated neurons regenerate into sciatic but not optic nerve explants in culture irrespective of neurotrophic factors. *J Neurosci*, 5, 2415-23.
- Schwamborn, J. C., Muller, M., Becker, A. H. M. & Puschel, A. W. 2007. Ubiquitination of the GTPase Rap1B by the ubiquitin ligase Smurf2 is required for the establishment of neuronal polarity. *EMBO J*, 26, 1410-1422.
- Serra, C., Palacios, D., Mozzetta, C., Forcales, S. V., Morante, I., Ripani, M., Jones, D. R., Du, K., Jhala, U. S., Simone, C. & Puri, P. L. 2007. Functional interdependence at the chromatin level between the MKK6/p38 and IGF1/PI3K/AKT pathways during muscle differentiation. *Mol Cell*, 28, 200-13.
- Shah, M., Patel, K., Mukhopadhyay, S., Xu, F., Guo, G. & Sehgal, P. B. 2006. Membrane-associated STAT3 and PY-STAT3 in the cytoplasm. *J Biol Chem*, 281, 7302-8.
- Silver, J. & Miller, J. H. 2004. Regeneration beyond the glial scar. *Nat Rev Neurosci*, 5, 146-56.
- Smith, P. D., Sun, F., Park, K. K., Cai, B., Wang, C., Kuwako, K., Martinez-Carrasco, I., Connolly, L. & He, Z. 2009. SOCS3 deletion promotes optic nerve regeneration in vivo. *Neuron*, 64, 617-23.
- Spencer, T. & Filbin, M. T. 2004. A role for cAMP in regeneration of the adult mammalian CNS. *J Anat*, 204, 49-55.
- Staerk, J., Kallin, A., Demoulin, J. B., Vainchenker, W. & Constantinescu, S. N. 2005. JAK1 and Tyk2 activation by the homologous polycythemia vera JAK2 V617F mutation: cross-talk with IGF1 receptor. *J Biol Chem*, 280, 41893-9.
- Subbiah, V., Naing, A., Brown, R. E., Chen, H., Doyle, L., Lorusso, P., Benjamin, R., Anderson, P. & Kurzrock, R. 2011. Targeted morphoproteomic profiling of Ewing's sarcoma treated with insulin-like growth factor 1 receptor (IGF1R) inhibitors: response/resistance signatures. *PLoS One*, 6, e18424.
- Tanaka, H., Yamashita, T., Yachi, K., Fujiwara, T., Yoshikawa, H. & Tohyama, M. 2004. Cytoplasmic p21(Cip1/WAF1) enhances axonal regeneration and functional recovery after spinal cord injury in rats. *Neuroscience*, 127, 155-64.
- Tedeschi, A. 2011. Tuning the orchestra: transcriptional pathways controlling axon regeneration. *Front Mol Neurosci*, 4, 60.
- Tedeschi, A. & Di Giovanni, S. 2009. The non-apoptotic role of p53 in neuronal biology: enlightening the dark side of the moon. *EMBO Rep*, 10, 576-83.
- Tedeschi, A., Nguyen, T., Puttagunta, R., Gaub, P. & Di Giovanni, S. 2009a. A p53-CBP/p300 transcription module is required for GAP-43 expression, axon outgrowth, and regeneration. *Cell Death Differ*, 16, 543-54.
- Tedeschi, A., Nguyen, T., Steele, S. U., Feil, S., Naumann, U., Feil, R. & Di Giovanni, S. 2009b. The tumor suppressor p53 transcriptionally regulates cGKI expression during

- neuronal maturation and is required for cGMP-dependent growth cone collapse. *J Neurosci*, 29, 15155-60.
- Teng, F. Y. & Tang, B. L. 2006. Axonal regeneration in adult CNS neurons--signaling molecules and pathways. *J Neurochem*, 96, 1501-8.
- Toledo, F. & Wahl, G. M. 2006. Regulating the p53 pathway: in vitro hypotheses, in vivo veritas. *Nat Rev Cancer*, 6, 909-23.
- Vassilev, L. T., Vu, B. T., Graves, B., Carvajal, D., Podlaski, F., Filipovic, Z., Kong, N., Kammlott, U., Lukacs, C., Klein, C., Fotouhi, N. & Liu, E. A. 2004. In vivo activation of the p53 pathway by small-molecule antagonists of MDM2. *Science*, 303, 844-8.
- Vogel, S. M., Bauer, M. R., Joerger, A. C., Wilcken, R., Brandt, T., Veprintsev, D. B., Rutherford, T. J., Fersht, A. R. & Boeckler, F. M. 2012. Lithocholic acid is an endogenous inhibitor of MDM4 and MDM2. *Proc Natl Acad Sci U S A*, 109, 16906-10.
- Wang, H.-R., Zhang, Y., Ozdamar, B., Ogunjimi, A. A., Alexandrova, E., Thomsen, G. H. & Wrana, J. L. 2003. Regulation of Cell Polarity and Protrusion Formation by Targeting RhoA for Degradation. *Science*, 302, 1775-1779.
- Wang, K. C., Koprivica, V., Kim, J. A., Sivasankaran, R., Guo, Y., Neve, R. L. & He, Z. 2002. Oligodendrocyte-myelin glycoprotein is a Nogo receptor ligand that inhibits neurite outgrowth. *Nature*, 417, 941-4.
- Windle, W. F. 1980. Inhibition of regeneration of severed axons in the spinal cord. *Exp Neurol*, 69, 209-11.
- Yamada, T., Yang, Y. & Bonni, A. 2013. Spatial organization of ubiquitin ligase pathways orchestrates neuronal connectivity. *Trends Neurosci*, 36, 218-26.
- Yang, X. J. & Seto, E. 2007. HATs and HDACs: from structure, function and regulation to novel strategies for therapy and prevention. *Oncogene*, 26, 5310-8.
- Yin, Y., Cui, Q., Li, Y., Irwin, N., Fischer, D., Harvey, A. R. & Benowitz, L. I. 2003. Macrophage-derived factors stimulate optic nerve regeneration. *J Neurosci*, 23, 2284-93.
- Yiu, G. & He, Z. 2006. Glial inhibition of CNS axon regeneration. *Nat Rev Neurosci*, 7, 617-27.
- Zhou, F. Q. & Snider, W. D. 2006. Intracellular control of developmental and regenerative axon growth. *Philos Trans R Soc Lond B Biol Sci*, 361, 1575-92.
- Zou, H., Ho, C., Wong, K. & Tessier-Lavigne, M. 2009. Axotomy-induced Smad1 activation promotes axonal growth in adult sensory neurons. *J Neurosci*, 29, 7116-23.
- Zweifel, L. S., Kuruvilla, R. & Ginty, D. D. 2005. Functions and mechanisms of retrograde neurotrophin signalling. *Nat Rev Neurosci*, 6, 615-25.

2 Publications

Contributions

1. Modulation of MDM4-p53-IGF1R axis promotes CNS axonal regeneration and sprouting after CNS injury (Submitted)

Yashashree Joshi^{1,2,3}, Giorgia Quadrato^{1*}, Marília Grando Sória^{1,2*}, Gizem Inak^{1,2}, Khizr Rathore¹, Mohamed Elnaggar^{1,2}, Jeanne Christophe Marine⁴, Simone Di Giovanni^{1,5}.

Research designed by: **YJ**, SDG

Experiments performed by: **YJ**, GQ, MGS, KR

Technical Assistance: GI, ME

Data analysed by: **YJ**, MGS

Manuscript written by: **YJ**, SDG

2. The histone acetyl transferase p300 promotes intrinsic axonal regeneration.

P Gaub, **Y Joshi**, Anja Wuttke, U Naumann, S Schnichels, P Heiduschka, S Di Giovanni

Brain 2011: 134; 2134–2148

Research designed by: PG, **YJ**, SDG

Experiments performed by: PG, **YJ**, AW

Data analysed by: PG, **YJ**

Manuscript written by: PG, SDG

3. PCAF-dependent epigenetic changes promote axonal regeneration in the central nervous system (under review Nature Letters)

Radhika Puttagunta^{1§}, Andrea Tedeschi^{2§}, Marilia Grando Soria^{1,3}, Arnau Hervera¹ Ricco Lindner^{1,3}, Khizr I. Rathore¹, Perrine Gaub^{1,3}, **Yashashree Joshi**^{1,3,4}, Tuan Nguyen¹, Antonio Schmandke¹, Claudia J. Laskowski², Anne-Laurence Boutillier⁵, Frank Bradke², and Simone Di Giovanni¹

Contributions:

Research Designed by: RP, AT, SDG

Experiments performed by: RP, AT, MGS, AH, **YJ**, RL, KR

Data analysed by: RP, MGS, AT, SDG, RL, **YJ**

Manuscript written by: RP, SDG

2.1 Modulation of MDM4-p53-IGF1R axis promotes CNS axonal regeneration and sprouting after CNS injury

Yashashree Joshi^{1,2,3}, Giorgia Quadrato^{1*}, Marília Grando Sória^{1,2*}, Gizem Inak^{1,2}, Khizr Rathore¹, Mohamed Elnaggar^{1,2}, Jeanne Christophe Marine⁴, Simone Di Giovanni^{1,5}.

¹Laboratory for NeuroRegeneration and Repair, Center for Neurology, Hertie Institute for Clinical Brain Research, University of Tuebingen, Tuebingen, Germany.

²Graduate School for Cellular and Molecular Neuroscience, University of Tuebingen, Tuebingen, Germany.

³German Centre for Neurodegenerative Diseases (DZNE), Tuebingen, Germany.

⁴Laboratory for Molecular Cancer Biology, Department of Molecular and Developmental Genetics, VIB-K.U.Leuven, Leuven, Belgium.

⁵Laboratory for Neuroregeneration, Division of Brain Sciences, Department of Medicine, Imperial College London, London, UK.

*These authors contributed equally.

To whom correspondence should be addressed:

Simone Di Giovanni, MD, PhD
Laboratory for NeuroRegeneration and Repair
Hertie Institute for Clinical Brain Research
University of Tuebingen
Otfried-Mueller Strasse 27
D-72076 Tuebingen, Germany
tel: 0049 (0) 7071 29 80449
fax: 0049 (0) 7071 29 4521
e.mail: simone.digiovanni@medizin.uni-tuebingen.de

Key words: MDM4, MDM2, IGF1R, p53, optic nerve, spinal cord, regeneration

Abstract

Regeneration of injured CNS axons is highly restricted causing neurological impairment. Despite recent advances, the complex signaling regulating the neuronal regenerative potential remains poorly defined limiting therapeutic options. Ubiquitin ligases and ubiquitin ligase binding proteins coordinate neuronal morphogenesis and connectivity during development and after axonal injury. However their role in CNS axonal regeneration remains unaddressed. Here we show that conditional deletion of the ubiquitin ligase-like protein MDM4 in retinal ganglion cells (RGCs) and sensory motor cortex promotes axonal regeneration following optic nerve crush and sprouting of the corticospinal tracts after spinal dorsal hemisection respectively. Use of double conditional deletion and small molecule inhibitors show that this regenerative phenotype depends upon MDM4 binding proteins p53 and MDM2, a ubiquitin ligase. Finally, genome wide gene expression analysis from ex vivo fluorescent-sorted MDM4 deficient RGCs identifies the downstream target IGF1R, whose activity was found to be required for regeneration elicited by MDM4 deletion. Thus, our results conclusively show MDM4-MDM2/p53-IGF1R as a novel signalling hub that may be targeted for regenerative therapy.

Introduction

The adult mammalian central nervous system (CNS) is unable to regenerate following axonal injury due to the presence of glial inhibition environment as well as to lack of neuronal intrinsic regeneration potential. Research in the past two decades has elucidated a number of key molecular mechanisms and pathways that limit axonal sprouting and regeneration following CNS axonal injury, including myelin or proteoglycan-dependent inhibitory signalling (Yiu and He, 2006, Giovanni, 2009, Bradke *et al.*, 2012). More recently, accumulating evidence has suggested that the modulation of the neuronal intrinsic potential via the manipulation of selected genes in specific neuronal populations may enhance axonal regeneration in the injured CNS (Smith *et al.*, 2009, Sun *et al.*, 2011, Moore *et al.*, 2009, Park *et al.*, 2008). Often, these are developmentally regulated pathways that contribute to lock adult CNS neurons in a non-regenerative mode. As remarkable examples, deletion of PTEN in retinal ganglia cells (RGCs) or in corticospinal axons (CST) enhances mTOR activity and leads to robust axonal regeneration after optic nerve or CST injury respectively (Park *et al.*, 2008, Liu *et al.*, 2010), which is further enhanced by conditional co-deletion of SOCS3 and PTEN (Sun *et al.*, 2011). In addition, modifications of the developmentally regulated neuronal transcriptional program can lead to increased axonal regeneration after optic nerve crush (ONC) or spinal cord injury (SCI) as shown by deletion of KLF4, by overexpression of p300 in RGCs (Moore *et al.*, 2009, Gaub *et al.*, 2011); by overexpression of KLF7 (Blackmore *et al.*, 2012) or RAR β in corticospinal neurons (Puttagunta *et al.*, 2011, Puttagunta and Di Giovanni, 2011). Despite this progress, viable translational therapeutic options for axonal regeneration are still very limited, and there is need for the identification of specific molecular pathways with translational potential.

Ubiquitin ligases and ubiquitin ligase like proteins coordinate neuronal morphogenesis and connectivity both during development and after axonal injury, and regulate the turnover, localization and activity of a number of proteins and transcription factors involved in the axonal regeneration program, including PTEN, p300, KLFs, Smads p21 and p53 (Yamada *et al.*, 2013). They may therefore represent a signalling hub orchestrating the regenerative neuronal response following injury. However their role in axonal regeneration remains unaddressed. The ubiquitin ligase like MDM4 can form inhibitory protein complexes with at least four key proteins involved in the axonal outgrowth program: Smad1/2, p300, p53 and MDM2 (Markey, 2011, Kadakia *et al.*, 2002). Additionally, MDM4 expression is developmentally regulated in the retina reaching its maximal levels in adulthood, potentially keeping the post-injury RGC growth program under check. Therefore, MDM4 appears to be a candidate molecule limiting the axonal regeneration program at first in the injured optic nerve.

In support of this, we found by pathway and gene network analysis using Genomatix bioinformatics tools that MDM4 lies at the centre of a signalling and transcriptional hub, potentially involved in repressing axonal regeneration signalling. Therefore we investigated whether disruption of MDM4 would affect the axonal regeneration program. Indeed, we found that MDM4 restricts the axonal regeneration program after optic nerve crush and also after corticospinal lesions, two classical models of non-regenerative axonal injury. In fact, MDM4 conditional deletion in RGCs and sensory motor cortex leads to enhanced axonal regeneration of RGC axons following ONC and of the CST after spinal dorsal hemisection. Additionally, conditional co-deletion of MDM4 and of the target protein p53 in RGCs after ONC limits nerve regeneration elicited by MDM4 deletion alone. Similarly, pharmacological inhibition of the interaction between the MDM4 co-factor MDM2 and p53 via the MDM2/p53 antagonist Nutlin-3a also enables robust regeneration after ONC, which is abolished in p53 deficient mice. Lastly, genome wide gene expression analyses from pure RGC population after conditional deletion of MDM4 showed enhancement of IGF1R expression suggesting IGF1R signaling as a downstream effector of MDM4 deletion. Indeed co-inhibition of MDM4 and IGF1R after ONC via a specific IGF1R antagonist impairs axonal regeneration.

Together, this work portrays MDM4-MDM2/p53-IGF1R signalling hub as a novel molecular target for axonal regeneration.

Materials and Methods

Mice

All experimental procedures were performed according to the animal protocols approved by Regierungspräsidium Tübingen. Mice were housed in a colony maintained at 24 °C with a 12h dark/light cycle and *ad libitum* food and water. For all surgeries, mice were anesthetized with xylazine (10mg/kg of body weight) and ketamine (100mg/kg of bodyweight), and eye ointment bepanthen was applied to protect cornea during the surgery.

Intravitreal injections

For intravitreal injections, pulled glass capillaries attached to a Hamilton syringe via a connector were inserted into the peripheral retina. A volume of vitreal fluid equal to the volume to be injected was removed to avoid intravitreal pressure elevation. The micropipette was deliberately angled in a way to avoid lens injury. Fundoscopic inspection was done after every intravitreal injection to check for any damage to the lens. Animals with lens injury were excluded from the study. For performing the optic nerve injury, the left optic nerve was exposed intraorbitally and crushed for 10s, 1 mm from the optic disc with forceps (Dumont 5, FST). Care was taken not to injure the ophthalmic artery to avoid retinal ischemia. Animals

with injury to the ophthalmic artery were excluded from the study. For anterograde tracing of the RGC axons, 1 μ l cholera subunit B (CtB) conjugated to Alexa fluor 555 (Invitrogen) was injected intravitreally at least 2 days before sacrificing the mice. Mice were killed with a lethal dose of anaesthesia and transcardially perfused with ice cold 0.1M PBS followed by 4% paraformaldehyde. Optic nerves and eyes were dissected and post fixed for 1 hr at 4 C, before cryoprotecting them with 30% sucrose solution.

AAV-cre in MDM4^{ff} mice and Nutlin-3a administration

MDM4^{ff} mice were a gift from the J.C.M lab and were produced as described previously (Grier *et al.*, 2006). Primers used for genotyping of the MDM4 mice were: a- (forward) - 5'-gggtgccttgaacttgctgtgtagaa-3'; b-(exon2 reverse) - 5'-ctgggcccagggtggaatgtgatgt-3'; c-(reverse) - 5'-tatccagtgctcttctggctt-3'. 1 μ l of the Adeno-associated virus expressing GFP (AAV GFP) or AAV CreGFP (titre in the range of 1 X10⁸) were intravitreally injected in male mice aged P21 and optic nerve crush was performed 14 days later (at P35). 26d post-optic nerve crush, CtB (Invitrogen, 2 μ g/ μ l) was intravitreally injected in the eye, 2 days before sacrifice by transcardial perfusion (28d). 1 μ l of 100nm Nutlin-3a or vehicle were intravitreally injected in C57/BL6 (Charles River) male mice aged P35 and optic nerve crush was performed on the same day. Another intravitreal dose of Nutlin-3a was given 7 days post-optic nerve crush. 26 days later, CtB (Invitrogen, 2 μ g/ μ l) was intravitreally injected, and mice were sacrificed by transcardial perfusion 28 days post-optic nerve crush. Both wildtype and *p53*^{+/+} mice were employed for Nutlin-3a experiments.

Experiments with MDM4^{ff}/p53^{ff} mice

MDM4^{ff} were crossed with P53^{ff} mice (Strain name: B6.129P2-Trp53tm1Brn/J, Stock Number: 008462, Jackson Labs) to generate MDM4^{ff}/p53^{ff} mice. The same experimental design including AAV delivery and ONC was conducted in MDM4^{ff}/p53^{ff} as in MDM4^{ff}.

Adeno associated virus preparation and purification

Details about production of adeno associated virus 2 (AAV2-GFP/AAV2-CreGFP) has been described elsewhere (Berton *et al.*, 2006, Grieger *et al.*, 2006). Plasmid vector for AAV-GFP and AAV-CreGFP production were a gift from Dr. Eric. J. Nestler. Briefly, GFP (control) or an N terminal fusion of GFP to Cre were cloned into a recombinant AAV-2 vector containing the human immediate early cytomegalovirus promoter with a splice donor acceptor sequence and polyadenylation signal from the human-globin gene. The vector was produced using a triple-transfection, helper-free method. The final purified virus was stored at -80°C. The titre was evaluated after infection in HeLa cells and successful infection was also tested *in vivo*.

Whole mount retinal staining

After perfusion, uninjured and injured eyes were dissected and post fixed for 1hr in PFA . Flat retinae were plated on a dish in PBS and then stained for Tuj1 to detect surviving RGCs and with DAPI to detect nuclei. The uninjured retinae were used as a control. The retinae were mounted with single coverslips with mounting medium (DAKO). At least 10 fields were imaged at 25X oil magnification specifically from the retinal ganglion cell layer using Zeiss Apotome. The number of Tuj1 positive cells was counted with the help of ImageJ. RGCs were quantified by an observer blind to the treatment. At least 15 high magnification images were taken from different parts of each retina and the total viable RGC number was obtained by multiplying the average number per field of TUJ1+ cells in the ganglion cell layer by the retinal area.

Immunostaining of retina sections

Post fixed and cryoprotected eyes were snap frozen and then cryosectioned longitudinally (10µm). Standard immunostaining procedures were followed. Antibody specificity was confirmed by using secondary antibody alone for each staining. The details of the antibodies are as follows: anti-p53 (1:200, Leica); anti-MDM4 (1:50, Sigma); anti-MDM2 (1:200, Novus Biologicals); anti-Cre (1:500, Novus Biologicals); anti-Tuj1 (1:1000, Covance and Promega), anti-GFP (1:500, Abcam); anti-p53ac 373 (1:200, Millipore), anti-GFAP (1:1000,Millipore). Detailed protocols are available upon request.

Densitometry analysis

A high-resolution image was obtained at 40X magnification using the Zeiss Axioplan Microscope (Axiovert 200, Zeiss Inc.). Images for the same antigen groups were processed with the same exposure time. Assessment of fluorescence intensity was performed using AlphaEaseFC 4.0.1 software by measuring the intensities specifically from retinal ganglion cells. Care was taken that the area analysed for each cell was the same for each set, 100 cells from at least 6 sections per condition were quantified. The intensity values of each cell were normalized to the 4',6'-diamidino-2-phenylindole signal and mean values of intensities were calculated for each animal (at least three animals per condition)(Gaub *et al.*, 2011).

Evaluation of regenerating axons

Regenerating axons were counted as described previously(Leon *et al.*, 2000, Park *et al.*, 2008). Longitudinal sections of nerves were mounted and imaged at 40X. Every 4th section and at least 4 sections per animal were quantified by drawing lines perpendicular to the crush site at a distance of 200 µm, 300 µm, 500 µm, 750 µm, 1000 µm, 1500 µm from the

crush site. CtB positive axons between these sections were counted and the cross sectional width of every nerve was also measured. An observer blind to the treatment counted the regenerating fibres. The number of axon per millimetre was calculated and averaged over all the sections Σ_{ad} , the total number of axons extending distance d in a nerve having a radius of r , was estimated by summing over all sections having a thickness t (10 μm)

$$\Sigma_{ad} = \pi r^2 \times [\text{average axons/mm}]/t$$

Cerebellar Granule Neuron Culture

Cerebellar granule neurons (CGN) were prepared from cerebella of P7 MDM4^{ff} mice as described earlier (Bradke *et al.*, 2012, Gaub *et al.*, 2010). Briefly, the minced cerebella were incubated for 15 min at 37°C in an ionic medium with 0.025% trypsin and 0.05% DNase I (Sigma). Then trypsin inhibitor (0.04%, Sigma) was added followed by centrifugation. The pellet was triturated, centrifuged and suspended in the growth medium (basal Eagle's medium supplemented with 10% bovine calf serum, 25 mM KCl, 4 mM glutamine and gentamycin (100 ng/ml)). Cells were plated at a density of 1×10^5 cells on PDL/myelin ($4 \mu\text{g}/\text{cm}^2$) coated plates followed by infection with AV5-GFP/AV5-Cre. Cells were then fixed with 4% PFA 24 h later followed by staining with anti-Tuj1 and anti-Cre. At least 100 single transduced cells per condition ($n=4$) were traced manually with Neurolucida software.

Quantitative RT-PCR

Total RNA was extracted from CGN cells 24h after transduction with Trizol Reagent (Invitrogen). Complementary DNA (cDNA) was synthesized from 1 μg of RNA using oligo dT and SuperScriptTM II Reverse Transcriptase kit (Invitrogen). Complementary DNA (1 μl of 1:5 dilution) was used in a reverse transcriptase polymerase chain reaction using Master Mix (Invitrogen) and for quantitative reverse transcriptase polymerase chain reaction, SYBR-greenER (ThermoScientific) was used. RPL13a or 18SRNA were used as controls. Melting curve analysis ensured single amplified products. Primers sequences have been summarized in Table 2.

Retinal Ganglion cell culture

Dissociated retinal ganglion cell culture has been described previously (Gaub *et al.*, 2011). Shortly, P7 eyes were dissected, and retinae were incubated in Dulbecco's modified Eagle's medium with Papain (Worthington, USA) and L-Cystein (Sigma) for 40 min. After incubation, retinae were dissociated in Dulbecco's modified Eagle's medium with B27 (Life Technologies) and penicillin/streptomycin (Sigma). Cells were plated at a density of 1×10^6 cells per 2 cm^2 . Plated cell were immediately infected with AV-GFP and AV-Cre at 100 MOI.

Following incubation, cells were fixed with 4% paraformaldehyde for 20 min. Cells were then blocked with 8% bovine serum albumin, 0.1% TritonX-100 in phosphate-buffered saline and finally incubated with the primary antibodies overnight at 4°C: mouse anti-Tuj1 (1:1000, Promega). Cells were then washed with phosphate-buffered saline and incubated with appropriate secondary antibodies (1:1000, Invitrogen) for 1 h at room temperature. At least 10 images were taken at 20X magnification with Axioplan inverted microscope (Zeiss) and were automatically analysed for neurite outgrowth with ImageJ, NeuriteTrace plugin.

Immunoblotting

For immunoblotting, entire retinæ were collected 6h after Nutlin-3a injection and ONC and flash frozen. Upon thawing, proteins were extracted with RIPA buffer (.50mM Tris., 150mM NaCl, 2mM EDTA, 1%NP-40, 0.1% SDS, 0.1 mM PMSF, 1X Protease inhibitor (Roche), 1X PhosphoStop (Roche)). A portion of the lysate (30–50 mg of protein) was then fractionated by SDS-polyacrylamide gel electrophoresis, and the separated proteins were transferred to a nitrocellulose membrane and following blocking probed for different antigens, as follows. Rabbit anti-p53 (1:500, Santa-Cruz). Mouse anti- β -actin (Sigma) was used as a loading and transfer control. Immune complexes were detected with appropriate secondary antibodies (goat anti-rabbit IgG, goat anti-mouse IgG, label with horseradish peroxidase (Thermo Scientific, Germany) and chemiluminescence reagents (Pierce ECL Western blotting Substrate).

Viral injections into the sensorimotor cortex

MDM4^{ff} mice were anesthetized with ketamine and xylazine and then placed on a stereotactic frame. To infect layer V neurons, AAV1-GFP or AAV1-CreGFP under CMV promoter were injected with a 5 μ l Hamilton syringe in the right sensorimotor cortex 5 weeks before spinal cord injury. The viruses were injected after craniotomy in a total of 4 sites [0.8 μ l/site of AAV1-GFP or AAV1-CreGFP (3.1×10^9 gc/ μ l) (SignaGen, MD, USA)]. The coordinates used were 1.0 mm lateral, 0.6 mm deep, and +0.5, - 0.2, -0.7, and -1 mm with respect to bregma (Steward *et al.*, 2008).

Spinal cord injury surgical procedure and post-operative care

The experimental procedure followed for SCI has been described previously (Floriddia *et al.*, 2012). Briefly, anesthetized Mdm4^{ff} mice (ketamine/xylazine) were kept on a heating pad to maintain the body temperature at 37°C during the whole procedure. An incision was made on the thoracic area after shaving and cleaning with Softasep N (Braun). Muscle tissue right below the incision was dissected to expose laminae T8–T10. A dorsal hemisection at T9 until

the central canal was performed with a microknife (FST). To ensure that the lesion was complete, the microknife was passed throughout the dorsal part of the spinal cord several times. This kind of injury damages the dorsal and lateral CST, the dorsal columns, the rubrospinal, the dorsal and lateral raphe-spinal, and part of the reticulospinal tracts. After surgery, mice were placed back in their cages warmed up with an infrared light to prevent hypothermia. Mice underwent daily check for general health, mobility within the cage, wounds, swelling, infections, or autophagy of the toes throughout the experiment. The animals showed neither skin lesions nor autophagy throughout the study. Mice were injected subcutaneously with 1 ml of 0.9% saline twice daily for 3 d and once daily from days 4 to 7 after surgery. Bladders were manually expressed twice daily for the first week after operation and once daily until needed. 2 weeks following spinal injury, the animals were injected with 1.4 μ l of a 10% (wt/vol) solution of BDA (fluorescent biotin dextran tetramethylrhodamine-BDA (10,000 MW, Molecular Probes, 10% w/v in PBS) into four injection sites of the right sensorimotor cortex of the hind limb region to trace the CST as previously described(Simonen *et al.*, 2003).

Quantification of Corticospinal tract (CST) sprouting

2 weeks following tracer injection, mice were perfused transcardially with 0.1 M PBS, pH 7.4, and 4% PFA in PBS, pH 7.4 under deep anesthesia. For each animal, at least three consecutive sagittal cryosections (18 μ m) from the most ventral part of the spinal cord using the central canal as landmark were chosen and analyzed with the software AxioVision (Zeiss) to measure the CST dieback or Stereo-Investigator 7 (MBF Bioscience) to count axons, sprouts, and end bulbs. Dieback of the dorsomedial CST was measured as the distance between the axon bundle and the border of the lesion site identified by GFAP immunoreactivity(Shen *et al.*, 2009). The quantification of the sprouting and end-bulb indexes of the dorsomedial CST was performed proximal to the lesion site at rostral and caudal level. For each section, the BDA-labeled sprouts, end bulbs, and axons were counted live. The sum of the total number of labeled sprouts or bulbs was normalized to the total number of labeled axons above the lesion site counted in all the analyzed sections for each animal, obtaining an inter animal comparable ratio considering the individual tracing variability(Schnell and Schwab, 1993, Steward *et al.*, 2008). Sprouts and re-growing fibers were defined following the anatomical reported criteria(Steward *et al.*, 2003, Joosten and Bar, 1999, Hill *et al.*, 2004, Erturk *et al.*, 2007).

Immunohistochemistry for brain sections

Coronal sections from brains (40 μ m) were processed and stained in free-floating to detect GFP signal in the sensorimotor cortex. GFP signal was also enhanced using chicken anti-

GFP antibody (1:500, Abcam). Sections were also stained with anti-CTIP2 antibody (1:500, Abcam) to mark layer V neurons.

Retrograde labelling of RGCs for FACS and Affymetrix gene expression analysis

Dil (Molecular Probes, Invitrogen, 2% in DMF) was injected in the superior colliculus of P28 mice. Anesthetized mice were placed in a stereotaxic holder and approximately 2 μ L Dil was then injected directly into the superficial SC (4.5 mm caudal to Bregma, 0.5 mm lateral to sagittal suture and 1-2 mm deep to brain surface) via 10 μ l gastight syringe (Hamilton) connected to an automated nano-injector. 7 days after superior colliculus injection, the optic nerve crush was performed. Three days (72h) after crush, retinae were dissected and incubated in digestion solution (20 U/ml papain, Worthington; 1mM L-cysteine HCL; 0.004% DNase; 0.5 mM EDTA in Neurobasal) for 25-40 min at 37°C, with gentle shaking every 5 min. Digestion was stopped by adding Ovomuroid solution before trituration. Retinae were then passed through a 40 μ m filter. The obtained suspensions of the retinae were then FACS sorted. For microarray, total RNA was isolated from the FACS sorted RGCs using PureLink RNA micro kit (Invitrogen, Carlsbad, CA, USA) according to manufacturer's instructions. Affymetrix, Mouse Genome 430 2.0 Array from triplicate samples was performed at the Microarray Genechip Facility at Universitäts Klinikum, Tübingen. Data processing and analysis was performed according to standard procedures (GC-RMA, RMA, MAS5). Genes differentially expressed were selected based upon a 2 fold change cut-off and significant statistical difference (Anova with Bonferroni correction). The microarray data analysis was carried out by Ingenuity Pathway Analysis software (Ingenuity System Inc., Redwood City, CA, USA). Cluster analysis for selected probe sets was performed in R 3.0.1. Signal intensities were scaled and centered and the distance between two expression profiles was calculated using euclidian distance measure. Hierarchical cluster analysis was performed with average linkage for genes. Heatmaps were generated with Bioconductor package *gplots*.

Results

MDM4 conditional deletion stimulates robust optic nerve regeneration following ONC and CST axonal sprouting after spinal cord dorsal hemisection

We performed conditional deletion of MDM4 specifically in RGC by intravitreal injection of AAV2-CreGFP virus in MDM4^{fl/fl} mice two weeks before ONC, while an AAV2-GFP vector was employed as control (Fig. 1a). AAV2 infects RGCs very efficiently and rather specifically due to physical proximity although about 5-10% of other neuronal populations can also be infected. Significantly, MDM4 deletion promoted robust axonal regeneration of the optic

nerve as measured 28d after ONC (Fig. 1b, c), while it did not affect RGC survival (Fig. 1d, e).

MDM4 was expressed as expected in RGCs predominately in the cytoplasm, and its expression remained elevated after ONC (Supp. Fig. 1a, b). Following AAV2-cre mediated infection (Supp. Fig. 1c) and conditional deletion we could confirm a strong reduction of MDM4 expression in infected cells (Supp. Fig. 1d). Additionally, AAV-cre mediated genetic deletion of MDM4 in primary retinal cells determined by semi quantitative PCR confirmed MDM4 deletion (Supp. Fig. 1e). In order to seek for generalization of this regenerative phenotype to another non-sensory clinically relevant CNS fiber tract, we investigated whether MDM4 conditional deletion may enhance axonal sprouting and regeneration of the CST after SCI. To this end, we performed AAV1-creGFP mediated MDM4 conditional deletion in the sensorimotor cortex (SMC) of MDM4^{fl/fl} mice (Fig. 2a; Supp. Fig. 2a-b) and subsequently performed a thoracic dorsal spinal hemisection, which severs the main components of the CST. An AAV1-GFP virus was employed as control. Importantly, MDM4 was found highly expressed in the SMC including in layer V neurons (Supp. Fig. 2c-d). In line with the data in the optic nerve, we found significant axonal sprouting and regeneration after MDM4 conditional deletion while control-infected mice displayed the expected collapse of the CST before reaching the lesion site (Fig. 2b, c; Supp. Fig. 3a-b). Indeed, in control mice collapsing bulbs were more prominent and already seen more rostrally, i.e. not only at the CST cut margin (data not shown).

In support of the *in vivo* axonal regeneration findings, we investigated neurite outgrowth in cultured RGCs and cerebellar granule neurons (CGN) on both outgrowth permissive and myelin inhibitory conditions. AV-cre or AV-GFP control virus were employed to infect RGCs or CGN at the time of plating on poly-D-Lysine or myelin and neurite outgrowth was analysed at 72h and 24h respectively. Results showed that MDM4 deletion enhances neurite outgrowth in both RGC and CGN on both permissive and inhibitory substrates (Supp. Fig. 4). Together, these data suggest that MDM4 conditional deletion significantly lifts the CNS regenerative block enhancing axonal regeneration and sprouting after optic nerve and spinal injury in sensory and motor neurons respectively.

MDM4 conditional deletion enhances optic nerve regeneration via p53 and is phenocopied by MDM2/p53 inhibition

To gain mechanistic insight into the regenerative phenotype observed with MDM4 conditional deletion, we investigated the role of the MDM4 associated proteins p53 and MDM2. MDM4 typically keeps p53 transactivation under check (Marine and Jochemsen, 2005), as supported by our findings in primary neurons where conditional deletion of MDM4 (Supp. Fig. 5a) enhances p53-dependent gene targets, including axon growth associated genes (Supp. Fig.

5b). Similarly to MDM4, p53 was expressed mainly in the cytoplasm of RGC both before and after ONC (Supp. Fig. 6). Therefore, we hypothesized that MDM4 deletion could enhance the regeneration program via p53 transactivation. To this end, we investigated whether double conditional deletion of MDM4 and p53 would block the regenerative phenotype observed with MDM4 deletion. We performed AAV2-cre conditional deletion of MDM4 and p53 in RGCs simultaneously in double MDM4^{fl/fl}/p53^{fl/fl} mice (Fig. 3a) and found that this abolished axonal regeneration induced by MDM4 deletion alone as the number of axons past the crush site were now similar to AAV2-GFP control infected mice (Fig. 3b, c), while RGC survival remained unaffected. This demonstrates that p53 is required for MDM4-dependent axonal regeneration. Next, we further explored the central role of ubiquitin ligase related signalling in this regenerative phenotype. Thus, we asked whether modulation of the MDM4 binding protein and ubiquitin ligase MDM2, also strongly expressed in RGCs (Supp. Fig. 7), would be phenocopying axonal regeneration as seen upon deletion of MDM4. Given that MDM2 controls p53 protein levels by ubiquitination and proteasome degradation, we inhibited MDM2/p53 interaction by intravitreal injection of the well-characterized small molecule MDM2/p53 antagonist Nutlin-3a (Vassilev *et al.*, 2004). Importantly, Nutlin-3a (100 nM) delivery at the time of ONC and 7 days later (Fig. 4a) promoted robust axonal regeneration of the optic nerve to a similar extent to MDM4 deletion without affecting the survival of RGC 28d after crush (Fig. 4b-c, e-f). Administration of Nutlin-3a enhanced p53 protein levels in the retina as expected (Fig. 4g). To investigate by genetic approach whether MDM2/p53 inhibition promotes axonal regeneration via p53, we performed an analogous set of Nutlin-3a experiments, but in p53^{+/-} mice that typically retain only 25% of p53 expression and do not display aberrant cell metabolism as opposed to p53^{-/-} mice. This would also address whether a “minimum” threshold p53 expression level is required for axonal regeneration similarly to p53 dosage effect found in cancer (Boehme and Blattner, 2009). Data analysis revealed that axonal regeneration of the optic nerve after crush was significantly reduced in Nutlin-3a treated p53^{+/-} mice as compared to wildtype (Fig. 4b, d) further supporting the overall model where regeneration after deletion of MDM4 and inhibition of MDM2 both depend upon p53 transactivation. Indeed Nutlin-3a delivery in primary neurons enhanced p53 transactivation as shown by Q-RT-PCR (Supp. Fig. 8).

Optic nerve axonal regeneration after conditional MDM4 deletion depends upon the IGF1R pathway

Data so far point to a model where disruption of MDM4-MDM2/p53 inhibitory protein complex triggers axonal regeneration after ONC. To explore directly *in vivo* in RGCs whether MDM4 deletion would affect the gene expression program supporting the regenerative phenotype, we performed Affymetrix based genome wide gene expression arrays from fluorescently

activated sorted RGCs after ONC. Dil positive retrogradely traced RGCs were sorted three days after ONC from MDM4^{fl/fl} mice that underwent either AAV2-creGFP or AAV2-GFP control intravitreal injections (Fig. 5a, b). Functional data analysis of differentially regulated and statistically significant transcripts was performed with Ingenuity pathway analysis platform. Unsupervised hierarchical clustering of the gene expression data showed a clear separation of the gene expression profiles between AAV2-cre and AAV2-GFP cells (Fig. 5c). Additionally, Ingenuity pathway analysis revealed that conditional MDM4 deletion was associated with a number of receptor-dependent signalling cascades involved in cell growth and metabolism (Fig. 5d, Table 1, Supp. Table 1-2). Highly ranked differentially regulated signalling were p53 and the related GADD45 signalling pathways (Fig. 5d, Supp. Table 2), supporting our model so far. Of special interest was the MDM4-deletion dependent activation of insulin and insulin receptor signalling pathways via overexpression of IGF1R, since insulin-dependent pathways have a key role in cell growth and are highly neurotrophic. However, a function in axonal regeneration remains unclear. Careful analysis of IGF1R protein expression in RGCs revealed that in most cells where MDM4 deletion occurred, IGF1R levels were particularly elevated while in control AAV-GFP positive RGC, IGF1R was expressed at lower levels (Fig 5e). Next, we asked whether the IGF1R pathway might be critical for the downstream regenerative signalling elicited by conditional deletion of MDM4. Therefore, we decided to inhibit IGF1R signalling after MDM4 deletion and ONC. We chose to employ picropodophyllin (PPP), a highly selective and potent inhibitor of IGF-1R (IC₅₀=6 nM) that efficiently blocks IGF-1R activity and expression *in vivo* without noticeable toxicity. In preparation to the *in vivo* experiment, we performed a dose response analysis of PPP in primary neurons in permissive growth conditions and monitored toxicity (active cleaved caspase 3 positive neurons) and neurite outgrowth. This allowed identifying a dose between 10 nM and 1 μ M that efficiently inhibited neuronal outgrowth without resulting in significant toxicity (Supp. Fig. 9a, b). After AAV2-cre MDM4 conditional deletion in RGCs of MDM4^{fl/fl} mice (Fig. 6a), PPP 1 μ M was delivered both intra vitreal and at the site of the nerve crush at the time of ONC and optic nerve regeneration was evaluated at 28d post-injury. Indeed, PPP delivery strongly reduced the expression of IGF1R (Fig. 6b) and drastically inhibited optic nerve regeneration induced by MDM4 deletion, without affecting RGC survival (Fig. 6c-f). Together, these data show that deletion of MDM4 triggers optic nerve regeneration via IGF1R signaling.

Discussion

The reasons underlying lack of a neuronal intrinsic regenerative potential after CNS axonal injury seem to be found in an inhibitory molecular environment, which either exists prior to axonal injury or is elicited by it. The present work defines MDM4-MDM2/p53 as a

novel regeneration-repressive protein complex, whose disruption activates the axonal regenerative program via IGF1R signalling. Therefore, the discovery of MDM4-MDM2/p53-IGF1R signalling pathway contributes to clarify the causes for failed regeneration and may provide a target for regenerative therapy after optic nerve and spinal cord damage.

MDM4 was first identified as a p53 binding protein including in selected cancers where it inhibits p53 transcriptional activity promoting tumour progression (Markey, 2011). Similarly, MDM4 regulates cell cycle, survival and apoptosis by forming an inhibitory complex with a selected set of proteins that include MDM2, ASPP1 and 2, p300 and Smad1/2 (Gaub *et al.*, 2011, Sabbatini and McCormick, 2002, Wade *et al.*, 2010). However a role for MDM4 in neuronal biology and in axonal regrowth was until now missing. Our work shows that MDM4 lies at the centre of a regeneration-inhibitory signalling hub formed by MDM4-MDM2/p53. In fact conditional deletion of MDM4 enhances axonal regeneration and sprouting after ONC and SCI and co-deletion of p53 or inhibition of MDM2/p53 interaction significantly diminish the MDM4-deletion dependent regenerative phenotype.

We have recently shown that the tumour suppressor and transcription factor p53 is required for neurite outgrowth, axonal sprouting and regeneration both after facial nerve injury and spinal cord hemisection in mice (Tedeschi *et al.*, 2009a, Floriddia *et al.*, 2012, Tedeschi and Di Giovanni, 2009, Tedeschi *et al.*, 2009b, Di Giovanni *et al.*, 2006). Specifically, transcriptionally active acetylated p53 at K372-3-82 and the acetyltransferases CBP/p300 and P/CAF form a transcriptional complex that occupies promoters of selected pro-regenerative genes, driving neurite outgrowth. P53 integrates numerous stress signals including following axonal injury and it undergoes tight regulation of its protein levels, subcellular localization and of its transcriptional activity by several factors, including the best defined negatively regulators MDM2 and MDM4. MDM2, a E3 ubiquitin ligase, targets p53 for degradation via the ubiquitin proteasome pathway and negatively regulates p53 cytoplasmic-nuclear shuttling. MDM4, although structurally similar to MDM2, is devoid of ubiquitin ligase activity, and rather regulates with MDM2 p53 cytoplasmic-nuclear shuttling and it occupies the p53 transcriptional activation domain thereby inhibiting p53 transactivation. MDM4 prevents p53 nuclear translocation in association with MDM2 and competes with the acetyltransferases CBP and p300 for binding to Lysines on p53 C-terminus, overall hindering p53 transcriptional activity.

Given the pro-neurite outgrowth and axon regeneration function of the MDM4 interacting proteins p300 and Smads (Gaub *et al.*, Zou *et al.*, 2009, Parikh *et al.*), it is plausible that p300-dependent acetylation of regenerative promoters as well as TGF β -Smad signalling may also contribute to axonal regeneration induced by MDM4 deletion. In support of this, we have recently shown that p300 acetylates p53 in RGC after ONC during p300-dependent axonal regeneration, supporting the presence of this signalling network during

axonal regeneration(Gaub *et al.*, 2011). Given the axon regenerative/sprouting function of p21(Tanaka *et al.*, 2004), the previously described inhibitory MDM4 protein complex with p21(Markey), which is also a classical p53-target gene, may also play a role in axonal regeneration. Interestingly, we found that MDM4 deletion in primary neurons enhanced p21 gene expression levels along with other classical regeneration associated genes, supporting the inhibitory role for MDM4 in repressing the regenerative gene expression program.

Further, genome wide analysis from FACS sorted pure RGCs after ONC revealed that MDM4 conditional deletion was associated with the enhancement of transcripts involved in cytoskeleton remodelling, axonal development and signalling, including genes involved in neuronal maturation (Table 1). This pattern of gene expression changes suggests that MDM4 deletion modulates developmentally regulated pathways, which may support axonal regrowth.

Additionally, here we show that IGF1R signalling is required for axonal regeneration of the crushed optic nerve induced by MDM4 deletion and it lays likely downstream the transcriptional complex formed by MDM4-p53/MDM2. The best characterized IGF1R targets include PI3K and JAK/STAT3, which are typically activated by IGF1R (Kim *et al.*, 2012, Subbiah *et al.*, 2011, Staerk *et al.*, 2005, Serra *et al.*, 2007). Both PI3K and JAK/STAT3 activation depends upon the phosphorylation status that has been shown to be necessary to promote axonal regeneration following deletion of PTEN or after JAK binding to IL-6 respectively(Park *et al.*, 2008, Cao *et al.*, 2006, Shah *et al.*, 2006, Teng and Tang, 2006, Hakkoum *et al.*, 2007). This suggests a likely cross-talk between MDM4-MDM2/p53-IGF1R signalling and these regenerative pathways, supporting the importance and soundness of our novel findings.

Given that genetic inhibition of MDM4 or pharmacological antagonism of MDM2-p53 interaction have been shown to induce tumour suppression and are currently being explored in the clinic for cancer treatment(Brown *et al.*, 2009), they may represent viable options for neuroregenerative therapy. The recent discovery of specific small molecule inhibitors of MDM4(Vogel *et al.*, 2012, Reed *et al.*, 2010) which are still awaiting confirmation in multiple studies, may also expand our regenerative therapeutic options.

Acknowledgments

We would like to thank the Hertie Foundation for financial support (SDG); the DAAD PhD fellowship (MGS); Wings for Life (SDG). Additionally we are grateful to Marco Benevento for technical support for some of the experiments with neuronal cultures and Anja Wuttke for excellent technical assistance.

References

- Aguayo, A. J., David, S. & Bray, G. M. 1981. Influences of the glial environment on the elongation of axons after injury: transplantation studies in adult rodents. *J Exp Biol*, 95, 231-40.
- Aigner, L. & Caroni, P. 1993. Depletion of 43-kD growth-associated protein in primary sensory neurons leads to diminished formation and spreading of growth cones. *J Cell Biol*, 123, 417-29.
- Aigner, L. & Caroni, P. 1995. Absence of persistent spreading, branching, and adhesion in GAP-43-depleted growth cones. *J Cell Biol*, 128, 647-60.
- Benson, M. D., Romero, M. I., Lush, M. E., Lu, Q. R., Henkemeyer, M. & Parada, L. F. 2005. Ephrin-B3 is a myelin-based inhibitor of neurite outgrowth. *Proc Natl Acad Sci U S A*, 102, 10694-9.
- Berger, S. L. 2007. The complex language of chromatin regulation during transcription. *Nature*, 447, 407-412.
- Bernstein, D. R. & Stelzner, D. J. 1983. Plasticity of the corticospinal tract following midthoracic spinal injury in the postnatal rat. *J Comp Neurol*, 221, 382-400.
- Berton, O., Mcclung, C. A., Dileone, R. J., Krishnan, V., Renthal, W., Russo, S. J., Graham, D., Tsankova, N. M., Bolanos, C. A., Rios, M., Monteggia, L. M., Self, D. W. & Nestler, E. J. 2006. Essential Role of BDNF in the Mesolimbic Dopamine Pathway in Social Defeat Stress. *Science*, 311, 864-868.
- Blackmore, M. G., Wang, Z., Lerch, J. K., Motti, D., Zhang, Y. P., Shields, C. B., Lee, J. K., Goldberg, J. L., Lemmon, V. P. & Bixby, J. L. 2012. Kruppel-like Factor 7 engineered for transcriptional activation promotes axon regeneration in the adult corticospinal tract. *Proc Natl Acad Sci U S A*, 109, 7517-22.
- Boehme, K. A. & Blattner, C. 2009. Regulation of p53--insights into a complex process. *Crit Rev Biochem Mol Biol*, 44, 367-92.
- Bomze, H. M., Bulsara, K. R., Iskandar, B. J., Caroni, P. & Skene, J. H. 2001. Spinal axon regeneration evoked by replacing two growth cone proteins in adult neurons. *Nat Neurosci*, 4, 38-43.
- Bradbury, E. J. & McMahon, S. B. 2006. Spinal cord repair strategies: why do they work? *Nat Rev Neurosci*, 7, 644-653.
- Bradbury, E. J., Moon, L. D., Popat, R. J., King, V. R., Bennett, G. S., Patel, P. N., Fawcett, J. W. & McMahon, S. B. 2002. Chondroitinase ABC promotes functional recovery after spinal cord injury. *Nature*, 416, 636-40.
- Bradke, F., Fawcett, J. W. & Spira, M. E. 2012. Assembly of a new growth cone after axotomy: the precursor to axon regeneration. *Nat Rev Neurosci*, 13, 183-93.
- Bregman, B. S., Kunkel-Bagden, E., Mcate, M. & O'Neill, A. 1989. Extension of the critical period for developmental plasticity of the corticospinal pathway. *J Comp Neurol*, 282, 355-70.
- Brown, C. J., Lain, S., Verma, C. S., Fersht, A. R. & Lane, D. P. 2009. Awakening guardian angels: drugging the p53 pathway. *Nat Rev Cancer*, 9, 862-73.
- Buffo, A., Holtmaat, A. J., Savio, T., Verbeek, J. S., Oberdick, J., Oestreicher, A. B., Gispen, W. H., Verhaagen, J., Rossi, F. & Strata, P. 1997. Targeted overexpression of the neurite growth-associated protein B-50/GAP-43 in cerebellar Purkinje cells induces sprouting after axotomy but not axon regeneration into growth-permissive transplants. *J Neurosci*, 17, 8778-91.
- Butler, S. J. & Tear, G. 2007. Getting axons onto the right path: the role of transcription factors in axon guidance. *Development*, 134, 439-48.
- Cai, D., Deng, K., Mellado, W., Lee, J., Ratan, R. R. & Filbin, M. T. 2002. Arginase I and polyamines act downstream from cyclic AMP in overcoming inhibition of axonal growth MAG and myelin in vitro. *Neuron*, 35, 711-9.
- Cao, Z., Gao, Y., Bryson, J. B., Hou, J., Chaudhry, N., Siddiq, M., Martinez, J., Spencer, T., Carmel, J., Hart, R. B. & Filbin, M. T. 2006. The cytokine interleukin-6 is sufficient but

- not necessary to mimic the peripheral conditioning lesion effect on axonal growth. *J Neurosci*, 26, 5565-73.
- Carmichael, S. T., Archibeque, I., Luke, L., Nolan, T., Momiy, J. & Li, S. 2005. Growth-associated gene expression after stroke: evidence for a growth-promoting region in peri-infarct cortex. *Exp Neurol*, 193, 291-311.
- Caroni, P. & Grandes, P. 1990. Nerve sprouting in innervated adult skeletal muscle induced by exposure to elevated levels of insulin-like growth factors. *J Cell Biol*, 110, 1307-17.
- Carulli, D., Buffo, A., Botta, C., Altruda, F. & Strata, P. 2002. Regenerative and survival capabilities of Purkinje cells overexpressing c-Jun. *Eur J Neurosci*, 16, 105-18.
- Cheng, P.-L., Lu, H., Shelly, M., Gao, H. & Poo, M.-M. 2011. Phosphorylation of E3 Ligase Smurf1 Switches Its Substrate Preference in Support of Axon Development. *Neuron*, 69, 231-243.
- Cho, K. S., Yang, L., Lu, B., Feng Ma, H., Huang, X., Pekny, M. & Chen, D. F. 2005. Re-establishing the regenerative potential of central nervous system axons in postnatal mice. *J Cell Sci*, 118, 863-72.
- David, S. & Aguayo, A. J. 1981. Axonal elongation into peripheral nervous system "bridges" after central nervous system injury in adult rats. *Science*, 214, 931-3.
- Di Giovanni, S. 2009. Molecular targets for axon regeneration: focus on the intrinsic pathways. *Expert Opin Ther Targets*, 13, 1387-98.
- Di Giovanni, S., Faden, A. I., Yakovlev, A., Duke-Cohan, J. S., Finn, T., Thouin, M., Knobloch, S., De Biase, A., Bregman, B. S. & Hoffman, E. P. 2005. Neuronal plasticity after spinal cord injury: identification of a gene cluster driving neurite outgrowth. *FASEB J*, 19, 153-4.
- Di Giovanni, S., Knights, C. D., Rao, M., Yakovlev, A., Beers, J., Catania, J., Avantaggiati, M. L. & Faden, A. I. 2006. The tumor suppressor protein p53 is required for neurite outgrowth and axon regeneration. *EMBO J*, 25, 4084-96.
- Di Giovanni, S. & Rathore, K. 2012. p53-Dependent pathways in neurite outgrowth and axonal regeneration. *Cell Tissue Res*, 349, 87-95.
- Dokmanovic, M., Clarke, C. & Marks, P. A. 2007. Histone deacetylase inhibitors: overview and perspectives. *Mol Cancer Res*, 5, 981-9.
- Erturk, A., Hellal, F., Enes, J. & Bradke, F. 2007. Disorganized microtubules underlie the formation of retraction bulbs and the failure of axonal regeneration. *J Neurosci*, 27, 9169-80.
- Eva, R., Andrews, M. R., Franssen, E. H. & Fawcett, J. W. 2012. Intrinsic mechanisms regulating axon regeneration: an integrin perspective. *Int Rev Neurobiol*, 106, 75-104.
- Fischer, D., Heiduschka, P. & Thanos, S. 2001. Lens-injury-stimulated axonal regeneration throughout the optic pathway of adult rats. *Exp Neurol*, 172, 257-72.
- Fishman, H. M. & Bittner, G. D. 2003. Vesicle-mediated restoration of a plasmalemmal barrier in severed axons. *News Physiol Sci*, 18, 115-8.
- Floriddia, E. M., Rathore, K. I., Tedeschi, A., Quadrato, G., Wuttke, A., Lueckmann, J. M., Kigerl, K. A., Popovich, P. G. & Di Giovanni, S. 2012. p53 Regulates the Neuronal Intrinsic and Extrinsic Responses Affecting the Recovery of Motor Function following Spinal Cord Injury. *J Neurosci*, 32, 13956-70.
- Francoz, S., Froment, P., Bogaerts, S., De Clercq, S., Maetens, M., Doumont, G., Bellefroid, E. & Marine, J. C. 2006. Mdm4 and Mdm2 cooperate to inhibit p53 activity in proliferating and quiescent cells in vivo. *Proc Natl Acad Sci U S A*, 103, 3232-7.
- Fraser, P. & Bickmore, W. 2007. Nuclear organization of the genome and the potential for gene regulation. *Nature*, 447, 413-417.
- Gao, Y., Deng, K., Hou, J., Bryson, J. B., Barco, A., Nikulina, E., Spencer, T., Mellado, W., Kandel, E. R. & Filbin, M. T. 2004. Activated CREB is sufficient to overcome inhibitors in myelin and promote spinal axon regeneration in vivo. *Neuron*, 44, 609-21.
- Gaub, P., Joshi, Y., Wuttke, A., Naumann, U., Schnichels, S., Heiduschka, P. & Di Giovanni, S. The histone acetyltransferase p300 promotes intrinsic axonal regeneration. *Brain*, 134, 2134-48.

- Gaub, P., Joshi, Y., Wuttke, A., Naumann, U., Schnichels, S., Heiduschka, P. & Di Giovanni, S. 2011. The histone acetyltransferase p300 promotes intrinsic axonal regeneration. *Brain*, 134, 2134-48.
- Gaub, P., Tedeschi, A., Puttagunta, R., Nguyen, T., Schmandke, A. & Di Giovanni, S. 2010. HDAC inhibition promotes neuronal outgrowth and counteracts growth cone collapse through CBP/p300 and P/CAF-dependent p53 acetylation. *Cell Death Differ*, 17, 1392-408.
- Giovanni, S. D. 2009. Molecular targets for axon regeneration: focus on the intrinsic pathways. *Expert Opinion on Therapeutic Targets*, 13, 1387-1398.
- Girnita, A., Girnita, L., Del Prete, F., Bartolazzi, A., Larsson, O. & Axelson, M. 2004. Cyclolignans as inhibitors of the insulin-like growth factor-1 receptor and malignant cell growth. *Cancer Res*, 64, 236-42.
- Gloster, A., Wu, W., Speelman, A., Weiss, S., Causing, C., Pozniak, C., Reynolds, B., Chang, E., Toma, J. G. & Miller, F. D. 1994. The T alpha 1 alpha-tubulin promoter specifies gene expression as a function of neuronal growth and regeneration in transgenic mice. *J Neurosci*, 14, 7319-30.
- Goldberg, J. L., Klassen, M. P., Hua, Y. & Barres, B. A. 2002. Amacrine-signaled loss of intrinsic axon growth ability by retinal ganglion cells. *Science*, 296, 1860-4.
- Grieger, J. C., Choi, V. W. & Samulski, R. J. 2006. Production and characterization of adeno-associated viral vectors. *Nat. Protocols*, 1, 1412-1428.
- Grier, J. D., Xiong, S., Elizondo-Fraire, A. C., Parant, J. M. & Lozano, G. 2006. Tissue-specific differences of p53 inhibition by Mdm2 and Mdm4. *Mol Cell Biol*, 26, 192-8.
- Hakkoum, D., Stoppini, L. & Muller, D. 2007. Interleukin-6 promotes sprouting and functional recovery in lesioned organotypic hippocampal slice cultures. *J Neurochem*, 100, 747-57.
- Hall, A. 1998. Rho GTPases and the actin cytoskeleton. *Science*, 279, 509-14.
- Hanz, S. & Fainzilber, M. 2006. Retrograde signaling in injured nerve--the axon reaction revisited. *J Neurochem*, 99, 13-9.
- Hanz, S., Perlson, E., Willis, D., Zheng, J. Q., Massarwa, R., Huerta, J. J., Koltzenburg, M., Kohler, M., Van-Minnen, J., Twiss, J. L. & Fainzilber, M. 2003. Axoplasmic importins enable retrograde injury signaling in lesioned nerve. *Neuron*, 40, 1095-104.
- Hellstrom, M., Muhling, J., Ehlert, E. M., Verhaagen, J., Pollett, M. A., Hu, Y. & Harvey, A. R. 2011. Negative impact of rAAV2 mediated expression of SOCS3 on the regeneration of adult retinal ganglion cell axons. *Mol Cell Neurosci*, 46, 507-15.
- Herdegen, T., Skene, P. & Bahr, M. 1997. The c-Jun transcription factor--bipotential mediator of neuronal death, survival and regeneration. *Trends Neurosci*, 20, 227-31.
- Hill, C. E., Proschel, C., Noble, M., Mayer-Proschel, M., Gensel, J. C., Beattie, M. S. & Bresnahan, J. C. 2004. Acute transplantation of glial-restricted precursor cells into spinal cord contusion injuries: survival, differentiation, and effects on lesion environment and axonal regeneration. *Exp Neurol*, 190, 289-310.
- Hollis, E. R., 2nd, Jamshidi, P., Low, K., Blesch, A. & Tuszynski, M. H. 2009. Induction of corticospinal regeneration by lentiviral trkB-induced Erk activation. *Proc Natl Acad Sci U S A*, 106, 7215-20.
- Joosten, E. A. & Bar, D. P. 1999. Axon guidance of outgrowing corticospinal fibres in the rat. *J Anat*, 194 (Pt 1), 15-32.
- Kadakia, M., Brown, T. L., Mcgorry, M. M. & Berberich, S. J. 2002. MdmX inhibits Smad transactivation. *Oncogene*, 21, 8776-85.
- Kamiguchi, H. & Lemmon, V. 2000. Recycling of the cell adhesion molecule L1 in axonal growth cones. *J Neurosci*, 20, 3676-86.
- Kim, A. H., Puram, S. V., Bilimoria, P. M., Ikeuchi, Y., Keough, S., Wong, M., Rowitch, D. & Bonni, A. 2009. A centrosomal Cdc20-APC pathway controls dendrite morphogenesis in postmitotic neurons. *Cell*, 136, 322-36.
- Kim, J. G., Kang, M. J., Yoon, Y. K., Kim, H. P., Park, J., Song, S. H., Han, S. W., Park, J. W., Kang, G. H., Kang, K. W., Oh Do, Y., Im, S. A., Bang, Y. J., Yi, E. C. & Kim, T. Y. 2012. Heterodimerization of glycosylated insulin-like growth factor-1 receptors and

- insulin receptors in cancer cells sensitive to anti-IGF1R antibody. *PLoS One*, 7, e33322.
- Kimura, K., Mizoguchi, A. & Ide, C. 2003. Regulation of growth cone extension by SNARE proteins. *J Histochem Cytochem*, 51, 429-33.
- Knoops, B. & Octave, J. N. 1997. Alpha 1-tubulin mRNA level is increased during neurite outgrowth of NG 108-15 cells but not during neurite outgrowth inhibition by CNS myelin. *Neuroreport*, 8, 795-8.
- Konishi, Y., Stegmuller, J., Matsuda, T., Bonni, S. & Bonni, A. 2004. Cdh1-APC controls axonal growth and patterning in the mammalian brain. *Science*, 303, 1026-30.
- Lane, M. A. & Bailey, S. J. 2005. Role of retinoid signalling in the adult brain. *Prog Neurobiol*, 75, 275-93.
- Leaver, S. G., Cui, Q., Plant, G. W., Arulpragasam, A., Hisheh, S., Verhaagen, J. & Harvey, A. R. 2006. AAV-mediated expression of CNTF promotes long-term survival and regeneration of adult rat retinal ganglion cells. *Gene Ther*, 13, 1328-41.
- Lee, J. K., Geoffroy, C. G., Chan, A. F., Tolentino, K. E., Crawford, M. J., Leal, M. A., Kang, B. & Zheng, B. 2010. Assessing spinal axon regeneration and sprouting in Nogo-, MAG-, and OMgp-deficient mice. *Neuron*, 66, 663-70.
- Leibinger, M., Muller, A., Andreadaki, A., Hauk, T. G., Kirsch, M. & Fischer, D. 2009. Neuroprotective and axon growth-promoting effects following inflammatory stimulation on mature retinal ganglion cells in mice depend on ciliary neurotrophic factor and leukemia inhibitory factor. *J Neurosci*, 29, 14334-41.
- Leon, S., Yin, Y., Nguyen, J., Irwin, N. & Benowitz, L. I. 2000. Lens injury stimulates axon regeneration in the mature rat optic nerve. *J Neurosci*, 20, 4615-26.
- Liu, K., Lu, Y., Lee, J. K., Samara, R., Willenberg, R., Sears-Kraxberger, I., Tedeschi, A., Park, K. K., Jin, D., Cai, B., Xu, B., Connolly, L., Steward, O., Zheng, B. & He, Z. 2010. PTEN deletion enhances the regenerative ability of adult corticospinal neurons. *Nat Neurosci*, 13, 1075-81.
- Liu, K., Tedeschi, A., Park, K. K. & He, Z. 2011. Neuronal intrinsic mechanisms of axon regeneration. *Annu Rev Neurosci*, 34, 131-52.
- Liu, R., Chen, X. P. & Tao, L. Y. 2008. Regulation of axonal regeneration following the central nervous system injury in adult mammalian. *Neurosci Bull*, 24, 395-400.
- Llinas, R. R. 2003. The contribution of Santiago Ramon y Cajal to functional neuroscience. *Nat Rev Neurosci*, 4, 77-80.
- Lu, P. & Tuszynski, M. H. 2008. Growth factors and combinatorial therapies for CNS regeneration. *Exp Neurol*, 209, 313-20.
- Makwana, M. & Raivich, G. 2005. Molecular mechanisms in successful peripheral regeneration. *FEBS J*, 272, 2628-38.
- Marine, J. C. 2011. MDM2 and MDMX in cancer and development. *Curr Top Dev Biol*, 94, 45-75.
- Marine, J. C. & Jochemsen, A. G. 2004. Mdmx and Mdm2: brothers in arms? *Cell Cycle*, 3, 900-4.
- Marine, J. C. & Jochemsen, A. G. 2005. Mdmx as an essential regulator of p53 activity. *Biochem Biophys Res Commun*, 331, 750-60.
- Markey, M. P. Regulation of MDM4. *Front Biosci*, 16, 1144-56.
- Markey, M. P. 2011. Regulation of MDM4. *Front Biosci*, 16, 1144-56.
- Mckerracher, L., David, S., Jackson, D. L., Kottis, V., Dunn, R. J. & Braun, P. E. 1994. Identification of myelin-associated glycoprotein as a major myelin-derived inhibitor of neurite growth. *Neuron*, 13, 805-11.
- Moore, D. L., Blackmore, M. G., Hu, Y., Kaestner, K. H., Bixby, J. L., Lemmon, V. P. & Goldberg, J. L. 2009. KLF Family Members Regulate Intrinsic Axon Regeneration Ability. *Science*, 326, 298-301.
- Moreau-Fauvarque, C., Kumanogoh, A., Camand, E., Jaillard, C., Barbin, G., Boquet, I., Love, C., Jones, E. Y., Kikutani, H., Lubetzki, C., Dusart, I. & Chedotal, A. 2003. The transmembrane semaphorin Sema4D/CD100, an inhibitor of axonal growth, is

- expressed on oligodendrocytes and upregulated after CNS lesion. *J Neurosci*, 23, 9229-39.
- Morgenstern, D. A., Asher, R. A. & Fawcett, J. W. 2002. Chondroitin sulphate proteoglycans in the CNS injury response. *Prog Brain Res*, 137, 313-32.
- Mukhopadhyay, G., Doherty, P., Walsh, F. S., Crocker, P. R. & Filbin, M. T. 1994. A novel role for myelin-associated glycoprotein as an inhibitor of axonal regeneration. *Neuron*, 13, 757-67.
- Muller, A., Hauk, T. G., Leibinger, M., Marienfeld, R. & Fischer, D. 2009. Exogenous CNTF stimulates axon regeneration of retinal ganglion cells partially via endogenous CNTF. *Mol Cell Neurosci*, 41, 233-46.
- Nadeau, S., Hein, P., Fernandes, K. J., Peterson, A. C. & Miller, F. D. 2005. A transcriptional role for C/EBP beta in the neuronal response to axonal injury. *Mol Cell Neurosci*, 29, 525-35.
- Naeve, G. S., Ramakrishnan, M., Kramer, R., Hevroni, D., Citri, Y. & Theill, L. E. 1997. Neuritin: a gene induced by neural activity and neurotrophins that promotes neurite outgrowth. *Proc Natl Acad Sci U S A*, 94, 2648-53.
- Nakazawa, T., Tamai, M. & Mori, N. 2002. Brain-derived neurotrophic factor prevents axotomized retinal ganglion cell death through MAPK and PI3K signaling pathways. *Invest Ophthalmol Vis Sci*, 43, 3319-26.
- Oblinger, M. & Lasek, R. 1984. A conditioning lesion of the peripheral axons of dorsal root ganglion cells accelerates regeneration of only their peripheral axons. *The Journal of Neuroscience*, 4, 1736-1744.
- Ogryzko, V. V., Schiltz, R. L., Russanova, V., Howard, B. H. & Nakatani, Y. 1996. The transcriptional coactivators p300 and CBP are histone acetyltransferases. *Cell*, 87, 953-9.
- Panicker, A. K., Buhusi, M., Thelen, K. & Maness, P. F. 2003. Cellular signalling mechanisms of neural cell adhesion molecules. *Front Biosci*, 8, d900-11.
- Parikh, P., Hao, Y., Hosseinkhani, M., Patil, S. B., Huntley, G. W., Tessier-Lavigne, M. & Zou, H. Regeneration of axons in injured spinal cord by activation of bone morphogenetic protein/Smad1 signaling pathway in adult neurons. *Proc Natl Acad Sci U S A*, 108, E99-107.
- Park, K. K., Liu, K., Hu, Y., Kanter, J. L. & He, Z. 2010. PTEN/mTOR and axon regeneration. *Exp Neurol*, 223, 45-50.
- Park, K. K., Liu, K., Hu, Y., Smith, P. D., Wang, C., Cai, B., Xu, B., Connolly, L., Kramvis, I., Sahin, M. & He, Z. 2008. Promoting axon regeneration in the adult CNS by modulation of the PTEN/mTOR pathway. *Science*, 322, 963-6.
- Perlson, E., Hanz, S., Ben-Yaakov, K., Segal-Ruder, Y., Seger, R. & Fainzilber, M. 2005. Vimentin-dependent spatial translocation of an activated MAP kinase in injured nerve. *Neuron*, 45, 715-26.
- Pernet, V. & Di Polo, A. 2006. Synergistic action of brain-derived neurotrophic factor and lens injury promotes retinal ganglion cell survival, but leads to optic nerve dystrophy in vivo. *Brain*, 129, 1014-26.
- Pernet, V., Hauswirth, W. W. & Di Polo, A. 2005. Extracellular signal-regulated kinase 1/2 mediates survival, but not axon regeneration, of adult injured central nervous system neurons in vivo. *J Neurochem*, 93, 72-83.
- Puttagunta, R. & Di Giovanni, S. 2011. Retinoic acid signaling in axonal regeneration. *Front Mol Neurosci*, 4, 59.
- Puttagunta, R., Schmandke, A., Floriddia, E., Gaub, P., Fomin, N., Ghyselinck, N. B. & Di Giovanni, S. 2011. RA-RAR-beta counteracts myelin-dependent inhibition of neurite outgrowth via Lingo-1 repression. *J Cell Biol*, 193, 1147-56.
- Qin, Q., Liao, G., Baudry, M. & Bi, X. 2010a. Cholesterol Perturbation in Mice Results in p53 Degradation and Axonal Pathology through p38 MAPK and Mdm2 Activation. *PLoS One*, 5, e9999.

- Qin, Q., Liao, G., Baudry, M. & Bi, X. 2010b. Role of calpain-mediated p53 truncation in semaphorin 3A-induced axonal growth regulation. *Proc Natl Acad Sci U S A*, 107, 13883-7.
- Raivich, G. & Behrens, A. 2006. Role of the AP-1 transcription factor c-Jun in developing, adult and injured brain. *Prog Neurobiol*, 78, 347-63.
- Raivich, G., Bohatschek, M., Da Costa, C., Iwata, O., Galiano, M., Hristova, M., Nateri, A. S., Makwana, M., Riera-Sans, L., Wolfer, D. P., Lipp, H. P., Aguzzi, A., Wagner, E. F. & Behrens, A. 2004. The AP-1 transcription factor c-Jun is required for efficient axonal regeneration. *Neuron*, 43, 57-67.
- Reed, D., Shen, Y., Shelat, A. A., Arnold, L. A., Ferreira, A. M., Zhu, F., Mills, N., Smithson, D. C., Regni, C. A., Bashford, D., Cicero, S. A., Schulman, B. A., Jochemsen, A. G., Guy, R. K. & Dyer, M. A. 2010. Identification and characterization of the first small molecule inhibitor of MDMX. *J Biol Chem*, 285, 10786-96.
- Reichardt, L. F. 2006. Neurotrophin-regulated signalling pathways. *Philos Trans R Soc Lond B Biol Sci*, 361, 1545-64.
- Richardson, P. M., Mcguinness, U. M. & Aguayo, A. J. 1980. Axons from CNS neurons regenerate into PNS grafts. *Nature*, 284, 264-5.
- Rishal, I., Michaelevski, I., Rozenbaum, M., Shinder, V., Medzihradzky, K. F., Burlingame, A. L. & Fainzilber, M. 2010. Axoplasm isolation from peripheral nerve. *Dev Neurobiol*, 70, 126-33.
- Rowland, B. D., Bernards, R. & Peeper, D. S. 2005. The KLF4 tumour suppressor is a transcriptional repressor of p53 that acts as a context-dependent oncogene. *Nat Cell Biol*, 7, 1074-1082.
- Sabbatini, P. & McCormick, F. 2002. MDMX inhibits the p300/CBP-mediated acetylation of p53. *DNA Cell Biol*, 21, 519-25.
- Saha, R. N. & Pahan, K. 2005. HATs and HDACs in neurodegeneration: a tale of disconcerted acetylation homeostasis. *Cell Death Differ*, 13, 539-550.
- Saha, R. N. & Pahan, K. 2006. HATs and HDACs in neurodegeneration: a tale of disconcerted acetylation homeostasis. *Cell Death Differ*, 13, 539-50.
- Santiago Ramón Y Cajal, J. D., Edward G. Jones 1991. *Cajal's Degeneration and Regeneration of the Nervous System*, Oxford, Oxford University Press.
- Schlaepfer, W. W. & Bunge, R. P. 1973. Effects of calcium ion concentration on the degeneration of amputated axons in tissue culture. *J Cell Biol*, 59, 456-70.
- Schmandke, A. & Strittmatter, S. M. 2007. ROCK and Rho: biochemistry and neuronal functions of Rho-associated protein kinases. *Neuroscientist*, 13, 454-69.
- Schnell, L. & Schwab, M. E. 1993. Sprouting and regeneration of lesioned corticospinal tract fibres in the adult rat spinal cord. *Eur J Neurosci*, 5, 1156-71.
- Schwab, M. E. & Thoenen, H. 1985. Dissociated neurons regenerate into sciatic but not optic nerve explants in culture irrespective of neurotrophic factors. *J Neurosci*, 5, 2415-23.
- Schwamborn, J. C., Muller, M., Becker, A. H. M. & Puschel, A. W. 2007. Ubiquitination of the GTPase Rap1B by the ubiquitin ligase Smurf2 is required for the establishment of neuronal polarity. *EMBO J*, 26, 1410-1422.
- Seiffers, R., Mills, C. D. & Woolf, C. J. 2007. ATF3 increases the intrinsic growth state of DRG neurons to enhance peripheral nerve regeneration. *J Neurosci*, 27, 7911-20.
- Serra, C., Palacios, D., Mozzetta, C., Forcales, S. V., Morante, I., Ripani, M., Jones, D. R., Du, K., Jhala, U. S., Simone, C. & Puri, P. L. 2007. Functional interdependence at the chromatin level between the MKK6/p38 and IGF1/PI3K/AKT pathways during muscle differentiation. *Mol Cell*, 28, 200-13.
- Shah, M., Patel, K., Mukhopadhyay, S., Xu, F., Guo, G. & Sehgal, P. B. 2006. Membrane-associated STAT3 and PY-STAT3 in the cytoplasm. *J Biol Chem*, 281, 7302-8.
- Shen, Y., Tenney, A. P., Busch, S. A., Horn, K. P., Cuascat, F. X., Liu, K., He, Z., Silver, J. & Flanagan, J. G. 2009. PTPsigma is a receptor for chondroitin sulfate proteoglycan, an inhibitor of neural regeneration. *Science*, 326, 592-6.

- Shin, J. E., Cho, Y., Beirowski, B., Milbrandt, J., Cavalli, V. & Diantonio, A. 2012. Dual leucine zipper kinase is required for retrograde injury signaling and axonal regeneration. *Neuron*, 74, 1015-22.
- Silver, J. & Miller, J. H. 2004. Regeneration beyond the glial scar. *Nat Rev Neurosci*, 5, 146-56.
- Simonen, M., Pedersen, V., Weinmann, O., Schnell, L., Buss, A., Ledermann, B., Christ, F., Sansig, G., Van Der Putten, H. & Schwab, M. E. 2003. Systemic Deletion of the Myelin-Associated Outgrowth Inhibitor Nogo-A Improves Regenerative and Plastic Responses after Spinal Cord Injury. *Neuron*, 38, 201-211.
- Smith, P. D., Sun, F., Park, K. K., Cai, B., Wang, C., Kuwako, K., Martinez-Carrasco, I., Connolly, L. & He, Z. 2009. SOCS3 deletion promotes optic nerve regeneration in vivo. *Neuron*, 64, 617-23.
- Spencer, T. & Filbin, M. T. 2004. A role for cAMP in regeneration of the adult mammalian CNS. *J Anat*, 204, 49-55.
- Staerk, J., Kallin, A., Demoulin, J. B., Vainchenker, W. & Constantinescu, S. N. 2005. JAK1 and Tyk2 activation by the homologous polycythemia vera JAK2 V617F mutation: cross-talk with IGF1 receptor. *J Biol Chem*, 280, 41893-9.
- Steward, O., Zheng, B. & Tessier-Lavigne, M. 2003. False resurrections: distinguishing regenerated from spared axons in the injured central nervous system. *J Comp Neurol*, 459, 1-8.
- Steward, O., Zheng, B., Tessier-Lavigne, M., Hofstadter, M., Sharp, K. & Yee, K. M. 2008. Regenerative growth of corticospinal tract axons via the ventral column after spinal cord injury in mice. *J Neurosci*, 28, 6836-47.
- Subbiah, V., Naing, A., Brown, R. E., Chen, H., Doyle, L., Lorusso, P., Benjamin, R., Anderson, P. & Kurzrock, R. 2011. Targeted morphoproteomic profiling of Ewing's sarcoma treated with insulin-like growth factor 1 receptor (IGF1R) inhibitors: response/resistance signatures. *PLoS One*, 6, e18424.
- Sun, F., Park, K. K., Belin, S., Wang, D., Lu, T., Chen, G., Zhang, K., Yeung, C., Feng, G., Yankner, B. A. & He, Z. 2011. Sustained axon regeneration induced by co-deletion of PTEN and SOCS3. *Nature*, 480, 372-5.
- Tanaka, H., Yamashita, T., Yachi, K., Fujiwara, T., Yoshikawa, H. & Tohyama, M. 2004. Cytoplasmic p21(Cip1/WAF1) enhances axonal regeneration and functional recovery after spinal cord injury in rats. *Neuroscience*, 127, 155-64.
- Tedeschi, A. 2011. Tuning the orchestra: transcriptional pathways controlling axon regeneration. *Front Mol Neurosci*, 4, 60.
- Tedeschi, A. & Di Giovanni, S. 2009. The non-apoptotic role of p53 in neuronal biology: enlightening the dark side of the moon. *EMBO Rep*, 10, 576-83.
- Tedeschi, A., Nguyen, T., Puttagunta, R., Gaub, P. & Di Giovanni, S. 2009a. A p53-CBP/p300 transcription module is required for GAP-43 expression, axon outgrowth, and regeneration. *Cell Death Differ*, 16, 543-54.
- Tedeschi, A., Nguyen, T., Steele, S. U., Feil, S., Naumann, U., Feil, R. & Di Giovanni, S. 2009b. The tumor suppressor p53 transcriptionally regulates cGKI expression during neuronal maturation and is required for cGMP-dependent growth cone collapse. *J Neurosci*, 29, 15155-60.
- Teng, F. Y. & Tang, B. L. 2006. Axonal regeneration in adult CNS neurons--signaling molecules and pathways. *J Neurochem*, 96, 1501-8.
- Toledo, F. & Wahl, G. M. 2006. Regulating the p53 pathway: in vitro hypotheses, in vivo veritas. *Nat Rev Cancer*, 6, 909-23.
- Vassilev, L. T., Vu, B. T., Graves, B., Carvajal, D., Podlaski, F., Filipovic, Z., Kong, N., Kammlott, U., Lukacs, C., Klein, C., Fotouhi, N. & Liu, E. A. 2004. In vivo activation of the p53 pathway by small-molecule antagonists of MDM2. *Science*, 303, 844-8.
- Vogel, S. M., Bauer, M. R., Joerger, A. C., Wilcken, R., Brandt, T., Veprintsev, D. B., Rutherford, T. J., Fersht, A. R. & Boeckler, F. M. 2012. Lithocholic acid is an endogenous inhibitor of MDM4 and MDM2. *Proc Natl Acad Sci U S A*, 109, 16906-10.

- Wade, M., Wang, Y. V. & Wahl, G. M. 2010. The p53 orchestra: Mdm2 and Mdmx set the tone. *Trends Cell Biol*, 20, 299-309.
- Wang, H.-R., Zhang, Y., Ozdamar, B., Ogunjimi, A. A., Alexandrova, E., Thomsen, G. H. & Wrana, J. L. 2003. Regulation of Cell Polarity and Protrusion Formation by Targeting RhoA for Degradation. *Science*, 302, 1775-1779.
- Wang, K. C., Koprivica, V., Kim, J. A., Sivasankaran, R., Guo, Y., Neve, R. L. & He, Z. 2002. Oligodendrocyte-myelin glycoprotein is a Nogo receptor ligand that inhibits neurite outgrowth. *Nature*, 417, 941-4.
- Windle, W. F. 1980. Inhibition of regeneration of severed axons in the spinal cord. *Exp Neurol*, 69, 209-11.
- Yamada, T., Yang, Y. & Bonni, A. 2013. Spatial organization of ubiquitin ligase pathways orchestrates neuronal connectivity. *Trends Neurosci*, 36, 218-26.
- Yang, X. J. & Seto, E. 2007. HATs and HDACs: from structure, function and regulation to novel strategies for therapy and prevention. *Oncogene*, 26, 5310-8.
- Yin, Y., Cui, Q., Li, Y., Irwin, N., Fischer, D., Harvey, A. R. & Benowitz, L. I. 2003. Macrophage-derived factors stimulate optic nerve regeneration. *J Neurosci*, 23, 2284-93.
- Yiu, G. & He, Z. 2006. Glial inhibition of CNS axon regeneration. *Nat Rev Neurosci*, 7, 617-27.
- Yudin, D., Hanz, S., Yoo, S., Iavnilovitch, E., Willis, D., Gradus, T., Vuppalanchi, D., Segal-Ruder, Y., Ben-Yaakov, K., Hieda, M., Yoneda, Y., Twiss, J. L. & Fainzilber, M. 2008. Localized regulation of axonal RanGTPase controls retrograde injury signaling in peripheral nerve. *Neuron*, 59, 241-52.
- Zhou, F. Q. & Snider, W. D. 2006. Intracellular control of developmental and regenerative axon growth. *Philos Trans R Soc Lond B Biol Sci*, 361, 1575-92.
- Zou, H., Ho, C., Wong, K. & Tessier-Lavigne, M. 2009. Axotomy-induced Smad1 activation promotes axonal growth in adult sensory neurons. *J Neurosci*, 29, 7116-23.
- Zweifel, L. S., Kuruvilla, R. & Ginty, D. D. 2005. Functions and mechanisms of retrograde neurotrophin signalling. *Nat Rev Neurosci*, 6, 615-25.

Figure Legends

Figure 1. **Conditional deletion of MDM4 in retinal ganglion cells enhances axonal regeneration after optic nerve crush**

a. Schematic of the experimental design showing AAV-Cre or AAV-GFP intra-vitreous infection of RGC in MDM4^{ff} mice 14 days before optic nerve crush. Regenerating axons were traced with Cholera toxin B (CtB). **b.** High magnification images of regenerating CtB labeled optic nerve axons 28d post-crush (asterisk) in MDM4^{ff} mice after infection with AAV-Cre or AAV-GFP. Scale bar 100 μ m. **c.** Quantification of regenerating optic nerve axons post-crush (experiment as in b). At least 4 serial sections were analysed from each animal (Student t-test, * $p < 0.05$ or ** $p < 0.01$ $n = 7$, each group). **d.** Anti-Tuj1 immunofluorescence shows surviving retinal ganglion cells (Tuj1+) 28 days post-optic nerve crush. Scale bar 50 μ m. **e.** Quantification of surviving RGC as total percentage of surviving cells as compared to the intact contralateral retina ($n=7$, AAV-Cre infected animals; $n=6$, AAV-GFP infected animals).

Figure 2. **Conditional deletion of MDM4 in the SMC enhances CST sprouting following T9 dorsal hemisection in MDM4^{ff} mice**

a. and b. Schematic diagrams summarizing the experimental design. AAV-CreGFP/AAV-GFP particles were injected in the SMC of adult MDM4^{ff} mice 5 weeks prior to T9 dorsal hemisection. BDA for CST labelling was injected 14 days before sacrificing the animal. **c.** Representative images of sagittal sections from MDM4^{ff} mice after cortical AAV-GFP/AAV-CreGFP infection. The CST were traced by BDA injection (red) in the cortex. Spinal cord sections were also stained with GFAP (green) and DAPI (blue). High magnification images show the sprouting axons past the lesion site, in the AAV-CreGFP infected mice. Scale bar 500 μ m **d.** Quantification of the BDA labelled sprouting CST axons in the spinal cord rostral and distal to the lesion site. (Mann Whitney test, ** $p < 0.001$ $n=10$ for AAV-GFP and $n=9$ for AAV-CreGFP).

Figure 3. **Conditional co-deletion of MDM4 and p53 does not lead to axonal regeneration**

a. Schematic of the experimental design showing AAV-Cre or AAV-GFP intra-vitreous infection of RGC in MDM4^{ff}p53^{ff} mice 14 days before optic nerve crush. Regenerating axons were traced with Cholera toxin B (CtB). **b.** Representative images of CtB labelled optic nerve axons from MDM4^{ff}p53^{ff} mice infected with AAV-CreGFP/AAV-GFP. No regenerating axons were observed past the lesion site (asterisk). Scale bar 100 μ m. **c.** Quantification of CtB labelled axons regenerating past the lesion site. At least 4 serial sections were analyzed from each animal ($n=5$, AAV-CreGFP group, $n=4$, AAV-GFP).

Figure 4. Inhibition of MDM2/p53 interaction enhances axonal regeneration after optic nerve crush

a. Schematic of the experimental design showing intra-vitreous injection of Nutlin-3a (100nm) on the day of optic nerve crush followed by second application 7 days later. Regenerating axons were traced with Cholera toxin B (CtB). **b.** High magnification images of regenerating CtB labeled optic nerve axons 28d post-crush (asterisk) in Nutlin treated wildtype mice. Only sporadic regenerating axons were observed 200 μ m post-ONC in Nutlin treated p53^{+/-} mice. Scale bar 100 μ m. **c.** and **d.** Quantification of regenerating optic nerve axons post-crush (experiment as in b). At least 4 serial sections were analysed from each animal (Student t-test, *p< 0.05 or **p<0.01 for each distance, n= 7, each group). **e.** Anti-Tuj1 immunofluorescence shows surviving retinal ganglion cells (Tuj1+) 28 days post-optic nerve crush. Scale bar 50 μ m. **f.** Quantification of surviving RGC as total percentage of surviving cells as compared to the intact contralateral retina (n=7, Nutlin; n=6, vehicle). **g.** Immunoblotting from retinae treated with vehicle or Nutlin (100nM) at the time of ONC, 3 days post-ONC. Nutlin enhances P53 expression. Blots from AV-p53 or control AV-GFP infected primary neurons were used as positive control of p53 expression.

Figure 5. Genome wide gene expression analysis in RGC after conditional MDM4 deletion and sorting by FACS

a. Schematic of the experimental design. MDM4^{fl/fl} animals were infected with AAV-CreGFP/AAV-GFP 14 days before the optic nerve crush. Dil was injected in the superior colliculus 7 days prior to crushing the optic nerve. Dil⁺ RGCs were sorted by FACS 3 days following ONC, and RNA extracted from these samples were used to perform gene expression analysis (Affymetrix). **b.** Whole mount retina showing highly efficient Dil tracing in the RGC layer. Scale bar 20 μ m. **c.** Heatmap showing clear-cut separation of gene expression levels (green: low; red: high) between AAV-GFP and AAV-creGFP infected RGC. **d.** Differentially regulated signaling pathways up regulated in MDM4 deleted RGCs analysed with Ingenuity Pathways Analysis (IPA). These include p53, Gadd45 and IGF1-IGFR signaling pathways. **e.** Immunofluorescence micrographs showing high IGF1R expression level 3d after optic nerve crush in retinal ganglion cells (Tuj1*) infected with AAV-CreGFP, while a faint signal was observed in AAV-GFP+ RGC in MDM4^{fl/fl} mice. Retinal ganglion cells have been counterstained with Tuj1. Scale bar 20 μ m.

Figure 6. Regeneration elicited by MDM4 deletion is reduced by inhibition of IGF1R signalling

a. Schematic of the experimental design. Conditional MDM4 deletion in MDM4^{fl/fl} mice was followed by ONC and pharmacologically inhibition of IGF1R with the antagonist

picropodophyllin (PPP). Axonal tracing was performed with CtB. **b.** Immunoblotting from retinæ 3d after ONC and administration of PPP or vehicle. Shown is a strong reduction in the expression of IGF1R. **c.** Representative images of optic nerves showing regenerating CtB labelled axons of MDM4^{fl/fl} animals after MDM4 conditional deletion and vehicle. Not a significant number of regenerating axons were found after PPP administration post-ONC (asterix). Scale bar 100 µm. **d.** Quantification of regenerating optic nerve axons post-crush (experiment as in c). At least 4 serial sections were analysed from each animal (Student t-test, $p < 0.05$ for each distance, $n = 6$, each group). The number of regenerating axons was significantly hampered following AAV-cre-PPP treatment versus AAV-cre-veh. **e.** Anti-Tuj1 immunofluorescence shows surviving retinal ganglion cells (Tuj1+) 28 days post-optic nerve crush. Scale bar 50 µm. **f.** Quantification of surviving RGC as total percentage of surviving cells as compared to the intact contralateral retina ($n = 6$).

Supplementary Figure 1.

a. Representative fluorescent images at 24h and 72h after ONC showing MDM4 expression in retinal ganglion cells. Retinal ganglion cells were counterstained with Tuj1. MDM4 co-localised with Tuj1. Scale bar 20 µm. **b.** Quantification of the expression level of MDM4 by fluorescence intensity measurement. MDM4 expression level did not change significantly at 24h and 72h following ONC. At least six sections were analysed from 3 animals in each group. **c.** Representative image of a retina infected with AAV-CreGFP showing specific highly efficient infection in retinal ganglion cells. Scale bar 50 µm. **d.** Immunofluorescence of retinal ganglion cells infected with AAV-GFP or AAV-CreGFP showing MDM4 deletion 14d after infection. MDM4 expression could be detected by immunostaining in control AAV-GFP infected samples only (arrowheads). Scale bar 20 µm. **e.** Semi quantitative PCR from dissociated retinal ganglion cell culture 3 days after infection with AAV-GFP/AAV-Cre. MDM4 expression was significantly reduced after Cre mediated recombination.

Supplementary Figure 2.

a. Shown are GFP and BDA labeling of the SMC after stereotaxic delivery of AAV-GFP or BDA. Inset shows layer V in the SMC. Scale bar 500 µm. **b.** Shown are cre-positive cells after anti-cre immunostaining in proximity of the injection site (asterix) of AAV-cre in the SMC. Scale bar 50 µm. **c.** Immunostaining for GFP and CTIP2 (layer V neurons marker) show AAV-GFP infection of layer V neurons in the SMC. Scale bar 20 µm.

Supplementary Figure 3.

a. Coronal section of a spinal cord 10 mm caudal to the lesion site showing completeness of the lesion with lack of BDA positive CST labelling after AAV-GFP infection in the SMC of MDM4^{ff} mice (5 weeks post-SCI). Scale bar 500 μ m. **b.** BDA+ CST sprouting axons (arrowheads) after AAV-cre delivery in the SMC of MDM4^{ff} mice (5 weeks post-injury). Scale bar 500 μ m.

Supplementary Figure 4.

a. Dissociated retinal ganglion cells from MDM4^{ff} postnatal day 7 mice were cultured on permissive (PDL) and inhibitory substrate (myelin) for 72h following Ad-Cre/Ad-GFP infection. Neurites were traced with Tuj1. **b.** Quantification of neurite outgrowth 72h after AV-GFP/AV-Cre infection. Semi-automatic analysis from more than 500 neurons per condition (n=3) showed a significantly higher outgrowth in the AV-Cre infected group. Student's t-test, $p < 0.05$. **c.** Cerebellar granule neurons from MDM4^{ff} mice were plated on permissive (PDL) and inhibitory (Myelin) substrate and infected with AV-GFP/AV-Cre. AV-Cre infected group showed a significantly higher neurite outgrowth 24h after infection. Neurites were traced with Tuj1. **d.** Quantification of neurite outgrowth of cultured CGN. Neurites were traced manually from single neurons that were infected with the virus. At least 100 neurons were analysed per condition per group. n= 4. Student's t-test, $p < 0.05$.

Supplementary Figure 5.

a. Semiquantitative PCR mice from MDM4^{ff} cerebellar granule neuron (CGN) cultures after infection with AV-Cre or AV-GFP. MDM4 expression was significantly reduced after Cre mediated recombination. **b.** Real time quantitative PCR from MDM4^{ff} CGN cultures 24h after infection with AV-GFP or AV-Cre showed enhanced expression of several p53-target genes. P53 expression was not altered due to MDM4 deletion.

Supplementary Figure 6.

a. Representative fluorescent images at 24h and 72h after ONC showing p53 expression in retinal ganglion cells. Retinal ganglion cells were counterstained with Tuj1. P53 co-localised with Tuj1. Scale bar 20 μ m. **b.** Quantification of the expression level of p53 by fluorescence intensity measurement. P53 expression level did not change significantly at 24h and 72h following ONC. At least six sections were analysed from 3 animals in each group.

Supplementary Figure 7.

a. Representative fluorescent images at 24h and 72h after ONC showing MDM2 expression in retinal ganglion cells. Retinal ganglion cells were counterstained with Tuj1. MDM2 co-localised with Tuj1. Scale bar 20 μm . **b.** Quantification of the expression level of MDM2 by fluorescence intensity measurement. MDM2 expression level did not change significantly at 24h and 72h following ONC. At least six sections were analysed from 3 animals in each group.

Supplementary Figure 8.

a. Quantitative RTPCR from CGN treated with Nutlin-3a or vehicle (24h). Shown is enhanced expression of axon growth associated and p53 target genes with Nutlin-3a 100nM versus vehicle. 18S RNA was used for normalization. $n=3$. (Student t-test, $*p < 0.05$ or $**p < 0.01$). **b.** Apoptosis was evaluated 24h after administration of Nutlin-3a or vehicle in CGN. Pyknotic cells were identified with DAPI staining. $n=3$. (Student t-test, $*p < 0.05$ or $**p < 0.01$).

Supplementary Figure 9.

a. Dose response of Picropodphylin (PPP, IGF1R antagonist) in cerebellar granule neurons was determined by counting the number of Cleaved Caspase 3 positive cells in a dose response curve. PPP 1 μM or above showed significant cell death as compared to vehicle control. $n=3$. Student's t-test, $p < 0.05$. **b.** Cells extending neuritis in response to PPP treatment (dose response) were counted. Cells treated with PPP 10nM or above showed reduced number of cells extending neurites. $n=3$. Student's t-test, $p < 0.05$.

<i>Functional Class</i>	<i>Fold change (Cre vs GFP)</i>	<i>p value</i>	<i>Function</i>
<u>Axonal signalling</u>			
IGF1R	2,12	0,0122	Intracell signalling
CXCR2	2,18	0,0222	Chemoattraction
Klf11	1,764	0,0391	Axonal transport
Cited4	1,69	0,0324	Transcription co-activ
Spr2b	1,866	0,004	Axon growth
<u>Neuronal morphology and cytoskeleton organization</u>			
DCC	-2,031	0,0476	Axon repulsion
GAD1	1,569	0,0365	Glut/GABA metab
Arf1	3,505	0,02	GTP-bind prot
FCER1A	1,71	0,018	IgE rec
NKX2-2	-1,66	0,014	NeuroD1-cofact
Nrg1	-1,84	0,006	Neuronal differ
Rab23	1,516	0,01	GTPase
Rin2	1,797	0,029	GTPase
Mast3	-1,797	0,043	Microtub ass kinase
<u>Neuronal development</u>			
GAD1	1,569	0,0365	Glut/GABA metab
CAMKK2	1,595	0,004	CREB activator
ZIC1	1,632	0,0385	Transc Activ-Neurogenesis
ZNF423	1,762	0,0226	Smad coact-Neurogenesis
LYNX1	2,222	0,0004	Synaptic plasticity
ST8SIA2	1,683	0,02704	NCAM1 binding protein-rec
DCC	-2,031	0,0476	Axon repulsion

Table 1. List of selected differentially regulated genes from RGC after ONC in MDM4^{fl/fl} mice- AAV GFP vs Cre

<i>Primers sequences</i>		
Gene	Primer forward	Primer Reverse
p21	CGGTGGAAC TTTGACTTCGT	AGAGTGCAAGACAGCGACAA
GADD45	CAGGGGAGGGACTCGCACTT	CGGGGTCTACGTTGAGCAGC
GAP43	AAGCTACCACTGATAACTCCCC	CTT CTTTACCCTCATCCTGTCTG
SCG10	AGACTCCTCTCTCGCTCTCTCCG C	AGCCTCTTGAGACTTTCTTCGCTCCT C
CAP23	GGCGGCAGCGCTCCAAC TCG	CCGCCTGGGGTTCGCTCTCC
p53	AGAGACCGCCGTACAGAAGA	CTGTAGCATGGGCATCCTTT
MDM4	CAGCTAGGAGGGGGAGCGACT	GCAGTTTTGGCCGCACCTGACTAA
β-actin	CTCTCSGCTGTGGTGGTGAA	AGCCATGTACGTAGCCATCC
L1CAM	ATGCTGCGGTACGTGTGGCCCT	CCACTTGGGGGCACCCTCGG
BDNF	AGTCTCCAGGACAGCAAAGC	TCGTCAGACCTCTCGAACCT
Spr1a	CCCCTCAACTGTCACTCCAT	CAGGAGCCCTTGAAGATGAG
18S RNA	CTCAACACCGGGAAACCTCAC	CGCTCCACCAACTAAGAACG
β-actin	CTCTCSGCTGTGGTGGTGAA	AGCCATGTACGTAGCCATCC
RPL13a	GGCTGAAGCCTACCAGAAAG	TTCTCCTCCAGAGTGGCTGT

Table 2. List of primer sequences

Figure 1

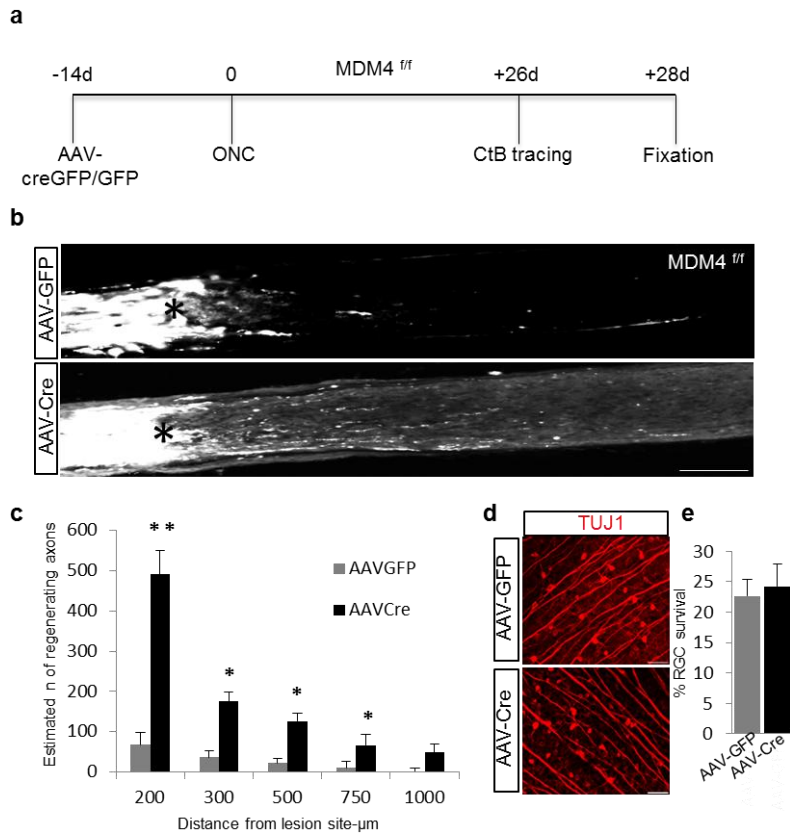


Figure 2

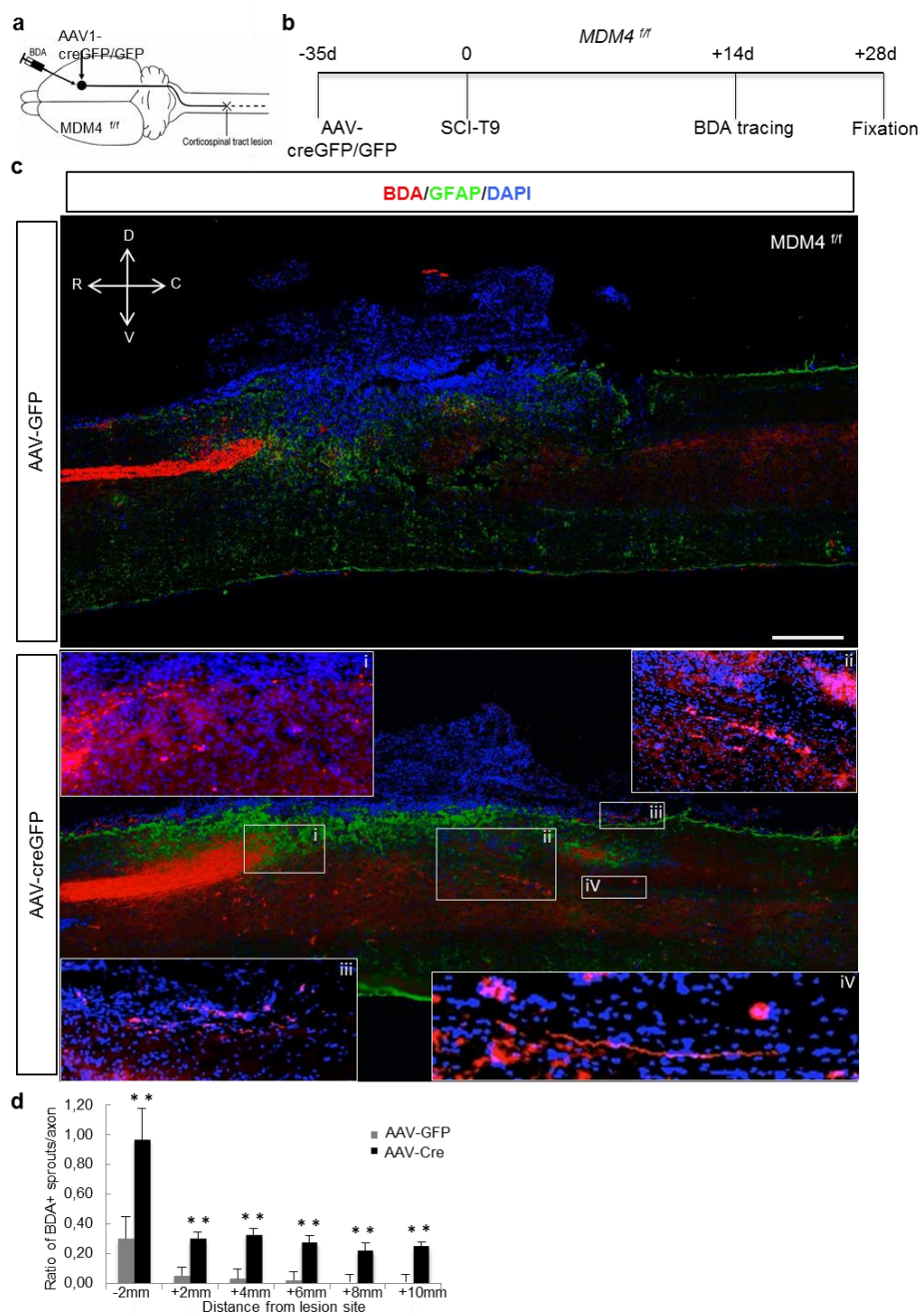


Figure 3

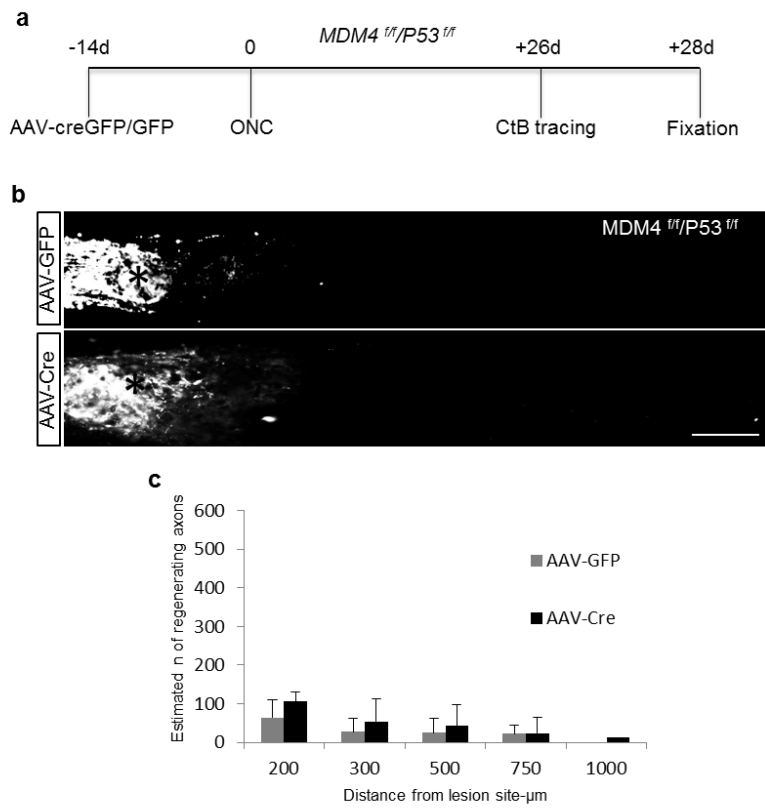


Figure 4

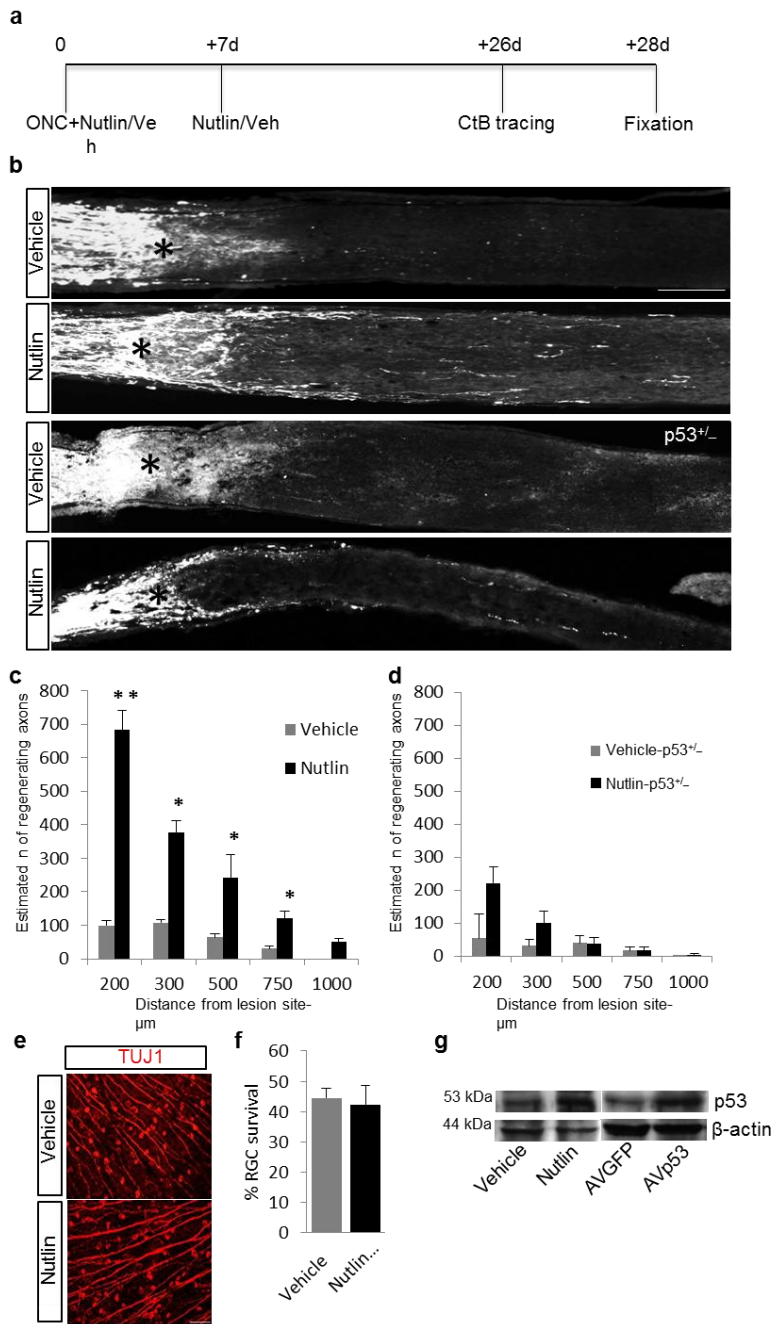


Figure 5

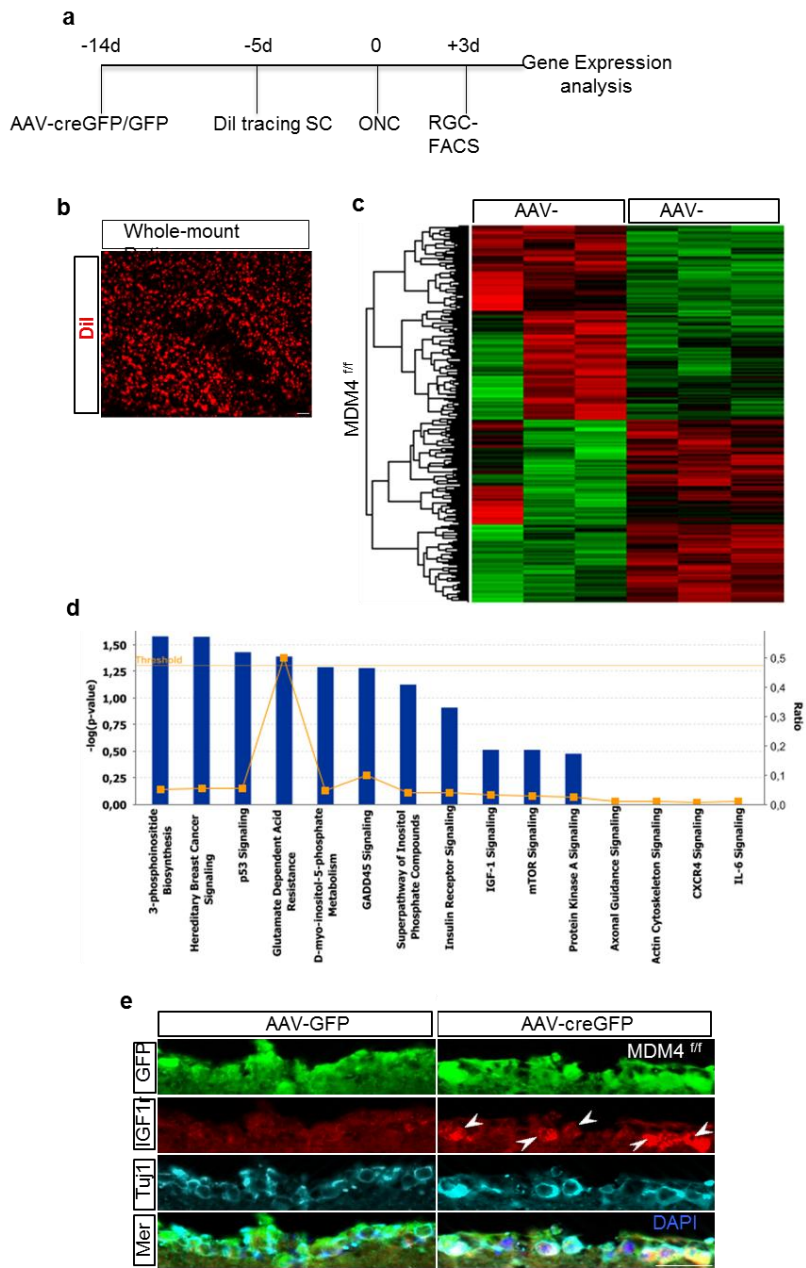
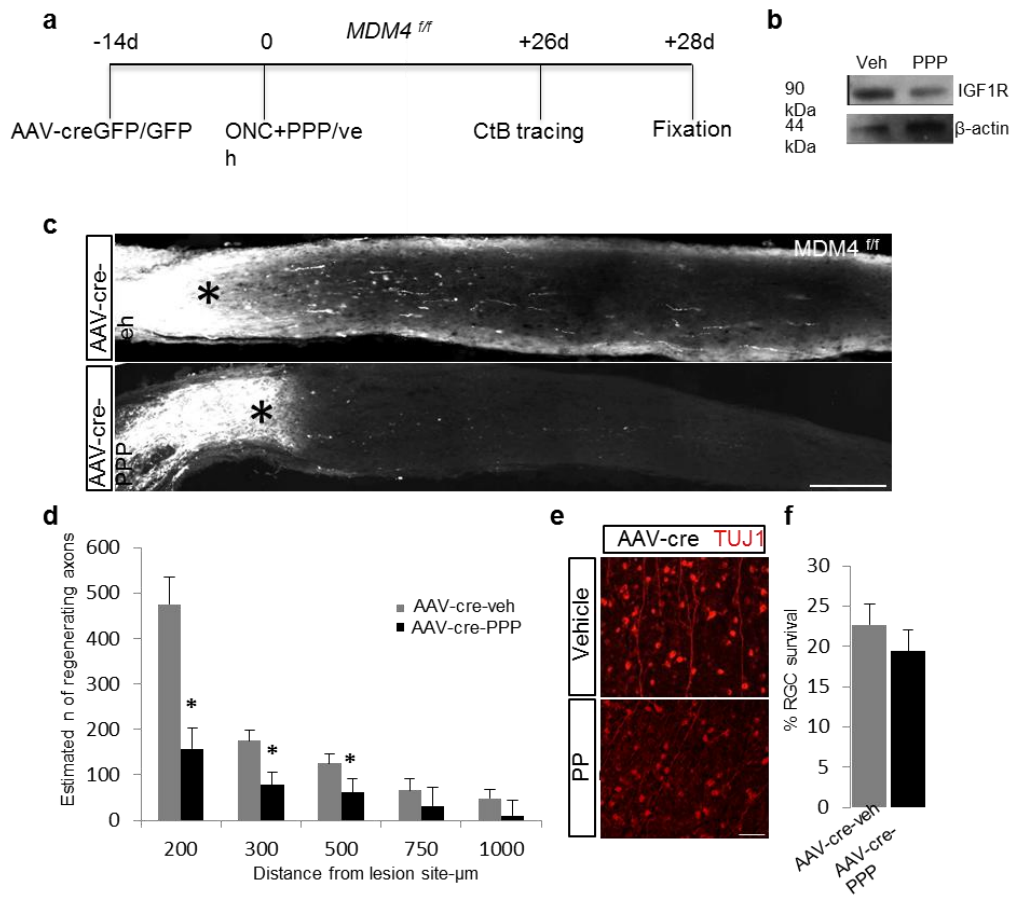
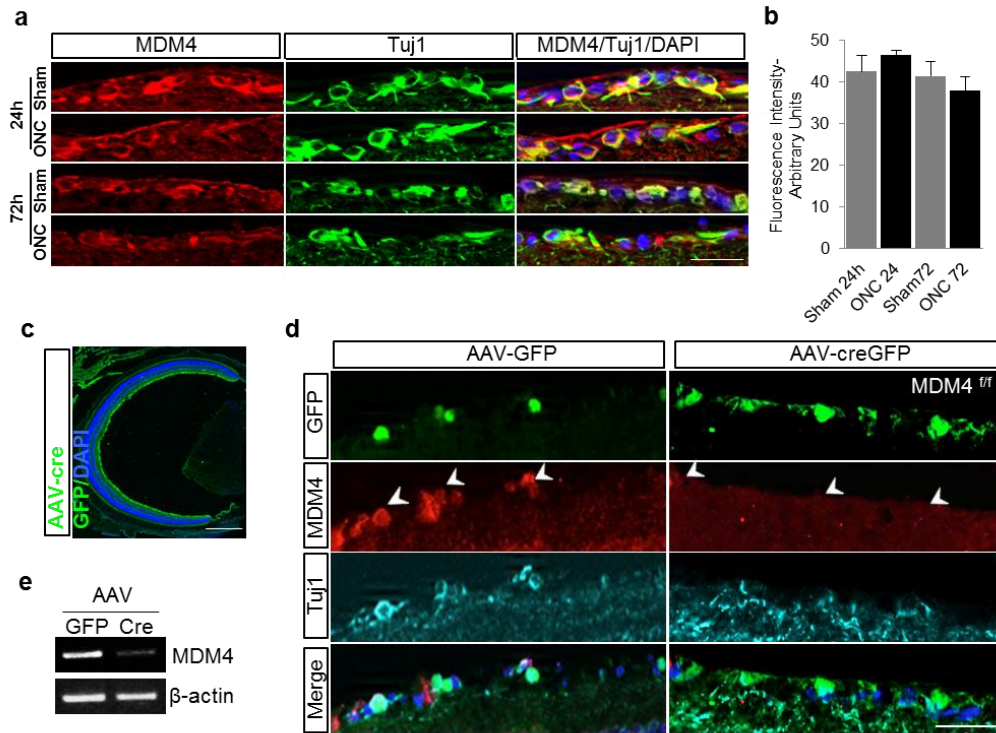


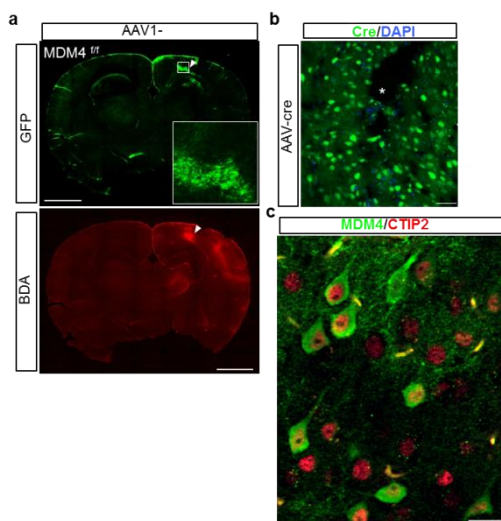
Figure 6



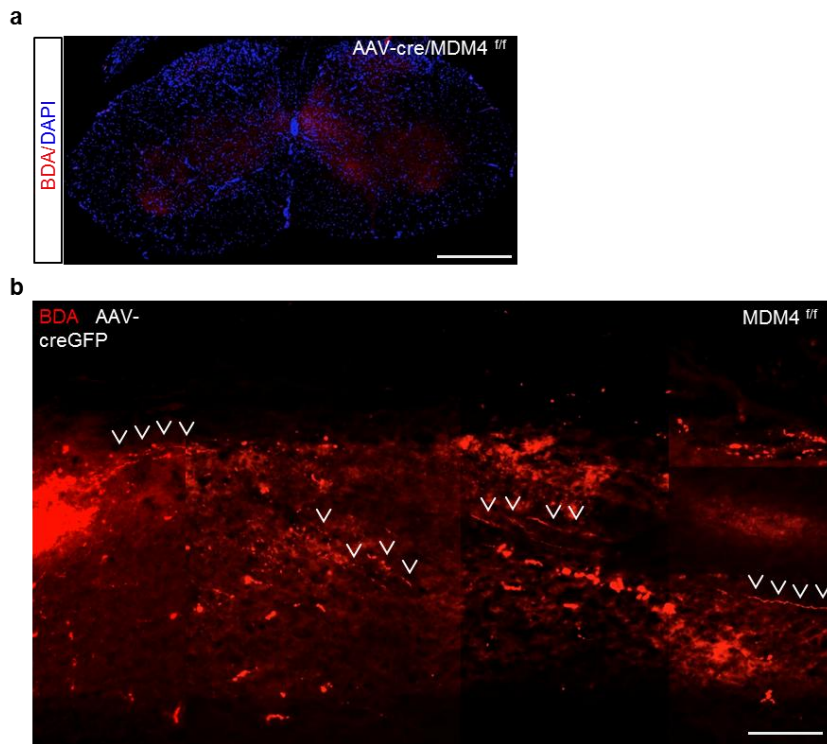
Supp. Figure
1



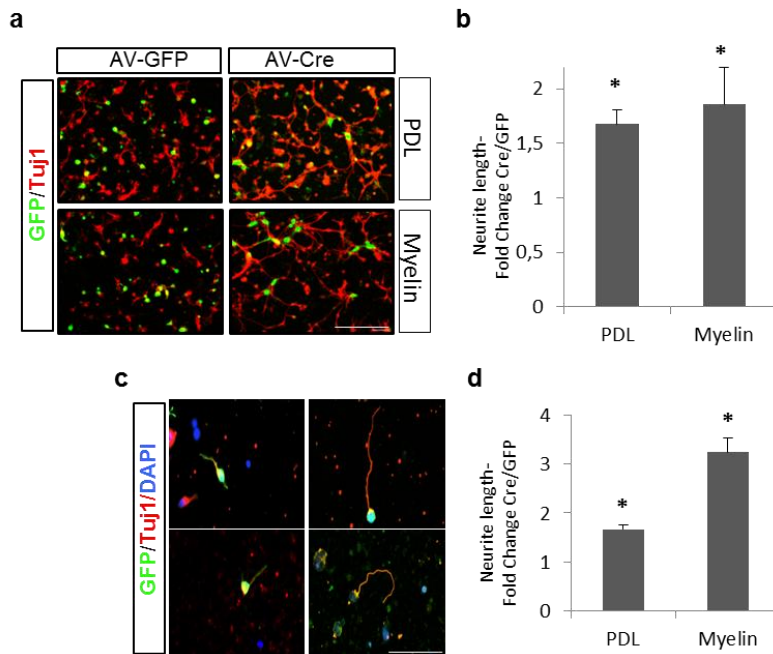
Supp. Figure 2



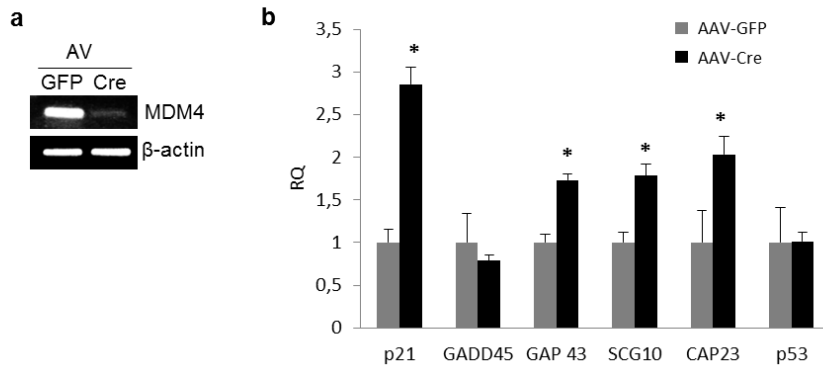
Supp. Figure 3



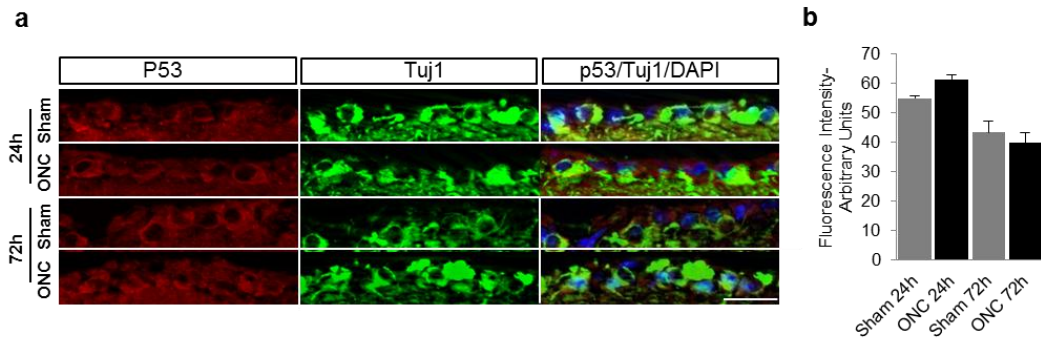
Supp. Figure 4



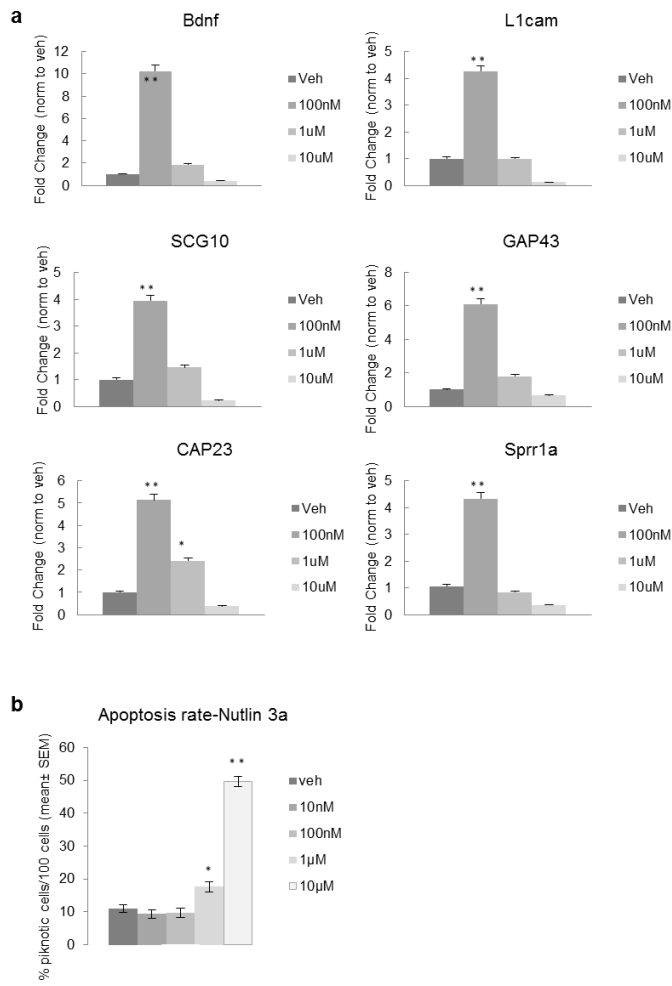
Supp. Figure 5



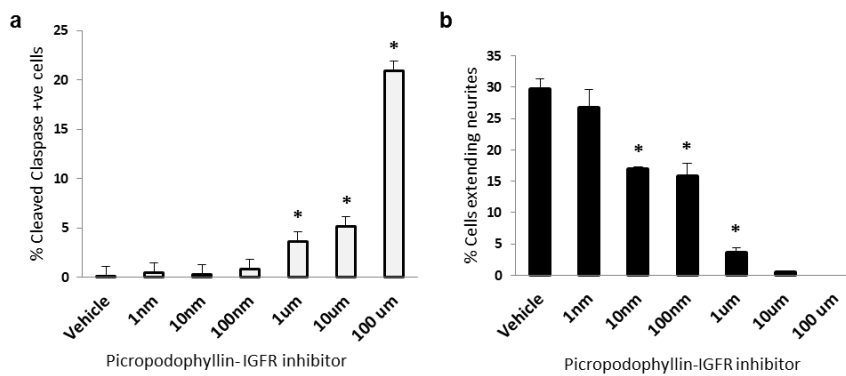
Supp. Figure 6



Supp. Figure 7



Supp. Figure 8



The histone acetyltransferase p300 promotes intrinsic axonal regeneration

Perrine Gaub,^{1,2} Yashashree Joshi,^{1,2} Anja Wuttke,¹ Ulrike Naumann,³ Sven Schnichels,⁴ Peter Heiduschka^{4,*} and Simone Di Giovanni¹

1 Centre for Neurology, Laboratory for NeuroRegeneration and Repair, Hertie Institute for Clinical Brain Research, University of Tübingen, Otfried Mueller str. 27, 72076 Tübingen, Germany

2 Graduate School for Cellular and Molecular Neuroscience, University of Tübingen, Otfried Mueller str. 27, 72076 Tübingen, Germany

3 Laboratory for Neuro-Oncology, Centre for Neurology, Hertie Institute for Clinical Brain Research, University of Tübingen, Schleichstr. 12-16, D-72076 Tübingen, Germany

4 Centre of Ophthalmology, University Eye Hospital, Domagkstr. 15, D-48149 Münster, Germany

*Present address: University Eye Hospital Muenster, Münster, Germany

Correspondence to: Simone Di Giovanni, MD, PhD,
Centre for Neurology,
Laboratory for NeuroRegeneration and Repair,
Hertie Institute for Clinical Brain Research,
University of Tübingen,
Otfried-Mueller Strasse 27,
Tübingen, Germany
E-mail: simone.digiovanni@medizin.uni-tuebingen.de

Axonal regeneration and related functional recovery following axonal injury in the adult central nervous system are extremely limited, due to a lack of neuronal intrinsic competence and the presence of extrinsic inhibitory signals. As opposed to what occurs during nervous system development, a weak proregenerative gene expression programme contributes to the limited intrinsic capacity of adult injured central nervous system axons to regenerate. Here we show, in an optic nerve crush model of axonal injury, that adenoviral (cytomegalovirus promoter) overexpression of the acetyltransferase p300, which is regulated during retinal ganglion cell maturation and repressed in the adult, can promote axonal regeneration of the optic nerve beyond 0.5 mm. p300 acetylates histone H3 and the proregenerative transcription factors p53 and CCAAT-enhancer binding proteins in retinal ganglia cells. In addition, it directly occupies and acetylates the promoters of the growth-associated protein-43, coronin 1 b and Sprr1a and drives the gene expression programme of several regeneration-associated genes. On the contrary, overall increase in cellular acetylation using the histone deacetylase inhibitor trichostatin A, enhances retinal ganglion cell survival but not axonal regeneration after optic nerve crush. Therefore, p300 targets both the epigenome and transcription to unlock a post-injury silent gene expression programme that would support axonal regeneration.

Keywords: p300; histone acetyltransferase; optic nerve; axonal regeneration; transcription

Abbreviations: AVGFP = adenovirus green fluorescent protein; CBP = cyclic adenosine monophosphate responsive element binding protein; C/EBP = CCAAT-enhancer binding protein; GFP = green fluorescent protein; P/CAF = p300/CBP-associated factor

Introduction

Mature neurons of the adult CNS lack axonal regeneration capacity following axonal injury. The reason for such a regenerative failure is 2-fold: (i) the presence of a non-permissive glial environment (Yiu and He, 2003, 2006); and (ii) an intrinsic lack of proregenerative ability (Lee *et al.*, 2010). This is in contrast to the potential for axonal regeneration and outgrowth present in the injured PNS (Huebner and Strittmatter, 2009) and in immature neurons during development (Cai *et al.*, 2001; Filbin, 2006).

The intrinsic properties of neurons are regulated by gene transcription, which regulates gene expression, and therefore tightly controls the neuronal intrinsic capacity to synthesize new proteins needed for pro-axonal regeneration signalling. Indeed, transcriptional regulation controls axonal outgrowth during development (Butler and Tear, 2007) as well as axon regrowth after injury in the adult (Goldberg *et al.*, 2002; Raivich *et al.*, 2004; Moore *et al.*, 2009). Intrinsic signals receive numerous inputs from extrinsic ones and are used here to describe those signals whose modulation is sufficient to promote axonal outgrowth without additional inhibition of the inhibitory environment.

Mature retinal ganglion cells fail to regenerate axons and undergo apoptosis following optic nerve damage; however, experimental evidence has shown that enhancement of the intrinsic properties of retinal ganglion cells can promote axonal regeneration of the injured optic nerve. Examples include the lens injury-dependent activation of a proregenerative state characterized by gene expression comparable with that seen after peripheral nerve injury (Leon *et al.*, 2000; Fischer *et al.*, 2001, 2004). In fact, a lens injury previous to the optic nerve crush induces, likely via inflammatory molecules (Yin *et al.*, 2006, 2009), the expression of pro-growth genes such as *Spr1a* and *Narp* as well as transcription factors such as cyclic adenosine monophosphate responsive element binding protein (CBP) and CCAAT-enhancer binding proteins (C/EBP). In addition to lens injury, the combined administration of several growth factors (Logan *et al.*, 2006), as well as the lens injury induced ciliary neurotrophic factor are other well-established means to enhance intrinsic axonal regeneration of the injured optic nerve (Lingor *et al.*, 2008; Leibinger *et al.*, 2009; Muller *et al.*, 2009).

Recent studies have demonstrated that the modulation of individual intrinsic molecules such as PTEN (phosphatase and tensin homologue) or the transcription factors KLF4 (Krupper-like factor 4) can promote axonal regeneration of retinal ganglion cells after optic nerve crush (Park *et al.*, 2008; Moore *et al.*, 2009). Both PTEN and KLF4 show repressive effects on neurite outgrowth, while their suppression in retinal ganglion cells strongly enhances axonal regeneration ultimately activating a proregenerative gene expression response. These lines of evidence suggest that as opposed to what occurs during development and in immature neurons, the gene expression programme in mature retinal ganglion cells does not allow mounting an axonal regenerative response unless modified by experimental manipulations.

We hypothesize that the proregenerative transcriptional machinery is silenced or repressed in adult CNS neurons after neuronal maturation and following axonal damage; however, it could be

reactivated by modulating genes that regulate the proregenerative gene expression programme. Gene expression is controlled by the state of chromatin as well as by the presence of specific transcriptional complexes near gene promoters. The balance between the histone acetyltransferases and histone deacetylases regulates the level of histone and transcription factor acetylation, which modifies the state of chromatin and the activity of transcription factors, and overall contributes to the fine-tuning of gene expression (Yang and Seto, 2007). We have recently reported that chromatin relaxation and transcription factor activation via histone deacetylases inhibition by trichostatin A enhances neurite outgrowth on permissive and non-permissive substrates. Specifically, this was due to an increased expression of the histone acetyltransferases CBP/p300 and p300/CBP-associated factor (P/CAF) that enhanced acetylation of H3 and p53, which stimulated the expression of several proregenerative genes (Gaub *et al.*, 2010). However, this work was performed *in vitro* and the role of histone acetyltransferases in axonal regeneration *in vivo* is yet to be investigated.

In the present study, we investigated the regulation of expression of the specific histone acetyltransferases p300, CBP and P/CAF during retinal ganglion cell maturation and whether they could thus become potential candidates to control the ability of retinal ganglion cells to regenerate axons following optic nerve crush. Indeed, we found that histone acetylation and the expression of CBP and p300 are repressed in mature retinal ganglion cells and after optic nerve crush. Importantly, overexpression of p300 but not histone deacetylases inhibition, promotes axonal regeneration after optic nerve crush. P300 leads to hyperacetylation of histone H3 and the transcription factors p53 and C/EBP, as well as to increased p300 occupancy and H3 acetylation of selected pro-axonal outgrowth gene promoters.

This is a first report showing that a specific modification of the transcriptional and epigenetic environments can promote axonal regeneration *in vivo*, likely by redirecting the transcriptional programme on proregeneration promoters.

Materials and methods

Viral construction, production and infection

AVp300 vector was created by using the AdEasy™ system (Luo *et al.*, 2007). p300 complementary DNA was purchased from Addgene (plasmid 10718) and subcloned into the pAdTrack-cytomegalovirus (CMV) shuttle vector (Addgene plasmid 16405). Preparation of adenovirus green fluorescent protein (AVGFP) has been described previously (Naumann *et al.*, 2001). The plasmid containing p300 and pAdTrack-CMV was then linearized and recombined with the viral backbone pAdEasy-1. All viruses were expanded in 293 cells (ATCC) and tested to be replication-deficient by polymerase chain reaction (primer: E1Afrwd GTTGGCGGTGCAGGAAGGGATTG and E1Arev CTCGGGCTCAGGCTCAGGTTTCAGA) and by immunoblot of the E1A gene product (mouse-anti E1A, 1:10 000, BD Biosciences 554155). Viral titres were assessed using a hexon titre kit (Clontech). The efficacy of adenoviral gene delivery and expression was ascertained by green fluorescent protein (GFP) fluorescence or by polymerase chain

reaction for p300 messenger RNA expression. Infection with recombinant viruses *in vitro* was accomplished by exposing cells *in vitro* to 100 multiplicity of infection (MOI) of adenovirus immediately after plating. *In vivo*, AVGFP as a control and AVp300 were injected intravitreally immediately after optic nerve crush.

Retinal ganglion cell survival assay

Assessment of retinal ganglion cell survival was performed on flat-mounted retinæ. Eyes were dissected and the retinæ removed from the eye cup. The retinæ were then washed in phosphate-buffered saline and blocked in a solution of 10% bovine serum albumin and 1% Triton X-100. After the blocking solution, the whole retina was incubated in the same solution with mouse anti- β -III tubulin (1:400) (Promega) overnight at 4°C. Retinæ were then washed with phosphate-buffered saline, incubated with the secondary antibody anti-mouse Alexa 568 (1:1000, Pierce) and flat mounted on slides with Fluorsave™ (Calbiochem).

Quantification was performed by taking pictures in the central, intermediate and peripheral region for each quarter of flat mounted retina under fluorescent illumination ($n = 3$) as previously reported (Park *et al.*, 2008; Kurimoto *et al.*, 2010). β -III tubulin-positive cells were then counted on each picture using the Neurolucida software and normalized as a percentage to sham retinæ ($n = 3$). Similarly, additional counting was performed by evaluating the number of GFP-positive infected cells (with a control AVGFP or AVp300) co-expressing β -III tubulin only. GFP/ β -III tubulin-positive cells were then counted on each picture using the Neurolucida software and normalized as a percentage to sham retinæ ($n = 3$).

Retinal cell culture

Primary culture of retinal cells was performed following a previously described protocol (Hauk *et al.*, 2010). Briefly, P6–P7 eyes were dissected, and retinæ were incubated in Dulbecco's modified Eagle's medium with Papain (Cellsystem) and L-cystein (Sigma). After incubation, retinæ were dissociated in Dulbecco's modified Eagle's medium with B27 (Life Technologies) and penicillin/streptomycin (Sigma) and $\sim 1 \times 10^6$ cells per 2 cm² were plated. Immediate infection by AV-GFP and AV-p300 was carried out using 100 MOI. Cells were then fixed with 4% paraformaldehyde for 30 min. Cells were washed with phosphate-buffered saline, then blocked with 8% bovine serum albumin, 0.2% TritonX-100 in phosphate-buffered saline and finally incubated with the primary antibodies overnight at 4°C: mouse anti- β -III tubulin (1:1000) (Promega). Cells were then washed with phosphate-buffered saline and incubated with an anti-mouse Alexa 564-coupled secondary antibody (1:1000) (Pierce) for 1 h at room temperature. As a control, we stained with Hoechst 33258 (Molecular Probes) and then washed in phosphate-buffered saline before mounting the coverslips on a slide with Fluorsave™ (Calbiochem).

Optic nerve crush surgery and intraocular injection

All animal experiments were conducted according to the European Union and German regulations under the allowance of the animal protocol number N03/07 and AK7/07 (University of Tübingen). Surgical procedures were based on those described previously (Berry *et al.*, 1996; Fischer *et al.*, 2000; Leon *et al.*, 2000). Adult (2–3 months old) Crl-CD1 rats (400–500 g) were anaesthetized

intraperitoneally with 80 mg/kg of ketamine and 50 mg/kg of xylazine. After shaving the head, rats were immobilized in an apparatus and a 1.5- to 2-cm incision was made in the skin in the middle of the head. Under microscopic illumination, a longitudinal section above the right orbit was made to access the orbital space below the bones. The lachrymal glands and extraocular muscles were resected and retracted to expose 3–4 mm of the optic nerve. The epineurium was slit open along the longitudinal axis and the nerve was crushed 2 mm behind the eye with angled jeweller's forceps (Dumont #5, FST) for 10 s, avoiding injury to the ophthalmic artery. Nerve injury was verified by the appearance of a clearing at the crush site, while the vascular integrity of the retina was evaluated by funduscopic examination. Cases in which the vascular integrity of the retina was in question were excluded from the study. For intraocular injections, the eye was rotated to expose its posterior aspect. Injections were made through the sclera and retina with a 30 gauge needle 1–2 mm superior to the optic nerve head, inserting the tip of the needle perpendicular to the axis of the nerve to a depth of 2 mm without infringing on the lens (minimally invasive injection). Injection volumes were dependent upon the solution. In a subset of rats, we performed lens injury as described previously (Schnichels *et al.*, 2011). Survival times ranged from 1–3 days and 14 days after the surgery. Groups included sham controls ($n = 3$), animals with optic nerve crush ($n = 3$), animals with optic nerve crush and phosphate-buffered saline ($n = 4$) or trichostatin A (T-8552, Sigma) (10 ng/ml; $n = 4$); animals with optic nerve crush and AVGFP (7.5×10^7 pfu; $n = 5$) or AVp300 (7.5×10^7 pfu; $n = 5$). Animals showing signs of lens injury or intravitreal haemorrhage after puncture were excluded from the study. The surgical site was sutured and closed. Animals were observed for postoperative recovery and were housed with *ad libitum* access to food and water.

Evaluation of axonal regeneration

For evaluation of optic nerve axon regeneration following optic nerve crush, GAP-43 immunofluorescence was performed. Photomicrographs were taken with a fluorescence microscope using the Zeiss Axioplan microscope (Axiovert 200, Zeiss Inc.). Images of whole sections were assembled from single pictures taken with a $\times 20$ objective. The number of regenerating axons at designated distances from the end of the crush sites was evaluated per section as previously reported (Planchamp *et al.*, 2008). The number of regenerating axons per nerve was then averaged over all sections of one nerve. The following experimental conditions after optic nerve crush were analysed ($n = 4$): AVGFP; AVp300; AV GFP + lens injury; and AVp300 + lens injury.

Tissue extraction

Postnatal CD rats at Days P0, P7 and P21, and adult rats were deeply anaesthetized using 100 mg/kg of ketamine and 80 mg/kg of xylazine and transcardially perfused with 100 ml of ice-cold phosphate-buffered saline followed by 50 ml of ice-cold 4% paraformaldehyde. The eyes were enucleated with the optic nerve and post-fixed overnight in 4% paraformaldehyde followed by cryoprotection using 30% sucrose in water. The eyes were later stored at -80°C . Three different retinæ were sacrificed at each time point.

Immunohistochemistry

Eyes and optic nerves were embedded in freezing medium and longitudinal serial sections (10 μm) were cut and mounted on glass slides. The sections were washed once with phosphate-buffered saline and incubated in 4% sucrose for 30 min followed by ice-cold 100%

methanol treatment for 15 min. For antigen retrieval, we used citrate buffer [2.1 g citric acid (monohydrated); 0.74 g EDTA; 0.5 ml Tween-20; in 1000 ml distilled water; pH 6.2] after the sucrose treatment and the slides were heated at 98°C. The sections were then washed with phosphate-buffered saline and blocked with 8% bovine serum albumin, 0.2% TritonX-100 in phosphate-buffered saline and then incubated in 2% bovine serum albumin, phosphate-buffered saline with the primary antibodies overnight at 4°C: rabbit anti-acetyl H3K18 (1:1000, Millipore); mouse anti-CBP (AC238, Abcam) (citrate buffer treatment, 1:50); mouse anti-p300 (3G230, Abcam), (citrate buffer treatment, 1:200); mouse anti- β -III tubulin (1:1000) (Promega); rabbit anti-acetyl-p53 lys373 (1:200, citrate buffer treatment) (06-916, Millipore); rabbit anti-p53 (1:200) (sc-6243, Santa-Cruz); rabbit anti-C/EBP acetylated 215-216 (1:200) (09-037, Millipore); rabbit anti-GAP-43 (1:500) (Chemicon, Schwalbach, Germany). Sections were then washed with phosphate-buffered saline and incubated with the respective secondary antibodies for 1 h at room temperature: Alexa 488, 546 or 564-coupled secondary antibodies (goat anti-rabbit IgG, goat anti-mouse IgG, Pierce). As a control, we stained with Hoechst 33258 (Molecular Probes) and then washed in phosphate-buffered saline before mounting on slides with FluorsaveTM (Calbiochem). For all experiments, a negative control was performed by immunostaining with the secondary antibody only.

Controls for anti-CBP and p300 antibody specificity were carried out previously by immunostaining after CBP and p300 gene silencing in both cell lines and primary neurons (Gaub *et al.*, 2010), which showed reduced signal intensity in agreement with gene silencing. Specificity for anti-p53 antibodies has been tested previously by both immunoblotting and immunocytochemistry after overexpression of p53 in both cell lines and primary neurons (Di Giovanni *et al.*, 2006; Tedeschi *et al.*, 2009; Gaub *et al.*, 2010). Specificity for antibodies anti-H3Ac has been supported by immunoblotting. In addition, the immunofluorescence signal has always been found specifically in the nucleus and to change as expected whenever we modified acetylation levels with either trichostatin A (T-8552, Sigma) or overexpression of CBP or p300 (Gaub *et al.*, 2010).

Assessment of fluorescence intensity

A high-resolution image was obtained at $\times 40$ magnification using the Zeiss Axioplan microscope (Axiovert 200, Zeiss Inc.). Images for the same antigen groups were processed with the same exposure time. Assessment of fluorescence intensity was performed using AlphaEaseFC 4.0.1 software by measuring the intensities specifically within the retinal ganglion cell layer. Care was taken that the area analysed for each cell was the same for each set, 20 cells per section and two sections per retina were quantified.

The intensity values of each cell were normalized to the 4',6'-diamidino-2-phénylindole signal and mean values of intensities were calculated for each animal (three animals per condition). For statistical analysis, ANOVA with Bonferroni test was performed using Origene software. At least 100 cells were analysed in triplicates at each time point and *P*-values of ≤ 0.05 (*) were considered significant.

Reverse transcriptase polymerase chain reaction and quantitative reverse transcriptase polymerase chain reaction

After the eyes were enucleated from the animal under deep anaesthesia, unfixed retinæ were dissected and RNA was extracted. RNA was extracted using TRIzol[®] reagent (Invitrogen) and complementary DNA

was synthesized from 1 μ g of RNA using oligo dT and random hexamers from the SuperScriptTM II Reverse Transcriptase kit (Invitrogen). Complementary DNA (1 μ l) was used in a reverse transcriptase polymerase chain reaction using Master Mix (Invitrogen) and for quantitative reverse transcriptase polymerase chain reaction, SYBR-greenER (Invitrogen) was used.

The *RPL13A* gene was used for normalization. The sequences of the primers used were p300 forward 5'-GGGACTAACCAATGGTGGTG-3' and reverse 5'-ATTGGGAGAAGTCAAGCCTG-3' (386 bp), GAP-43 forward 5'-AAGCTACCACTGATAACTCGCC-3' and reverse 5'-CTTCTTTACCTCATCTGTGCG-3' (246 bp); coronin 1b forward 5'-GACCTGTGCCACATAACGATCAGG5C-3' and reverse 5'-CACGATGCCGACTCTTTTGA-3'; α -tubulin 1a forward 5'-GCTTCTGGTTTCCACAGC-3' and reverse 5'-TGGAATTGTAGGGCTCAACC-3' (162 bp); SCG10 forward 5'-CCACCATTGCCTAGTGACCT-3' and reverse 5'-GAAGCACACACTCCACGAGA-3' (202 bp); Chl1 forward 5'-CGCCTACACAGGAGCTAAGG-3' and reverse 5'-TTCTTTTGAAGGAGTGTCT-3' (231 bp); L1cam forward 5'-CATCGCCTTTGTGAGTGA-3' and reverse 5'-CTGTACTCGCCGAAGGTCTC-3' (162 bp); Lgals1 forward 5'-GCTGGTGGAGCAGGTCTCAGGAATCT-3' and reverse 5'-AAGGTGATGCACTCCTCTGTGATGCTC-3' (314 bp); Sprr1A like forward 5'-CTGATCACCAGATGCTGAGG-3' and reverse 5'-TCCTGAGCATGGAAGATT-3' (202 bp); RPL13A forward 5'-CCCTCCACCCTATGACAAGA-3' and reverse 5'-CCTTTTCTTCCGTTTCTCC-3' (167 bp). All primers were initially tested for their specificity by running reverse transcriptase polymerase chain reaction samples on an agarose gel. Only primers that under specific polymerase chain reaction conditions gave a single band of the appropriate molecular weight were then used for real-time polymerase chain reaction experiments. For quantitative reverse transcriptase polymerase chain reaction, fold changes were calculated following manufacture instructions (Invitrogen) and normalized to the levels of a housekeeping gene (*RPL13A*).

Chromatin immunoprecipitation assays

Chromatin immunoprecipitation assays were performed according to the manufacturer's recommendations (Upstate). Briefly, three retinæ per condition (AVGFP versus AVp300 at 24 h) were dissected and subsequently fixed in a 1% formaldehyde solution for 10 min at 37°C. Following cell lysis (0.5% sodium dodecyl sulphate, 100 mM NaCl, 50 mM Tris-HCl, pH 8.0, 5 mM EDTA), extracts were sonicated to shear DNA to lengths of 200–600 bp.

Chromatin solutions were incubated overnight with rotation using 4 μ g of rabbit polyclonal anti-acetyl histone H3 K9-14 antibody (Upstate) and mouse anti-p300 antibody (Abcam). The following day protein A agarose beads, which had been blocked with salmon sperm DNA, were added to each reaction to precipitate antibody complexes. The precipitated complexes were washed and then incubated for 4 h at 65°C in parallel with input samples to reverse the cross-link. DNA was isolated by phenol chloroform iso-amyl alcohol extraction, which was followed by ethanol precipitation in the presence of sodium acetate.

'Input', 'IP' and 'Mock' fractions were then analysed by quantitative polymerase chain reaction (ABI 7000) analysis with appropriate primer pairs. The primers used were as follows: coronin 1b 5' site <1 kb forward 5'-CTCCCAGCGTTATCATGTCA-3' and reverse 5'-GGGAGACTCGAATGTCCTCA-3'; GAP-43 5' site <1 kb forward 5'-GCAGCTGTAACCTGTGTGCA-3' and reverse 5'-GGTCCAGATTGGAGGTGTTTA-3'; Sprr1al 5' site <200 bp forward 5'-ACCCTCTCACAAACAAGCA-3' and reverse 5'-GAAACACACTTGCCCCAGAT-3'. For real-time quantitation of polymerase chain reaction products and fold-change measurements after chromatin immunoprecipitation,

each experimental sample was normalized to 'input' and 'Mock' fractions in triplicate from three independent samples, following the manufacturer instructions (Upstate).

Results

The expression of the acetyltransferase p300 is regulated during retinal ganglion cell maturation, and is repressed following optic nerve crush

Active gene expression is essential for axonal growth during development (Condrón, 2002). On the contrary, an active proregenerative gene expression programme is deficient after nerve injury in the adult CNS, contributing to the lack of axonal regeneration (Cai *et al.*, 2001). First, we analysed the expression profile of selected epigenetic markers for active gene expression including H3 lysine K18 acetylation (H3AcK18), p300, CBP and P/CAF during retinal ganglion cell maturation, as these three histone acetyltransferases are responsible for H3K18 acetylation. Importantly, in these initial experiments, although retinal ganglion cells are organized in a clearly distinguishable layer of the retina, the identity of retinal ganglion cells was confirmed by β -III tubulin immunostaining (Supplementary Fig. 1). To tag retinal ganglion cell maturation, we used sequential maturation steps of retinal ganglion cells leading to full myelination of the optic nerve (Tennekoon *et al.*, 1977). Within the retina, the retinal ganglion cell layer was stained by immunohistochemistry for H3AcK18, p300, CBP and P/CAF before (P0), during (P7 and P21) and after (adult) full myelination of the optic nerve (Fig. 1A). Assessment of fluorescence intensity showed an increase of H3AcK18 at P7 and P21 followed by a decrease in the adult stage (Fig. 1B). All fluorescence signal measurements for the protein of interest were normalized to the nuclear 4',6'-diamidino-2-phenylindole signal (data not shown). The expression pattern observed for H3AcK18 correlates with the expression of p300, which increases during retinal ganglion cell maturation to decrease in the adult (Fig. 1A and B). Conversely, CBP expression was stable throughout the maturation of retinal ganglion cells, while P/CAF appeared at very low and even expression levels along the time course (data not shown).

Hence, H3 K18 acetylation seems to be regulated similarly to the corresponding HAT p300 during retinal ganglion cell maturation and to decrease in adult cells.

We then investigated the expression of H3K18 acetylation and its acetyltransferases p300 and CBP by immunofluorescence at 24 and 72 h following optic nerve crush to investigate the post-injury regulation of this developmental epigenetic signature, potentially involved in axonal outgrowth. We chose a time window between 24 and 72 h for this experiment as optic nerve crush induces the expression of early genes as early as at 24 h after injury (Robinson, 1994; Bormann *et al.*, 1998), although the pro-regenerative programme is not spontaneously triggered. In addition, proregenerative gene expression is activated at \sim 72 h in case of axonal

regeneration after optic nerve crush mediated by lens injury (Fischer *et al.*, 2004).

By immunofluorescence, we did not observe any change in H3K18 acetylation level in the retinal ganglion cell layer after optic nerve crush compared with sham neither at 24 nor at 72 h (Fig. 1C and D). However, p300 and CBP expression decreased significantly at 72 h after optic nerve crush (Fig. 1C and D). Importantly, we also observed decreased acetylation of the transcription factor p53 at lysine 373 (p53 K373) (Fig. 1C and D), which is acetylated specifically by CBP/p300 at K373, and together with CBP/p300 can regulate neurite outgrowth in cultured neurons (Tedeschi *et al.*, 2009; Gaub *et al.*, 2010). Significantly, p53 basal level was not modified after optic nerve crush at neither 24 nor 72 h compared with sham (Fig. 1C and D).

Double immunofluorescence experiments with antibodies anti- β -III tubulin/p300, anti- β -III tubulin/CBP or anti- β -III tubulin/H3AcK18 confirmed that the expression observed in the granular cell layer is indeed localized almost exclusively in retinal ganglion cells (Supplementary Fig. 2). In brief, optic nerve crush does not modify the chromatin environment through histone H3 acetylation, which remains at similar lower levels in the adult as compared with retinal ganglion cells during maturation even after injury. However, optic nerve crush further downregulates the enzymes responsible for lysine acetylation such as CBP and p300, likely leading to deacetylation of p53 at K373.

The histone deacetylases inhibitor trichostatin A enhances CBP expression, induces retinal ganglion cell survival, but not axonal regeneration

We have previously demonstrated that the histone deacetylases I/II inhibitor trichostatin A induces CBP and p300 expression as well as p53 acetylation leading to an increase of p53 binding on specific progrowth gene promoters, thereby inducing neurite outgrowth in cultured neurons on permissive and non-permissive substrates (Gaub *et al.*, 2010). In order to explore whether the administration of trichostatin A would enhance axonal regeneration after optic nerve crush via similar mechanisms, we injected either trichostatin A (1, 10 or 100 ng/ml) or vehicle into the vitreous at the time of injury. Optic nerves as well as retinae were subsequently analysed 14 days post-optic nerve crush. Trichostatin A injection resulted in a significant increase of retinal ganglion cell survival compared with vehicle 14 days post-injury based upon the number of β -III tubulin-positive cells (Fig. 2A and B). Then we performed immunohistochemistry for GAP-43 on optic nerve sections to quantify axonal regeneration between trichostatin A versus vehicle-treated animals. Trichostatin A-treated rats showed a very limited non-significant increase of labelled axons past the lesion site independently of the dose delivered, while control animals receiving vehicle showed as expected no axonal regeneration past the lesion site (Fig. 2C). As opposed to what we observed previously in cultured cerebellar granule cells (Gaub *et al.*, 2010), trichostatin A did not induce p300 expression and p53 K373-associated acetylation in the retinal ganglion cell layer following optic nerve crush (Fig. 3A and B). Importantly, however,

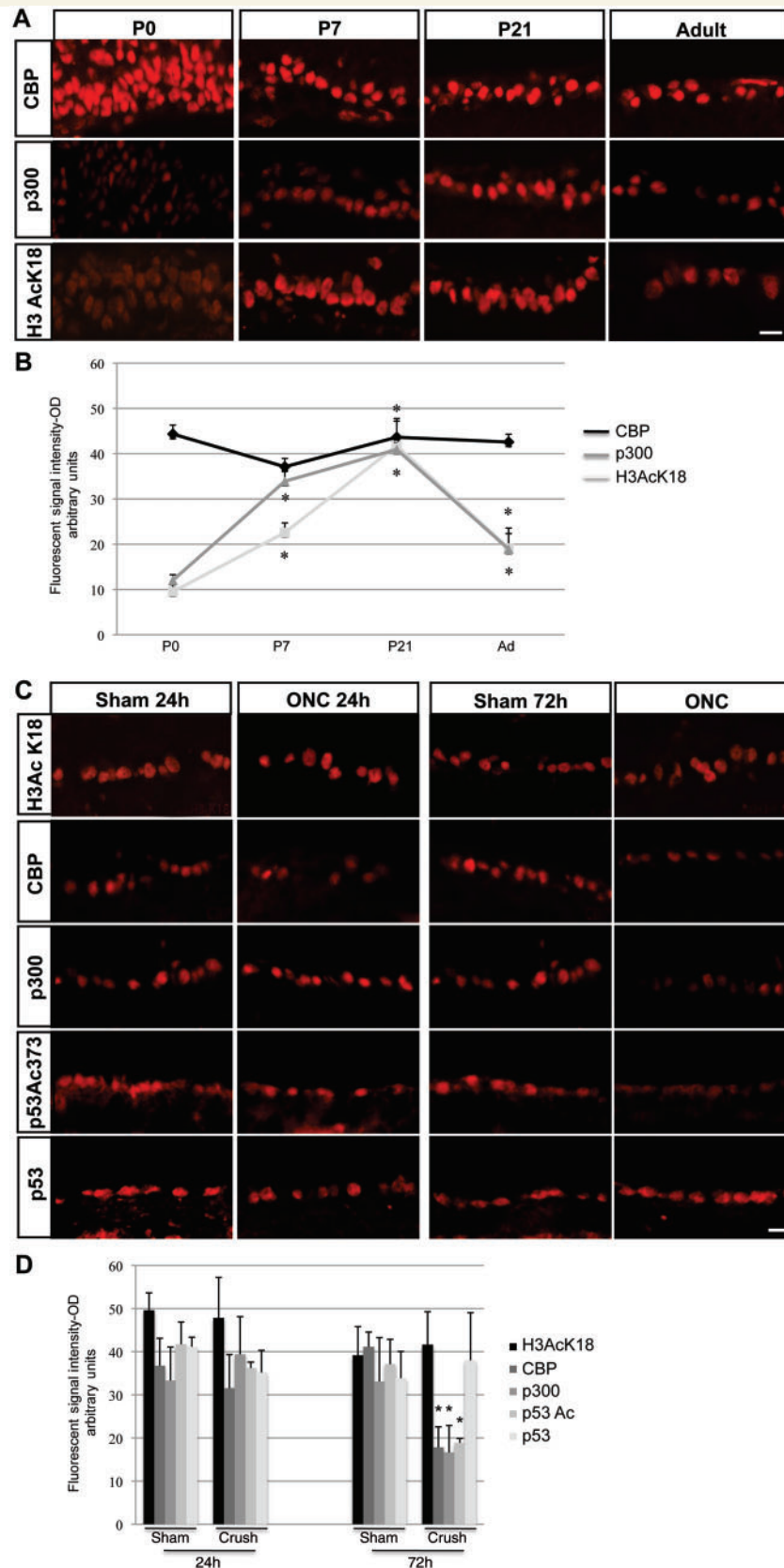


Figure 1 Maturation and optic nerve crush are associated with a decrease of histone acetyltransferase p300 in the retinal ganglion cell layer. (A) Representative pictures of the retinal ganglion cell layer at different time points during retinal ganglion cell maturation (P0, P7, P21 and adult) immunostained against CBP, p300 and H3AcK18. Scale bar = 20 μ m. (B) The level of protein expression was quantified by analysis of fluorescence intensity and represented on the graph. The graphs show an increase of H3AcK18 and p300 between P0 and P21

(continued)

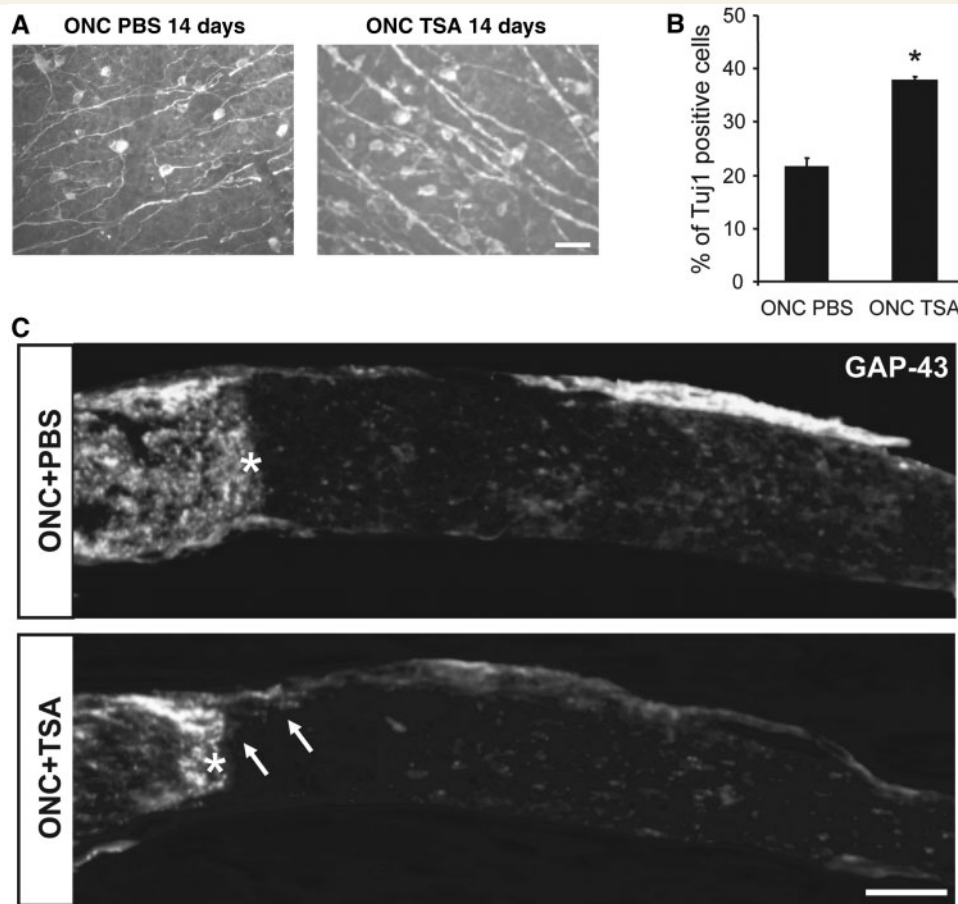


Figure 2 Histone deacetylases inhibition induces survival of retinal ganglion cells but not a significant enhancement of axonal regeneration. (A) Representative pictures of whole mount retina immunostained against β -III tubulin showing an increase of retinal ganglion cell survival 14 days after optic nerve crush (ONC) and injection of trichostatin A (TSA) 10 ng/ml, compared with optic nerve crush with phosphate-buffered saline (PBS). Scale bar = 50 μ m. (B) The bar graph shows quantification of retinal ganglion cells β -III tubulin (Tuj1)-positive cells after optic nerve crush with phosphate-buffered saline or trichostatin A injection compared with sham. Asterisk = unpaired two-tailed *t*-test, **P*-value < 0.05; *n* = 3. Error bars represent SD. (C) Optic nerve longitudinal sections were immunostained against GAP-43 14 days after optic nerve crush with phosphate-buffered saline or trichostatin A 10 ng/ml. Representative pictures show sporadic short axons past the lesion site after trichostatin A stimulation. Scale bar = 100 μ m.

trichostatin A did increase H3 acetylation, which is considered a read-out of the activity of histone deacetylases I/II inhibitors as well as of CBP (Fig. 3C and D). Hence, trichostatin A promotes the survival of retinal ganglion cells concomitantly with induction of histone acetylation and CBP expression. However, it is not able to stimulate axonal regeneration at any of the doses employed and does not promote the expression of p300 and of p53 acetylation, previously shown to enhance neurite outgrowth in cerebellar neurons cultured on inhibitory substrates (Gaub *et al.*, 2010).

p300 induces axonal regeneration and modifies the epigenome on select proregeneration promoters

Since intravitreal trichostatin A administration fails to promote axonal regeneration and is able to neither increase p300 expression nor p300-related p53K373 acetylation after optic nerve crush, we decided to overexpress p300 in order to enhance axonal

Figure 1 Continued

and a decrease in adult, whereas CBP expression was not altered. P300 and H3 AcK18 level show a similar expression pattern during retinal ganglion cell maturation (*n* = 3). Asterisks = unpaired two-tailed *t*-test, **P*-value < 0.01; *n* = 3. Each average value per time point was measured against the average value of all time points together. Error bars represent SD. (C) Immunohistochemistry of retinae shows immunostaining of retinal ganglion cell layer against H3 AcK18, CBP, p300, p53 Ac373 and p53, 24 h and 72 h after optic nerve crush (ONC) compared with sham. No change is observed for H3K18 acetylation at either 24 h or at 72 h after optic nerve crush compared with sham, whereas a decrease of p300 and CBP expression is shown along with a decrease of p53 Ac373, while p53 basal level was stable. Scale bar = 20 μ m. (D) The graph represents quantification of the protein level obtained by measurement of the fluorescence signal. Asterisks = unpaired two-tailed *t*-test, **P*-value < 0.01; *n* = 3. Error bars represent SD. OD = optical density.

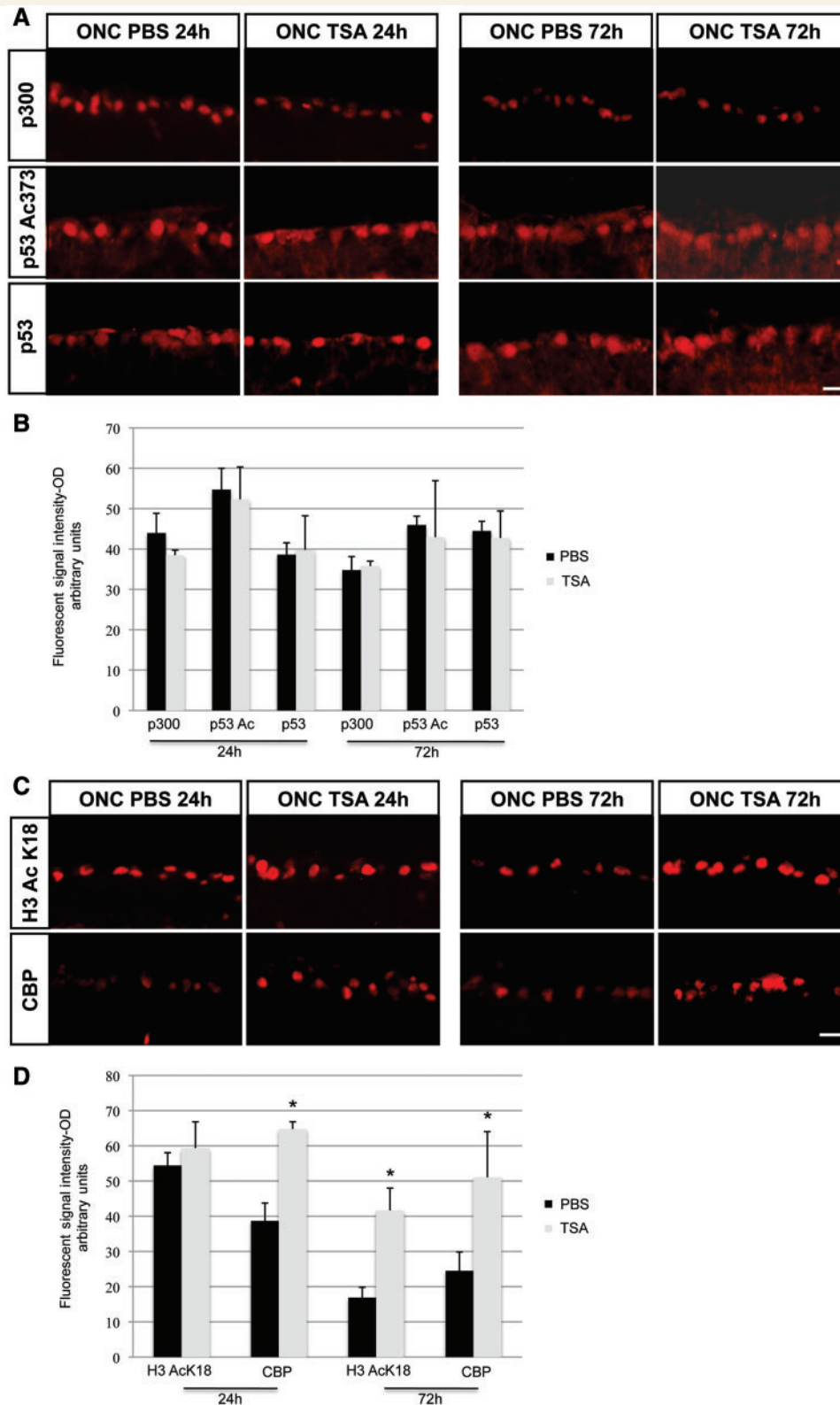


Figure 3 Histone deacetylases inhibition does not modify p300 expression or p53-dependent acetylation. (A) Retinae were immunostained against p300, p53Ac373 and p53 24 h and 72 h after optic nerve crush (ONC) with or without trichostatin A (TSA; 10 ng/ml). Shown are representative pictures of retinal ganglion cells showing no change for p300, p53 or p53Ac373 expression at 24 h or at 72 h after trichostatin A, compared with phosphate-buffered saline (PBS)-injected animals. Scale bar = 20 μ m. (B) The bar graphs show quantification of p300, p53Ac373 and p53 protein level analysed by measurement of the fluorescence signal. (C) Immunostaining against H3AcK18 and CBP on retinal ganglion cells 24 h and 72 h after optic nerve crush with phosphate-buffered saline or trichostatin A represented in the pictures show a significant increase of H3AcK18 and CBP 72 h after trichostatin A injection compared with phosphate-buffered saline. Scale bar = 20 μ m. (D) Quantification of expression levels of H3AcK18 and CBP are represented in the bar graphs. Asterisks = unpaired two-tailed *t*-test, **P*-value < 0.05. Error bars represent SD.

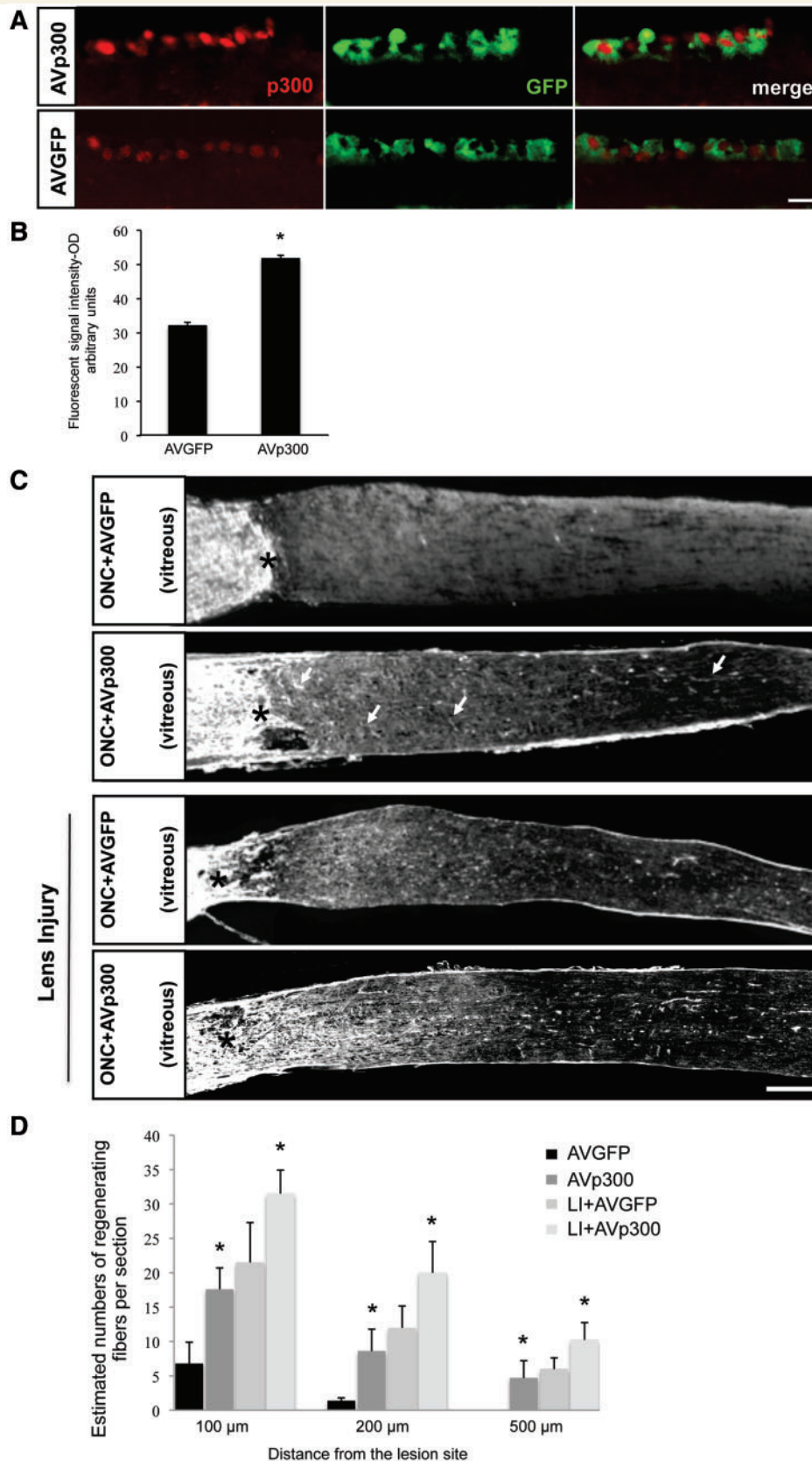


Figure 4 p300 over-expression by adenovirus infection induces axonal regeneration of the optic nerve. (A) Representative pictures of retinal ganglion cell layer after immunostaining in the retina against p300 shows expression of p300 in green fluorescence protein (GFP)-positive cells 24 h after optic nerve crush (ONC) and AVp300 or AVGFP infection. An increase of p300 expression in the retinal ganglion cell layer is shown following AVp300-GFP versus AVGFP infection. Scale bar = 20 μm. (B) Bar graph represents quantification of p300

(continued)

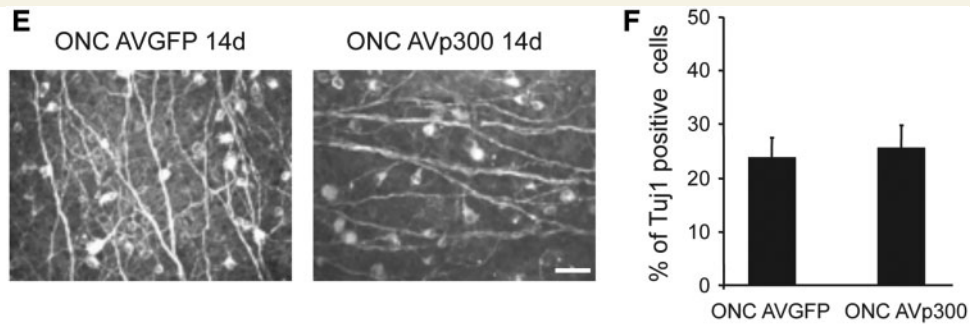


Figure 4 Continued.

protein levels analysed by measurement of the fluorescence signal. Asterisks = unpaired two-tailed *t*-test, **P*-value < 0.01; *n* = 3. Error bars represent SD. (C) Representative pictures of longitudinal optic nerve sections immunostained against GAP-43 14 days after optic nerve crush and infected with AVGFP or AVp300-GFP (alone or in combination with lens injury) show axonal regeneration in AVp300-infected rats, which is enhanced by lens injury. Scale bar = 100 μ m. (D) Adenoviral overexpression of p300 alone or in combination with lens injury induces a significant increase in the number of axons past the lesion site compared with AVGFP-infected nerves alone or in combination with lens injury as shown in the bar graph (*n* = 4 per condition). Asterisks = unpaired two-tailed *t*-test, **P*-value < 0.05. Error bars represent SD. (E) Representative pictures of whole flat retina immunostained against β -III tubulin (Tuj1) 14 days after optic nerve crush with AVGFP or AVp300 infection. Scale bar = 50 μ m. (F) Bar graphs show quantification of retinal ganglion β -III tubulin-positive cells on whole flat retina (*n* = 3) that reveals no difference in retinal ganglion cell survival (as compared with sham) 14 days after optic nerve crush with AVGFP or AVp300. OD = optical density.

regeneration via both increased proregenerative transcription and histone acetylation on select target promoters. Due to the large size of p300 (8 kb), we decided to clone full-length p300 in a size-compatible adenoviral vector carrying two cytomegalovirus promoters driving either p300 or GFP for intravitreal *in vivo* infection experiments. AVGFP virus was employed as a control. AVp300/GFP (AVp300) or AVGFP were injected into the vitreous at the time of injury. Optic nerves were extracted 14 days post-injury and immunostained for GAP-43 to identify regenerating axons. Infection of p300 significantly increased p300 expression as early as at 24 h after infection (Fig. 4A and B) in the retinal ganglion cell layer. More importantly, it resulted in a significant increase in the number of regenerating axons compared with control GFP (Fig. 4C and D). Additionally, the combination of lens injury, a well-known strategy to enhance neuronal intrinsic-dependent axonal regeneration after optic nerve crush, and p300 overexpression led to further enhancement of axonal regeneration as compared with lens injury or p300 overexpression alone (Fig. 4C and D). However, we observed that AVp300 does not induce survival of retinal ganglion cells compared with AVGFP when counting the overall number of β -III tubulin-positive neurons (Fig. 4E and F), therefore the pool of regenerating axons stems from the limited pool of spontaneously surviving retinal ganglion cells. This was confirmed by evaluating the number of double β -III tubulin/GFP-positive cells in p300 and control virus-infected retinæ, which showed no difference (Supplementary Fig. 3).

A percentage of retinal ganglion cells ($17.7 \pm 3.4\%$ SE of β -III tubulin-positive cells, *n* = 3) were successfully infected as shown by co-localization of GFP with β -III tubulin within the ganglion cell layer *in vivo* (Supplementary Fig. 4). A number of cells were

also infected in the retina inner nuclear layer, corresponding presumably to bipolar/amacrine and Müller cells (Supplementary Fig. 4). In order to prove the cell autonomous effects of p300 overexpression specifically in neurons, we cultured primary retinal cells and infected them with either AVGFP or AVp300. Retinal ganglion cells were infected in culture as shown by expression of GFP in β -III tubulin-positive cells (Fig. 5A). More importantly, we found that overexpression of p300 induced a significant increase in neurite outgrowth as compared with control-infected neurons (Fig. 5B and C). All together, these data suggest that p300 overexpression can promote axonal regeneration but not survival of retinal ganglion cells following optic nerve crush and that these effects are at least in part mediated by neuronal intrinsic mechanisms.

Immunofluorescence experiments further showed that overexpression of p300 induced both pro-axonal regeneration transcription factor and histone H3 hyperacetylation in the retinal ganglion cell layer following optic nerve crush. At both 24 and 72 h post-optic nerve crush, we observed a significantly increased p53K373 acetylation in the retinal ganglion cell layer in AVp300 versus AVGFP infection, while total p53 levels remained unchanged (Fig. 6A and B). Similarly, we found that the acetylation of the pro-axonal regeneration transcription factor C/EBP, which can be acetylated on lysine 215 and 216 (Cesena *et al.*, 2007; Wang *et al.*, 2007), was enhanced at 24 and 72 h after optic nerve crush by p300 overexpression (Fig. 6A and B). Lastly, we confirmed as expected that p300 overexpression was able to induce H3K18 acetylation (Fig. 6A and B).

Therefore, induction of p300 resulted in an increased acetylation of p53 and C/EBP, which is associated with their increased

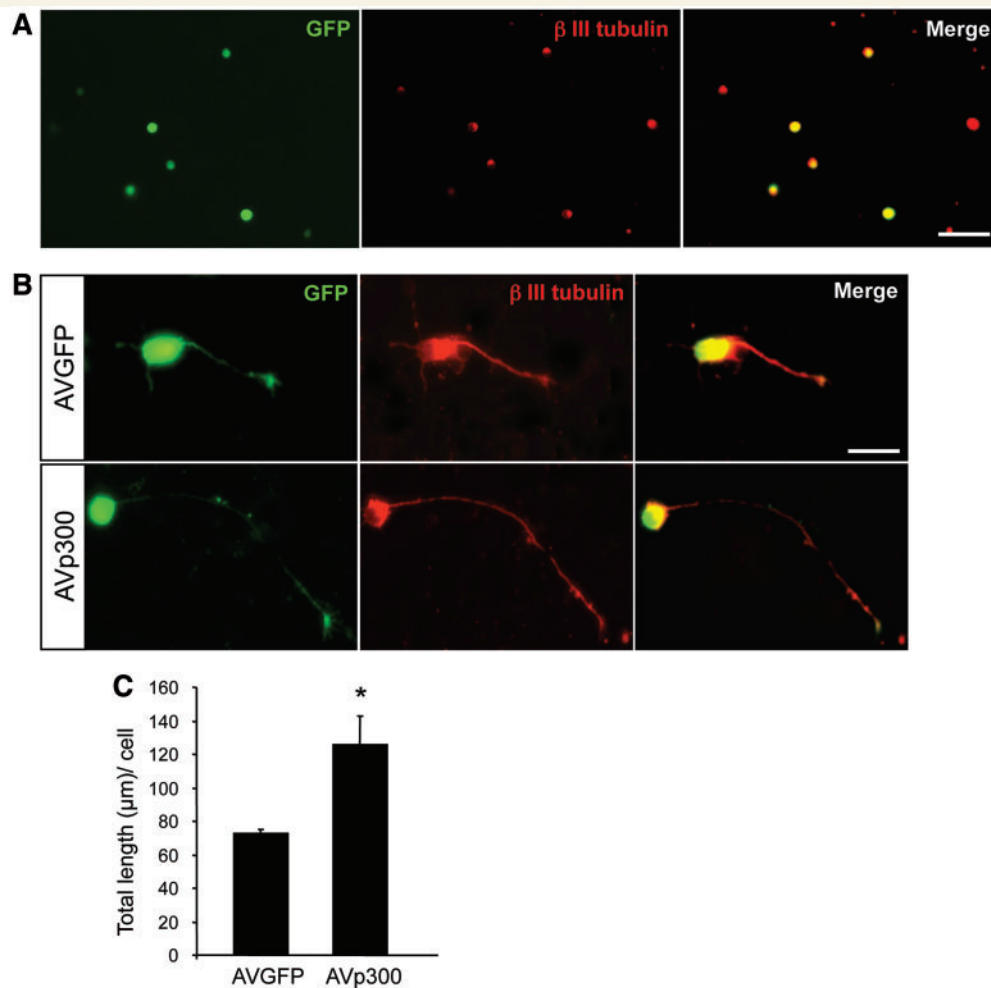


Figure 5 Overexpression of p300 induces neurite outgrowth in cultured cells. (A) Retinal cells were cultured on poly-D-lysine for 24 h and infected with AVGFP or AVp300 at MOI 100. Immunostaining against β -III tubulin for retinal ganglion cells shows a colocalization with infected green fluorescence protein (GFP)-positive cells. Scale bar = 20 μ m. (B) Representative pictures of dissociated retinal primary culture immunostained against β III-tubulin show enhanced neurite outgrowth in p300-infected GFP-positive cells compared with control virus infection. Scale bar = 20 μ m. (C) Quantification of neurite length shows an increase in neurite outgrowth 72 h after infection of AVp300 compared with AVGFP-infected cells. Asterisk = unpaired two-tailed *t*-test, **P*-value < 0.01; *n* = 3. Error bars represent SD. MOI = multiplicity of infection.

transcriptional activity, and with H3 hyperacetylation, signature of active chromatin. However, in order to assess whether AVp300, in addition to enhancing axonal regeneration, is also directly capable of occupying and acetylating the promoters of proregenerative gene targets, we performed chromatin immunoprecipitation assays from dissected retinae after optic nerve crush and infection with either AVp300 or AVGFP. Selected gene targets included *Sprr1a* and *GAP-43* as markers of pro-regenerative state of retinal ganglion cells (Benowitz and Routtenberg, 1997; Fischer *et al.*, 2004), and *coronin 1B* as a pro-neurite outgrowth gene and target of p53-dependent acetylation (Di Giovanni *et al.*, 2006). Following p300 overexpression, we found a significant increase of p300 proximal promoter occupancy on *GAP-43*, *coronin 1b* and *Sprr1a* (Fig. 7A), which was paralleled by a strongly enhanced promoter acetylation of H3 (Fig. 7B). Importantly, as p300 promoter occupancy and p300-dependent promoter

acetylation are associated with gene transcription, we measured gene expression by real-time reverse transcriptase polymerase chain reaction post-optic nerve crush and AVp300 or AVGFP infection. Indeed, we observed an increase in messenger RNA expression of several pro-axonal outgrowth genes, including *GAP-43*, *Sprr1a* and *coronin 1b* (Fig. 7C), as well as α -tubulin 1a, *Chl1* and *Lgals1* (Fig. 7D). Interestingly, all of these genes contain p300-related p53 putative binding sites, and their induction is likely to contribute to the pro-axonal regenerative properties of p300. In summary, overexpression of p300 induces axonal regeneration upon optic nerve crush, acetylates the proregenerative transcription factors p53 and C/EBP, directly occupies and acetylates the promoters of the regeneration-associated genes *GAP-43*, *coronin 1b* and *Sprr1a* and drives the gene expression programme of several regeneration-associated genes.

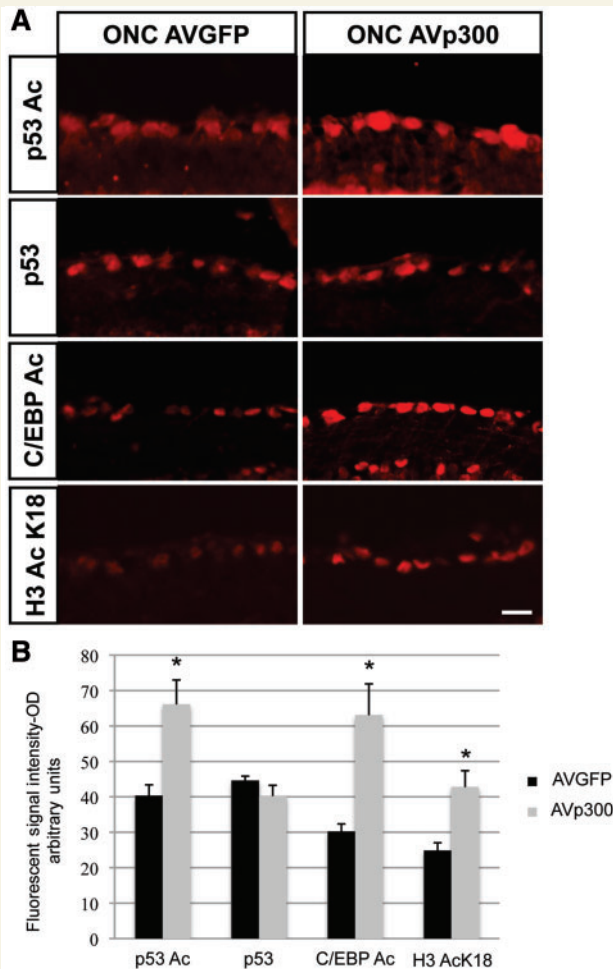


Figure 6 p300 overexpression leads to increased acetylation of p53, C/EBP and H3 K18. (A) Immunohistochemistry of retinæ against p53 Ac373, p53, C/EBP Ac215/216 and H3AcK18 shows expression in the retinal ganglion cell layer 24 h after optic nerve crush (ONC) and AVGFP or AVp300 infection. Shown is an increase of H3AcK18, p53 and C/EBP acetylation. The basal level of p53 is unchanged. Scale bar = 20 μ m. (B) The bar graphs represent assessment of fluorescence signal in retinal ganglion cells for the different antigens. Asterisk = unpaired two-tailed *t*-test, **P*-value < 0.01; *n* = 3. Error bars represent SD. OD = optical density.

Discussion

Variable degrees of axonal regeneration of the optic nerve have been achieved by both inhibiting the extrinsic environment or by enhancing the intrinsic capacity of retinal ganglion cells (Bertrand *et al.*, 2005, 2007; Park *et al.*, 2008; Moore *et al.*, 2009). As far as the intrinsic strategies are concerned, lens injury, the pro-inflammatory molecule oncomodulin, the Bcl-2 inhibitor BAG-1 or ciliary neurotrophic factor have all led to substantial axonal regeneration (Yin *et al.*, 2006, 2009; Planchamp *et al.*, 2008). More recently, direct modifications of transcription or of protein synthesis via KLF4 or PTEN deletion, respectively,

promoted axonal regeneration after optic nerve crush (Park *et al.*, 2008; Moore *et al.*, 2009), and to a substantial distance in the case of combinatory treatment with PTEN deletion, cyclic adenosine monophosphate and oncomodulin (Kurimoto *et al.*, 2010).

Here, we show for the first time that intrinsic axonal regeneration of the optic nerve can be achieved by a different class of molecules, via overexpression of a transcriptional coactivator and epigenetic modifier, the acetyltransferase p300. Overexpression of p300 induces axonal regeneration of the optic nerve following crush, hyperacetylates histone H3, acetylates the promoters of several regeneration-associated genes and induces their gene expression. In addition, overexpression of p300 results in the acetylation of the pro-axonal outgrowth transcription factors p53 and C/EBP. p53 K373 acetylation has been previously shown to promote neurite outgrowth in primary neurons and to be a signature of active p53 that is required for axonal regeneration (Tedeschi *et al.*, 2009; Gaub *et al.*, 2010). Acetylated C/EBP, whose acetylation enhances its transcription potential, has been shown to be induced in retinal ganglion cells during lens injury-mediated axonal regeneration, and has been reported to be required for axonal regeneration in the PNS (Nadeau *et al.*, 2005).

It is therefore conceivable that p300 may unlock a silent pro-regenerative gene expression programme by driving the expression of several regeneration-associated genes via enhanced transcription.

We found initially that p300 was regulated during retinal ganglion cell maturation to decrease in the mature retinal ganglion cells as well as following optic nerve crush. Importantly, the signal for p300 and the related proteins does not follow the same pattern of expression in the inner nuclear layer (data not shown), suggesting that it is specific to the retinal ganglion cell layer. In addition, in the ganglion cell layer, the expression of histone acetyltransferases is largely restricted to retinal ganglion cells, and is only sporadically found in neighbouring glial cells.

Since mature adult neurons are known to be less plastic and to express a less vigorous pro-regenerative gene expression programme, we wondered whether p300 downregulation might be in part responsible for the lack of intrinsic neuronal proregenerative capacity. Indeed, after ruling out the pro-regenerative potential of a more general epigenetic strategy with the histone deacetylase inhibitor trichostatin A, which does not enhance p300 expression, we found that overexpression of p300 was able to promote axonal regeneration of surviving retinal ganglion cells. This supports the model where reactivating a silenced developmental programme in the adult may favour axonal regeneration.

P300 is a transcriptional coactivator and histone-modifying enzyme (Ogryzko *et al.*, 1996), thus contributing to epigenetic changes responsible for enhanced transcriptional activity. Recently, we have shown that a transcriptional complex formed by CBP/p300 and p53 occupies the promoter of GAP-43 driving its expression during axonal regeneration following facial nerve axotomy (Tedeschi *et al.*, 2009). Subsequently, we also observed that overexpression of CBP and p300 was able to promote neurite outgrowth on permissive and inhibitory myelin substrates in

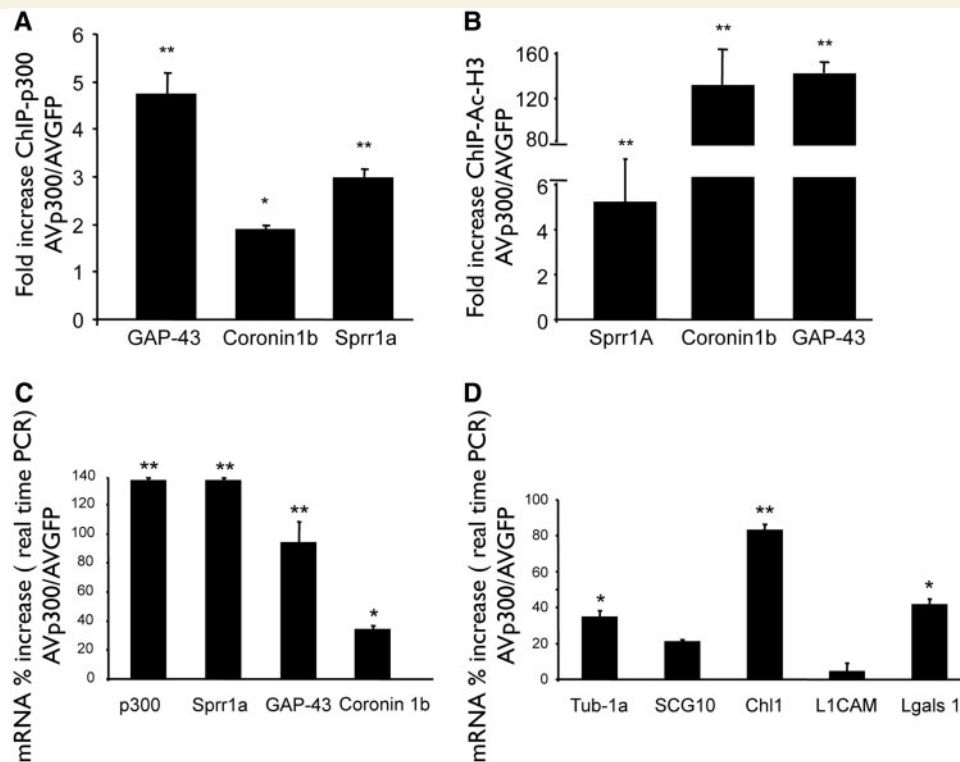


Figure 7 Infection of AVp300 enhances promoter occupancy of p300 and histone acetylation on specific proregenerative genes along with an increase of their gene expression level. (A) Chromatin immunoprecipitation (ChIP) assay from dissected retina shows increased occupancy of the GAP-43, coronin 1 b and Sprr1a promoters by p300 following 24 h of optic nerve crush plus AVp300 injection versus AVGFP. Fold change was calculated as a ratio of promoter occupancy between AVp300 treated versus AVGFP in three independent animals in triplicate samples. Asterisks = unpaired two-tailed *t*-test, **P*-value < 0.05, ***P*-value < 0.01. Error bars represent SD. (B) Bar graph shows an increase of histone H3 acetylation on Sprr1a, coronin 1 b and GAP-43 promoter 24 h after optic nerve crush with AVp300 compared with AVGFP infection. Fold change was calculated as a ratio of promoter occupancy between AVp300 treated versus AVGFP in three independent animals in triplicate samples. Asterisks = unpaired two-tailed *t*-test, **P*-value < 0.05, ***P*-value < 0.01. Error bars represent SD. (C and D) Bar graphs show real-time reverse transcriptase polymerase chain reaction (PCR) messenger RNA (mRNA) expression data for p300 and a number of regeneration-associated genes including Sprr1a, GAP-43 and coronin 1 b (C) or for α -tubulin1a, SCG10, Chl1, L1CAM and Lgals1 (D). Optic nerve crush with AVp300 induces an increase of several of these genes compared with optic nerve crush with AVGFP in three independent animals. Asterisks = unpaired two-tailed *t*-test, **P*-value < 0.05, ***P*-value < 0.01. Error bars represent SD.

primary cerebellar neurons (Gaub *et al.*, 2010). Here we show for the first time that p300 can promote neurite outgrowth in retinal ganglion cells, supporting the neuronal intrinsic effect of p300 in axonal regeneration. We used adenoviral infection to achieve p300 overexpression due to the large size of p300 (~8 kb), which is too large for other viral vectors such as adeno-associated virus (maximum insert size < 5 kb) that have become the gold standard for retinal ganglion cell infection *in vivo* in recent years (Dinculescu *et al.*, 2005). However, adenoviruses have been extensively used to infect both non-neuronal and neuronal cells in the eye, both via intravitreal (Jomary *et al.*, 1994; Li *et al.*, 1994; Weise *et al.*, 2000; Zhang *et al.*, 2008) or axonal retrograde injection (Cayouette and Gravel, 1996; Isenmann *et al.*, 2001), and our findings suggest that our adenovirus is able to infect primary neurons at very high efficiency in culture and at a lower efficiency *in vivo*. It is possible that infection of bipolar/amacrine cells also plays an important role in determining the intrinsic growth ability

of retinal ganglion cells (Goldberg *et al.*, 2002), and that the infection of glial cells may contribute to stimulating intrinsic axonal regeneration of retinal ganglion cells. Conceptually, the specificity of p300-dependent axonal regeneration is supported by the negative findings following trichostatin A treatment, where overall pro-transcriptional epigenetic changes do not enhance axonal regeneration. Interestingly, trichostatin A does induce survival of retinal ganglion cells 14 days after optic nerve crush, as well as increased CBP expression and H3K18 acetylation, but fails to promote p300 expression and p53 acetylation. Conversely, overexpression of p300 does not induce retinal ganglion cell survival but promotes axonal regeneration in surviving retinal ganglion cells, suggesting that histone deacetylases inhibition and p300 activate two independent pathways. Axonal regeneration is not always linked to neuronal survival, as in the case of deletion of the transcription factor KLF4 (Moore *et al.*, 2009), which results in a significant increase in axonal regeneration

from surviving retinal ganglion cells but not in increased retinal ganglion cell survival. Here, neuronal survival was assessed by β -III tubulin staining, which although it cannot discern among specific cell death mechanisms, is widely used to count retinal neurons. If lack of enhanced p300-dependent retinal ganglion cell survival is disappointing, it highlights the efficacy and specificity of p300 in promoting the axonal regeneration programme.

We have in fact shown, for the first time, that a selective modification of the transcriptional environment is capable of promoting axonal regeneration in the CNS by enhancing the intrinsic pre-generative programme. Moreover, the enhanced axonal regeneration achieved by the overexpression of p300, along with lens injury, suggests that p300 may further stimulate the intrinsic gene expression programme known to be activated by lens injury. Therefore, future combinatory experiments with molecules such as oncomodulin, deletion of PTEN or delivery of ciliary neurotrophic factor are also expected to enhance the level of p300-dependent axonal regeneration by boosting the intrinsic retinal ganglion cell regeneration potential.

Acknowledgements

We would like to thank our collaborators in the adenovirus core facility for viral production. We would also like to thank Jeffrey Goldberg for critically reading our manuscript.

Funding

Hertie Foundation; the Fortüne Program, University of Tübingen (both granted to S.D.G.); a DZNE Fellowship (granted to Y.J.).

Supplementary material

Supplementary material is available at *Brain* online.

References

- Benowitz LI, Routtenberg A. GAP-43: an intrinsic determinant of neuronal development and plasticity. *Trends Neurosci* 1997; 20: 84–91.
- Berry M, Carlile J, Hunter A. Peripheral nerve explants grafted into the vitreous body of the eye promote the regeneration of retinal ganglion cell axons severed in the optic nerve. *J Neurocytol* 1996; 25: 147–70.
- Bertrand J, Winton MJ, Rodriguez-Hernandez N, Campenot RB, McKerracher L. Application of Rho antagonist to neuronal cell bodies promotes neurite growth in compartmented cultures and regeneration of retinal ganglion cell axons in the optic nerve of adult rats. *J Neurosci* 2005; 25: 1113–21.
- Bormann P, Zumsteg VM, Roth LW, Reinhard E. Target contact regulates GAP-43 and alpha-tubulin mRNA levels in regenerating retinal ganglion cells. *J Neurosci Res* 1998; 52: 405–19.
- Butler SJ, Tear G. Getting axons onto the right path: the role of transcription factors in axon guidance. *Development* 2007; 134: 439–48.
- Cai D, Qiu J, Cao Z, McAtee M, Bregman BS, Filbin MT. Neuronal cyclic AMP controls the developmental loss in ability of axons to regenerate. *J Neurosci* 2001; 21: 4731–9.
- Cayouette M, Gravel C. Adenovirus-mediated gene transfer to retinal ganglion cells. *Invest Ophthalmol Vis Sci* 1996; 37: 2022–8.
- Cesena TI, Cardinaux JR, Kwok R, Schwartz J. CCAAT/enhancer-binding protein (C/EBP) beta is acetylated at multiple lysines: acetylation of C/EBPbeta at lysine 39 modulates its ability to activate transcription. *J Biol Chem* 2007; 282: 956–67.
- Condron B. Gene expression is required for correct axon guidance. *Curr Biol* 2002; 12: 1665–9.
- Di Giovanni S, Knights CD, Rao M, Yakovlev A, Beers J, Catania J, et al. The tumor suppressor protein p53 is required for neurite outgrowth and axon regeneration. *EMBO J* 2006; 25: 4084–96.
- Dinculescu A, Glushakova L, Min SH, Hauswirth WW. Adeno-associated virus-vectored gene therapy for retinal disease. *Hum Gene Ther* 2005; 16: 649–63.
- Filbin MT. Recapitulate development to promote axonal regeneration: good or bad approach? *Philos Trans R Soc Lond B Biol Sci* 2006; 361: 1565–74.
- Fischer D, Heiduschka P, Thanos S. Lens-injury-stimulated axonal regeneration throughout the optic pathway of adult rats. *Exp Neurol* 2001; 172: 257–72.
- Fischer D, Pavlidis M, Thanos S. Cataractogenic lens injury prevents traumatic ganglion cell death and promotes axonal regeneration both in vivo and in culture. *Invest Ophthalmol Vis Sci* 2000; 41: 3943–54.
- Fischer D, Petkova V, Thanos S, Benowitz LI. Switching mature retinal ganglion cells to a robust growth state in vivo: gene expression and synergy with RhoA inactivation. *J Neurosci* 2004; 24: 8726–40.
- Gaub P, Tedeschi A, Puttagunta R, Nguyen T, Schmandke A, Di Giovanni S. HDAC inhibition promotes neuronal outgrowth and counteracts growth cone collapse through CBP/p300 and P/CAF-dependent p53 acetylation. *Cell Death Differ* 2010; 17: 1392–408.
- Goldberg JL, Klassen MP, Hua Y, Barres BA. Amacrine-signaled loss of intrinsic axon growth ability by retinal ganglion cells. *Science* 2002; 296: 1860–4.
- Hauk TG, Leibinger M, Muller A, Andreadaki A, Knippschild U, Fischer D. Stimulation of axon regeneration in the mature optic nerve by intravitreal application of the toll-like receptor 2 agonist Pam3Cys. *Invest Ophthalmol Vis Sci* 2010; 51: 459–64.
- Huebner EA, Strittmatter SM. Axon regeneration in the peripheral and central nervous systems. *Results Probl Cell Differ* 2009; 48: 339–51.
- Isenmann S, Engel S, Kugler S, Gravel C, Weller M, Bahr M. Intravitreal adenoviral gene transfer evokes an immune response in the retina that is directed against the heterologous lacZ transgene product but does not limit transgene expression. *Brain Res* 2001; 892: 229–40.
- Jomary C, Piper TA, Dickson G, Couture LA, Smith AE, Neal MJ, et al. Adenovirus-mediated gene transfer to murine retinal cells in vitro and in vivo. *FEBS Lett* 1994; 347: 117–22.
- Kurimoto T, Yin Y, Omura K, Gilbert HY, Kim D, Cen LP, et al. Long-distance axon regeneration in the mature optic nerve: contributions of oncomodulin, cAMP, and pten gene deletion. *J Neurosci* 2010; 30: 15654–63.
- Lee JK, Geoffroy CG, Chan AF, Tolentino KE, Crawford MJ, Leal MA, et al. Assessing spinal axon regeneration and sprouting in Nogo-, MAG-, and OMgp-deficient mice. *Neuron* 2010; 66: 663–70.
- Leibinger M, Muller A, Andreadaki A, Hauk TG, Kirsch M, Fischer D. Neuroprotective and axon growth-promoting effects following inflammatory stimulation on mature retinal ganglion cells in mice depend on ciliary neurotrophic factor and leukemia inhibitory factor. *J Neurosci* 2009; 29: 14334–41.
- Leon S, Yin Y, Nguyen J, Irwin N, Benowitz LI. Lens injury stimulates axon regeneration in the mature rat optic nerve. *J Neurosci* 2000; 20: 4615–26.
- Li T, Adamian M, Roof DJ, Berson EL, Dryja TP, Roessler BJ, et al. In vivo transfer of a reporter gene to the retina mediated by an adenoviral vector. *Invest Ophthalmol Vis Sci* 1994; 35: 2543–9.
- Lingor P, Tonges L, Pieper N, Bermel C, Barski E, Planchamp V, et al. ROCK inhibition and CNTF interact on intrinsic signalling pathways and differentially regulate survival and regeneration in retinal ganglion cells. *Brain* 2008; 131 (Pt 1): 250–63.

- Logan A, Ahmed Z, Baird A, Gonzalez AM, Berry M. Neurotrophic factor synergy is required for neuronal survival and disinhibited axon regeneration after CNS injury. *Brain* 2006; 129 (Pt 2): 490–502.
- Luo J, Deng ZL, Luo X, Tang N, Song WX, Chen J, et al. A protocol for rapid generation of recombinant adenoviruses using the AdEasy system. *Nat Protoc* 2007; 2: 1236–47.
- Moore DL, Blackmore MG, Hu Y, Kaestner KH, Bixby JL, Lemmon VP, et al. KLF family members regulate intrinsic axon regeneration ability. *Science* 2009; 326: 298–301.
- Muller A, Hauk TG, Leibinger M, Marienfeld R, Fischer D. Exogenous CNTF stimulates axon regeneration of retinal ganglion cells partially via endogenous CNTF. *Mol Cell Neurosci* 2009; 41: 233–46.
- Nadeau S, Hein P, Fernandes KJ, Peterson AC, Miller FD. A transcriptional role for C/EBP beta in the neuronal response to axonal injury. *Mol Cell Neurosci* 2005; 29: 525–35.
- Naumann U, Kugler S, Wolburg H, Wick W, Rascher G, Schulz JB, et al. Chimeric tumor suppressor 1, a p53-derived chimeric tumor suppressor gene, kills p53 mutant and p53 wild-type glioma cells in synergy with irradiation and CD95 ligand. *Cancer Res* 2011; 71: 5833–42.
- Ogryzko VV, Schiltz RL, Russanova V, Howard BH, Nakatani Y. The transcriptional coactivators p300 and CBP are histone acetyltransferases. *Cell* 1996; 87: 953–9.
- Park KK, Liu K, Hu Y, Smith PD, Wang C, Cai B, et al. Promoting axon regeneration in the adult CNS by modulation of the PTEN/mTOR pathway. *Science* 2008; 322: 963–6.
- Planchamp V, Bermel C, Tonges L, Ostendorf T, Kugler S, Reed JC, et al. BAG1 promotes axonal outgrowth and regeneration in vivo via Raf-1 and reduction of ROCK activity. *Brain* 2008; 131 (Pt 10): 2606–19.
- Raivich G, Bohatschek M, Da Costa C, Iwata O, Galiano M, Hristova M, et al. The AP-1 transcription factor c-Jun is required for efficient axonal regeneration. *Neuron* 2004; 43: 57–67.
- Robinson GA. Immediate early gene expression in axotomized and regenerating retinal ganglion cells of the adult rat. *Brain Res Mol Brain Res* 1994; 24: 43–54.
- Schnichels S, Heiduschka P, Julien S. Different spatial and temporal protein expressions of repulsive guidance molecule a and neogenin in the rat optic nerve after optic nerve crush with and without lens injury. *J Neurosci Res* 2011; 89: 490–505.
- Tedeschi A, Nguyen T, Puttagunta R, Gaub P, Di Giovanni S. A p53-CBP/p300 transcription module is required for GAP-43 expression, axon outgrowth, and regeneration. *Cell Death Differ* 2009; 16: 543–54.
- Tennekoon GI, Cohen SR, Price DL, McKhann GM. Myelinogenesis in optic nerve. A morphological, autoradiographic, and biochemical analysis. *J Cell Biol* 1977; 72: 604–16.
- Wang H, Larris B, Peiris TH, Zhang L, Le Lay J, Gao Y, et al. C/EBPbeta activates E2F-regulated genes in vivo via recruitment of the coactivator CREB-binding protein/P300. *J Biol Chem* 2007; 282: 24679–88.
- Weise J, Isenmann S, Klockner N, Kugler S, Hirsch S, Gravel C, et al. Adenovirus-mediated expression of ciliary neurotrophic factor (CNTF) rescues axotomized rat retinal ganglion cells but does not support axonal regeneration in vivo. *Neurobiol Dis* 2000; 7: 212–23.
- Yang XJ, Seto E. HATs and HDACs: from structure, function and regulation to novel strategies for therapy and prevention. *Oncogene* 2007; 26: 5310–8.
- Yin Y, Cui Q, Gilbert HY, Yang Y, Yang Z, Berlinicke C, et al. Oncomodulin links inflammation to optic nerve regeneration. *Proc Natl Acad Sci USA* 2009; 106: 19587–92.
- Yin Y, Henzl MT, Lorber B, Nakazawa T, Thomas TT, Jiang F, et al. Oncomodulin is a macrophage-derived signal for axon regeneration in retinal ganglion cells. *Nat Neurosci* 2006; 9: 843–52.
- Yiu G, He Z. Glial inhibition of CNS axon regeneration. *Nat Rev Neurosci* 2006; 7: 617–27.
- Yiu G, He Z. Signaling mechanisms of the myelin inhibitors of axon regeneration. *Curr Opin Neurobiol* 2003; 13: 545–51.
- Zhang C, Li H, Liu MG, Kawasaki A, Fu XY, Barnstable CJ, et al. STAT3 activation protects retinal ganglion cell layer neurons in response to stress. *Exp Eye Res* 2008; 86: 991–7.

Supplementary Figures

Supplementary Figure 1.

Representative immunofluorescence of the retina performed with Ab against β III tubulin and counterstained with DAPI. Shown in a higher magnification on the right are β III-tubulin positive retinal ganglion cells (retinal ganglion cell) in the ganglion cell layer (GCL). Scale bar: 50 μ m.

Supplementary Figure 2.

Representative double immunofluorescence of the retina performed with Ab anti- β III tubulin and anti-p300, anti-CBP, or anti-H3AcK18 in sham as well as after optic nerve crush (72 hours). As shown in the merged images, almost all p300, CBP or H3AcK18 positive cells are also β -III tubulin positive (retinal ganglion cells). Scale bar: 10 μ m.

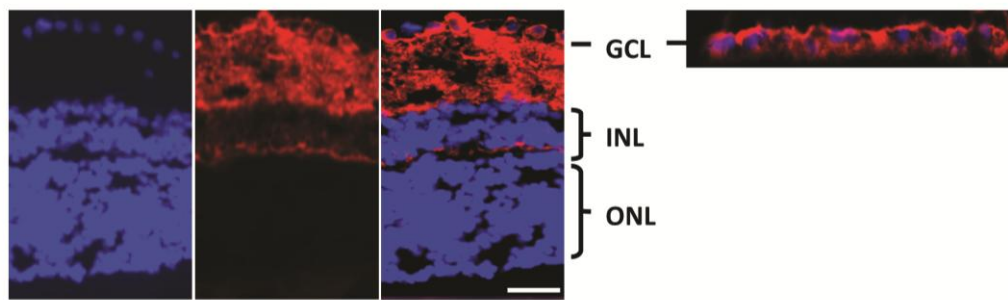
Supplementary Figure 3.

Bar graphs show quantification of β III tubulin/green fluorescent protein double positive retinal ganglion cells on whole flat retina (n : 3) that reveals no difference in retinal ganglion cells survival (as compared to sham) 14 days after optic nerve crush with AVgreen fluorescent protein or AVp300.

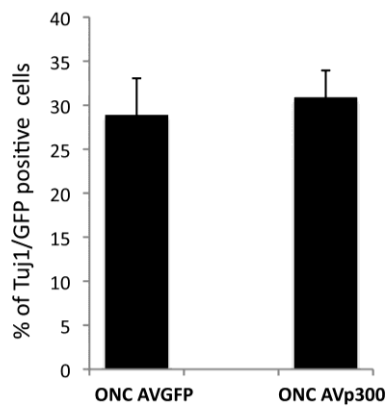
Supplementary Figure 4.

Confocal microscopy images of immunohistochemistry in the retina for β III-tubulin 24h after intravitreal injection of AVgreen fluorescent protein and optic nerve crush. Shown is infection of retinal ganglion cells in the ganglion cell layer (GCL) in several double positive green fluorescent protein and β III-tubulin infected cells (arrows). Scale bar: 20 μ m

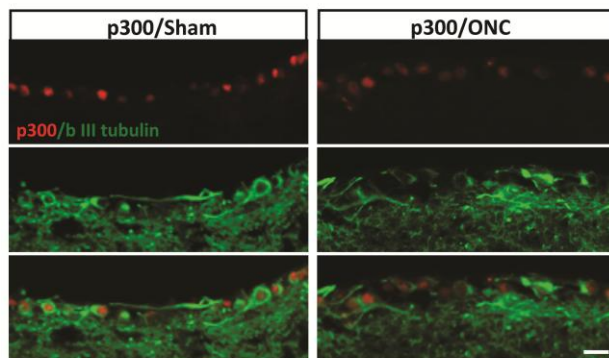
Supplementary Figure 1



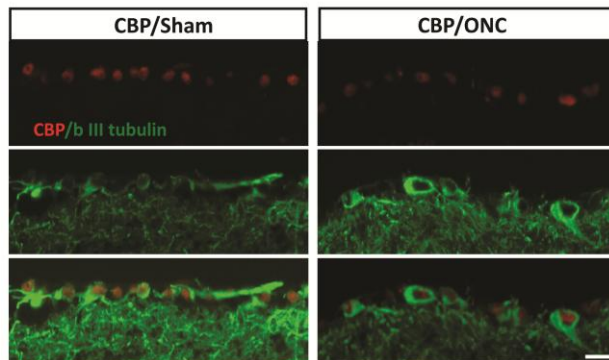
Supplementary Figure 2



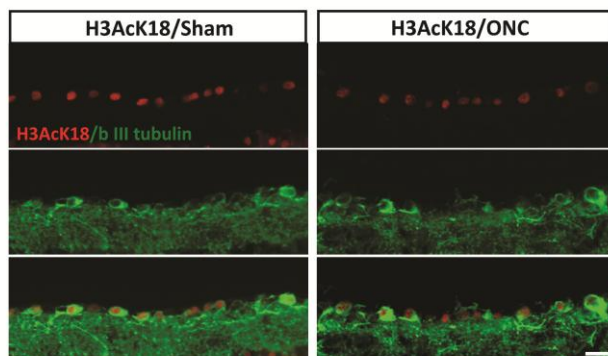
Supplementary Figure 3



B.



C.



ARTICLE

Received 13 Dec 2013 | Accepted 27 Feb 2014 | Published 1 Apr 2014

DOI: 10.1038/ncomms4527

PCAF-dependent epigenetic changes promote axonal regeneration in the central nervous system

Radhika Puttagunta^{1,*}, Andrea Tedeschi^{2,*}, Marilia Grando Sória^{1,3}, Arnau Hervera^{1,4}, Ricco Lindner^{1,3}, Khizr I. Rathore¹, Perrine Gaub^{1,3}, Yashashree Joshi^{1,3,5}, Tuan Nguyen¹, Antonio Schmandke¹, Claudia J. Laskowski², Anne-Laurence Boutillier⁶, Frank Bradke² & Simone Di Giovanni^{1,4}

Axonal regenerative failure is a major cause of neurological impairment following central nervous system (CNS) but not peripheral nervous system (PNS) injury. Notably, PNS injury triggers a coordinated regenerative gene expression programme. However, the molecular link between retrograde signalling and the regulation of this gene expression programme that leads to the differential regenerative capacity remains elusive. Here we show through systematic epigenetic studies that the histone acetyltransferase p300/CBP-associated factor (PCAF) promotes acetylation of histone 3 Lys 9 at the promoters of established key regeneration-associated genes following a peripheral but not a central axonal injury. Furthermore, we find that extracellular signal-regulated kinase (ERK)-mediated retrograde signalling is required for PCAF-dependent regenerative gene reprogramming. Finally, PCAF is necessary for conditioning-dependent axonal regeneration and also singularly promotes regeneration after spinal cord injury. Thus, we find a specific epigenetic mechanism that regulates axonal regeneration of CNS axons, suggesting novel targets for clinical application.

¹Laboratory for NeuroRegeneration and Repair, Center for Neurology, Hertie Institute for Clinical Brain Research, University of Tübingen, 72076 Tübingen, Germany. ²Department of Axonal Growth and Regeneration, German Center for Neurodegenerative Disease, 53175 Bonn, Germany. ³Graduate School for Cellular and Molecular Neuroscience, University of Tübingen, 72076 Tübingen, Germany. ⁴Division of Brain Sciences, Department of Medicine, Imperial College London, Hammersmith Campus, London W12 0NN, UK. ⁵DZNE, German Center for Neurodegenerative Diseases, D-72076 Tübingen, Germany. ⁶Laboratoire de Neurosciences Cognitives et Adaptatives (LNCA), Université de Strasbourg-CNRS, GDR CNRS, Strasbourg 67000, France. *These authors contributed equally to this work. Correspondence and requests for materials should be addressed to R.P. (email: radhika.puttagunta@medizin.uni-tuebingen.de) or to S.D.G. (email: s.di-giovanni@imperial.ac.uk).

The regenerative response initiated following axonal injury in the peripheral nervous system (PNS) versus the central nervous system (CNS) leads to differential growth capacities and repair. In fact, the lack of pro-neuronal growth gene expression and glial inhibitory signals leads to regenerative failure following CNS but not PNS injury^{1–4}. Immediately after a peripheral nerve injury, rapid ion fluxes increase, followed by a rise in cAMP levels, axonal translation occurs, phosphorylation retrograde cascades activate transcription factors, gene expression is induced and finally regeneration occurs^{5,6}. However, the final link between axonal injury-induced retrograde signalling and the regulation of essential regenerative gene expression remains elusive. The dorsal root ganglia (DRG) sensory neurone system has a central as well as a peripheral axonal branch departing from a single cell body. This allows for bimodal injury inputs with differing regenerative capacities into one central transcriptional hub. Interestingly, the lack of regeneration of injured ascending sensory fibres in the spinal cord can be partially enhanced by an injury to the peripheral branch (conditioning lesion) of DRG neurones⁷. In search of key regulatory mechanisms that may clarify the molecular nature of this regenerative gene expression programme, we hypothesized that as an ‘orchestrator of gene regulation’ epigenetic changes would direct expression of genes crucial for regeneration only in the presence of pro-regenerative signalling following peripheral but not central damage.

Identification of a specific regulatory mechanism shared by several essential genes may lead to novel molecular strategies recapitulating the conditioning effect, thus non-surgically enhancing axonal regeneration in the CNS. To this end, we employed the first systematic approach to understand the epigenetic environment in DRG neurones. We examined both DNA methylation and various key histone modifications with regards to gene regulation following axonal injury. We found that p300/CBP-associated factor (PCAF)-dependent acetylation of histone 3 lysine 9 (H3K9ac), paralleled by a reduction in methylation of H3K9 (H3K9me2), occurred at the promoters of select genes only after PNS axonal injury. In addition, we observed that extracellular signal-regulated kinase (ERK) axonal retrograde signalling is required for PCAF-dependent acetylation at these promoters and for their enhancement in gene expression. Finally, we established that PCAF is required for regeneration following a conditioning lesion and PCAF overexpression promotes axonal regeneration similar to that of a conditioning lesion after CNS injury in spinal ascending sensory fibres. Our results show the first evidence of immediate retrograde signalling leading to long-term epigenetic reprogramming of gene expression of select genes whose modulation leads to axonal regeneration in the hostile spinal environment.

Results

Histone codes are shaped by a peripheral not by a central lesion. Given that epigenetic changes are a rapid and dynamic way to translate external stimuli into targeted and long-lasting gene regulation, such has been observed in learning and memory, seizures, stroke and neuronal differentiation^{8–11}, we hypothesized that retrograde signals following axonal injury could lead to an epigenetic environmental shift facilitating the expression of genes critical to regeneration. We believed that a positive retrograde signal initiated by PNS injury could relax the chromatin environment surrounding specific promoters and allow for gene expression; however, a negative signal following CNS injury may restrict promoter accessibility and inhibit gene expression. Following equidistant CNS (dorsal column axotomy, DCA) or PNS (sciatic nerve axotomy, SNA) axotomies, from L4–L6 DRG we assessed both high-throughput promoter

and CGI DNA methylation (DNA methylation microarrays) and histone modifications (quantitative chromatin immunoprecipitation (ChIP) assays) at the proximal promoters of genes previously established to be critical to regeneration such as growth-associated protein 43 (GAP-43)¹², Galanin¹³ and brain-derived neurotrophic factor (BDNF)^{14,15} (Fig. 1a).

DNA methylation arrays showed a modest number of genes differentially methylated between injuries (Supplementary Fig. 1a–e); however, none of the genes associated with regeneration displayed significant levels of methylation nor were they differentially methylated between SNA and DCA (Supplementary Fig. 2a). More importantly, and as opposed to a recent study investigating folate and its DNA methylation after sciatic and spinal injury¹⁶, quantitative RT-PCR analysis of the differentially methylated genes, and DNA methyltransferases did not show a consistent correlation between DNA methylation levels and gene expression (Supplementary Figs 2b–e and 3). Therefore, promoter and CGI DNA methylation does not appear to be a key factor in the differential regenerative response between CNS and PNS injuries in the DRG system.

Next, we investigated whether key histone modifications would be specifically enriched on established critical genes for the regenerative programme in DRG neurones. Of all histone modifications that correlate with active gene transcription (H3K9ac, H3K18ac, H3K4me2)¹⁷ or gene repression (H3K9me2 and H3K27me3)¹⁷ that were screened, H3K9ac, H3K9me2 and H3K27me3 were enriched compared with IgG on most promoters; however, only H3K9ac and H3K9me2 were found to be differentially enriched at *GAP-43*, *Galanin* and *BDNF* promoters, consistently correlating with early and sustained increased expression following SNA (1–7 days; Figs 1b,c and 2a–d; Tables 1 and 2). Additionally, these three genes presented common promoter motifs in CpG content as well as transcription-binding sites that together with increased H3K9ac at their promoters suggest common transcriptional regulation (Fig. 1b,c). H3K9ac and the H3K9ac-specific acetyltransferase, PCAF, are typically found in the proximity of transcriptional start sites of actively transcribing genes¹⁷, and accordingly PCAF was also enriched at these promoters (Fig. 1c). Interestingly, H3K9me2, which is associated with gene silencing¹⁷, was found to be decreased at these promoters and inversely correlated to gene expression following SNA (Fig. 1c). In contrast, *SCG-10*, whose gene expression is unaltered after 24 h and only modestly increased following 3- and 7-day SNA (Fig. 1b), did not show an enhancement of H3K9ac or PCAF at its promoter (Fig. 1c). Given that a preconditioning lesion (SNA preceding DCA) activates the regenerative capacity of the CNS⁷, we questioned whether a PNS epigenetic signal overrides a CNS signal. We observed an increase in the gene expression of these genes following preconditioned DCA versus DCA alone, which correlated with an increase in PCAF at these promoters (Fig. 1d,e). Furthermore, a broader picture of post-axotomy gene expression profiles and H3K9ac promoter enrichment is depicted by regeneration-associated (*Chl1*, *L1cam*, *SPRR1a*)¹⁸, axonal growth (*ATF3* and *Bcl-xL*)^{19,20} housekeeping (*ribosomal unit 18S*) genes and axonal structure (*NF-L*) genes²¹ (Fig. 2a,b). Importantly, these experiments show that H3K9ac, a marker of actively transcribing genes, is selectively enriched on the promoters of *GAP-43*, *Galanin* and *BDNF*, but not on the promoters of other SNA-induced genes such as *SPRR1a*, *ATF3* and *HSP27* (Fig. 2a–d; Table 1), suggesting that their common regulation maybe linked to their importance in regeneration.

NGF-MEK-ERK signalling regulates PCAF and H3K9ac. Next, we turned our attention to understanding whether retrograde signalling following SNA plays a role in this positive chromatin

remodelling. Immediately following peripheral injury, pERK levels rise in the injured axon and ERK signalling modules are retrogradely transported to the DRG cell body^{22,23}, where we show that global PCAF and H3K9ac levels rise (Fig. 3a–c). In adult primary DRG neuronal cultures, nerve growth factor (NGF), an activator of ERK signalling and neurite outgrowth²⁴, increased the expression of PCAF and H3K9ac, while the ERK kinase (MEK) inhibitor, PD98059 (PD), prevented PCAF and H3K9ac induction²⁵ (Fig. 4a,b). NGF induces PCAF expression, nuclear localization and activation of acetyltransferase activity specifically by threonine phosphorylation at its histone acetyltransferase domain²⁶. In L4-L6 DRG, SNA induced the expression of nuclear PCAF and PCAF threonine but not serine

phosphorylation (Fig. 4c,d). This correlated with an increase in pERK in DRG, as well as nuclear PCAF translocation and acetylation of H3K9, all of which are dependent on ERK activation following SNA (Fig. 4e–i). As predicted, inhibition of ERK activation following SNA decreased gene expression as well as PCAF and H3K9ac at the promoters of *GAP-43*, *Galanin* and *BDNF* (Fig. 4j–l). However, in conjunction with our theory of specificity of regulation, H3K9ac did not correlate with gene expression at other promoters following inhibition of ERK activation (Supplementary Fig. 4a,b). Remarkably, cAMP signalling in adult DRG neuronal cultures did not induce nuclear PCAF translocation (Supplementary Fig. 5), suggesting that cAMP-mediated mechanisms only partially supporting

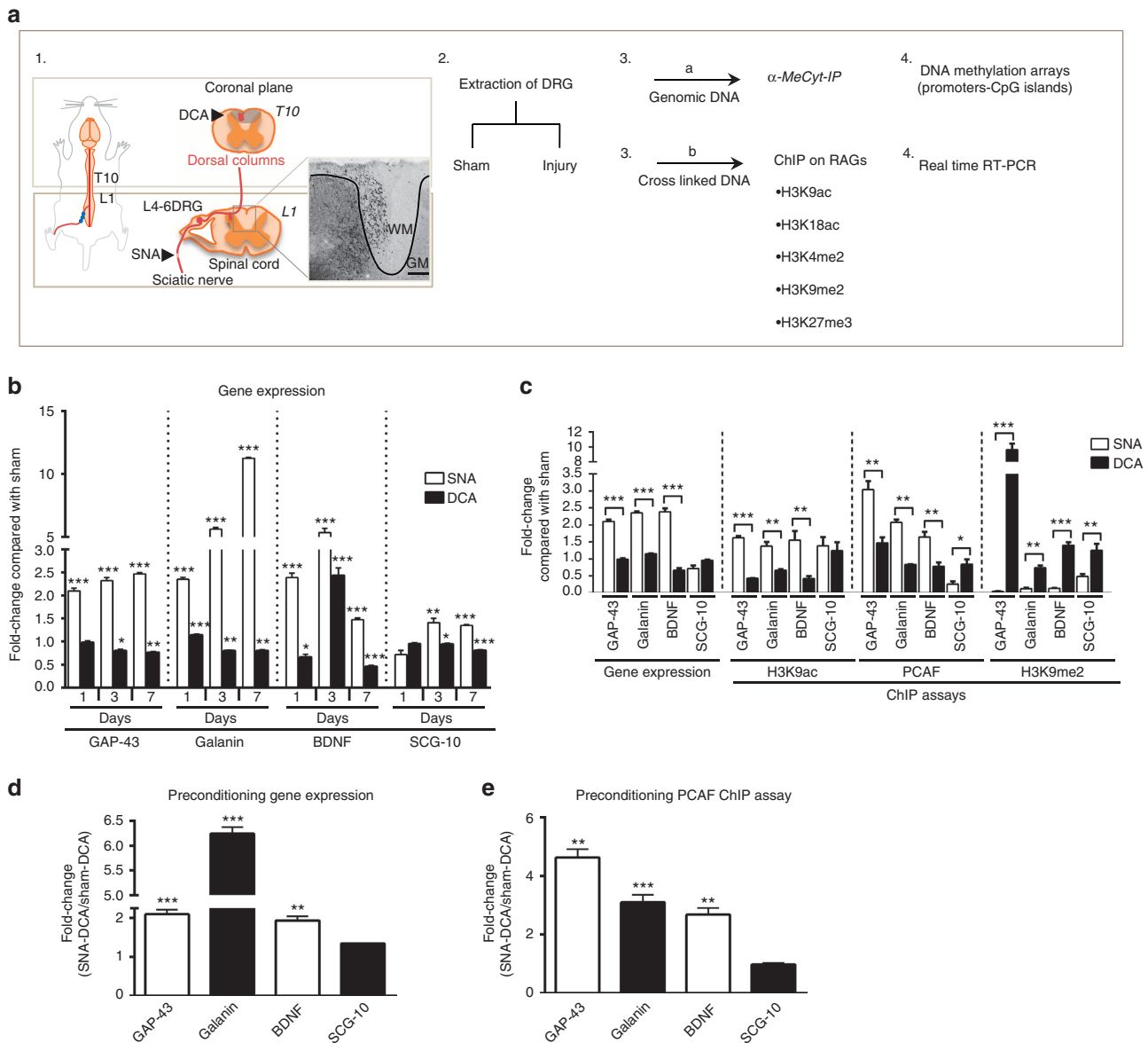


Figure 1 | H3K9ac and PCAF involvement in the regulation of regeneration genes. (a) Schematic diagram of SNA and DCA injury models used for epigenetic screens involving DNA methylation arrays and quantitative ChIP assays from L4-L6 DRG. Scale bar, 100 μ m. (b) Fold change increases observed in *GAP-43*, *Galanin* and *BDNF* gene expression at 1, 3 and 7 days post SNA but not DCA and at 3 and 7 days for *SCG-10*. (c) Increased gene expression, H3K9ac, PCAF and decreased H3K9me2 at *GAP-43*, *Galanin* and *BDNF*, but not *SCG-10* (*SCG-10* had decreased H3K9me2 enrichment to a lesser extent) promoters following 1 day post-SNA versus DCA. (d) A preconditioning lesion performed 1 week before DCA still induced 24 h later gene expression of *GAP-43*, *Galanin* and *BDNF* but not *SCG-10*. (e) This correlated with an increase in PCAF at the promoters of activated regeneration genes. Q-PCR. (b,c) $N = 3$ per group; ChIP assays (c–e) $N = 6$ per group, Student's t -test, error bars, s.e. * $P < 0.05$, ** $P < 0.01$, *** $P < 0.001$. All experiments were performed in triplicate.

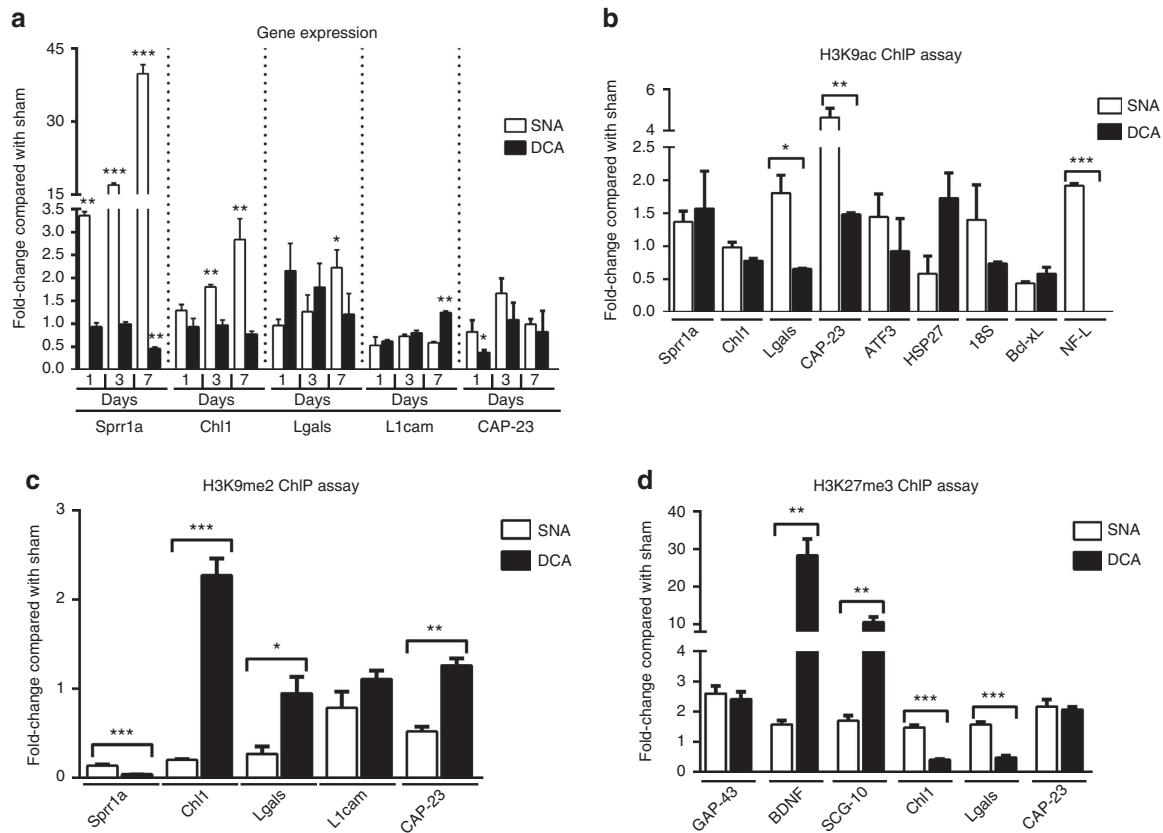


Figure 2 | Histone modifications that do not correlate with gene expression. (a) Gene expression of genes associated with regeneration found to be induced (*Sprr1a* and *Chl1*) or not changed (*Lgals*, *L1cam* and *CAP-23*) at various timepoints. (b) H3K9ac ChIP assays at the promoters of several genes previously found to be either induced (*Sprr1a*, *HSP27* and *ATF3*), unchanged (*Chl1* and *18S*) or repressed (*Bcl-xL* and *NF-L*) in gene expression 24 h post SNA only showed a correlation between expression and H3K9ac promoter occupancy for *Bcl-xL*. No enrichment to IgG was found for *L1cam* promoter. (c) ChIP assay for H3K9me2 24 h post SNA and DCA compared with Shams shows no correlation with 24-h gene expression time point for *Sprr1a*, *Chl1*, *Lgals* and *CAP-23*, but for *L1cam* there is no change observed, which is in agreement with no change in gene expression. (d) No consistent pattern of correlation with gene expression was found with H3K27me3 24 h post SNA by ChIP assay. No enrichment was found compared with IgG for *L1cam* and *Galanin*. (ChIP assays, $N = 6$ per group, performed in triplicate). Error bars, s.e. (a,c,d) Student's t -test, * $P < 0.05$, ** $P < 0.001$ and *** $P < 0.001$.

Table 1 | Correlation between gene expression and H3K9ac ChIP data.

		H3K9ac at promoters		
		Increase	No change	Decrease
Gene expression	Increase	<u>BDNF, Galanin, GAP-43</u>	ATF3, HSP27	<i>Sprr1a</i>
	No change	CAP-23	<u>SCG-10</u> , <i>Chl1</i> , <i>L1cam</i> , <i>18S</i> , <i>Lgals</i>	
	Decrease	NF-L		<i>Bcl-xL</i>

BDNF, brain-derived neurotropic factor; ChIP, chromatin immunoprecipitation; H3K9ac, acetylation of histone 3 lysine 9. A table displaying our gene expression data for genes associated with regeneration or known data for control genes and our H3K9ac ChIP data at their promoters, showing a clear correlation between increased gene expression and H3K9ac at the promoters of the genes BDNF, Galanin and GAP-43.

Table 2 | Enrichment of histone modifications over IgG.

Histone modifications	Enrichment compared with IgG
H3K9ac	Yes
H3K18ac	No
H3K4me2	No
H3K9me2	Yes
H3K27me3	Yes

Of the histone modifications examined, those shown in the table in white are inducers and those in grey are repressors of gene expression. Two of the histone modifications screened for this study, H3K18ac and H3K4me2, did not show enrichment compared with IgG for any of the genes examined.

conditioning-dependent axonal regeneration²⁷ operate independently from pERK-induced epigenetic PCAF-mediated long-term mechanisms. These data present the first link between retrogradely transported PNS-injury-related signals and epigenetic modifications at the promoters of specific established regenerative genes.

PCAF supports axonal regeneration mimicking a conditioning lesion. As a preconditioning lesion is able to induce neurite outgrowth in primary adult DRG neurones cultured on permissive (laminin) or non-permissive (myelin) substrates²⁸, we tested whether increased PCAF expression by adeno-associated virus

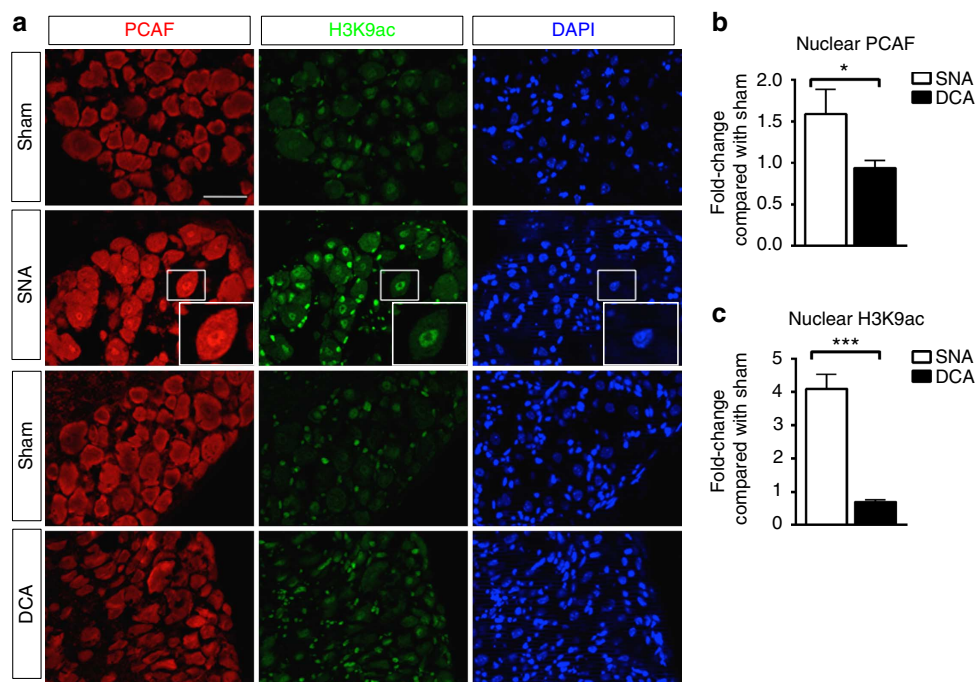


Figure 3 | Increased nuclear PCAF and H3K9ac following SNA but not DCA. (a) IHC co-staining with PCAF and H3K9ac of L4-L6 DRG following Sham/SNA or Sham/DCA. Insert shows high nuclear expression of PCAF and H3K9ac after SNA. Scale bar, 50 μ m. (b) IHC intensity density analysis reveals an increase in nuclear PCAF following SNA/Sham but not DCA/Sham. (c) Intensity density analysis of IHC stained with H3K9ac reveals a significant fold increase following SNA but not DCA when compared with respective Sham. Student's *t*-test, error bars, s.e., **P* < 0.05, ****P* < 0.001, *N* = 3 per group, performed in triplicate.

(AAV, Supplementary Fig. 6a–c) could also drive neurite outgrowth. Indeed, neurite outgrowth increased on laminin and myelin by PCAF overexpression in DRG (Fig. 5a,b) as well as another CNS primary culture, cerebellar granule neurones (CGN, Supplementary Fig. 7a). In CGN (employed for its ease of culture and greater cell number for use in immunoblotting, ChIP and transfections for luciferase assays) there was a significant decrease in H3K9ac when plated on myelin (Supplementary Fig. 7b,c) and a reduction of H3K9ac at select promoters, which was reverted to permissive levels with overexpression of PCAF (Supplementary Fig. 7d). Likewise, PCAF overexpression reversed myelin repression of select genes in DRGs (Fig. 5c). Furthermore, the drug Garcinol (5 μ M), which inhibits PCAF acetyltransferase activity²⁹, reduced neurite outgrowth in DRG (Fig. 5d,e) and CGN (Supplementary Fig. 7e,f), decreased the luciferase expression of a *GAP-43* promoter luciferase construct in CGN (Supplementary Fig. 7g) and decreased select gene expression in DRG (Fig. 5f). In *ex vivo* experiments, the inhibition of PCAF activity by Garcinol was able to significantly limit neurite outgrowth on both laminin and myelin as well as repress H3K9ac induced by SNA (Fig. 5g–i). Correspondingly, *PCAF*^{−/−} mice provided full abolishment of neurite outgrowth induced by SNA in *ex vivo* cultured DRG neurones (Fig. 5j,k). Additionally, SNA-dependent neurite outgrowth in *ex vivo* cultured DRG neurones was blocked by ERK inhibition via delivery of PD at the nerve stump (Fig. 6a–c), phenocopying PCAF loss of function experiments.

Thus far our data suggest that PCAF is integral to the signalling involved following PNS injury leading to regeneration by altering the epigenetic landscape and stimulating intrinsic competence through crucial gene expression. To validate these observations *in vivo*, we studied regeneration of ascending sensory fibres following a preconditioning lesion (SNA 7 days before DCA) in the absence of PCAF and found that PCAF is required for

regeneration induced by a conditioning lesion and for the expression of *GAP-43*, *Galanin* and *BDNF* in DRG (Fig. 7a–g). Importantly, axonal tracing in SCI experiments in a cohort of *PCAF*^{−/−} mice and strain-matched controls showed that *PCAF*^{−/−} mice did not display any abnormalities or overt phenotype in axonal tracing or regarding the lesion site (Fig. 7a).

Next, we wondered whether PCAF overexpression alone would mimic regeneration induced by a conditioning lesion and enhance regeneration of ascending sensory fibres in the spinal cord following dorsal column lesion. Indeed, similar to that previously reported for a preconditioning lesion^{7,30}, PCAF overexpression (Supplementary Fig. 8) significantly increased the number of regenerating fibres across the lesion and up to a distance of 1 mm rostral of the lesion site (Fig. 8a–c and Supplementary Fig. 9). Important to note, the depth of the lesion (Supplementary Fig. 10) and lack of tracing rostral to the lesion site (Supplementary Fig. 11) allowed excluding the presence of spared fibres. Furthermore, the introduction of the AAV directly into the sciatic nerve is in and of itself a PNS injury that does induce minimal sprouting towards the lesion in the GFP control.

Discussion

Our work demonstrates that PCAF is required for conditioning-dependent spinal regeneration and that PCAF overexpression alone is able to promote regeneration of sensory fibres across the injured spinal cord and beyond similarly to previously established conditioning paradigms. Furthermore, PCAF-induced regeneration correlated with a significant increase in the expression of H3K9ac, *GAP-43*, *Galanin* and *BDNF* in the L4-L6 DRG. The definition of regeneration-associated genes (RAGs) is genes differentially induced between the regenerating PNS and non-regenerating CNS systems; however, this does not validate the

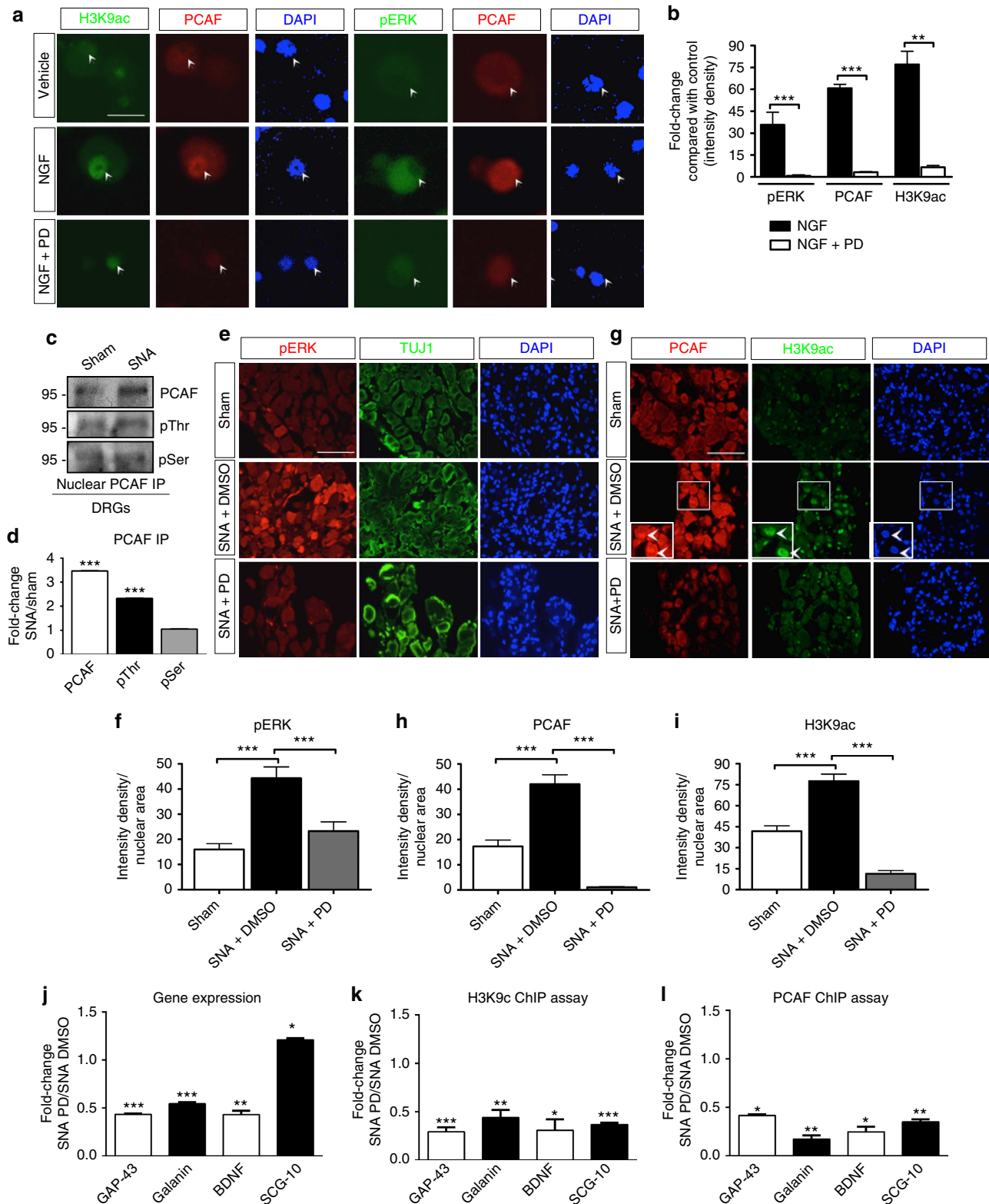


Figure 4 | ERK retrograde signalling controls PCAF activation. (a,b) NGF stimulates pERK, PCAF and H3K9ac expressions in adult DRG cultures after 3-h treatment, which is abrogated by the ERK kinase inhibitor PD98059 (PD), ICC (a) and fold change analysis of intensity density (b). Scale bar, 20 μ m, $N=3$ per group, performed in triplicate. (c,d) Nuclear PCAF immunoprecipitation from *in vivo* L4-L6 DRG 24 h following Sham or SNA reveals an increase in PCAF expression and threonine phosphorylation following SNA but not serine phosphorylation, immunoblot (c) and fold change of density analysis (d). $N=5$ per group, performed in triplicate. (e-i) In L4-L6 DRG, 24 h following SNA we observe an increase in pERK (e,f), PCAF (g,h) and H3K9ac (g,i) expression, which is significantly decreased by ERK inhibition with PD at the nerve stump. Insert shows high nuclear expression of PCAF and H3K9ac after SNA. Scale bars, 75 μ m, $N=3$ per group, performed in triplicate. (j-l) PD also inhibits gene expression (Q-PCR, $N=3$ per group) (j) as well as H3K9ac (k) and PCAF (l) at the promoters of GAP-43, Galanin and BDNF 24 h following SNA (ChIPs). $N=6$ per group, performed in triplicate. Error bars, s.e. (b,f,h,i) $P<0.0001$, ANOVA, Bonferroni *post hoc* tests, $**P<0.001$ and $***P<0.001$, (d,j-l) Student's *t*-test, $*P<0.05$, $**P<0.001$ and $***P<0.001$. Original immunoblot images are shown in Supplementary Fig. 12.

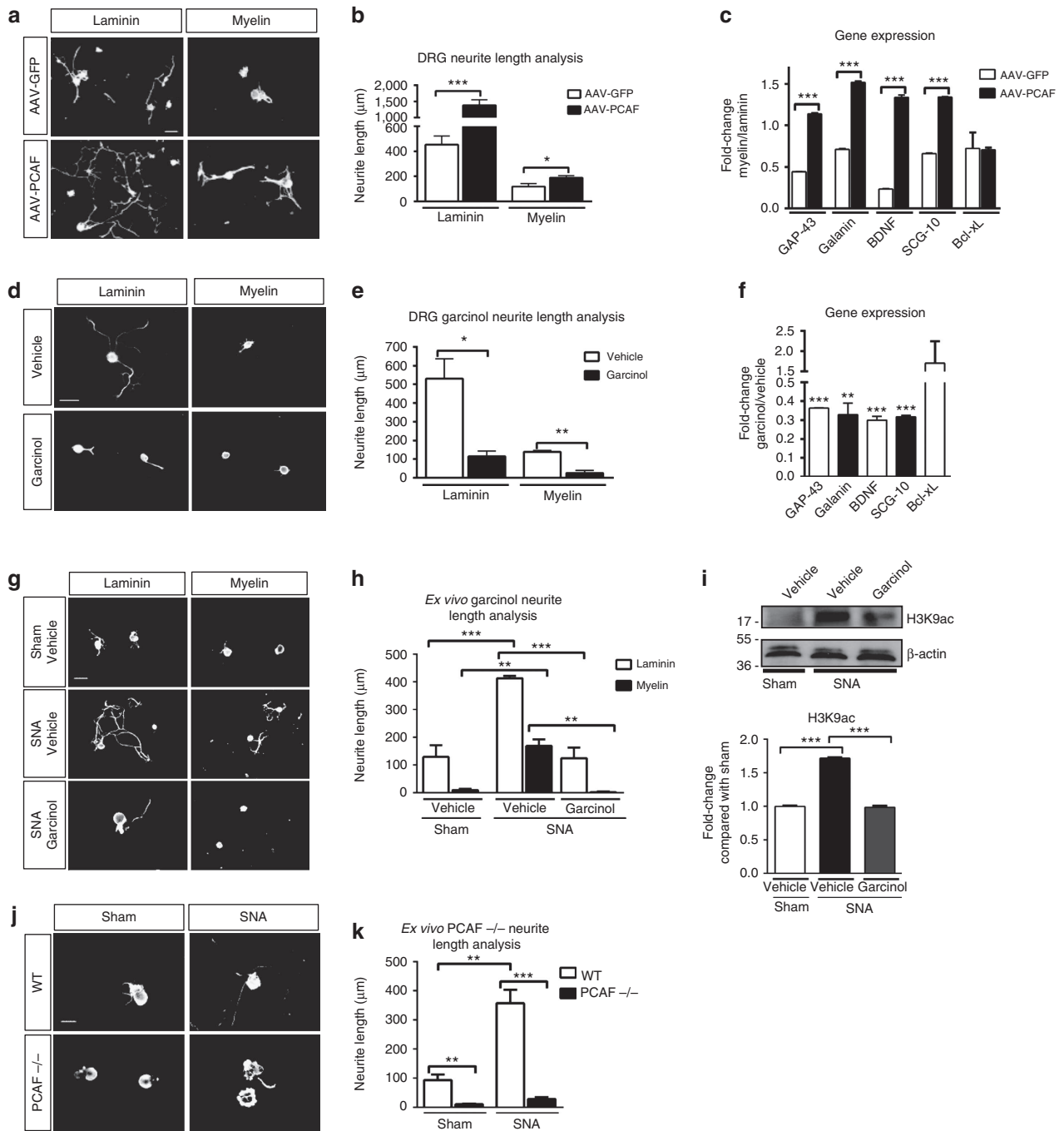


Figure 5 | PCAF promotes neurite outgrowth *in vitro* and *ex vivo* following SNA. (a,b) On both laminin and myelin substrates, adult DRG infected with AAV-PCAF (48 h) showed an increase in neurite outgrowth compared with AAV-GFP-infected DRG, ICC (βIII Tubulin) (a) and average neurite length analysis (b). Scale bars, 100 µm. (c) Q-PCR fold changes of myelin/laminin 48-h post-AAV infection reveals inhibitory myelin-dependent reduction in gene expression of regeneration genes, which was restored by PCAF overexpression. (d-f) On laminin and myelin substrates, the PCAF activity inhibitor Garcinol (24 h) represses neurite outgrowth as well as the gene expression of regeneration genes, ICC (βIII Tubulin) Scale bars, 50 µm (d), average neurite length analysis (e) and Q-PCR (f-i) Garcinol when applied intrathecally compared with Vehicle at the time of a conditioning lesion significantly repressed neurite outgrowth of the given lesion 24 h later in *ex vivo* cultures on both laminin and myelin substrates as well as the acetylation of H3K9, ICC (βIII Tubulin). Scale bars, 50 µm (g), average neurite length analysis (h) and western blot and intensity analyses (i). (j,k) In addition, neurite outgrowth in *ex vivo* cultures from PCAF^{-/-} mice showed PCAF to be required for neurite outgrowth induced by a conditioning lesion, ICC (βIII Tubulin). Scale bars, 50 µm (j), average neurite length analysis (k). Error bars, s.e. (b,c,e,h,i,k) $P < 0.0001$, ANOVA, Bonferroni *post hoc* tests, * $P < 0.05$, ** $P < 0.001$ and *** $P < 0.001$. (f) Student's *t*-test, ** $P < 0.001$ and *** $P < 0.001$, $N = 3-6$, performed in triplicate. Original immunoblot images are shown in Supplementary Fig. 13.

entire class of genes as essential for immediate and sustained axonal regeneration. In support of this, our data show that PCAF-dependent regulation of *GAP-43*, *Galatinin* and *BDNF* is at the essential core of the regenerative programme.

An immediate response to the external stimulus of a peripheral axonal injury is to seal the wound. This is followed by electrical impulses and calcium fluxes that are the first messages relayed from the lesion site to the cell body requesting assistance. Next, is

a rise in cAMP levels and phosphorylation signalling by multiple players involved in transmitting further information to the cell body^{5,6}. Recently, it has been shown that calcium influx ejects histone deacetylase 5 (HDAC5) from the DRG nucleus correlating to increased global H3ac and gene expression³¹. It has been hypothesized that merely shifting the balance from a deacetylated to a globally acetylated chromatin environment by inhibition of HDACs could recapitulate the conditioning lesion and could lead to regeneration. However, recent experimental evidence³² and our own work using HDAC class I and HDAC class I and II inhibitors³³ has proven this to be insufficient in producing post-lesion regeneration of sensory fibres following a spinal or optic nerve injury and therefore unlikely the key to unlocking the molecular mechanisms of regeneration. While our work here describes that specific epigenetic codes are induced endogenously following a conditioning lesion that leads to CNS regeneration, it is also consistent with previous findings from our laboratory that showed the presence of a transcriptional complex formed by p53, p300 and PCAF in the proximity of several RAGs including *GAP-43*, *Coronin 1b* and *Rab13* in primary neurones as well as facial motor neurones in a PNS facial nerve axotomy model^{34–36}. Additionally, we found that the histone acetyltransferase p300 (which may form a complex with PCAF) is developmentally regulated in retinal ganglion cells and whose overexpression drives axonal regeneration of the injured optic nerve³³.

While it is known that signals are sent via retrograde transport machinery^{23,37–39}, how they are decoded into the gene expression of key axonal regeneration players for growth towards re-innervation of the lost target has not been known until now. Here, we have shown the first systematic study of various epigenetic modifications revealing specifically that increased H3K9ac and PCAF as well as decreased H3K9me2 at the promoters of *GAP-43*, *Galanin* and *BDNF* are due to retrogradely induced pERK activation of PCAF leading to essential gene activation, which is sufficient to mimic the regenerative response assembled by a conditioning lesion, thus driving regeneration in the CNS.

The fundamentals of decoding the regenerative retrograde signal by understanding the specific epigenetic changes that occur to chromatin surrounding essential genes is paramount in our ability to recapitulate this mechanism when the signal is lacking, such as after spinal cord injury (SCI). Here we take the first steps in this understanding that may lead to the design of epigenetic-related regenerative therapies for SCI patients.

Methods

Reagents. PD 98059 (Calbiochem), Garcinol (Sigma-Aldrich), NGF (BD Biosciences) and dbcAMP (Enzo Life Sciences) were purchased from respective companies. The following antibodies were purchased and utilized, rabbit anti-PCAF (ab12188, Abcam), mouse anti-PCAF (E8, sc-13124, Santa Cruz Biotechnology), rabbit anti-AcH3K9 (no. 9671, Cell Signalling), rabbit anti-H3K9me2 (no. 9753, Cell Signalling), mouse anti-H3K27me3 (ab6002, Abcam), mouse anti-H3K4me2 (no. 9726, Cell Signalling), rabbit anti-H3K18ac (ab15823, Abcam), mouse anti-NeuN (MAB 377, Millipore), rabbit anti-phospho-Erk 1/2 (no. 9101, Cell Signalling), mouse anti-βIII tubulin (no. G712A, Promega), mouse β-actin (A2228, Sigma), rabbit anti-Phospho-Threonine (no. 600-403-263, Rockland), rabbit anti-Phospho-Serine (no. ADI-KAP-ST2103-E, Enzo Life Sciences), rabbit anti-MAP2 (sc20172, Santa Cruz Biotechnology), rat anti-Glial fibrillary acidic protein (GFAP) (no. 13-0300, Invitrogen), rabbit anti-BDNF (sc-546, Santa Cruz Biotechnology), rabbit anti-Galanin (T-4334, Bachem Peninsula Laboratories) and sheep anti-GAP-43 (no. NBP1-41123, Novus Biologicals).

Mice. All mice used for this work were treated according to the Animal Welfare Act and to the ethics committee guidelines of the University of Tübingen. Equally distributed male and female C57Bl6/J (bred from Charles River Laboratories), CD1 or CD1 PCAF $-/-$ (generated in Dr Boutillier's laboratory) mice ranging from 6 to 8 weeks of age were used for all experiments. C57Bl6/J were used for all studies except those specifying PCAF null mice. For surgeries, mice were anesthetized with ketamine (100 mg kg⁻¹ body weight) and xylazine (10 mg kg⁻¹ body weight). For all experiments, we employed a target for the appropriate expected power calculation linked to an *ad hoc* statistical test.

Dorsal column axotomy. Surgeries were performed as previously reported⁴⁰. Briefly, mice were anesthetized and a T10 laminectomy was performed (~20 mm from the L4-L6 DRGs), the dura mater was removed, taking care of not damaging the spinal cord. A dorsal hemisection until the central canal was performed with a microknife (FST). For the control laminectomy surgery, the dura mater was removed but the dorsal hemisection was not performed.

Sciatic nerve axotomy. Mice were anesthetized. At ~20 mm far from L4-L6 DRG, a 10-mm incision was performed on the gluteal region and muscles were displaced to expose the sciatic nerve for a complete transection with spring micro-scissors. For the PD study 30 s before transection, 2.5 μl of 100% DMSO or 2.0 μl of PD 98059 were slowly pipetted on the nerve. Finally, skin was closed with two suture clips. The nerve fibre was left uninjured in sham surgery.

Methylated DNA immunoprecipitation from DRG ex vivo. For each of the three time points (1, 3 and 7 days post SNA or DCA and naive), L4-L6 DRG were collected from two mice per time point and condition in triplicate for injury samples and naive, and in duplicate for shams. Frozen tissue was ground and digested with 0.2 mg ml⁻¹ Proteinase K. The lysate was then sonicated to average size of 700 bp and cleared of remaining tissue by centrifugation. Genomic DNA was extracted from the lysate via standard phenol–chloroform extraction and DNA precipitation protocols. MeDIP was then performed according to the manufacturer's protocol for the ChIP Kit from Upstate/Millipore. A total of 10 μg

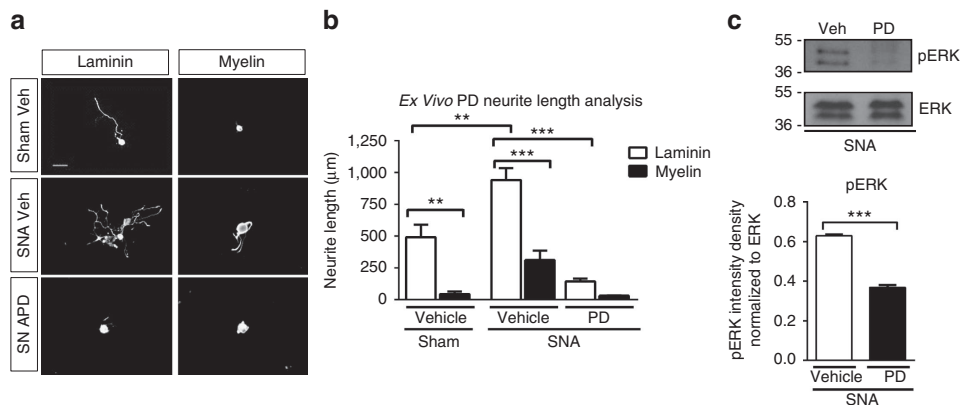


Figure 6 | ERK kinase inhibition blocks neurite outgrowth after conditioning lesion. (a–c) PD98059 when applied at the nerve stump compared with Vehicle at the time of a conditioning lesion or in Sham significantly repressed neurite outgrowth 12 h later in *ex vivo* cultures on both laminin and myelin substrates, ICC (βIII Tubulin). Scale bars, 50 μm (a), average neurite length analysis (b) and western blot and intensity analysis showing significant reduction in pERK after PD98059 delivery (c). (b) $P < 0.0001$, ANOVA, Bonferroni post hoc tests, $**P < 0.001$ and $***P < 0.001$. (c) Student's *t*-test, $***P < 0.001$, $N = 3-6$, performed in triplicate. Original immunoblot images are shown in Supplementary Fig. 14.

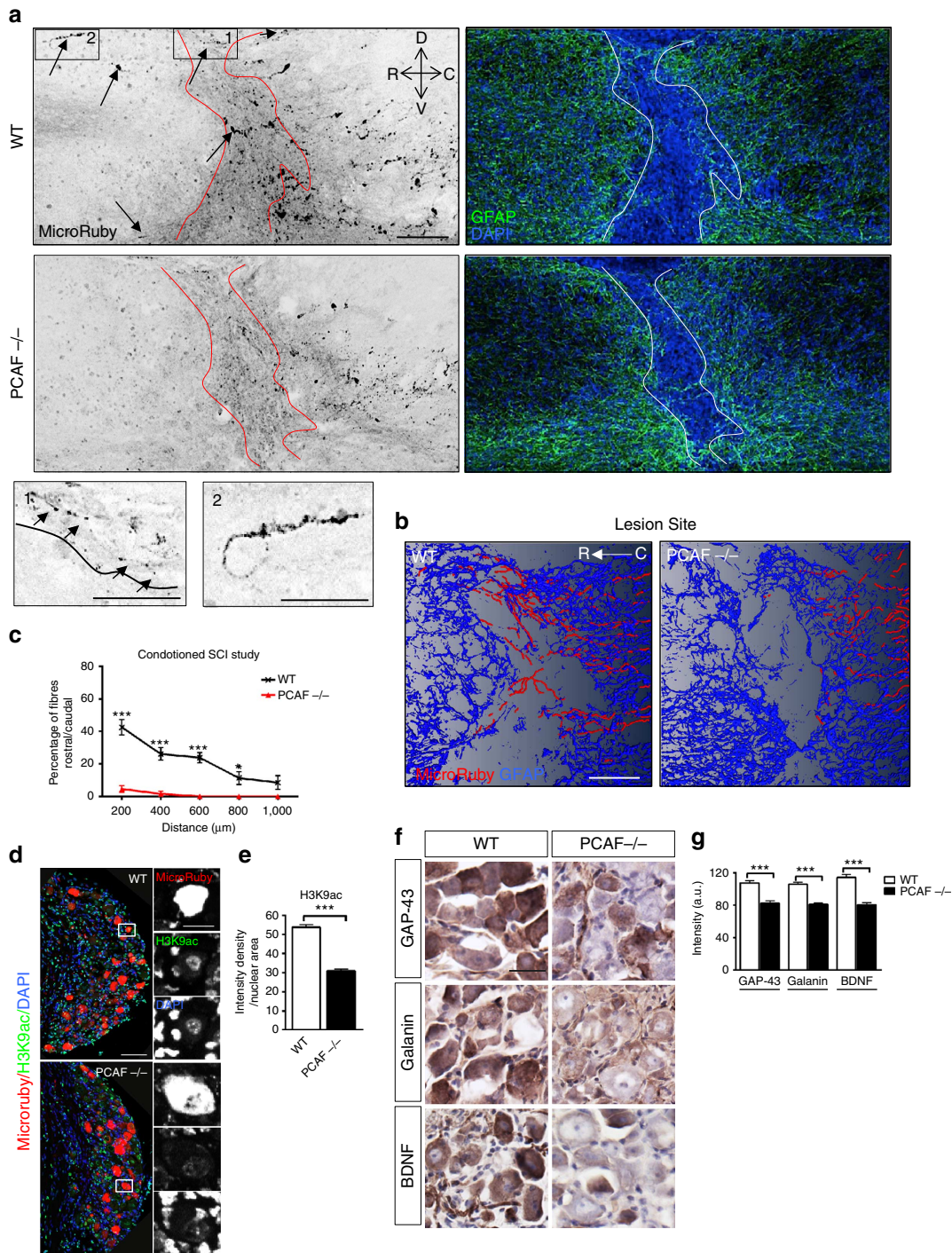


Figure 7 | PCAF is required for conditioning-dependent axonal regrowth after SCI. (a) MicroRuby tracing of the dorsal columns shows regenerating fibres invading into and past the lesion site (upper) in WT but not in PCAF^{-/-} (lower) after conditioning injury (SNA followed by DCA; left panels). The red dotted lines indicate the lesion site. Insets (1 and 2) show higher magnification of regenerating axons. D-R-C-V: anatomical coordinates, dorsal-rostral-caudal-ventral. Right panels show the lesion site. Arrows indicate axonal sprouts. Scale bar, 100 µm. (b) Amira 3D reconstruction of regenerating dorsal column axons and glial scar in a sagittal projection (~25 µm) of the lesion site from WT and PCAF^{-/-} mice. (c) Quantification of regenerating axons, N=6 (WT), N=6 (PCAF^{-/-}), Welch's *t*-test, **P*<0.05 and ****P*<0.001. (d,e) Lack of CNS regeneration correlates with a significant decrease in H3K9ac expression in L4-L6 PCAF^{-/-} traced DRG neurones when compared with WT, IHC (d), bar graphs (e). Inset shows high nuclear expression of H3K9ac in WT but not PCAF^{-/-} traced DRG neurones. Student's *t*-test, error bars, s.e., ****P*<0.001, N=6, performed in triplicate. (f,g) IHC and 3,3'-Diaminobenzidine (DAB) intensity analysis of L4-6 DRG neurones shows a decrease in GAP-43, BDNF and Galanin expression in PCAF^{-/-} DRG neurones when compared with WT after SNA followed by SCI. Scale bar, 25 µm. Student's *t*-test, ****P*<0.001, N=4 per group, performed in triplicate.

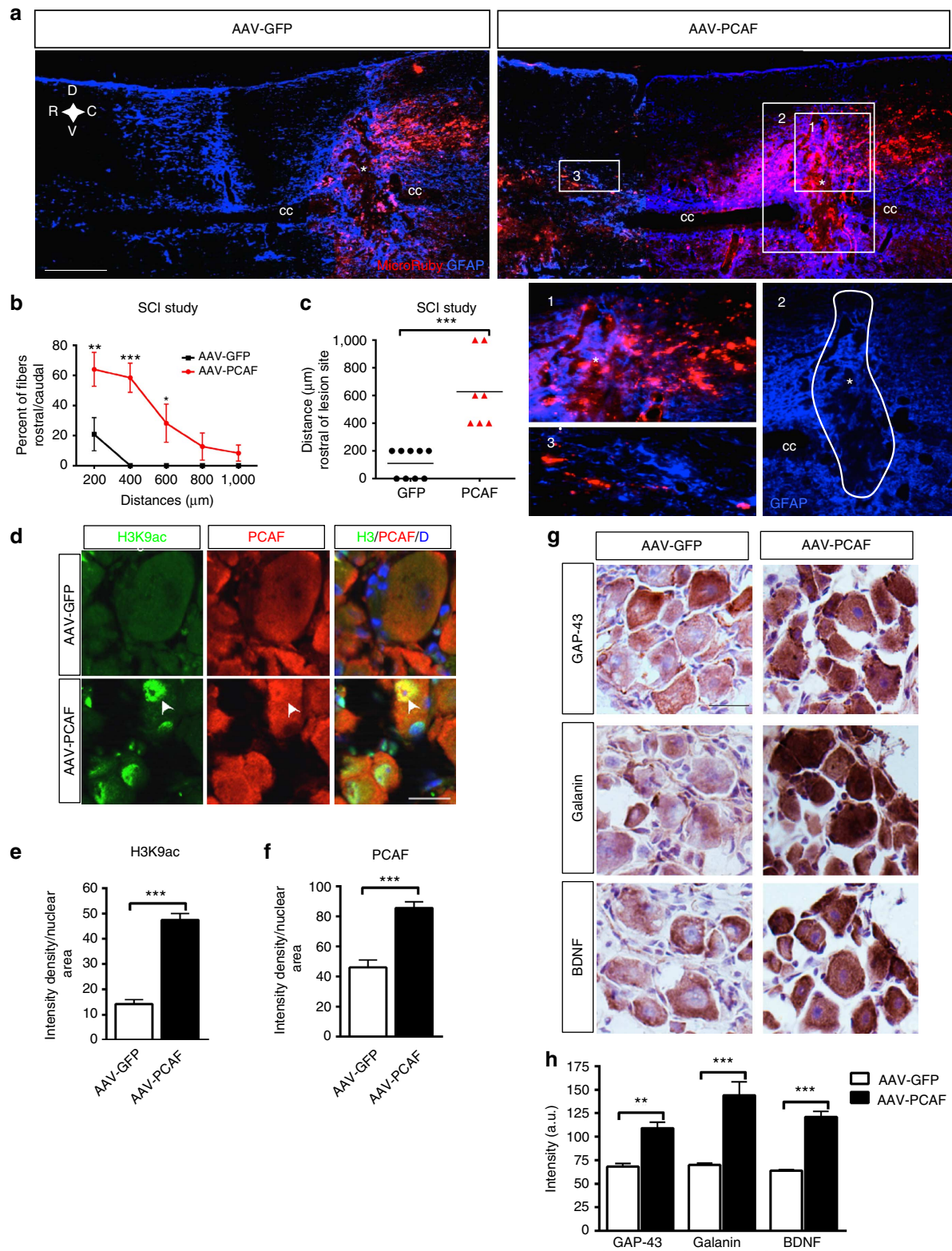


Figure 8 | PCAF overexpression induces spinal axonal regeneration. (a) MicroRuby tracing of the dorsal columns shows regenerating fibres invading into and past the lesion site after AAV-PCAF overexpression (upper right) versus a control AAV-GFP virus (upper left). Insets show higher magnification of regenerating axons. D-R-C-V: anatomical coordinates, dorsal-rostral-caudal-ventral. cc: central canal. Scale bar, 250 μm . (b) Quantification of regenerating axons, $N = 9$ (AAV-GFP), $N = 7$ (AAV-PCAF). (c) Quantification of longest regenerating axon per animal. (d-f) Overexpression of AAV-PCAF in the SCI study promotes H3K9ac (8 weeks post infection; arrowheads) as shown by IHC (d). Nuclear intensity density analysis of H3K9ac (e) and PCAF (f) show enhanced PCAF and H3K9ac after PCAF overexpression. (g,h) GAP-43, Galanin and BDNF IHC analysis of corresponding L4-L6 DRG from infected AAV-PCAF and AAV-GFP animals show an increase in GAP-43, Galanin and BDNF expression, IHC (g) and DAB intensity analysis (h). Scale bars, 25 μm . Error bars, s.e., (b) Welch's t -test, $*P < 0.05$, $**P < 0.01$ and $***P < 0.001$. (c,h) $P < 0.0001$, ANOVA, Bonferroni *post hoc* tests, $**P < 0.01$ and $***P < 0.001$, (e,f) Student's t -test, $***P < 0.001$, $N = 3$, performed in triplicate.

of genomic DNA and 5 µg of a 5-methyl-Cytosine antibody (Eurogentec, BI-MECY-0100) were added to immunoprecipitate methylated DNA fragments. The Whole Genome Amplification Kit (Sigma-Aldrich) was applied to amplify 20 ng of genomic samples to a maximum yield of 3–7 µg, followed by subsequent column purification using the GenElute PCR Clean-Up Kit (Sigma). MeDIP efficiency was tested with previously published primers for methylated H19 ICR⁴¹.

DNA methylation microarray. Whole-genome amplified, high-quality⁴² samples (input genomic DNA, immunoprecipitated methylated DNA or no-antibody control) were sent to Roche/NimbleGen for DNA methylation microarray analysis. NimbleGen processed the samples as described in its ‘NimbleChip Arrays User’s Guide for DNA Methylation Analysis’. A ‘2007-02-27 MM8 CpG Island Promoter (385K RefSeq)’ tiling microarray, covering proximal promoter regions and CGIs by close-set oligonucleotide probes. Fluorescence intensity raw data were obtained from scanned images of the tiling arrays using the NimbleScan extraction software. For each spot on the array, Cy5/Cy3 ratios were normalized and calculated to obtain log₂ values. Then, the bi-weight mean of log₂ ratios of a certain region was subtracted from each data point; this procedure is similar to mean normalization of each channel.

Promoter CGI analysis. Several known RAGs and of differentially methylated genes that emerged from the DNA methylation microarray analysis within this study were analyzed for CpG islands (CGIs). The complete genomic region, together with the promoter region (5,000 bp upstream of the transcription start site (TSS)), was analysed with the *EMBOSS CpGPlot* online tool from EMBL-EBI. Characteristic parameters of reported CGIs were used.

Gene-regulatory region bioinformatics analysis. We performed a MatInspector (Genomatix) and UCSD genome browser-based bioinformatics analysis of the regulatory regions of RAG genes (*GAP-43*, *Galanin*, *BDNF*, *SCG-10*, *Sprr1a*, *Chll*, *Lgals*, *L1cam* and *CAP-23*) spanning 1,000 bp upstream and 1,500 bp downstream of the TSS. These regions overlap and further extend what we studied for DNA methylation (500 bp upstream and 1,500 bp downstream of the TSS). Significant transcription-binding sites displayed at least two of the three classically required criteria: a *P*-value < 0.05, matrix similarity > 0.8 and core similarity > 0.8. Additionally, CGI and DNA methylation were examined in these regions for all of the RAGs investigated with the EMBO DNA methylation analysis online software. Results of the combined analysis suggested that *GAP-43*, *Galanin* and *BDNF* had common gene regulatory regions with low levels of DNA methylation and absence of typical CpG islands, presented transcriptional-binding sites for transcription factors that are typically acetylated and active in the proximity of acetylated histones, including, *Klf*, *NFκB*, *SRF*, *p53*, *YY1*, *CREB* and *c-jun*.

Quantitative real-time RT-PCR analysis. RNA was extracted using PeqGOLD TriFast reagent (peqlab), cDNA was synthesized from 1 µg of total RNA using both oligodT and random hexamers from the SuperScript II Reverse Transcriptase kit (Invitrogen) and a real time RT-PCR was performed using Absolute QPCR SYBR low ROX master mix (Thermo Scientific). Quantities and fold changes were calculated following the manufacturer’s instructions (ABI 7,500) and as previously reported^{35,43}. Primer sequences are shown in Supplementary Table 1. *RPL13A*, *GAPDH* or β -actin were used for normalization.

Quantitative chromatin immunoprecipitation. The SimpleCHIP Enzymatic Chromatin IP Kit with magnetic beads (Cell Signalling) was used according to previously published methods⁴⁴. Antibodies used were H3K9ac, PCAF (rabbit), H3K9me2, H3K27me3, H3K4me3 and H3K18ac. Real-time Q-PCR was run using Absolute QPCR SYBR low ROX master mix (Thermo Scientific). Quantities and fold changes were calculated following the manufacturer’s instructions (ABI 7,500) and as previously reported^{35,43}. Primers were designed in proximity (within 500 bp upstream) of the TSS. Primer sequences are shown in Supplementary Table 2.

Immunohistochemistry. DRG were fixed in 4% paraformaldehyde (PFA) and transferred to 30% sucrose. The tissue was embedded in OCT compound (Tissue-Tek), frozen at –80 °C and sectioned at 10-µm thickness. DRG sections underwent antigen retrieval with 0.1 M citrate buffer (pH 6.2) at 98 °C and were incubated with 120 µg ml⁻¹ goat anti-mouse IgG (Jackson ImmunoResearch). They were blocked for 1 h with 8% BSA, 1% PBS-TX100 or 0.3% PBS-TX100, respectively, and then incubated with NeuN (1:100), PCAF (mouse, 1:500) and AcH3K9 (1:500) antibodies or phospho-Erk 1/2 (1:500) and β III tubulin (1:1,000) antibodies O/N. This was followed by incubation with Alexa Fluor 568-conjugated goat anti-mouse and Alexa Fluor 488-conjugated goat anti-rabbit or Alexa Fluor 568-conjugated goat anti-rabbit and Alexa Fluor 488-conjugated goat anti-mouse (1:1,000, Invitrogen), respectively. Slides were counterstained with DAPI (1:5,000, Molecular Probes). Photomicrographs were taken with an Axio Imager.Z1/Apotome (Zeiss) microscope as 0.800 µm Z-stacks at $\times 40$ magnification and processed with the software AxioVision (Zeiss). In order to determine the nuclear intensity density (ID) of pixels, Image J (Fiji) was used. Each neuronal nuclear

area was selected in the DAPI channel (about 25 nuclei/picture). The same selection was then used to delineate the nuclei in the other channels. The threshold of the nuclear area was set for each different channels, and based on that the pixel ID of the nucleus was determined and divided by its nuclear area. Triplicates of each treatment were analysed.

Immunoblotting and immunoprecipitation. For whole-cell extract immunoblotting, DRG or CGN were collected, lysed on ice in RIPA lysis buffer containing protease inhibitors (Complete Mini; Roche Diagnostics), sonicated briefly, centrifuged and the supernatant collected. The NE-PER Nuclear and Cytoplasmic Extraction Reagents (Thermo Scientific) was used according to the manufacturer’s instructions for nuclear enriched fractions. H3K9ac (1:1,000), PCAF (rabbit, 1:500), β -actin (1:1,000) and β III Tubulin (1:1,000) were employed as primary antibodies. Quantitation of protein expression was performed by densitometry (Image J) of the representative bands of the immunoblots and normalized to the respective levels of loading controls.

For immunoprecipitation, the nuclear enriched fractions were bound to rabbit PCAF antibody (8 µg), pulled down with Protein G magnetic beads, washed with low and high salt buffers (ChIP kit, Cell Signalling) and was eluted with loading buffer (Thermo Scientific). The IP was stained with PCAF (rabbit, 1:500), Phospho-Threonine (1:1,000) or Phospho-Serine (1:1,000).

DRG culture. Adult DRG were dissected and collected in Hank’s balanced salt solution on ice. DRGs were transferred to a digestion solution (5 mg ml⁻¹ Dispase II (Sigma), 2.5 mg ml⁻¹ Collagenase Type II (Worthington) in DMEM (Invitrogen)) and incubated at 37 °C for 35 min with occasional mixing. Following which DRGs were transferred to media containing 10% heat-inactivated fetal bovine serum (Invitrogen), 1 \times B27 (Invitrogen) in DMEM:F12 (Invitrogen) mix and were briefly triturated with a Sigma-cote (Sigma) fire-polished pipette to manually dissociate the remaining clumps of DRG. After which the single cells were spun down, resuspended in media containing 1 \times B27 and Penicillin/Streptomycin in DMEM:F12 mix and plated at 4,000–5,000 per coverslip. The culture was maintained in a humidified atmosphere of 5% CO₂ in air at 37 °C. Neurones were infected with either AAV-GFP or AAV-PCAF (1 \times 10¹² ml⁻¹) a few hours post-plating and fixed with 4% PFA 48 h later. For the Garcinol study, cells were exposed to Vehicle (5% EtOH) or Garcinol (5 µM per well, Sigma-Aldrich) for 24 h and fixed. For the ERK/PD study, the day following plating DRG were exposed for 1 h to PD 98059 (50 µM per well), then to NGF (100 ng ml⁻¹) for 3 h and fixed.

CGN culture. CGNs were prepared from the cerebellum of 7-day-old C57Bl6/J mice following standard procedures⁴⁵. These disassociated CGNs were plated on either PDL (with or without 5 µM Garcinol) or myelin for 24 h in a humidified atmosphere of 5% CO₂ in air at 37 °C. Neurones were infected at the time of plating with a CMV promoter AV-GFP or AV-PCAF (1 \times 10¹⁰ ml⁻¹).

Immunocytochemistry. Glass coverslips were coated with 0.1 mg ml⁻¹ PDL, washed and coated with mouse Laminin (2 µg ml⁻¹; Millipore). For myelin experiments, they were additionally coated with 4 µg cm⁻² rat myelin. Cells were plated on coated coverslips for 24 or 48 h, at which time they were fixed with 4% PFA/4% sucrose. Immunocytochemistry was performed as previously reported⁴⁵ using β III Tubulin (1:1,000), MAP2 (1:100), PCAF (mouse, 1:400), AcH3K9 (1:1,000) or pErk1/2 (1:500). This was followed by incubation with Alexa Fluor 568-conjugated goat anti-mouse and Alexa Fluor 488-conjugated goat anti-rabbit (1:1,000, Invitrogen). To visualize the nucleus, we stained the cells with DAPI (1:5,000, Molecular Probes).

Image analysis for immunocytochemistry. DRG pictures were taken at $\times 20$ magnification with an Axioplan 2 (Zeiss) microscope and processed with the software AxioVision (Zeiss). Using Image J, a threshold was set. On the basis of the threshold, for each picture the ID of pixels was calculated in each channel and then divided by its respective number of cells (about 225 cells per picture). This was carried out in triplicate.

Neurite length analysis. Immunofluorescence was detected using an Axiovert 200 microscope (Zeiss) and pictures were taken as a mosaic at $\times 10$ magnification using a CDD camera (AxioCam MRm, Zeiss). Neurite analysis and measurements were performed using the NeuroLucida software (MicroBrightField) in triplicate with 50 cells per triplicate.

Luciferase assays. Experiments were performed in CGN using electroporation with the rat neurone nucleofactor kit (Amaxa Biosystems) according to the provided protocol. Briefly, five million neurones were used for each cuvette, with 2–4 µg of total DNA (*GAP-43-Luc reporter*⁴⁶ and 25 ng of *pRL-TK-Renilla-luciferase* (Promega)). Neurones were plated in 24-well plates at a density of 0.4 million cells per well with or without 5 µM Garcinol and incubated for a total

of 24 h. Cells were harvested and lysed with 100 μ l of passive lysis buffer, and luciferase activities were determined using the Dual-Luciferase kit (Promega).

Ex vivo DRG culture. Intrathecal (i.t.) injection was performed using the Wilcox technique⁴⁷. Mice were briefly anaesthetized with isoflurane (2%), and a lumbar cutaneous incision (1 cm) was made. I.t. injections were performed with 30-gauge 15-mm needles mated to a 5- μ l luer tip syringe (Hamilton, Reno, NV, USA). The needle was inserted into the tissue between the L5 and L6 spinous processes and inserted \sim 0.5 cm with an angle of 20°. Vehicle (10% DMSO in 0.9% NaCl) or Garcinol (80 μ M) was slowly injected in a final volume of 5 μ l. Directly after i.t. injection of Vehicle or Garcinol, mice underwent Sham or SNA surgeries. Twenty-four hours after surgery, mice were killed and L4–L6 DRG were collected and cultured for 24 h, and were then fixed and stained. We used three animals per group and plated in triplicate. L4–L6 DRG were also collected for total protein extraction for western blot analysis of H3K9ac.

For PCAF null *ex vivo* study, WT or PCAF^{-/-} mice (generated in Dr Boutilier's laboratory) underwent Sham or SNA surgeries. Twenty-four hours after surgery, mice were killed and L4–L6 DRG were collected and cultured for 18 h, and were then fixed and stained. We used three animals per group and the DRG were plated in triplicate.

SCI study

AAV-GFP/PCAF injection. All experimental procedures were performed in accordance with protocols approved by the University of Tübingen. PCAF expression plasmid was obtained from Addgene (Plasmid 8941). AAVs were prepared as described previously⁴⁸. Mice were anaesthetized and the left sciatic nerve was injected with 1.5–2 μ l of either AAV-GFP or AAV-PCAF (1×10^{12} ml⁻¹) using a glass-pulled micropipette. Standardized randomization and blinding strategies were adopted. Randomization of samples was performed by random assignment and labelling of control and test groups while between one to three experimenters were blind to the groups for each experiment performed.

Spinal cord injury. Two weeks after AAV injection, a T9–10 laminectomy was performed and the dorsal half of the spinal cord was crushed with no. 5 forceps (Dumont, Fine Science Tools) for 2 s (ref. 49). The forceps were deliberately positioned to sever the dorsal column axons completely. Four weeks after the spinal cord lesion, dorsal column axons were traced by injecting 2 μ l of Microruby tracer (3,000 molecular weight, 10%, Invitrogen) into the left sciatic nerve⁵⁰. Mice were kept for an additional 2 weeks before termination. CD1 WT and PCAF^{-/-} mice underwent the same spinal cord surgery as above. Additionally, they received a conditioning sciatic nerve lesion 1 week before the spinal surgery. One week after the spinal cord lesion, dorsal column axons were traced by injecting 2 μ l of Microruby tracer (3,000 molecular weight, 10%, Invitrogen) into the left sciatic nerve⁵⁰. These mice were kept for an additional 2 weeks before termination. Animals were deeply anaesthetized and were perfused transcardially. Spinal cords were dissected and post-fixed in 4% PFA in phosphate-buffered saline (PBS) at 4 °C for 2 h and 30% sucrose O/N. Then the tissue was embedded in Tissue-Tek OCT compound, frozen at -80 °C and cut in 18- μ m-sagittal and coronal sections (3 mm caudal and 5 mm rostral to the lesion were taken to confirm the completeness of the lesion and to quantify tracing efficiency among experimental groups). Brain stem from each cord was also dissected, and sections of the nuclei gracilis and cuneatus were generated to monitor tracing from spared fibres. Mice with incomplete lesions were excluded. Staining for GFAP (1:2,000) was performed following the standard protocols⁴⁰. Confocal laser scanning microscopy was performed using a Zeiss LSM700. Semi-automatic skeletonization of regenerating axons was performed on confocal scans using the three-dimensional (3D) imaging software Amira (FEI Visualization Sciences Group). An isosurface was applied to the GFAP signal.

Quantification of axonal regeneration. For each spinal cord after dorsal column crush, the number of fibres caudal to the lesion and their distance from the lesion epicentre were analysed in four to six sections per animal with a fluorescence Axioplan 2 (Zeiss) microscope and with the software StereoInvestigator 7 (MBF bioscience). The lesion epicentre (GFAP) was identified in each section at a $\times 40$ magnification. The sum total number of labelled axons rostral to the lesion site was normalized to the total number of labelled axons caudal to the lesion site counted in all the analysed sections for each animal, obtaining an inter-animal comparable ratio considering the individual tracing variability. Sprouts and regrowing fibres were defined following the anatomical criteria reported by Steward *et al.*⁵¹ Samples falling short of standard quality for each specific experiment or altered by clear experimental flaw were excluded from the analysis.

DAB immunostaining. Peroxidase activity was blocked in 0.3% H₂O₂, followed by incubation in 8% bovine serum albumin (BSA) and 0.3% TBS-TX-100. BDNF (1:500), Galanin (1:2,000) or GAP-43 (1:500) antibodies in 2% BSA and 0.2% TBS-TX100 were used. Labelled cells were visualized using the ABC system

(Vectastain Elite; Vector Laboratories) with DAB as chromogen. The sections then were counterstained with haematoxylin (Vector Laboratories).

Statistical analysis. Data are plotted as the mean \pm s.e. All experiments were performed in triplicate. Asterisks indicate a significant difference analysed using analysis of variance with Bonferroni *post hoc* tests, Student's *t*-test, Welch's *t*-test or two-way analysis of variance as indicated (**P* < 0.05; ***P* < 0.01; ****P* < 0.001).

References

- Skene, J. H. Axonal growth-associated proteins. *Annu. Rev. Neurosci.* **12**, 127–156 (1989).
- Schmitt, A. B. *et al.* Identification of regeneration-associated genes after central and peripheral nerve injury in the adult rat. *BMC Neurosci.* **4**, 8 (2003).
- Stam, F. J. *et al.* Identification of candidate transcriptional modulators involved in successful regeneration after nerve injury. *Eur. J. Neurosci.* **25**, 3629–3637.
- Starkey, M. L. *et al.* Expression of the regeneration-associated protein SPRR1A in primary sensory neurons and spinal cord of the adult mouse following peripheral and central injury. *J. Comp. Neurol.* **513**, 51–68 (2009).
- Hanz, S. & Fainzilber, M. Retrograde signaling in injured nerve—the axon reaction revisited. *J. Neurochem.* **99**, 13–19 (2006).
- Rishal, I. & Fainzilber, M. Retrograde signaling in axonal regeneration. *Exp. Neurol.* **223**, 5–10 (2010).
- Neumann, S. & Woolf, C. J. Regeneration of dorsal column fibers into and beyond the lesion site following adult spinal cord injury. *Neuron* **23**, 83–91 (1999).
- Maurice, T. *et al.* Altered memory capacities and response to stress in p300/CBP-associated factor (PCAF) histone acetylase knockout mice. *Neuropsychopharmacology* **33**, 1584–1602 (2008).
- Tsankova, N. M., Kumar, A. & Nestler, E. J. Histone modifications at gene promoter regions in rat hippocampus after acute and chronic electroconvulsive seizures. *J. Neurosci.* **24**, 5603–5610 (2004).
- Qureshi, I. A. & Mehler, M. F. Emerging role of epigenetics in stroke: part 1: DNA methylation and chromatin modifications. *Arch. Neurol.* **67**, 1316–1322 (2010).
- Lunyak, V. V. *et al.* Corepressor-dependent silencing of chromosomal regions encoding neuronal genes. *Science* **298**, 1747–1752 (2002).
- Basi, G. S., Jacobson, R. D., Virag, L., Schilling, J. & Skene, J. H. Primary structure and transcriptional regulation of GAP-43, a protein associated with nerve growth. *Cell* **49**, 785–791 (1987).
- Skofitsch, G. & Jacobowitz, D. M. Immunohistochemical mapping of galanin-like neurons in the rat central nervous system. *Peptides* **6**, 509–546 (1985).
- Lindsay, R. M. Nerve growth factors (NGF, BDNF) enhance axonal regeneration but are not required for survival of adult sensory neurons. *J. Neurosci.* **8**, 2394–2405 (1988).
- Geremia, N. M. *et al.* Endogenous BDNF regulates induction of intrinsic neuronal growth programs in injured sensory neurons. *Exp. Neurol.* **223**, 128–142 (2010).
- Iskandar, B. J. *et al.* Folate regulation of axonal regeneration in the rodent central nervous system through DNA methylation. *J. Clin. Invest.* **120**, 1603–1616 (2010).
- Wang, Z. *et al.* Combinatorial patterns of histone acetylations and methylations in the human genome. *Nat. Genet.* **40**, 897–903 (2008).
- Liu, K., Tedeschi, A., Park, K. K. & He, Z. Neuronal intrinsic mechanisms of axon regeneration. *Annu. Rev. Neurosci.* **34**, 131–152 (2011).
- Seiffers, R., Mills, C. D. & Woolf, C. J. ATF3 increases the intrinsic growth state of DRG neurons to enhance peripheral nerve regeneration. *J. Neurosci.* **27**, 7911–7920 (2007).
- Kretz, A., Kugler, S., Happold, C., Bahr, M. & Isenmann, S. Excess Bcl-XL increases the intrinsic growth potential of adult CNS neurons *in vitro*. *Mol. Cell Neurosci.* **26**, 63–74 (2004).
- Julien, J. P., Meyer, D., Flavell, D., Hurst, J. & Grosfeld, F. Cloning and developmental expression of the murine neurofilament gene family. *Brain Res* **387**, 243–250 (1986).
- Hanz, S. & Fainzilber, M. Integration of retrograde axonal and nuclear transport mechanisms in neurons: implications for therapeutics. *Neuroscientist* **10**, 404–408 (2004).
- Perlson, E. *et al.* Vimentin-dependent spatial translocation of an activated MAP kinase in injured nerve. *Neuron* **45**, 715–726 (2005).
- Averill, S. *et al.* Nerve growth factor modulates the activation status and fast axonal transport of ERK 1/2 in adult nociceptive neurones. *Mol. Cell Neurosci.* **18**, 183–196 (2001).
- Alessi, D. R., Cuenda, A., Cohen, P., Dudley, D. T. & Saltiel, A. R. PD 098059 is a specific inhibitor of the activation of mitogen-activated protein kinase kinase *in vitro* and *in vivo*. *J. Biol. Chem.* **270**, 27489–27494 (1995).
- Wong, K. *et al.* Nerve growth factor receptor signaling induces histone acetyltransferase domain-dependent nuclear translocation of p300/CREB-binding protein-associated factor and hGCN5 acetyltransferases. *J. Biol. Chem.* **279**, 55667–55674 (2004).

27. Blesch, A. *et al.* Conditioning lesions before or after spinal cord injury recruit broad genetic mechanisms that sustain axonal regeneration: superiority to camp-mediated effects. *Exp. Neurol.* **235**, 162–173 (2012).
28. Qiu, J. *et al.* Spinal axon regeneration induced by elevation of cyclic AMP. *Neuron* **34**, 895–903 (2002).
29. Balasubramanyam, K. *et al.* Polyisoprenylated benzophenone, garcinol, a natural histone acetyltransferase inhibitor, represses chromatin transcription and alters global gene expression. *J. Biol. Chem.* **279**, 33716–33726 (2004).
30. Ylera, B. *et al.* Chronically CNS-injured adult sensory neurons gain regenerative competence upon a lesion of their peripheral axon. *Curr. Biol.* **19**, 930–936 (2009).
31. Cho, Y., Sloutsky, R., Naegle, K. M. & Cavalli, V. Injury-induced HDAC5 nuclear export is essential for axon regeneration. *Cell* **155**, 894–908 (2013).
32. Finelli, M. J., Wong, J. K. & Zou, H. Epigenetic regulation of sensory axon regeneration after spinal cord injury. *J. Neurosci.* **33**, 19664–19676 (2013).
33. Gaub, P. *et al.* The histone acetyltransferase p300 promotes intrinsic axonal regeneration. *Brain* **134**, 2134–2148 (2011).
34. Di Giovanni, S. *et al.* The tumor suppressor protein p53 is required for neurite outgrowth and axon regeneration. *EMBO J.* **25**, 4084–4096 (2006).
35. Tedeschi, A., Nguyen, T., Puttagunta, R., Gaub, P. & Di Giovanni, S. A p53-CBP/p300 transcription module is required for GAP-43 expression, axon outgrowth, and regeneration. *Cell Death Differ.* **16**, 543–554 (2009).
36. Gaub, P. *et al.* HDAC inhibition promotes neuronal outgrowth and counteracts growth cone collapse through CBP/p300 and P/CAF-dependent p53 acetylation. *Cell Death Differ.* **17**, 1392–1408 (2010).
37. Hanz, S. *et al.* Axoplasmic importins enable retrograde injury signaling in lesioned nerve. *Neuron* **40**, 1095–1104 (2003).
38. Yudin, D. *et al.* Localized regulation of axonal RanGTPase controls retrograde injury signaling in peripheral nerve. *Neuron* **59**, 241–252 (2008).
39. Shin, J. E. *et al.* Dual leucine zipper kinase is required for retrograde injury signaling and axonal regeneration. *Neuron* **74**, 1015–1022 (2012).
40. Floriddia, E. M. *et al.* p53 regulates the neuronal intrinsic and extrinsic responses affecting the recovery of motor function following spinal cord injury. *J. Neurosci.* **32**, 13956–13970 (2012).
41. Weber, M. *et al.* Chromosome-wide and promoter-specific analyses identify sites of differential DNA methylation in normal and transformed human cells. *Nat. Genet.* **37**, 853–862 (2005).
42. Komashko, V. M. *et al.* Using ChIP-chip technology to reveal common principles of transcriptional repression in normal and cancer cells. *Genome Res.* **18**, 521–532 (2008).
43. Tedeschi, A. *et al.* The tumor suppressor p53 transcriptionally regulates cGKI expression during neuronal maturation and is required for cGMP-dependent growth cone collapse. *J. Neurosci.* **29**, 15155–15160 (2009).
44. Floriddia, E., Nguyen, T. & Di Giovanni, S. Chromatin immunoprecipitation from dorsal root ganglia tissue following axonal injury. *J. Vis. Exp.* **20** pii 2803 (2011).
45. Puttagunta, R. *et al.* RA-RAR-beta counteracts myelin-dependent inhibition of neurite outgrowth via Lingo-1 repression. *J. Cell Biol.* **193**, 1147–1156 (2011).
46. Nguyen, T. *et al.* NFAT-3 is a transcriptional repressor of the growth associated protein 43 during neuronal maturation. *J. Biol. Chem.* **284**, 18816–18823 (2009).
47. Hylden, J. L. & Wilcox, G. L. Intrathecal morphine in mice: a new technique. *Eur. J. Pharmacol.* **67**, 313–316 (1980).
48. Park, K. K. *et al.* Promoting axon regeneration in the adult CNS by modulation of the PTEN/mTOR pathway. *Science* **322**, 963–966 (2008).
49. Liu, K. *et al.* PTEN deletion enhances the regenerative ability of adult corticospinal neurons. *Nat. Neurosci.* **13**, 1075–1081 (2010).
50. Parikh, P. *et al.* Regeneration of axons in injured spinal cord by activation of bone morphogenetic protein/Smad1 signaling pathway in adult neurons. *Proc. Natl Acad. Sci. USA* **108**, E99–107 (2011).
51. Steward, O., Zheng, B. & Tessier-Lavigne, M. False resurrections: distinguishing regenerated from spared axons in the injured central nervous system. *J. Comp. Neurol.* **459**, 1–8 (2003).

Acknowledgements

This work was supported by funds granted by the Hertie Foundation, by the Wings for Life Spinal Cord Research Foundation, by the DFG-DI 140731 and DFG-DI 149741 (all granted to Simone Di Giovanni), the DAAD PhD fellowship (granted to Marilia Grando Soria) and a DZNE PhD fellowship (granted to Yashashree Joshi). We would like to thank Bernd Knöll for Galanin antibody and for discussion of our work, Torsten Plosch and Philipp Kahle for giving us feedback on the manuscript and for providing phospho-antibodies, and Marlies Knipper for BDNF antibody. We would also like to thank Yingchun Ni for discussion on AAV production and purification, and Giorgia Quadrato for discussion on immunohistochemistry.

Author contributions

S.D.G. designed the project; R.P., A.T., M.G.S., A.H., R.L., K.I.R., P.G., Y.J., T.N., A.S. and C.J.L. performed the experiments; R.P., A.T., M.G.S., A.H. and R.L. analysed data, A.-L.B. provided mice, F.B. provided support and feedback, R.P. and S.D.G. supervised the research as well as co-wrote the paper. A.T. contributed to editing the manuscript.

Additional information

Accession code: DNA methylation microarray data have been deposited in the NCBI Gene Expression Omnibus (GEO) database under the accession number GSE55514.

Supplementary Information accompanies this paper at <http://www.nature.com/naturecommunications>

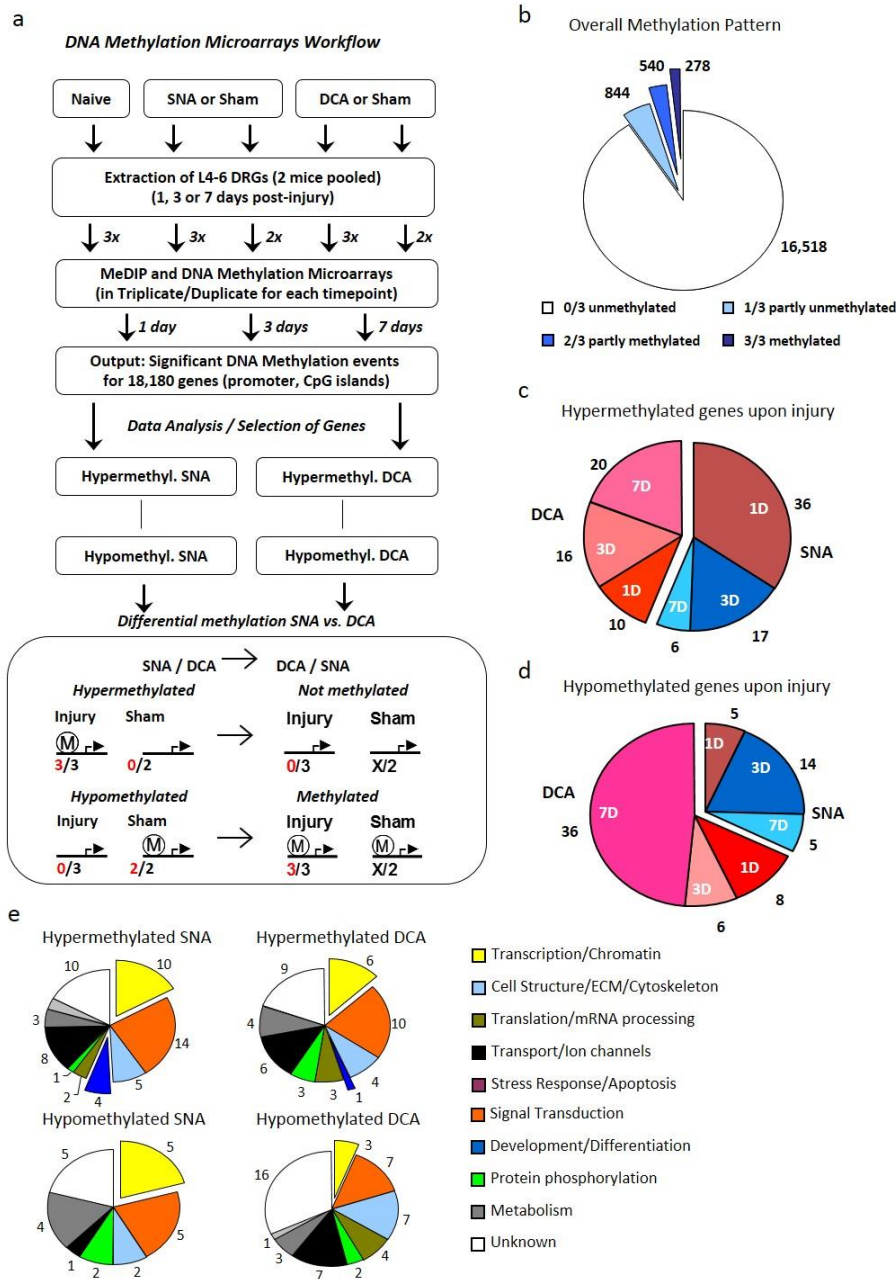
Competing financial interests: The authors declare no competing financial interests.

Reprints and permission information is available online at <http://npg.nature.com/reprintsandpermissions/>

How to cite this article: Puttagunta, R. *et al.* P/CAF-dependent epigenetic changes promote axonal regeneration in the central nervous system. *Nat. Commun.* 5:3527 doi: 10.1038/ncomms4527 (2014).

Supplementary Information

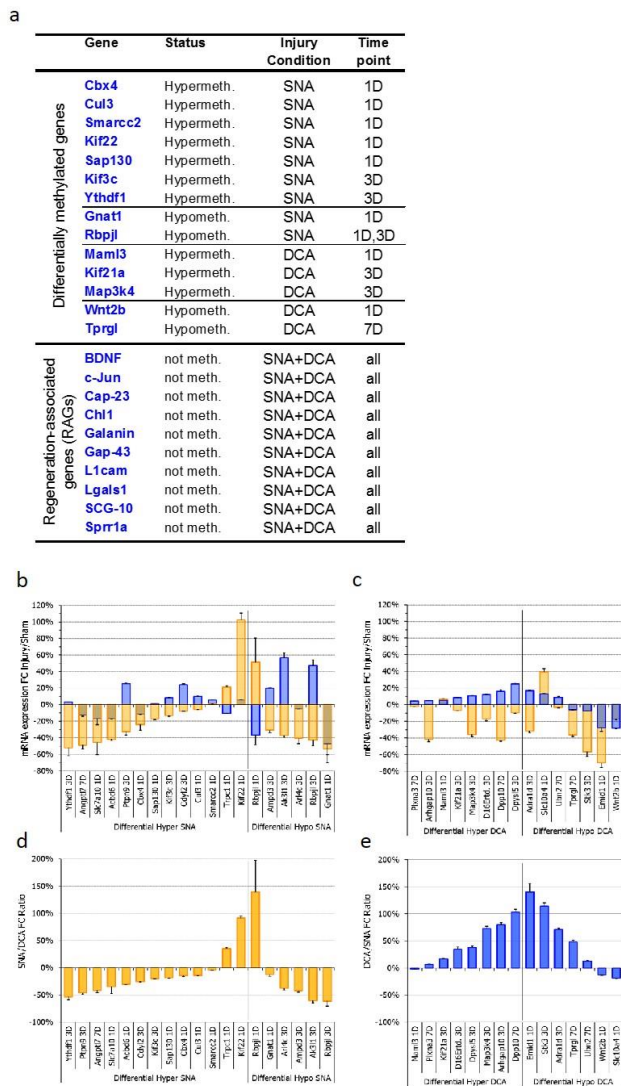
Supplementary Figure 1



Supplementary Figure 1 Promoter and CpG island DNA methylation arrays

a, Schematic diagram summarizing the experimental design of promoter and CpG island DNA methylation arrays from L4-L6 DRGs after SNA and DCA. **b**, Pie chart summarizing the overall number of methylated genes irrespective of injury, showing only a minority of methylated genes. **c**, Pie charts showing the number of fully hypermethylated or hypomethylated genes (3/3) after either SNA or DCA in comparison with Shams. **e**, Pie charts showing the limited number and respective functional classes of differentially methylated genes (comparison to Shams) after SNA and DCA.

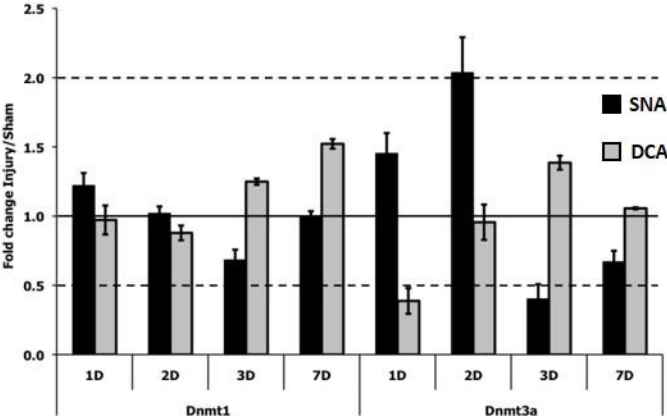
Supplementary Figure 2



Supplementary Figure 2 Methylation of genes and correlation with expression

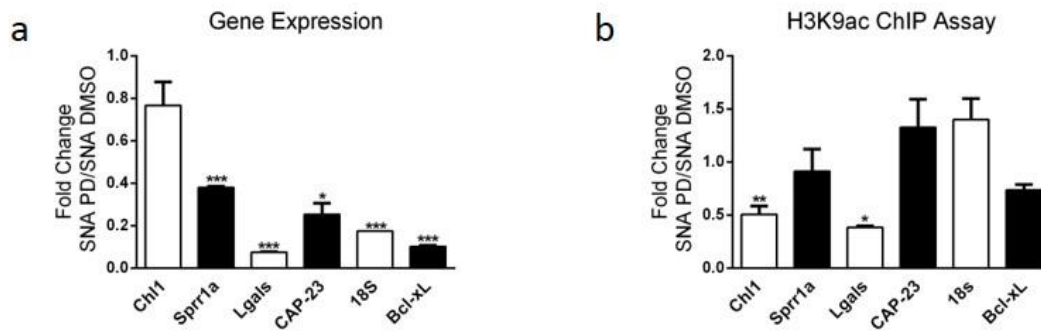
a, Table shows a selection of differentially methylated genes belonging to chromatin remodelling and retrograde signalling functional classes and the lack of methylation of RAGs after axonal injury. Relative mRNA expression fold changes upon SNA or DCA for a subset of differentially methylated genes do correlate with methylation status, but not as a general rule. **b-e**, For each differentially methylated gene, mRNA levels were detected for the relevant time point for SNA and DCA samples (injury and sham). Most differentially hypermethylated genes upon SNA exhibit decreased mRNA expression levels (injury/sham fold change, in orange), while levels upon DCA varied (blue). In contrast to the hypothesis, most differentially hypomethylated genes upon SNA are downregulated, except for *Rbpjl* (**b**). Upon DCA, some differentially hypomethylated genes are upregulated while differentially hypermethylated genes were marginally upregulated as well (**c**). To investigate the correlation between gene expression and DNA methylation, the SNA/DCA FC ratio was calculated, showing lack of correlation between promoter and CpG island methylation and gene expression (**d, e**). Error bars, s.e.m.

Supplementary Figure 3



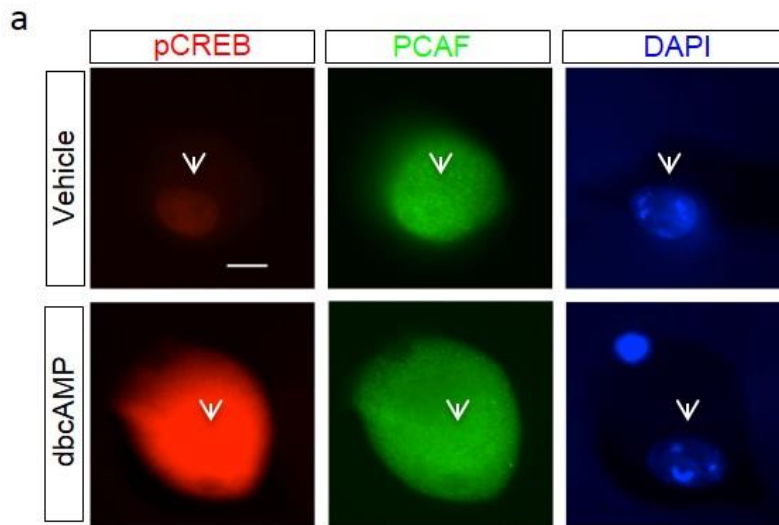
Supplementary Figure 3 DNMT 1 and 3a gene expression after SNA and DCA
Quantitative RT-PCR shows a modest change in gene expression for DNMT1 and DNMT3a after SNA and DCA. All values are fold changes to Shams, N = 3, triplicate experiments. Error bars, s.d.

Supplementary Figure 4



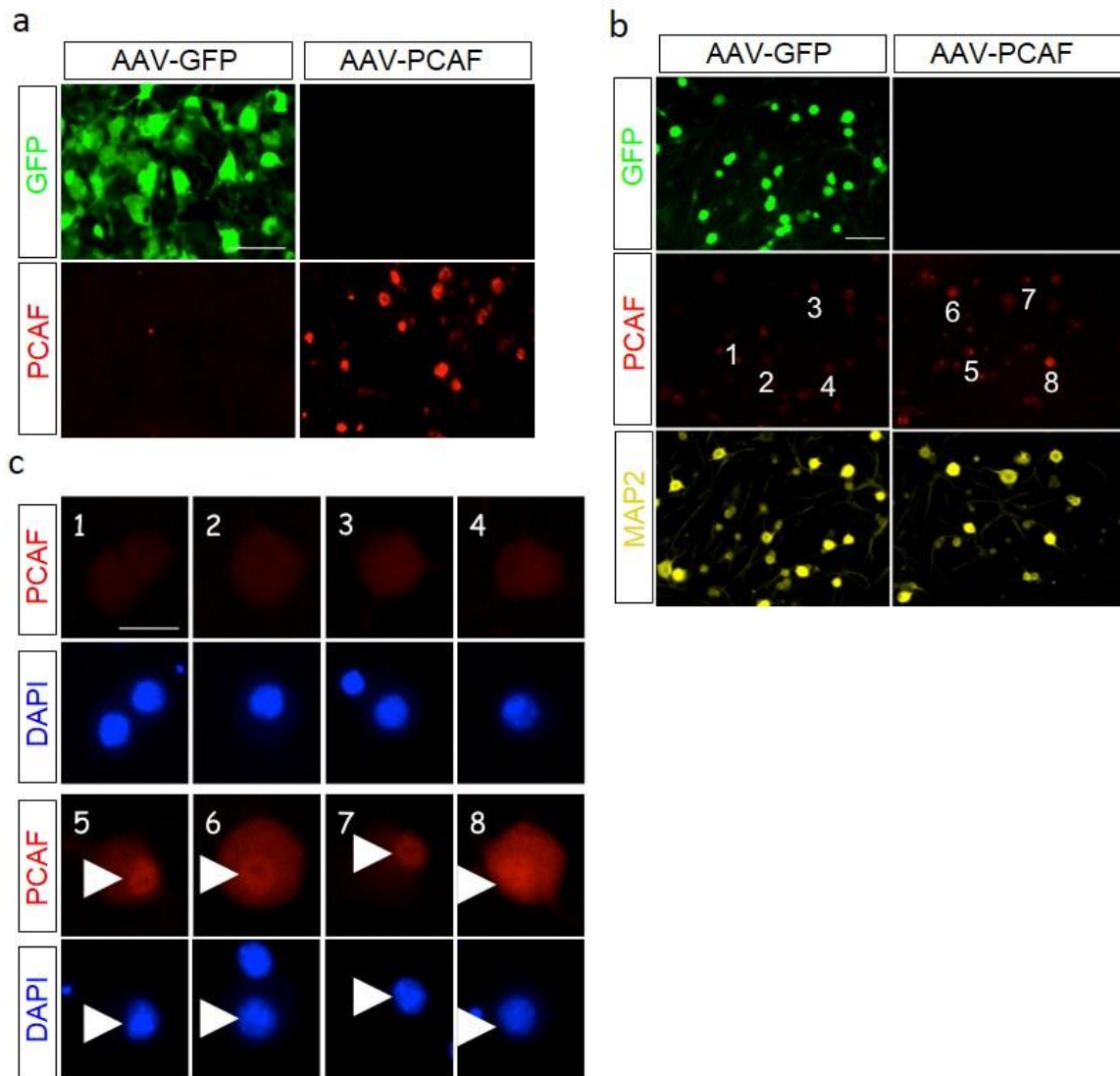
Supplementary Figure 4 Inhibition of ERK on gene expression and promoters **a**, One day following SNA with PD treatment showed a decrease in gene expression of most genes tested compared to SNA with DMSO (Quantitative RT-PCR, N = 3 per group). **b**, No correlation with H3K9ac at the promoters of these genes was found except for Lgals (ChIPs). N = 6 per group, performed in triplicate. Error bars, s.e.m. (a,b) Student's *t*-test, *P<0.05, **P<0.001 and ***P<0.001.

Supplementary Figure 5



Supplementary Figure 5 dbcAMP does not alter PCAF in cultured DRG neurons
a, dbcAMP (1 mM) delivered at the time of plating enhances pCREB expression as expected (24 h), but does not alter expression level nor localization of PCAF. N = 3. Arrow head shows selected cell and nuclear localization. (Scale bar: 10 μ m)

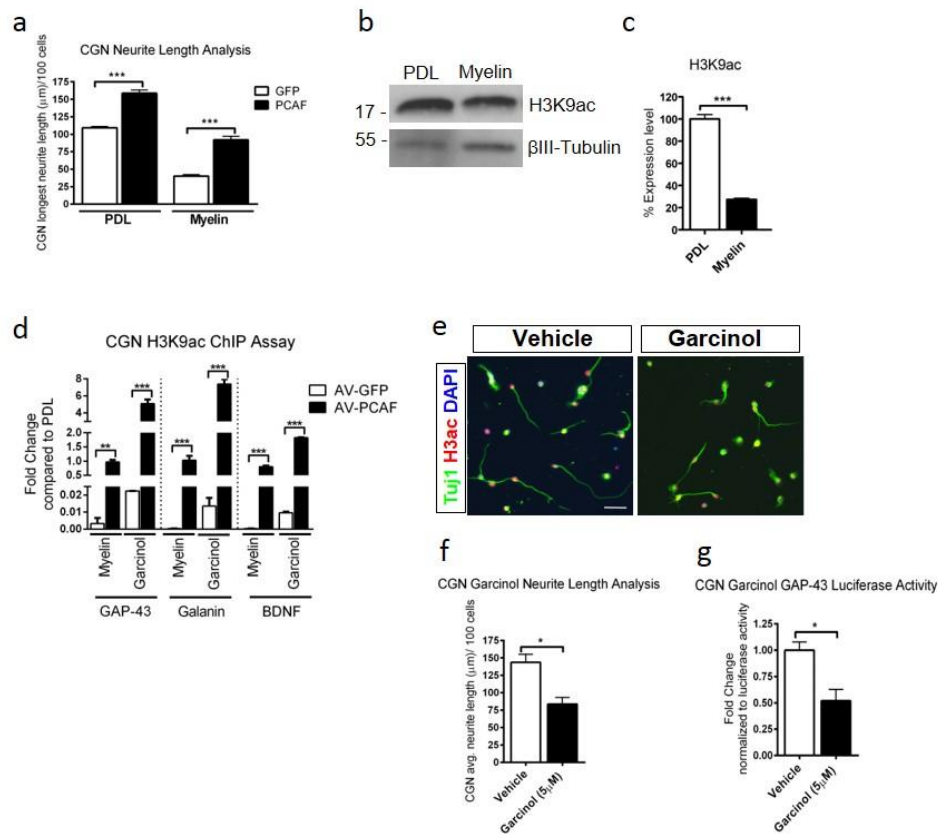
Supplementary Figure 6



Supplementary Figure 6 AAV overexpression leads to enhanced PCAF levels

a, HEK cells infected with AAV-GFP or AAV-PCAF for 48 h. Scale bar, 100 μ m. **b**, Cultured DRG neurons from adult mice were infected with AAV-GFP or AAV-PCAF for 48 h. Scale bar, 100 μ m. **c**, High magnification of numbered PCAF positive cells in **(b)** showing nuclear accumulation after PCAF overexpression. Scale bar, 25 μ m.

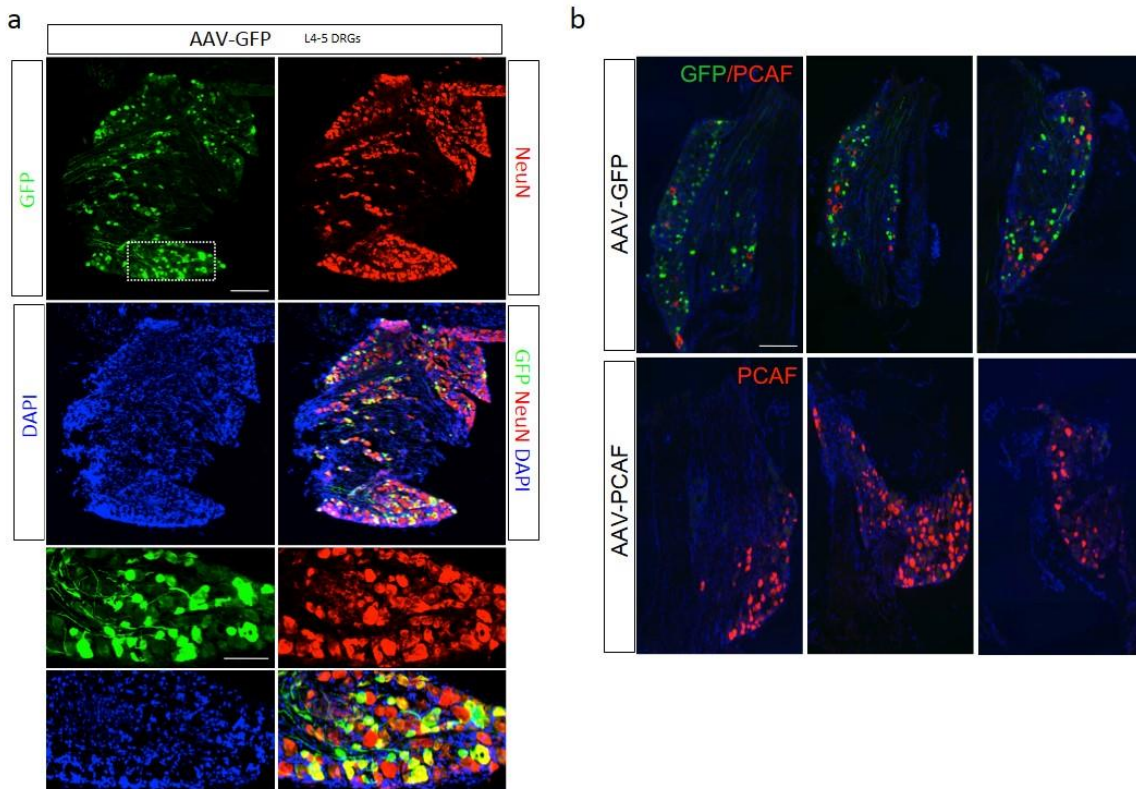
Supplementary Figure 7



Supplementary Figure 7 PCAF overexpression in CGN

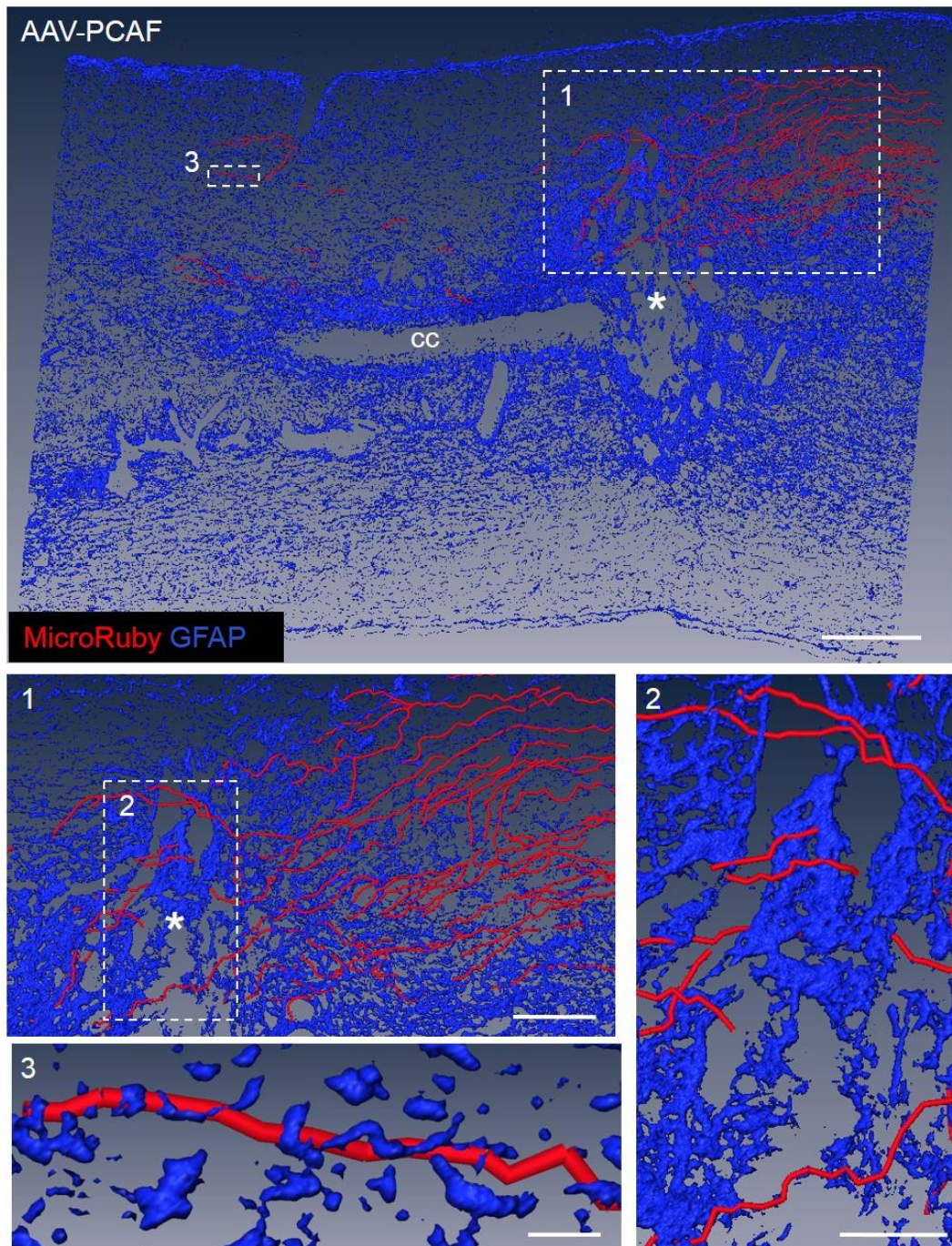
a, CGN electroplated with PCAF for 24 h showed an increase in neurite length on PDL and myelin. **b, c**, Immunoblot (**b**) shows decreased H3K9ac expression in CGN following 24 h of plating on myelin, intensity analysis (**c**). **d**, Myelin significantly decreases H3K9ac at the promoters of RAGs, which is restored by AV-PCAF overexpression (24 h) in CGN. **e, f**, CGN plated for 24 h and treated with 5 μM of the PCAF inhibitor Garcinol showed a decrease in neurite outgrowth on PDL, ICC (**e**) and neurite length analysis (**f**). Scale bars, 50 μm. **g**, GAP-43 proximal promoter luciferase construct shows decreased expression after 24h treatment with 5 μM Garcinol. Error bars, s.e.m., (a, d) $P < 0.0001$, ANOVA, Bonferroni post-hoc tests, * $P < 0.05$, ** $P < 0.001$ and *** $P < 0.001$ (c, f, g) Student's *t*-test, * $P < 0.05$, ** $P < 0.001$ and *** $P < 0.001$, $N = 3-6$, performed in triplicate. Original immunoblot images are shown in Supplementary Figure 15.

Supplementary Figure 8



Supplementary Figure 8 Infection efficiency of AAV in DRGs from SCI study
a, AAV injected in the sciatic nerve specifically targets DRG neurons (8 weeks post-infection) as seen by the overlap in GFP expression and NeuN staining. Scale bars, 250 and 100 μm respectively. **b**, Sciatic nerve injected AAV-GFP and AAV-PCAF shows infection and expression of PCAF protein levels in the L4-L6 DRGs (8 weeks post-infection). Scale bar, 250 μm .

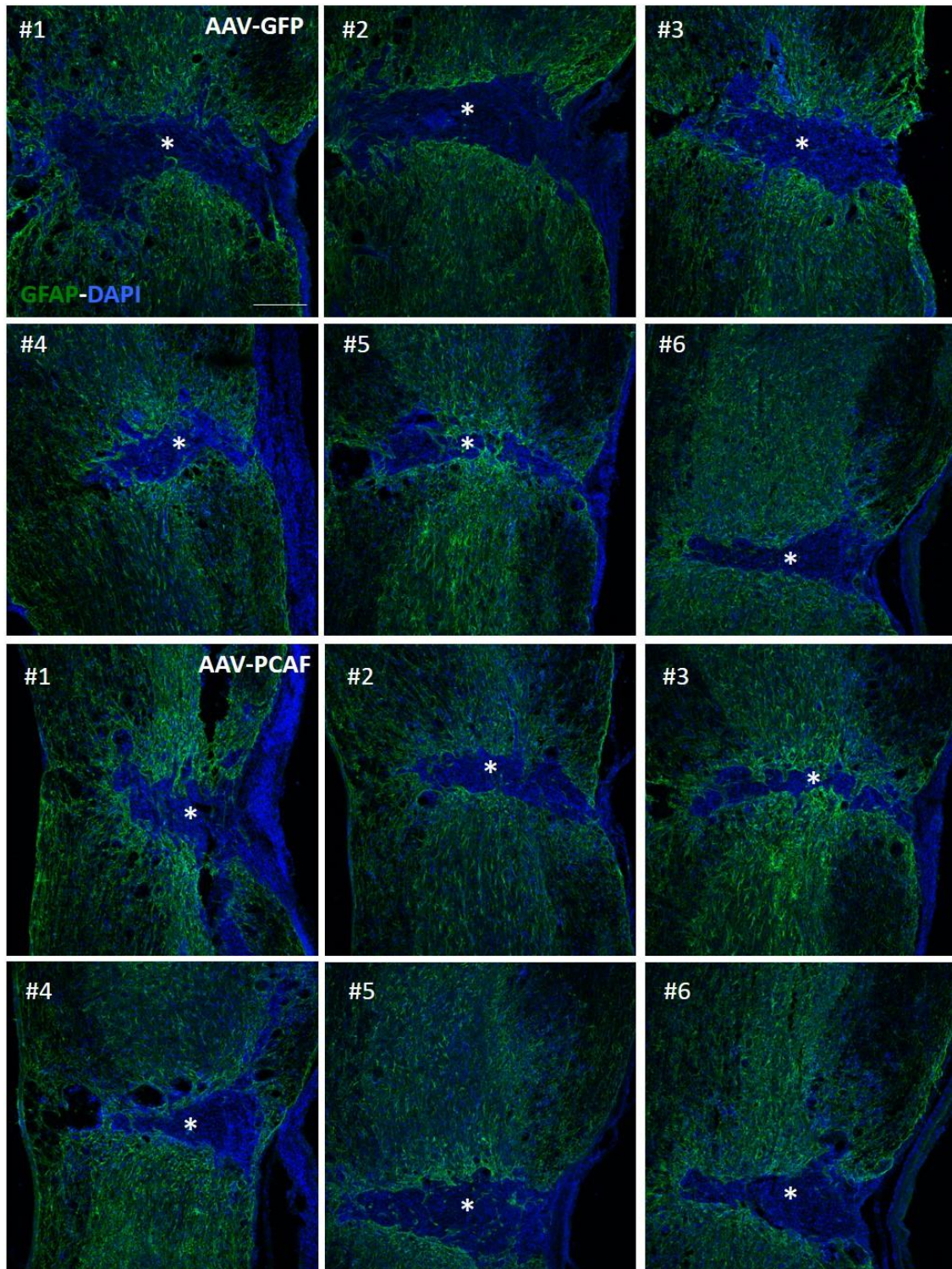
Supplementary Figure 9



Supplementary Figure 9 3D visualization of regenerating axons

Amira 3D reconstruction of regenerating dorsal column axons and glial scar in a sagittal projection (~25 μm) of the spinal cord after PCAF overexpression. * Lesion site. cc: central canal. Scale bars, 200 μm (top panel), 100 μm (1), 50 μm (2) and 10 μm (3).

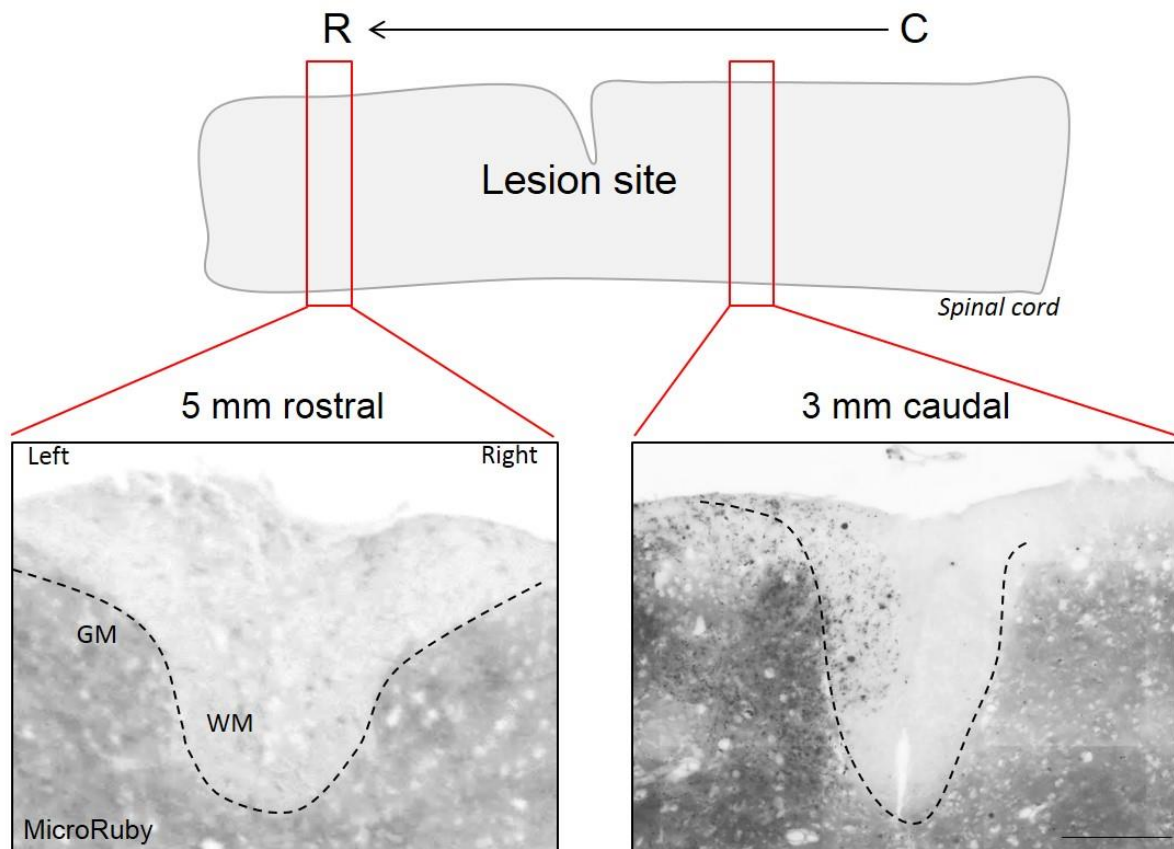
Supplementary Figure 10



Supplementary Figure 10 Lesion sites after SCI

Micrographs show spinal cord lesion sites from individual mice (#1,2, etc...) after SCI as indicated in Figure 8. Asterisk indicates the lesion site. Scale bar, 250 μ m. 40X Scale bar: 250 μ m

Supplementary Figure 11

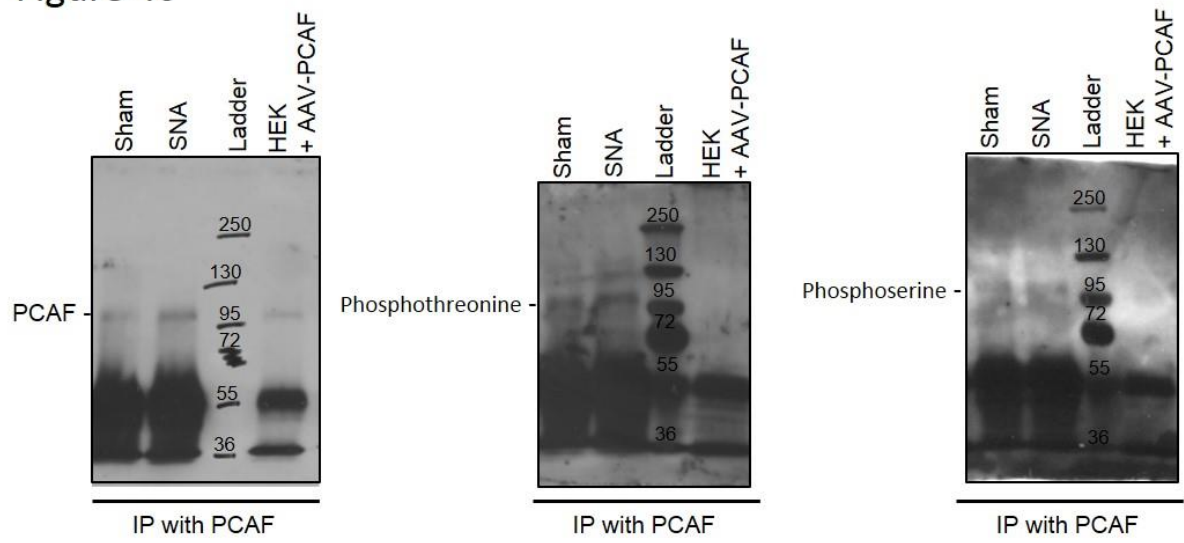


Supplementary Figure 11 Tracer in the dorsal columns after SCI

Micrographs show tracing in representative coronal sections of the dorsal columns after SCI cord. The dotted line indicates dorsal columns. Tracer is visible 3 mm caudal to the lesion site (right panel), but not 5 mm rostral to it (left panel). Scale bar, 150 μ m.

Supplementary Figure 12

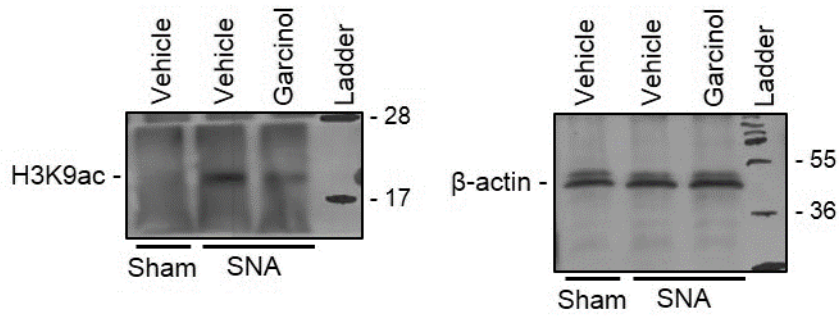
Figure 4c



Supplementary Figure 12 Full scan images of western blot data in Figure 4

Supplementary Figure 13

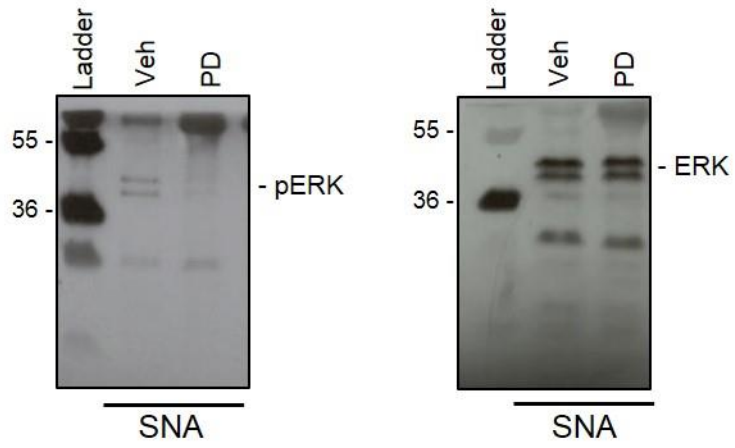
Figure 5i



Supplementary Figure 13 Full scan images of western blot data in Figure 5i

Supplementary Figure 14

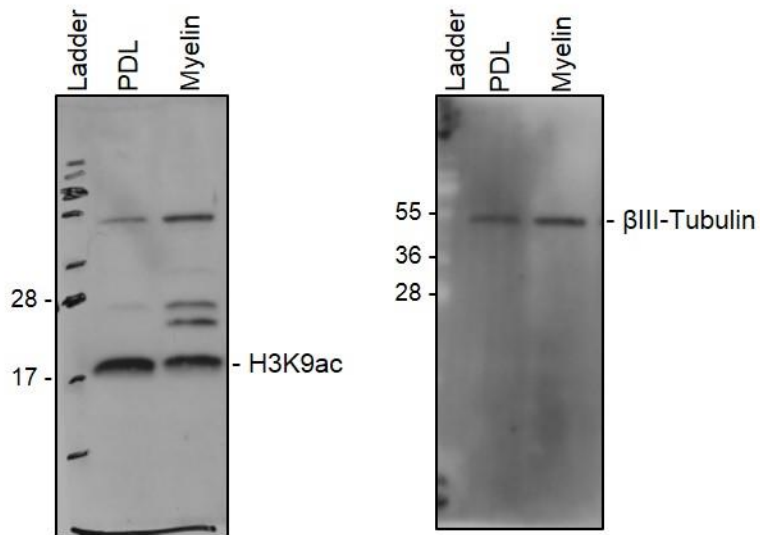
Figure 6c



Supplementary Figure 14 Full scan images of western blot data in Figure 6c

Supplementary Figure 15

Supplemental Figure 7b



Supplementary Figure 15 Full scan images of western blot data in Supplemental Figure 7

Supplementary Table 1

Quantitative-RT-PCR Primers

Gene	Forward Primer	Reverse Primer
GAP-43	5'-CTTCTTTACCCTCATCCTGTCG-3'	5'- CAGGAAAGATCCCAAGTCCA-3'
Galanin	5'- GTGACCCTGTCAGCCACTCT -3'	5'- GGTCTCCTTTCCTCCACCTC-3'
BDNF	5'- AGTCTCCAGGACAGCAAAGC-3'	5'- TCGTCAGACCTCTCGAACCT -3'
SCG-10	5'- GCAATGGCCTACAAGGAAAA -3'	5'- GGTGGCTTCAAGATCAGCTC-3'
L1cam	5'-GGGTGAGTGGAATCTGGCTA-3'	5'- TGGCTCTAGCACATGGTGTC-3'
Sprr1a	5'-CCCCTCAACTGTCACTCCAT-3'	5'-CAGGAGCCCTTGAAGATGAG-3'
CAP-23	5'-GGGAGAGAGAGAGCCTTTGC-3'	5'-CTTCGGCCTTCTTGTCTTTG-3'
Lgals	5'-TCAAACCTGGGGAATGTCTC-3'	5'-ATGCACACCTCTGTGATGCT-3'
Chl1	5'-ATTGCGGCTAACAATTCAGG-3'	5'-GAGGGTTGCAGGGTAAGACA-3'
Bcl-xL	5'- CTGGTGGTTGACTTTCTCTCC-3'	5'- CAAGGCTCTAGGTGGTCATTC-3'
18S	5'-CGGCTACCACATCCAAGGAA-3'	5'-GCTGGAATTACCGCGGCT-3'
Dnmt1	5'- GTGGTGTCTGTGAGGTCTGTC-3'	5'- AAGTTAGGACACCTCCTCTTGAG-3'
Dnmt3a	5'- AGGGAGGCTGAGAAGAAAGC-3'	5'- GGCTGCTTTGGTAGCATTCT-3'
Dnmt3b	5'- AGTTTCCGGCTACCAGGTCT-3'	5'- TGTGCTGTCTCCATCTCTGC -3'
RPL13A	5'-CCCTCCACCCTATGACAAGA-3'	5'-CCTTTTCCTTCCGTTTCTCC-3'
GAPDH	5'-ACCCTGTTGCTGTAGCCGTATCA-3'	5'- TCAACAGCAACTCCCCTCTCCA-3'
β-actin	5'-GAACGGAACATTGCACACAC-3'	5'-ACAGCTTCACCACCACAGCTGA-3'

Supplementary Table 2

ChIP Primers

Gene	Forward Primer	Reverse Primer
GAP-43	5'- CTGCGCGTAAAATCTAATGG-3'	5'- TGGAGAGATTGGATGGAACA-3'
Galanin	5'- TACACCTCCGGTCCTGAGAC-3'	5'- GGTAGGGAAGCTGCAGTCAC-3'
BDNF	5'- GGAGACTAGCGCCGATCTTC-3'	5'- CGAGCCACTAGTTGCCACACA-3'
SCG-10	5'- AAGGAGGCTTCCAGGCTAAG-3'	5'- GCTCAAGCAGATTGGCTCTC-3'
CAP-23	5'-GTCCCCCAACTTCTCTCCAC-3'	5'-GGGCGTGTAAGGAGGGAATA-3'
Sprr1a	5'-TCCCCTAGTTCACCTCTGA-3'	5'-AGGACCACTTCAACCTCCT-3'
Lgals	5'-CTGACTGGTCACCTCTGCTC-3'	5'-CAGTCAGAAGACTCCACCCGA-3'
Ch11	5'-TGTCCCCTTTCGCGGTTTTTC-3'	5'-TGAAGGCTCGATGCCCAAGT-3'
L1cam	5'-GCTGCACCATCCACTCTTT-3'	5'-TCACGACCATCTTGCTGTCAG-3'
Bcl-xL	5'- CGACATCGAAAGGAAAAAGC -3'	5'-ATCGAGACATGGGAGAGCAG-3'
NF-L	5'-CAGGGAAGTTATGGGGTCT -3'	5'-TTATACGCCGGGACTCTGAC-3'
HSP27	5'-TTGCTCCCCAGGAGATACAC-3'	5'-GATTCCCCTGTCGGGTTTA-3'
ATF3	5'-GCTGGTCAAAGAAGGCACAT-3'	5'-ATCTCTCCCTCCGCTAGGTT-3'
18S	5'-GGCCGAACCGGAAGTTATAG-3'	5'-AAGAGAGAGCGGAAGTGACG-3'

YASHASHREE JOSHI

EDUCATION

- Ph. D. Neurodegeneration/ Neuroregeneration May 2014
M. S. Cellular and Molecular Neuroscience May 2010
GPA: 3.75/4 (approx.)
- Advisor: Dr. Simone Di Giovanni.
 - Hertie Institute of Clinical Brain Research, University of Tuebingen, Germany.
 - 🏆 Awarded fellowship by German Centre for Neurodegenerative Diseases (DZNE).
 - 🏆 Awarded scholarship by the Graduate Training Centre, University of Tuebingen, Germany.
 - 🏆 Received German academic exchange service (DAAD) Grant.
- B. Sc. Biotechnology June 2008
GPA: 3.75/4 (approx.)
- University of Pune, India.
 - 🏆 Received J. N. Tata endowment trust Scholarship.

EXPERIENCE

- Research Assistant, University of Tuebingen, Germany 2010-2014
- Optimized and tested drugs *in vivo* to promote neuronal survival and regeneration after injury.
 - Established *in vitro* (virus production, primary neuronal cultures) and *in vivo* models (optic nerve crush).
 - Demonstrated an *ex-vivo* genotyping method to reduce experiment duration by 60%, cost by 10%.
 - Monitored adherence to guidelines for animal handling and experimentation.
- Industrial Internship, Vaccine Trial Division, VH Biologicals, Pune 2007
- Performed qualitative and quantitative estimation of extraneous pathogens in vaccine batches.
 - Assisted in chicken embryonic primary culture preparation.

SKILL SET

- *In vivo* rodent surgeries: Optic nerve crush, Intravitreal injection, Stereotactic injection, Middle cerebral artery occlusion (MCAO), Sciatic Nerve Injury.
- *In vitro*: Retinal ganglion cell culture, Dorsal root ganglia culture, Cerebellar granule neuron culture, Hippocampal culture, Cell line maintenance, Virus production (Adeno associated, Adeno, and Lenti), FACS.
- Protein chemistry: Anion exchange chromatography, Inclusion body purification, Sucrose density gradient ultracentrifugation.
- Basic techniques: Immunohistochemistry, Western blotting, qRT-PCR.
- Softwares: Ingenuity pathway analysis, Image J, GraphPad Prism, AxioVision, NeuroLucida.

CERTIFICATIONS

- Accreditation Course on Animal Handling and Experimentation 2011
- Certification by Federation for Laboratory Animal Science Associations, University of Zurich.
- Cerebral Ischemia: *in vivo* and *in vitro* models 2011
- Charite Universitätsmedizin, Centre for Stroke Research, Berlin.
- In vivo* Rodent CNS Injury Model 2010
- Harvard Medical School, Boston

PUBLICATIONS

2013

J1. Y Joshi, G Quadrato, M Grando Soria, A Hervera, G Inak, K Rathore, JC Marine, S Di Giovanni. *Modulation of MDM4-p53-IGF1R axis promotes CNS axonal regeneration and sprouting after CNS injury*. Under Review PLoS Biology

J2. R Puttagunta, A Tedeschi, M Grando Soria, R Lindner, K I. Rathore, P Gaub, YJoshi, T Nguyen, A Schmandke, C Laskowski, A Boutillier, F Bradke, S Di Giovanni. *Epigenetic changes promoting axonal regeneration in the central nervous system*. Nature Communication 2014, 5:3527.

C1. Y Joshi, G Quadrato, M Grando Soria, A Hervera, R Puttagunta, G Inak, K Rathore, JC Marine, S Di Giovanni. *Modulation of MDM2/MDM4 signaling promotes axonal regeneration in the CNS*.

Annual Meeting of Society to Neuroscience, San Diego, USA, 2013.

C2. R Puttagunta, A Tedeschi, M Grando Soria, R Lindner, Y Joshi, Tuan Nguyen, Tony Schmandke, Frank Bradke, and S Di Giovanni. *PCAF-dependent epigenetic changes promote axonal regeneration in the central nervous system*. Annual Meeting of Society to Neuroscience, San Diego, USA, 2013.

2012

C2. Y Joshi et al *p53 transactivation via conditional MDMX deletion leads to enhanced axonal outgrowth in vivo after optic nerve crush*: Ab No A-471-0088-03505 8th Federation of European Neuroscience Societies Forum, Barcelona.

2011

J3 P Gaub, Y Joshi, A Wuttke, U Naumann, P Heiduschka, S Schnichels, S Di Giovanni. *The histone acetyltransferase promotes p300 promotes intrinsic axonal regeneration* Brain 2011: 134; 2134–2148

2010

C3 P Gaub, Y Joshi, P Heiduschka, S Schnichels, S Di Giovanni. *Characterization of neuronal acetylation actors during development and axonal regeneration*. 7th Federation of European Neuroscience Societies Forum, Amsterdam